PREPARATION AND CHARACTERIZATION OF POLYMER MATRIX COMPOSITE USING NATURAL FIBER LANTANA-CAMARA

A THESIS SUBMITTED IN PARTIAL FULFILMENT OF THE REQUIREMENT FOR THE DEGREE OF

Doctor of Philosophy

in

Mechanical Engineering

By

Chitta Ranjan Deo

Department of Mechanical Engineering
National Institute of Technology
Rourkela -769 008 (India)
June-2010

PREPARATION AND CHARACTERIZATION OF POLYMER MATRIX COMPOSITE USING NATURAL FIBER LANTANA-CAMARA

A THESIS SUBMITTED IN PARTIAL FULFILMENT OF THE REQUIREMENTSFOR THE DEGREE OF

Doctor of Philosophy

in

Mechanical Engineering

Submitted to

National Institute of Technology, Rourkela

(Deemed University)

By

Chitta Ranjan Deo

Under the supervision of

Dr. Samir Kumar Acharya

Department of Mechanical Engineering
National Institute of Technology
Rourkela -769 008 (India)
June-2010

Dedicated to

My Parents

Late Purushottam Deo

&

Late Adaramani Deo

National Institute of Technology
Rourkela-769008 (Orissa), INDIA

CERTIFICATE

This is to certify that the thesis entitled "**Preparation and Characterization of Polymer Matrix Composite Using Natural Fiber Lantana-Camara"** submitted to the National Institute of Technology, Rourkela (Deemed University) by Chitta Ranjan Deo, Roll No. 507-ME-009 for the award of the Degree of Doctor of Philosophy in Mechanical Engineering is a record of bonafide research work carried out by him under my supervision and guidance. The results presented in this thesis has not been, to the best of my knowledge, submitted to any other University or Institute for the award of any degree or diploma.

The thesis, in my opinion, has reached the standards fulfilling the requirement for the award of the degree of **Doctor of Philosophy** in accordance with regulations of the Institute.

Date: - -June-2010

(Dr. S. K. Acharya)
Associate Professor
Mechanical Engineering Department

ACKNOWLEDGEMENT

It is a great pleasure to express my gratitude and indebtedness to my supervisor Dr. S. K. Acharya for his guidance, encouragement, moral support and affection through the course of my work.

I am also grateful to Prof. Sunil Kumar Sarangi, Director, NIT, Rourkela who took keen interest in the work. My special thanks to Prof. R. K. Sahoo, Head of Mechanical Engineering Department and QIP coordinator, Prof. Akrur Behera and all staff members of the department for their timely help in completion of this work.

Besides my advisors, I would like to thank Mr. Rajesh Pattanaik, Mr. Samir Pradhan & Mr. Uday Kumar Sahoo Metallurgical & Materials Engineering Department for helping me to complete the experimental work. I am also thankful to all my lab mates Mrs Punyapriya Mishra, Mr. S. K. Mehar and Mr. G. Raghavendra for their valuable support and maintaining a nice research environment in the laboratory.

This work is also the outcome of the blessing guidance and support of my uncle Mr. B. K. Deo & elder sister Mrs. Basanti Bala. This work could have been a distant dream if I did not get the moral encouragement and help from my wife, Reena. She equally shared my success and failures with me. My son Swadhin missed me a lot and sacrificed many of his pleasant dreams for me. This thesis is the outcome of the sincere prayers and dedicated support of my family.

Finally, I wish to acknowledge the financial support given to me by the Ministry of Human Resource Development, Government of India and the authorities of SIET, Dhenkanal, for granting three years study leave to carry out this research work at NIT Rourkela.

Date: - -June-2010 **(Chitta Ranjan Deo)**

ABSTRACT

Environmental awareness today motivates the researchers, worldwide on the studies of natural fiber reinforced polymer composite and cost effective option to synthetic fiber reinforced composites. The availability of natural fibers and ease of manufacturing have tempted researchers to try locally available inexpensive fibers and to study their feasibility of reinforcement purposes and to what extent they satisfy the required specifications of good reinforced polymer composite for different applications. With low cost and high specific mechanical properties, natural fiber represents a good renewable and biodegradable alternative to the most common synthetic reinforcement, i.e. glass fiber. Despite the interest and environmental appeal of natural fibers, there use is limited to non-bearing applications, due to their lower strength compared with synthetic fiber reinforced polymer composite. The stiffness and strength shortcomings of biocomposites can be overcome by structural configurations and better arrangement in a sense of placing the fibers in specific locations for highest strength performance. Accordingly extensive studies on preparation and properties of polymer matrix composite (PMC) replacing the synthetic fiber with natural fiber like Jute, Sisal, Pineapple, Bamboo, Kenaf and Bagasse were carried out. These plant fibers have many advantages over glass fiber or carbon fiber like renewable, environmental friendly, low cost, lightweight and high specific mechanical performance.

There are many potential natural resources, which India has in abundance. Most of it comes from the forest and agriculture. Lantana-Camara, locally called 'Putus' is one such natural resource whose potential as fiber reinforcement in polymer composite has not been explored till date.

Lantana-Camara was introduced in India in 1809 as an ornamental plant. Since then it has spread all over the country. This weed at present is posing serious problems in plantation forestry at various locations. It chokes all other vegetation and becomes the dominant species. Complete eradication of Lantana-Camara from every area is a very-very difficult task. The various measures to control this weed have almost failed or are not cost effective, therefore none of them have become popular. Some of the use of Lantana-Camara is to make cheap furniture, utility articles, mosquito repellent and as medicine for various cures particularly for skin related diseases. On the other hand the plant is an

invasive weed and is almost treated like bamboo in some part of India. Stems of larger Lantana-Camara are also thin and the wood is very tough and durable. Against this back ground the present research work has been undertaken with an objective to explore the use of natural fiber Lantana-Camara, as a reinforcement material in epoxy base.

The work presented in this dissertation involves investigation of two distinct problems of natural fiber composites:

i. A study of favourable mechanical properties of Lantana-Camara fiber in thermosetting matrix composite.

ii. An experimental investigation of tribological potential of Lantana-Camara fiber reinforced composite.

To study the mechanical properties of the composite, different volume fraction of fiber have been taken. These fibers were randomly distributed in the matrix. Usual hand-lay-up technique has been adopted for manufacturing the composite. To find out the critical fiber length Single fiber Pull-out test has been carried out. To have a good compatibility between the fiber and matrix, chemical modification of fibers such as Acetone, Alkali and Benzoyl-Chloride treatments has been carried out. It was found that benzoyl-chloride treated fiber composite exhibits favourable strength and stiffness in comparison to other treatments. Moisture absorption behaviour of both treated and untreated fiber composite was also carried out. The moisture sorption kinetics of the composite has also been studied. The study confirms that the Fickian's diffusion can be used to adequately describe the moisture absorption in the composite.

For studying the tribo-potential of Lantana-Camara fiber, different wear tests like abrasive wear test (multi-pass condition) on Pin-on-Disc wear testing machine, two body abrasion wear test (Single pass condition) by Two-body abrasion wear tester and Solid particle erosion behaviour by Air jet erosion test rig, have been carried out. All these tests have been carried out as per ASTM standard. The abrasive wear test results shows that the wear rate of pure epoxy reduces significantly with the addition of LCF up to 40 vol%. The wear anisotropy of the composite studied with Two-body abrasion tester shows wear

characteristics follow the following the trends: $W_{NO} < W_{APO} < W_{PO}$. The solid particle erosion test clearly indicates that the composite behaviour is semi-ductile in nature.

Two different mathematical models have been developed to predict the abrasive wear and erosive wear of Lantana-Camara fiber reinforced epoxy composite separately under various testing conditions by using Response Surface Methodology (RSM). The full factorial design experimentation has been intended to model the abrasive and erosive wear response. These two different second order regression equations for abrasive wear rate (Δw) and erosion rate (ER) have been evaluated after implementation of Analysis of variance (ANOVA) at 95% confidence level. To have an assessment of pure error and model fitting error, some of the experimental trials are replicated in both the cases and the adequacy of the models is also investigated by the examination of residuals. The mathematical models which are developed to predict the abrasive and erosive wear characteristics has been found to be statistically valid and sound within the range of the factors.

There are other fabrication techniques available like injection moulding, compression moulding and extrusion, where the volume fraction of reinforcement can be increased. In addition there are other chemical methods by which the fiber surface modification can be done. This work can be further extended to those techniques. However the results reported here can act as a starting point for both industrial designer and researchers to design and develop polymer matrix composite components using Lantana-Camara fiber as reinforcement.

The whole dissertation has been divided in to eight chapters to put the analysis independent of each other as far as practicable. Major works on moisture absorption characteristics, dry sliding wear behaviour, anisotropic wear behaviour, erosive wear characteristics and validation of results through RSM technique are given in chapter 3, 4, 5, 6 and 7 respectively.

TABLE OF CONTENTS

LIST OF TABLES

LIST OF FIGURES

LIST OF SYMBOLS

ANOVA	Analysis of variance
APO	Anti-parallel orientation
D_x	Diffusion coefficient
E_r	Erosion rate
FFD	Full factorial design
FTIR	Fourier Transform Infrared
GS	Abrasive grit size
H (t)	Sample thickness at any time‘t’
I_c	Crystallinity index
k_0	Specific Wear rate
K_{SR}	Thickness swelling parameter
L	Applied Normal Load
LCF	Lantana-Camara Fiber
M_m	Maximum percentage of moisture content
M_t	Moisture absorption
n	Anisotropy coefficient
NO	Normal orientation
P_{break}	Maximum load at failure
PO	Parallel orientation
R^2	Coefficient of determination
R^2_{adj}	Adjusted coefficient of determination
R_e	Volume fraction of reinforcement

RSM	Response Surface Methodology
S_d	Sliding Distance
SEM	Scanning electron microscope
t	Time
T(s)	Thickness swelling
Vv	Voids content
W	Wear rate
W_0	Oven-dry weight
W_t	Weight after time‘t’
XRD	X-ray Diffraction
Δw	Wear loss/ Weight loss
$\hat{w}$	Cumulative weight loss
α	Impingement / Impact angle
η	Erosion efficiency
μ	Coefficient of friction
ρ	Density

Chapter 1

INTRODUCTION

Chapter-1

1.1 BACKGROUND

It is a truism that technological development depends on advances in the field of materials. One dose not have to be an expert to realize the most advanced turbine or air-craft design is of no use if adequate materials to bear the service loads and conditions are not available. Whatever the field may be, the final limitation on advancement depends on materials. Composite materials in this regard represent nothing but a giant step in the ever-constant endeavour of optimization in materials.

Strictly speaking, the idea of composite materials is not a new or recent one. Nature is full of examples wherein the idea of composite materials is used. The coconut palm leaf, for example, is nothing but a cantilever using the concept of fiber reinforcement. Wood is a fibrous composite: cellulose fibers in a lignin matrix. The cellulose fibers have high tensile strength but are very flexible (i.e. low stiffness), while the lignin matrix joins the fibers and furnishes the stiffness. Bone is yet another example of a natural composite that supports the weight of various members of the body. It consists of short and soft collagen fibers embedded in a mineral matrix called apatite. In addition to these naturally occurring composites, there are many other engineering materials that are composites in a very general way and that have been in use for very long time. The carbon black in rubber, Portland cement or asphalt mixed with sand, and glass fibers in resin are common examples. Thus, we see that the idea of composite materials is not that recent. Nevertheless, one can safely mark the origin of the distinct discipline of the composite materials as the beginning of the 1960s. It would not be too much off the mark to say that a concerted research and development effort in composite materials began in 1965. Since the early 1960s, there has been an increasing demand for materials that are stiffer and stronger yet lighter in fields as diverse as aerospace, energy and civil constructions. The demands made on materials for better overall performance are so great and diverse that no one material can satisfy them. This naturally led to a resurgence of the ancient concept of combining different materials in an integral-composite material to satisfy the user requirement. Such composite material systems result in a performance unattainable by the individual constituents, and they offer

the great advantage of a flexible design; that is, one can, in principle, tailor-make the material as per specifications of an optimum design.

1.2 COMPOSITES

1.2.1 Why a composite?

Over the last thirty years composite materials, plastics and ceramics have been the dominant emerging materials. The volume and number of applications of composite materials have grown steadily, penetrating and conquering new markets relentlessly. Modern composite materials constitute a significant proportion of the engineered materials market ranging from everyday products to sophisticated niche applications.

While composites have already proven their worth as weight-saving materials, the current challenge is to make them cost effective. The efforts to produce economically attractive composite components have resulted in several innovative manufacturing techniques currently being used in the composite industries. It is obvious, especially for composites, that the improvement in manufacturing technology alone is not enough to overcome the cost hurdle. It is essential that there be an integrated effort in designing, material processing, tooling, quality assurance, manufacturing, and even programme management for composites to become competitive with metals.

The composites industry has begun to recognize that the commercial applications of composites promise to offer much larger business opportunities than the aerospace sector due to the sheer size of transportation industry. Thus the shift of composite applications from aircraft to other commercial uses has become prominent in recent years.

Increasingly enabled by the introduction of newer polymer resin matrix materials and high performance reinforcement fibers of glass, carbon and aramid, the penetration of these advanced materials has witnessed a steady expansion in uses and volume. The increased volume has resulted in an expected reduction in costs. High performance FRP can now be found in such diverse applications as composite armoring designed to resist

explosive impacts, fuel cylinders for natural gas vehicles, windmill blades, industrial drive shafts, support beams of highway bridges and even paper making rollers. For certain applications, the use of composites rather than metals has in fact resulted in savings of both cost and weight. Some examples are cascades for engines, curved fairing and fillets, replacements for welded metallic parts, cylinders, tubes, ducts, blade containment bands etc.

Further, the need of composites for lighter construction materials and more seismic resistant structures has placed high emphasis on the use of new and advanced materials that not only decreases dead weight but also absorbs the shock & vibration through tailored microstructures. Composites are now extensively being used for rehabilitation/ strengthening of pre-existing structures that have to be retrofitted to make them seismic resistant, or to repair damage caused by seismic activity.

Unlike conventional materials (e.g., steel), the properties of the composite material can be designed considering the structural aspects. The design of a structural component using composites involves both material and structural design. Composite properties (e.g. stiffness, thermal expansion etc.) can be varied continuously over a broad range of values under the control of the designer. Careful selection of reinforcement type enables finished product characteristics to be tailored to almost any specific engineering requirement.

Whilst the use of composites will be a clear choice in many instances, material selection in others will depend on factors such as working lifetime requirements, number of items to be produced (run length), complexity of product shape, possible savings in assembly costs and on the experience & skills the designer in tapping the optimum potential of composites. In some instances, best results may be achieved through the use of composites in conjunction with traditional materials.

1.2.2 What is a composite?

A typical composite material is a system of materials composing of two or more materials (mixed and bonded) on a macroscopic scale.

Generally, a composite material is composed of reinforcement (fibers, particles, flakes, and/or fillers) embedded in a matrix (polymers, metals, or ceramics). The matrix holds the reinforcement to form the desired shape while the reinforcement improves the overall mechanical properties of the matrix. When designed properly, the new combined material exhibits better strength than would each individual material.

As defined by Jartiz, [1] Composites are multifunctional material systems that provide characteristics not obtainable from any discrete material. They are cohesive structures made by physically combining two or more compatible materials, different in composition and characteristics and sometimes in form.

Kelly [2] very clearly stresses that the composites should not be regarded simple as a combination of two materials. In the broader significance; the combination has its own distinctive properties. In terms of strength or resistance to heat or some other desirable quality, it is better than either of the components alone or radically different from either of them.

Berghezan [3] defines as "The composites are compound materials which differ from alloys by the fact that the individual components retain their characteristics but are so incorporated into the composite as to take advantage only of their attributes and not of their shortcomings", in order to obtain an improved material

Van Suchetclan [4] explains composite materials as heterogeneous materials consisting of two or more solid phases, which are in intimate contact with each other on a microscopic scale. They can be also considered as homogeneous materials on a microscopic scale in the sense that any portion of it will have the same physical property.

1.2.3 Characteristics of the Composites

Composites consist of one or more discontinuous phases embedded in a continuous phase. The discontinuous phase is usually harder and stronger than the continuous phase and is called the 'reinforcement' or 'reinforcing material', whereas the continuous phase is termed as the ' matrix'.

Properties of composites are strongly dependent on the properties of their constituent materials, their distribution and the interaction among them. The composite properties may be the volume fraction sum of the properties of the constituents or the constituents may interact in a synergistic way resulting in improved or better properties. Apart from the nature of the constituent materials, the geometry of the reinforcement (shape, size and size distribution) influences the properties of the composite to a great extent. The concentration distribution and orientation of the reinforcement also affect the properties.

The shape of the discontinuous phase (which may by spherical, cylindrical, or rectangular cross-sanctioned prisms or platelets), the size and size distribution (which controls the texture of the material) and volume fraction determine the interfacial area, which plays an important role in determining the extent of the interaction between the reinforcement and the matrix.

Concentration, usually measured as volume or weight fraction, determines the contribution of a single constituent to the overall properties of the composites. It is not only the single most important parameter influencing the properties of the composites, but also an easily controllable manufacturing variable used to alter its properties.

1.2.4 Classification of Composites

Composite materials can be classified in different ways [5]. Classification based on the geometry of a representative unit of reinforcement is convenient since it is the geometry of the reinforcement which is responsible for the mechanical properties and high performance of the composites. A typical classification is presented in Table-1.1. The two broad classes of composites are:

(i) Fibrous composites

(ii) Particulate composites

Table- 1.1 Classification of composite

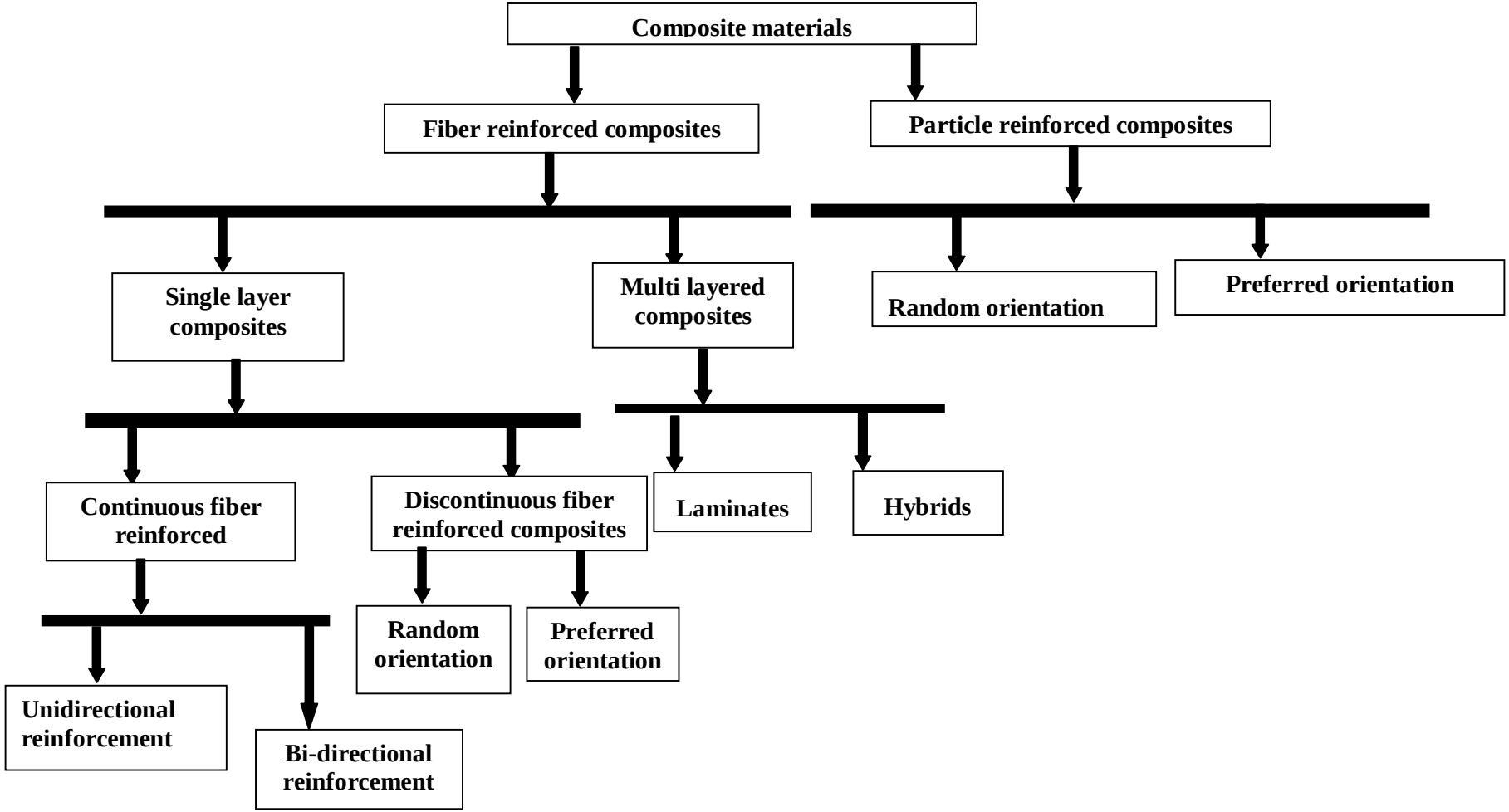

1.2.4.1 Particulate Composites

As the name itself indicates, the reinforcement is of particle nature (platelets are also included in this class). It may be spherical, cubic, tetragonal, a platelet, or of other regular or irregular shape, but it is approximately equiaxed. In general, particles are not very effective in improving fracture resistance but they enhance the stiffness of the composite to a limited extent. Particle fillers are widely used to improve the properties of matrix materials such as to modify the thermal and electrical conductivities, improve performance at elevated temperatures, reduce friction, increase wear and abrasion resistance, improve machinability, increase surface hardness and reduce shrinkage.

1.2.4.2 Fibrous composites

A fiber is characterized by its length being much greater compared to its cross-sectional dimensions. The dimensions of the reinforcement determine its capability of contributing its properties to the composite. Fibers are very effective in improving the fracture resistance of the matrix since a reinforcement having a long dimension discourages the growth of incipient cracks normal to the reinforcement that might other wise lead to failure, particularly with brittle matrices.

Man-made filaments or fibers of non polymeric materials exhibit much higher strength along their length since large flaws, which may be present in the bulk material, are minimized because of the small cross-sectional dimensions of the fiber. In the case of polymeric materials, orientation of the molecular structure is responsible for high strength and stiffness.

Fibers, because of their small cross- sectional dimensions, are not directly usable in engineering applications. They are, therefore, embedded in matrix materials to form fibrous composites. The matrix serves to bind the fibers together, transfer loads to the fibers, and protect them against environmental attack and damage due to handling. In discontinuous fiber reinforced composites, the load transfer function of the matrix is more critical than in continuous fiber composites.

1.3 COMPONENTS OF A COMPOSITE MATERIAL

In its most basic form a composite material is one, which is composed of at least two elements working together to produce material properties that are different to the properties of those elements on their own. In practice, most composites consist of a bulk material (the 'matrix'), and a reinforcement of some kind, added primarily to increase the strength and stiffness of the matrix.

1.3.1 Role of matrix in a composite

Many materials when they are in a fibrous form exhibit very good strength but to achieve these properties the fibers should be bonded by a suitable matrix. The matrix isolates the fibers from one another in order to prevent abrasion and formation of new surface flaws and acts as a bridge to hold the fibers in place. A good matrix should possess ability to deform easily under applied load, transfer the load onto the fibers and evenly distributive stress concentration.

A study of the nature of bonding forces in laminates [6] indicates that upon initial loading there is a tendency for the adhesive bond between the reinforcement and the matrix to be broken. The frictional forces between them account for the high strength properties of the laminates.

1.3.2 Materials used as matrices in composites

In its most basic form a composite material is one, which is composed of at least two elements working together to produce material properties that are different to the properties of those elements on their own. In practice, most composites consist of a bulk material (the matrix) and a reinforcement of some kind, added primarily to increase the strength and stiffness of the matrix.

1.3.2.1 Bulk-Phases

(a) Metal Matrices

Metal matrix composites possess some attractive properties, when compared with organic matrices. These include (i) strength retention at higher temperatures, (ii) higher transverse strength, (iii) better electrical conductivity, (iv) superior thermal conductivity, (v) higher erosion resistance etc. However, the major disadvantage of metal matrix composites is their higher densities and consequently lower specific mechanical properties compared to polymer matrix composites. Another notable difficulty is the high-energy requirement for fabrication of such composites.

In the aerospace industry interest has been concentrated primarily on fiber reinforced aluminium and titanium. Boron and to a lesser extent silicon carbide (SiC), have been investigated as the reinforcing fibers. Aluminium alloys reinforced with boron have been extensively produced by a variety of methods. Titanium reinforced with SiC, boron (coated with SiC) and even with beryllium, used for compressor blades.

Good elastic modulus properties can be achieved by the unidirectional incorporation of fibers or whiskers in the metal matrix even though the bonding between them may be poor. But, strong metallic matrices rather than weak metal or polymer matrices are essential for good transverse modulus and shear strength.

Carbon/graphite fibers have been used with metal matrices on a laboratory / experimental scale only, because most basic fabrication techniques involve high temperatures which have detrimental effects on the fiber. However, research on these lines is continuing in view of the potential of the composites.

(b) Polymer Matrices

A very large number of polymeric materials, both thermosetting and thermoplastic, are used as matrix materials for the composites. Some of the major advantages and limitations of resin matrices are shown in Table-1.2.

Table- 1.2 Advantages and limitations of polymer matrix materials

Advantages	Limitations
Low densities	Low transverse strength
Good corrosion resistance	Low operational temperature limits
Low thermal conductivities	
Low electrical conductivities	
Transluscence	
Aesthetic Colour effects	

Usually the resinous binders (polymer matrices) are selected on the basis of adhesive strength, fatigue resistance, heat resistance, chemical and moisture resistance etc. The resin must have mechanical strength commensurate with that of the reinforcement. It must be easy to use in the fabrication process selected and also stand up to the service conditions. Apart from these properties, the resin matrix must be capable of wetting and penetrating into the bundles of fibers which provide the reinforcement, replacing the dead air spaces therein and offering those physical characteristics capable of enhancing the performance of fibers.

Shear, chemical and electrical properties of a composite depend primarily on the resin. Again, it is the nature of the resin that will determine the usefulness of the laminates in the presence of a corroding environment.

Generally speaking, it can be assumed that in composites, even if the volume fraction of the fiber is high (of the order of 0.7), the reinforcement is completely covered by the matrix material; and when the composite is exposed to higher temperatures it is the matrix, which should withstand the hostile environment. Of course, the strength properties of the composite also show deterioration, which may be due to the influence of the temperature on the interfacial bond. Thus, the high temperature resistant properties of the composites are directly related more to the matrix, rather than to the reinforcement. The search for polymers which can withstand high temperatures has pushed the upper limit of

the service temperatures to about 300-350^{0}C. This range of operational temperatures can be withstood by polyimides, which are the state-of-the-art high temperature polymers for the present.

Table-1.3 and 1.4 indicate the approximate service temperature ranges for the resins and composites [7, 8]. It should be remembered that there is no place for compromise as to the nature of the matrix material, particularly when it comes to the application temperature of the composite. If the application temperature exceeds 300-350^{0}C metal matrix appears to be the only alternative, at least for the present.

(c) Ceramic Matrices

Ceramic fibres, such as alumina and SiC (Silicon Carbide) are advantageous in very high temperature applications, and also where environment attack is an issue. Since ceramics have poor properties in tension and shear, most applications as reinforcement are in the particulate form (e.g. zinc and calcium phosphate). Ceramic Matrix Composites (CMCs) used in very high temperature environments, these materials use a ceramic as the matrix and reinforce it with short fibres, or whiskers such as those made from silicon carbide and boron nitride.

Table- 1.3 Application temperatures of some matrix material

Matrix material	**Limit of**	
	Long term exposure, ^{0}C	**Short term exposure,^{0}C**
Unsaturated polyesters	70	100
Epoxies	125	200
Phenolics	250	1600
Polyimides	315	400
Aluminium	300	350

Table - 1.4 Trends for temperature application of heat resistant composites

Fiber reinforced Composite	Maximum service temperature, ^{0}C	Specific weight gm/cm3
Carbon / Epoxy	180	1.4
Boron/Epoxy	180	2.1
Borsic / Aluminium	310	2.8
Carbon/Polyimide	310	1.4
Boron/Polyimide	310	2.1
Carbon/Polyaminoxaline	350	1.4
Carbon/Polybenzthiazole	400	14
Borsic/Titanium	540	3.6
Carbon/Nickel	930	5.3
Whisker/Metals	1800	2.8-5.6

1.3.2.2 Reinforcement

The role of the reinforcement in a composite material is fundamentally one of increasing the mechanical properties of the neat resin system. All of the different fibres used in composites have different properties and so affect the properties of the composite in different ways. For most of the applications, the fibres need to be arranged into some form of sheet, known as a fabric, to make handling possible. Different ways for assembling fibers into sheets and the variety of fiber orientations possible to achieve different characteristics.

1.3.2.3 Interface

It has characteristics that are not depicted by any of the component in isolation. The interface is a bounding surface or zone where a discontinuity occurs, whether physical, mechanical, chemical etc. The matrix material must “wet” the fiber. Coupling agents are

frequently used to improve wettability. Well “wetted” fibers increase the interface surfaces area. To obtain desirable properties in a composite, the applied load should be effectively transferred from the matrix to the fibers via the interface. This means that the interface must be large and exhibit strong adhesion between fibers and matrix. Failure at the interface (called de-bonding) may or may not be desirable.

1.4 TYPES OF COMPOSITE MATERIALS

The composite materials are broadly classified into the following categories as shown in Figure-1.1 (a - e).

1.4.1 Fiber-reinforced composites

Reinforced-composites are popularly being used in many industrial applications because of their inherent high specific strength and stiffness. Due to their excellent structural performance, the composites are gaining potential also in tribological applications. Fiber reinforced composites materials consists of fiber of high strength and modulus in or bonded to a matrix with distinct interfaces (boundary) between them [4, 5]. In this form both fibers and matrix retain their physical and chemical identities. Yet they produce a combination of properties that cannot be achieved with either of the constituents acting alone. In general, fibers are the principal load carrying candidates, while the surrounding matrix keeps them in the desired location and orientation [5, 6]. A Fibrous composite can be classified into two broad groups: continuous (long) fiber composite and discontinuous (short) fiber composite.

1.4.1.1 Continuous or long fiber composite

Continuous or long fiber composite consists of a matrix reinforced by a dispersed phase in the form of continuous fibers. A continuous fiber is geometrically characterized as having a very high length-to- diameter ratio. They are generally stronger and stiffer than bulk material. Based on the manner in which fibers are packed within the matrix, it is again subdivided in to two categories: (a) unidirectional reinforcement and (b) bidirectional reinforcement. In unidirectional reinforcement, the fibers are oriented in one direction only

where as in bidirectional reinforcement the fibers are oriented in two directions either at right angle to one another (cross-ply), or at some desired angle (angle-ply). When fibers are large and continuous, they impart certain degree of anisotropy to the properties of the composites particularly when they are oriented. Multi-axially oriented continuous fiber composites are also display near isotropic properties.

1.4.1.2 Discontinuous or short fiber composite

Short-fiber reinforced composites consist of a matrix reinforced by a dispersed phase in form of discontinuous fibers (length < 100×diameter). The low cost, ease of fabricating complex parts, and isotropic nature are enough to make the short fiber composites the material of choice for large-scale production. Consequently, the short-fiber reinforced composites have successfully established its place in lightly loaded component manufacturing. Further the discontinuous fiber reinforced composite divided into: (a) biased or preferred oriented fiber composite and (b) random oriented fiber composite. In the former, the fibers are oriented in predetermined directions, whereas in the latter type, fibers remain randomly. The orientation of short fibers can be done by sprinkling of fiber on to given plane or addition of matrix in liquid or solid state before or after the fiber deposition.The discontinuities can produce a material response that is anisotropic, but the random reinforcement produces nearly isotropic properties.

1.4.2 Laminate Composites

Laminate Composites are composed of layers of materials held together by matrix. Generally, these layers are arranged alternatively for the better bonding between reinforcement and the matrix. These laminates can have uni- directional or bi-directional orientation of the fiber reinforcement according to the end use of the composite. The different types of composite laminates are unidirectional, angle-ply, cross-ply and symmetric laminates. A hybrid laminate can also be fabricated by the use of different constituent materials or of the same material with different reinforcing pattern. In most of the applications of laminate composites, man-made fibers are used due to their good combination of physico-mechanical and thermal behaviour.

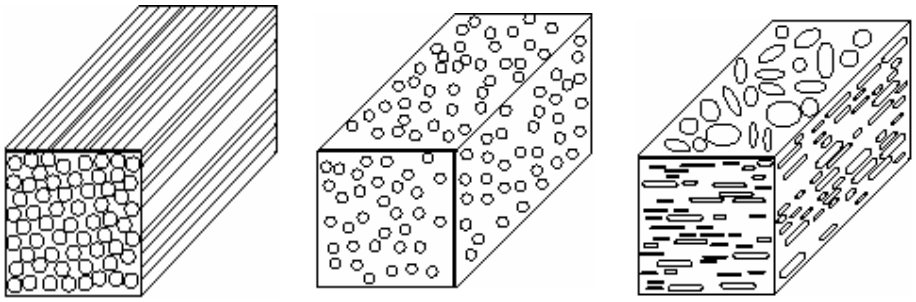

(a) Continuous fiber composite **(b) Particulate composites** **(c) Flake composites**

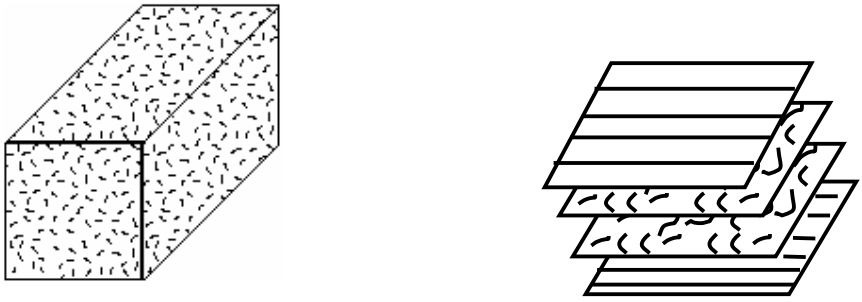

(d) Random fiber (short fiber) Composite **(e) Laminate Composite**

Figure-1.1 (a-e) Schematic diagram of different types of Composite

1.5 NATURAL FIBER COMPOSITES: Initiative in Product Development

Environmental awareness today motivates the researchers worldwide on the studies of natural fiber reinforced polymer composite and cost effective option to synthetic fiber reinforced composites. The availability of natural fibers and ease of manufacturing have tempted researchers to try locally available inexpensive fibers and to study their feasibility of reinforcement purposes and to what extent they satisfy the required specifications of good reinforced polymer composite for different applications. With low cost and high specific mechanical properties, natural fiber represents a good renewable and biodegradable alternative to the most common synthetic reinforcement, i.e. glass fiber.

The term “natural fiber” covers a broad range of vegetable, animal and mineral fibers. However in the composite industry, it is usually refers to wood fiber and agro based bast, leaf, seed, and stem fibers. These fibers often contribute greatly to the structural performance of plant and, when used in plastic composites, can provide significant reinforcement.

Despite the interest and environmental appeal of natural fibers, there use is limited to non-bearing applications due to their lower strength compared with synthetic fiber reinforced polymer composite. The stiffness and strength shortcomings of bio composites can be overcome by structural configurations and better arrangement in a sense of placing the fibers in specific locations for highest strength performance. Accordingly extensive studies on preparation and properties of polymer matrix composite (PMC) replacing the synthetic fiber with natural fiber like Jute, Sisal, Pineapple, Bamboo, Kenaf and Bagasse were carried out [9-14]. These plant fibers have many advantages over glass fiber or carbon fiber like renewable, environmental friendly, low cost, lightweight, high specific mechanical performance.

Increased technical innovation, identification of new applications, continuing political and environmental pressure and government investments in new methods for fiber harvesting and processing are leading to projections of continued growth in the use of natural fibers in composites, with expectation of reaching 100,000 tones per annum by 2010 [15]. The easy availability of natural fibers and manufacturing have motivated researchers world wide recently to try locally available inexpensive fibers and to study their feasibility of reinforcement purposes and to what extent they satisfy the required specifications of good reinforced polymer composite for tribological applications [16].

There are many potential natural resources, which India has in abundance. Most of it comes from the forest and agriculture. Lantana-Camara, locally called, as ‘Putus’ is one such natural resource whose potential as fiber reinforcement in polymer composite has not been explored to date.

Lantana-Camara has been known by at least five different polynomial descriptive names, including Lantana, Viburnum and Periclymenum [17]. Linnaeus first described and gave it its binomial name, Lantana-Camara, in 1753 [18]. The genus Lantana L. belongs to the Verbenaceae family and about 600 varieties now exist worldwide. In India about 7-8

species of Lantana are found. Some important species of Lantana (Figure-1.2) found in India are Lantana Camara, Lantana Indica, Lantana Trifolia, Lantana Canulata etc.

Lantana was introduced to India at the National Botanical Gardens, Calcutta in 1807 as an ornamental plant by the British and, since then, the plant has successfully invaded virtually all parts of the country. This weed is now posing serious problems in plantation forestry and has been considered recently as one of the ten worst weeds in the world. It chokes all other vegetation and becomes the dominant species. Hence various measures have been taken to eradicate this species like manual eradication, biological control, chemical methods, etc. But unfortunately efforts to manage the weed have not been successful. Alternatively, visualizing the luxuriant growth and vigorous survival of this weed, researchers world wide are trying to find out the potential economic value for its utilization into value added products and effective method for its management.

Different avenues of utilization of this weed is presently in India are going on at a very slow pace. Survey of literature on utilization of Lantana-Camara published so far reveals that its use is limited to development of furniture products, baskets, mulch, compost, drugs and other biologically active agents [19-21]. It has also been used for producing pulp for paper suitable for writing and printing and manufacturing rubber [22], but the economic viability of production has not been examined. The research and development work on utilization Lantana-Camara are under process in India, are presented in Table-1.5.

Table- 1.5 Effective use of Lantana-Camara in India

Organization	Use
Social Institute of Deliberate Human Immanence (SIDHI)	Cheap furniture, Utility articles, Mosquito repellent & a medicine, for various cures particularly for skin related diseases.
Ashoka Trust of Research in Ecology and the Environment (ATREE)	60 Nos. of products, from modest baskets to corporate office furniture

Growing through available information on the utilization of Lantana-Camara, it is seen that use of Lantana-Camara fiber as reinforcement for preparation of composite has not been explored till date.

The main objective of this work therefore is to prepare a Polymer Matrix Composite (PMC) using epoxy resin as matrix material and Lantana-Camara fiber as reinforcement. Out of the available manufacturing processes, we have adopted hand-lay-up technique to prepare the composite. Different volume fraction by weight of Lantana-Camara fiber has been mixed with matrix material and specimens were prepared for structural and tribological studies. In the process fiber properties like strength and density, critical fiber length and optimum volume fraction of fiber reinforcement have also been found out. For increasing bonding strength between fiber and matrix, fiber surface modification has also been carried out. Different tribological test have been conducted under simulated laboratory condition for specific application of developed composite. The surface of fracture and worn out samples have been studied using Scanning Electron Microscope (SEM) to have an idea about the fracture behaviour of the composite.

In the second chapter detailed discussion on reinforcement material, overview of fabrication processes and work related to present investigation available in literature are presented.

In the third chapter effect of environment on mechanical properties of both untreated and treated fiber reinforced composite along with moisture absorption characteristics have been presented.

In the fourth chapter abrasive wear behaviour of the composite has been studied.

Fifth chapter discusses the anisotropic wear behaviour of the composite.

In the sixth chapter solid particle erosion wear behaviour of the composite is presented.

Seventh chapter discusses the Response surface methodology (RSM) to predict the abrasive and erosive wear behaviour of the composite.

In the eighth chapter conclusions have been drawn from the above studies mentioning scope for the future work.

Fig. 1.2 (a)

Fig. 1.2 (b)

Figure-1.2 Photographs of Lantana-Camara plant

Chapter 2

LITERATURE SURVEY

Chapter-2

2.1 NATURAL FIBERS: Source and Classification

Growing environmental awareness has triggered the researchers world wide to develop and utilize materials that are compatible with the environment. In the process natural fibers have become suitable alternatives to traditional synthetic or manmade fibers and have the potential to be used in cheaper, more sustainable and more environmentally friendly composite materials. Natural organic fibers can be derived from either animal or plant sources. The majority of useful natural textile fibers are plant derived, with the exceptions of wool and silk. All plant fibers are composed of cellulose, whereas fibers of animal origin consist of proteins. Natural fibers in general can be classified based on their origin, and the plant-based fibers can be further categorized based on part of the plant they are recovered from. An overview of natural fibers is presented in Figure-2.1 [23].

Generally, plant or vegetable fibers are used to reinforce polymer matrices and a classification of vegetable fibers is given in Figure-2.2 [24]. Plant fibers are a renewable resource and have the ability to be recycled. The plant fibers leave little residue if they are burned for disposal, returning less carbon dioxide (CO_2) to the atmosphere than is removed during the plant's growth.

The leading driver for substituting natural fibers for glass is that they can be grown with lower cost than glass. The price of glass fiber is around Rs. 300.00/- per kg and has a density of 2.5 g/cc. On the other hand, natural fiber costs Rs. 15.00/- to 25.00/- per kg and has a density of 1.2-1.5 g/cc. As can be seen from Table-2.1 [23], the tensile strength of natural fibers is substantially lower than that of glass fibers though the modulus is of the same order of magnitude. However, when the specific modulus of natural fibers (modulus per unit specific gravity) is considered, the natural fibers show values that are comparable to or even better than glass fibers. Material cost savings, due to the use of natural fibers and high fiber filling levels, coupled with the advantage of being non-abrasive to the mixing and moulding equipment make natural fibers an exciting prospect. These benefits mean natural fibers could be used in many applications, including building, automotive, household appliances, and other applications.

Table-2.1 Properties of glass and natural fibers

Properties	Fiber						
	E-glass	Hemp	Flax	Jute	Sisal	Coir	Ramie
Density (gm/cc)	2.25	1.48	1.4	1.46	1.33	1.25	1.5
Tensile strength (MPa)	2400	550-900	800-1500	400-800	600-700	220	500
Young's Modulus (GPa)	73	70	60-80	10-30	38	6	44
Specific Modulus (GPa)	29	-	26-46	7-21	29	5	2
Failure Strain (%)	3	1.6	1.2-1.6	1.8	2-3	15-25	2
Moisture absorption(%)	-	8	7	12	11	10	12-17

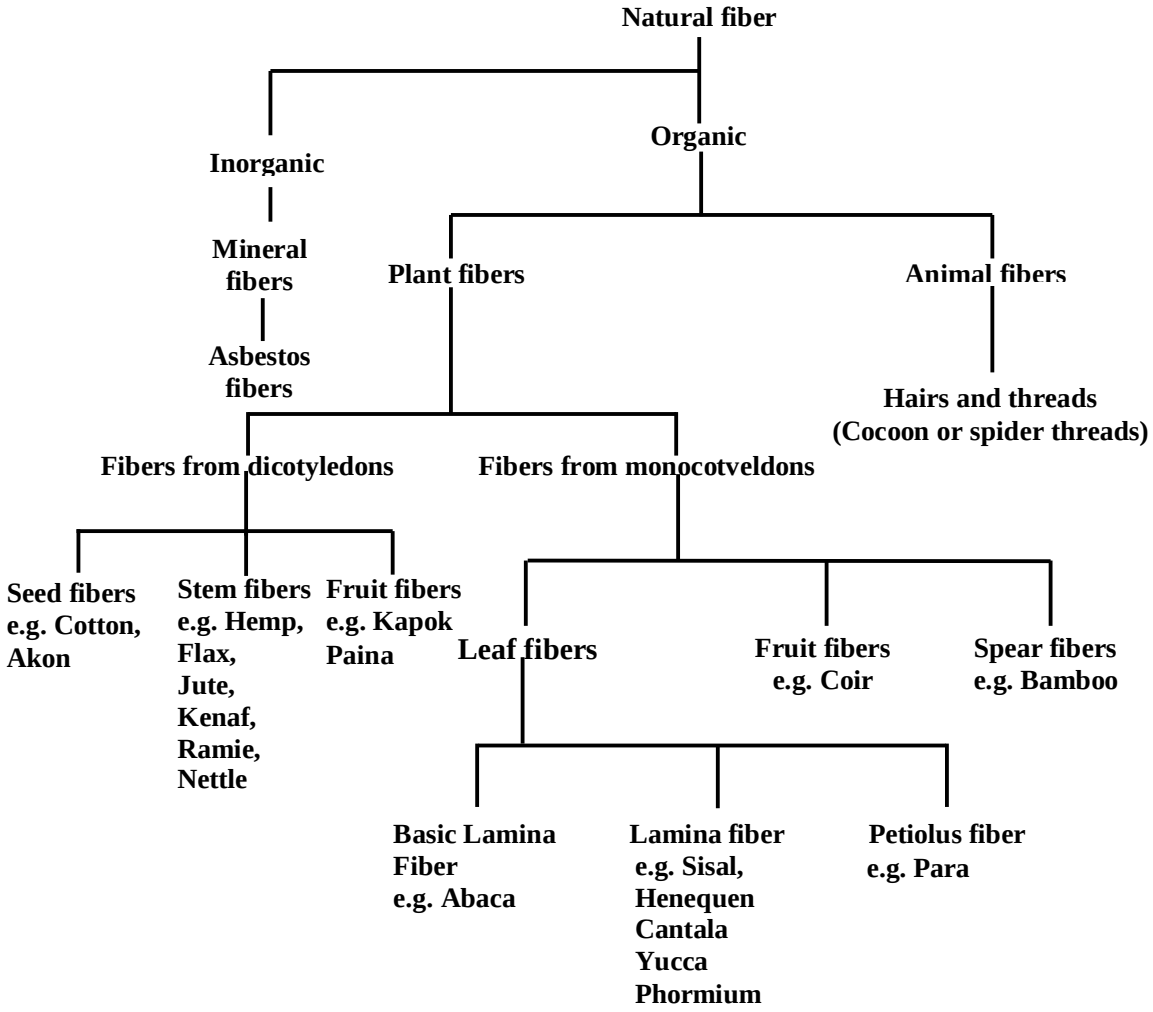

Figure-2.1 Overview of natural fibers

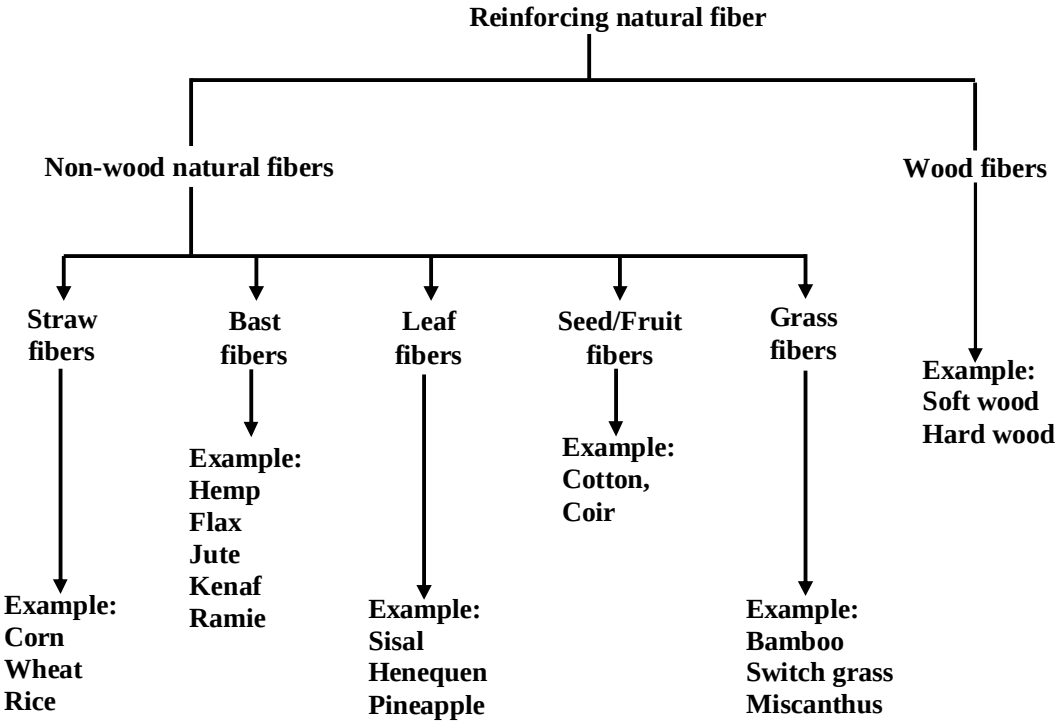

Figure-2.2 Classification of natural fiber that can be used as reinforcements in polymers

2.2 STRUCTURE OF PLANT FIBER

Natural plant fibers are constituents of cellulose fibers, consisting of helically wound cellulose micro fibrils, bound together by an amorphous lignin matrix. Lignin keeps the water in fibers; acts as a protection against biological attack and as a stiffener to give stem its resistance against gravity forces and wind. Hemicellulose found in the natural fibers is believed to be a compatibilizer between cellulose and lignin. The cell wall in a fiber (Figure-2.3) is not a homogenous membrane [25]. Each fiber has a complex, layered structure consisting of a thin primary wall which is the first layer deposited during cell growth encircling a secondary wall. The secondary wall is made up of three layers and the thick middle layer determines the mechanical properties of the fiber. The middle layer consists of a series of helically wound cellular micro-fibrils formed from long chain cellulose molecules. The angle between the fiber axis and the micro-fibrils is called the microfibrillar angle. The characteristic value of microfibrillar angle varies from one fiber to

another. These micro-fibrils have typically a diameter of about 10-30 nm and are made up of 30-100 cellulose molecules in extended chain conformation and provide mechanical strength to the fiber.

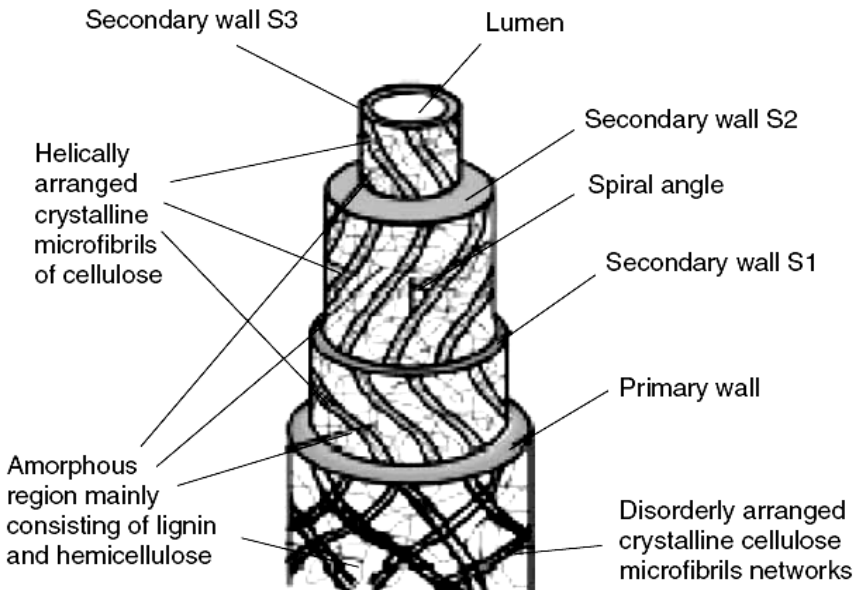

Figure-2.3 Structure of an elementary plant fiber (cell)

2.3 CHEMICAL COMPOSITION OF NATURAL FIBERS

The constituent of any natural fiber vary with origin, area of production, variety and maturation of plant. The major constituent of a fully developed natural fiber cell walls are cellulose, hemicellulose, lignin and pectin. These hydroxyl-containing polymers are distributed throughout the fiber wall [26].

2.3.1 Cellulose

The long thin crystalline micro-fibrils in the secondary cell wall are made of cellulose. It is the reinforcing material and is responsible for the high mechanical strength of fibers. It consists of a linear polymer of D-anhydroglucose units where two adjacent glucose units are linked together by β-1, 4-glycosidic linkages with elimination of one water

molecule between their -OH groups at carbon atoms 1 and 4. Chemically, cellulose is defined as a highly crystalline segment alternating with regions of non-crystalline or amorphous cellulose [27, 28].

The glucose monomers in cellulose form hydrogen bonds both within its own chain (intramolecular) forming fibrils and with neighboring chains (intermolecular), forming micro-fibrils. These hydrogen bonds lead to formation of a linear crystalline structure with high rigidity and strength. The amorphous cellulose regions have a lower frequency of intermolecular hydrogen bonding, thus exposing reactive intermolecular -OH groups to be bonded with water molecules. Amorphous cellulose can therefore be considered as hydrophilic in nature due to their tendency to bond with water. On the other hand, very few accessible intermolecular –OH are available in crystalline cellulose and it is far less hydrophilic than amorphous cellulose. Crystalline micro-fibrils have tightly packed cellulose chains within the fibrils, with accessible –OH groups present on the surface of the structure. Only very strong acids and alkalis can penetrate and modify the crystalline lattice of cellulose.

2.3.2 Hemicelluloses

Hemicelluloses differ from cellulose in three different ways. Firstly, unlike cellulose (containing only 1,4-β-D-glucopyranose units) they contain several different sugar units. Secondly, they exhibit a considerable degree of chain branching, whereas cellulose is a linear polymer. Thirdly, the degree of polymerization of native cellulose is ten to hundred times higher than that of hemicelluloses. Unlike cellulose, the constituents of hemicelluloses differ from plant to plant. Hemicelluloses contain substituents like acetyl (-COCH3) groups and glucoronic acid. By attaching ferulic acid and p-coumaric residues, hemicelluloses can form covalent bonds to lignin [29]. Due to this linking ability of hemicelluloses, degradation of it leads to disintegration of the fibers into cellulose micro-fibrils resulting in lower fiber bundle strength [30].

Mainly the acid residues attached to hemicelluloses make it highly hydrophilic and increase the fiber water uptake, which increases the risk of microbiological fiber degradation. It has been found that hemicelluloses thermally degrade more at lower temperatures (150-180°C) than cellulose (200-230°C) [31].

2.3.3 Lignin

Together with cellulose, lignin is the most abundant and important polymeric organic substance in the plant world. Lignin increases the compression strength of plant fibers by gluing the fibers together to form a stiff structure, making it possible for trees of 100 meters to remain upright. Lignin is essentially a disordered, polyaromatic, and cross-linked polymer arising from the free radical polymerizations of two or three monomers structurally related to phenyl-propane [32]. Free radical coupling of the lignin monomers gives rise to a very condensed, reticulated, and cross-linked structure. The lignin matrix is therefore analogous to a thermoset polymer in conventional polymer terminology. The dissolution of lignin using chemicals aids fiber separation. When exposed to ultraviolet light, lignin undergoes photochemical degradation [33]. The lignin seems to act like a matrix material within the fibers, making stress transfer on a micro-fibril scale and single fiber scale possible.

2.3.4 Pectin

Pectin is a complex branched structure of acidic structural polysaccharides, found in fruits and bast fibers. The majority of the structure consists of homopolymeric partially methylated poly-α-(1-4)-D-galacturonic acid residues, but there are substantial 'hairy' non-gelling areas of alternating α-(1-2)-L-rhamnosyl-α-(1-4)-Dgalacturonosyl sections containing branch-points with mostly neutral side chains (1-20 residues) of mainly L-arabinose and D-galactose (rhamnogalacturonan-I). Pectin is the most hydrophilic compound in plant fibres due to the carboxylic acid groups and is easily degraded by defibration with fungi [27]. Pectin along with lignin and hemicelluloses present in natural fibres can be hydrolysed at elevated temperatures.

2.4 MATRIX MATERIAL

Many materials when they are in fibrous form exhibit very good strength properties but to achieve these properties the fiber should be bonded by a suitable matrix. The matrix isolates the fibers from one another in order to prevent abrasion and formation of new surface flaws and acts as a bridge to hold the fibers in place. A good matrix should possess

ability to deform easily under applied load, transfer the load on to the fibers and evenly distribute stress concentration.

A study of the nature of bonding forces in laminates [34] indicates that upon initial loading there is a tendency for the adhesive bond between them to account for the high strength properties of the of the laminates.

The polymer matrix binds the fibers together so as to transfer the load to and between them and protect them from environments and handling. Polymer or resin systems used to manufacture advanced Polymer Matrix Composites (PMCs) are of two basic types, thermosets and thermoplastics (including bio-derived ones).

2.4.1 Thermosets

Much of the early work used thermosetting resins as matrix material for composite production. Products like tufnol which is made from cotton fibres and epoxy resin, have been available for some time, having good stiffness and strength [35]. In the last few years there has been renewed interest in these products for use in automotive applications [36]. To achieve reinforcing effects in composites it is necessary to have good adhesion between the fibres and resins. Epoxy and phenolic thermosetting resins are known to be able to form covalent cross-links with plant cell walls via -OH groups [37]. Composite manufacture can be achieved using low viscosity epoxy and phenolic resins that cure at room temperature. In addition epoxy resin does not produce volatile products during curing which is most desirable in production of void free composites. Therefore, although epoxy resins are relatively more expensive than polyester, they have potential for the development of high added value plant fiber composites, where long fibres at a high content are required.

The functional group in epoxy resins is called the oxirane, a three-membered strained ring containing oxygen. Epoxy resins, depending on their backbone structure, may be low or high viscosity liquids or solids. In low viscosity resin, it is possible to achieve a good wetting of fibres by the resin without using high temperature or pressure. The impregnation of fibres with high viscosity resins is done by using high temperature and pressure.

A wide range of starting materials can be used for the preparation of epoxy resins thereby providing a variety of resins with controllable high performance characteristics. These resins generally are prepared by reacting to a polyfunctional amine or phenol with epichlorohydrin in the presence of a strong base. The commercially available diglycidyl ether of bisphenol-A (DGEBA), Figure-2.4, is characterized by epoxy equivalent weight, which can be determined either by titration or quantitative infrared spectroscopy. The presence of glycidyl units in these resins enhances the processability but reduces thermal resistance.

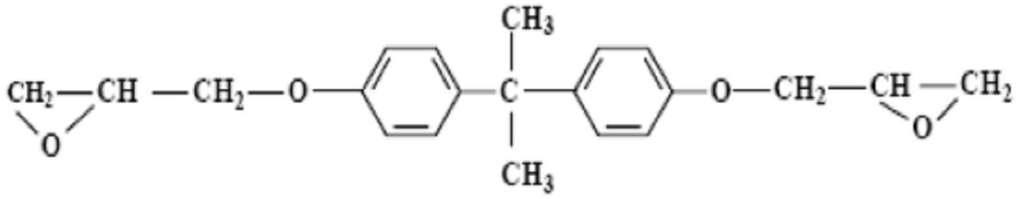

Figure-2.4 Chemical structure of DGEBA

The most widely used curing agents for epoxy resins are primary and secondary amines. The overall reaction rate of an amine with an epoxide is influenced by the steric hindrance and the electron withdrawing or electron donating groups present in the amine [38].

During curing, epoxy resins can undergo three basic reactions:

1. Epoxy groups are rearranged and form direct linkages between themselves.
2. Aromatic and aliphatic -OHs link up to the epoxy groups.
3. Cross-linking takes place with the curing agent through various radical groups.

The advantages of epoxy resins are low polymerisation shrinkages unlike polyesters during cure, good mechanical strength, excellent resistance to chemicals and solvents, and excellent adhesion to fibres. The epoxy molecule also contains two ring groups at its centre, which are able to absorb both mechanical and thermal stresses better than linear groups, giving epoxy resin very good stiffness, toughness and heat resistance.

The primary disadvantages of the epoxy resins are that they require long curing times and, in general, their mould release characteristics are poor. The epoxy resins are characterized by their high adhesive strengths. This property is attributed to the polarity of aliphatic -OH groups and ether groups that exist in both the initial resin and cured system. The polarity associated with these groups promotes electromagnetic bonding forces between epoxy molecules and the polar fibres.

2.4.2 Bio-derived Thermoplastic Matrices

Cellulose fibres (e.g. hemp, flax, jute) are widely used with conventional thermoplastic polymers (e.g. PP, PE) as reinforcement in composite production to improve mechanical properties. In fact, the history of composites from renewable resources is far longer than conventional polymers. The study and utilization of natural polymers is an ancient science. Typical examples, such as paper, silk, skin, and bone arts, can easily be found in museums around the world. In the biblical Book of Exodus, Moses's mother built the ark from rushes, pitch and slime- a kind of fiber reinforced composite, according to the current classification of material. During the opium war more than 1000 years ago, the Chinese built their castles to defend against invaders using a kind of mineral particle reinforced composite made from gluten rice, sugar, calcium carbonate and sand [39].

However, the availability of petroleum at a lower cost and the bio-chemical inertness of petroleum based products have proven disastrous for the market of natural polymers. It is only about last two decades when the significance of eco-friendly materials has been realized. Now polymers from renewable resources have started drawing an increasing amount of attention. The two main reasons for that are environmental concerns [40], and the realization that the petroleum resources are limited.

Generally, polymers from renewable resources can be classified into three groups: (1) natural polymers such as starch, protein, and cellulose (2) synthetic polymers from natural monomers, such as PLA and (3) polymers from microbial fermentation, such as polyhydroxy butyrate (PHB). Like numerous other petroleum based polymers, many properties of polymers from renewable resources can be improved through composite production [39].

The development of synthetic polymers like PLA using monomers from natural resources has been a driving force for the development of biodegradable polymers from renewable resources. Therefore, in today's world PLA is the most promising among bio-derivable polymers [39]. PLA can be processed (e.g. compression moulding, pultrusion, extrusion and injection moulding) like petroleum based polyolefins and its mechanical property is better than the widely used polymer PP [41]. On degradation PL does not emit any carbon dioxide to the environment like other biodegradable materials from renewable resources. The degradation occurs by hydrolysis to lactic acid, which is metabolized by micro-organisms to water and carbon dioxide. If PLA is comprised together with other biomass, the biodegradation occurs within a couple of weeks and the material can fully disappear within a month [42]. Chemically, it is linear aliphatic polyester of lactic acid which can be obtained by fermentation of renewable agricultural materials like corn, sugarcane and sugar beets. Lactic acid is converted to a cyclic lactide dimer which is then polymerized to PLA through a ring opening reaction.

The major applications of PLA products are in household wastes as plastic bags, barriers for sanitary products and diapers, planting, and disposable cups and plates. However, a number of authors reported the possibilities of developing fully bio-degradable composite products by using biodegradable polymers as matrix and natural fibres as reinforcements [43, 44]. Keller et al. [45] reported that PLA should produce fiber reinforced composites with high mechanical properties for light weight construction materials. Oksman et al. [41] observed that PLA had good potential as a polymer matrix in flax fiber reinforcement for composites production. They reported that the composite strength produced with PLA/flax was about 50% better than that of PP/flax composites. Due to the increasing commercial interest for natural fiber reinforced polymer composites for use in automotive applications and building constructions as well as demands for environmentally friendly materials, the development of fully biodegradable composites for many applications could be an interesting area of research.

2.5 NATURAL FIBER REINFORCED POLYMER COMPOSITES

Natural fiber reinforced polymer composites are hybrid with their properties, with characteristics of both natural fibres and polymers. In the beginning of the 20th century

wood- or cotton fiber reinforced phenol- or melamine formaldehyde resins were fabricated and used in electrical applications for their non-conductive and heat-resistant properties. Incorporation of natural fibers in to polymer is now a standard technology to improve the mechanical properties of polymer. Mechanical properties like tensile strength and young's modulus are enhanced in the end products (composites) as the fibres in the composites determine the tensile strength and young's modulus of the materials [46].

One of the largest areas of recent growth in natural fiber plastic composites in world-wide is the automotive industry, where natural fibers are advantageously used as a result of their low density and increasing environmental pressures. Natural fibers composites found application where load bearing capacity and dimensional stability under moist and high thermal conditions are of second order importance. For example, flax fiber reinforced polyolefins are extensively used today in the automotive industry, but the fiber acts mainly as filler material in non-structural interior panels [47]. Natural fiber composites used for structural purposes do exist, but then usually with synthetic thermo-set matrices which of course limit the environmental benefits [48, 49].

Plant fibers, such as hemp, flax and wood, have large potential as reinforcement in structural materials due to the high aspect ratio and high specific strength- and stiffness of the fibers [50-53]. Apart from good specific mechanical properties and positive environmental impact, other benefits from using natural fibers worth mentioning are low cost, friendly processing, low tool wear, no skin irritation and good thermal and acoustic insulating properties [53].

A complete biodegradable system may be obtained if the matrix material also comes from a renewable resource. Examples of such materials are lignophenolics, starch and polylactic acid (PLA). Some of these systems show encouraging results. For example Oksman et al. [41] have reported that flax fiber composites with PLA matrix can compete with and even outperform flax/polypropylene composites in terms of mechanical properties. In a recent study [54] it was found that composites of poly-L-lactide acid (PLLA) reinforced by flax fibers can show specific tensile modulus equivalent to that of glass/polyester short fiber composites. The specific strength of flax/PLLA composites was lower than that of glass/polyester, but higher than that of flax/polyester.

The limited use of natural fiber composites is also connected with some other major disadvantages still associated with these materials. The fibers generally show low ability to adhere to common non-polar matrix materials for efficient stress transfer. Furthermore, the fibers inherent hydrophilic nature makes them susceptible to water uptake in moist conditions. Natural fiber composites tend to swell considerably with water uptake and as a consequence mechanical properties, such as stiffness and strength, are negatively influenced. However, the natural fiber is not inert. The fiber-matrix adhesion may be improved and the fiber swelling reduced by means of chemical, enzymatic or mechanical modifications [51].

There are many application of natural fiber composite in every day life. For example, jute is a common reinforcement for composites in India. Jute fibers with polyester resins are used in buildings, elevators, pipes, and panels [55]. Natural fiber composites can also be very cost effective material for application in building and construction areas (e.g. walls, ceiling, partition, window and door frames), storage devices (e.g. bio-gas container, post boxes, etc.), furniture (e.g. chair, table, tools, etc.), electronic devices (outer casting of mobile phones), automobile and railway coach interior parts (inner fenders and bumpers), toys and other miscellaneous applications (helmets, suitcases).

During the last few years, a series of works have been done to replace the conventional synthetic fiber with natural fiber composites [56–63]. For instant, hemp, sisal, jute, cotton, flax and broom are the most commonly fibers used to reinforce polymers like polyolefins [63, 64], polystyrene [65], and epoxy resins [37]. In addition, fibers like sisal, jute, coir, oil palm, bamboo, bagasse, wheat and flax straw, waste silk and banana [58, 59, 64–73] have proved to be good and effective reinforcement in the thermoset and thermoplastic matrices. Nevertheless, certain aspects of natural fiber reinforced composite behaviour still poorly understood such as their visco-elastic, visco-plastic or time-dependent behaviour due to creep and fatigue loadings [74], interfacial adhesion [75, 76], and tribological properties. Little information concerning the tribological performance of natural fiber reinforced composite material [69–71, 77] has been available in the literatures. In this context, long plant fibers, like hemp, flax [75, 76], bagasse [16] and bamboo [70, 71] have considerable potential in the manufacture of composite materials for tribo applications. Likewise, Lantana-Camara fibers may also have considerable potential as reinforcement for

polymer and may provide advantages when used as a substitute for conventional synthetic glass fiber.

After reviewing the exiting literature available on the natural fiber composite efforts are put to understand the basic needs of the growing composite industry. The conclusions drawn from this is that, the success of combining vegetable natural fibers with polymer matrices results in the improvement of mechanical properties of the composite compared with the matrix material. These fillers are cheap and non toxic can be obtain from renewable source and are easily recyclable. Moreover despite of their low strength, they can lead to composites with high specific strength because of their low density.

Thus priority of this work is to prepare polymer matrix composites (PMCs) using Lantana-Camara fiber as reinforcement material. To improve the interfacial strength between the fiber and the matrix, the surface modification of the fiber has to be done by chemical treatment. The composite will then be subjected to different weathering condition like steam, saline and subzero condition. The fiber characterization will be done by Fourier Transform Infrared (FTIR) spectroscopy and X-Ray Diffraction (XRD) before and after the treatment of the fibers. The mechanical properties of the composite will be evaluated along with moisture absorption characteristics.

The potential of Lantana-Camara fiber for tribological application has to be investigated through performing different tribological tests like abrasive wear test, two-body abrasion test and solid particle erosion test as per ASTM standards.

Chapter 3

MECHANICAL CHARACTERIZATION OF LANTANA-CAMARA FIBER EPOXY COMPOSITE

CHAPTER – 3

3.1 INTRODUCTION

In general natural fibers are hygroscopic in nature and they absorb or release moisture depending on environmental conditions. Amorphous cellulose and hemicellulose that are present in the natural fiber are mostly responsible for the high moisture absorption, since they contain numerous easily accessible hydroxyl groups which give a high level of hydrophilic character to fiber. The high moisture absorption of the fiber occurs due to hydrogen bonding of water molecules to the hydroxyl groups within the fiber cell wall. This leads to a moisture build-up in the fiber cell wall (fiber swelling) and also in the fiber-matrix interface. This in turn becomes responsible for changes in the dimensions of cellulose-based composites, particularly in the thickness and the linear expansion due to reversible and irreversible swelling of the composites [78]. Another problem associated with fiber swelling is a reduction in the adhesion between the fiber and the matrix, leading to deterioration in the mechanical properties of the composite [79]. A good fiber-matrix bonding can decrease the rate and amount of moisture absorbed by the composite as well as improving the mechanical properties [80]. However in order to overcome this problem, chemical treatment has been considered as a good technique to reduce the hydroxyl group in the fibers. Different chemical treatments such as mercerization or alkali treatment, isocyanate treatment, acrylation, benzoylation, permanganate treatment, acetone treatment, acetylation, silane treatment etc. are reported by several researchers [63, 81-83].

The moisture absorption by composites containing natural fibers has several adverse effects on their properties and thus affects their long-term performance. In view of the severity of moisture absorption and its effects on composite properties, a numerous efforts have already been made by several researchers to address this issue.

George et al. [84] investigated the relationship between the moisture absorption of pineapple-leaf fiber reinforced low density polyethylene (LDPE) composites with different fiber loadings. They found that the moisture absorption increased almost linearly with the fiber loading.

Joseph et al. [85] studied the environmental effects on sisal fiber reinforced PP composites. Water uptake of the composite was found to increase with fiber content and leveled off at longer periods. The chemically modified fiber composites showed a reduction in water uptake because of better interfacial bonding. Water uptake of the composite was found to increase with temperature since temperature activates the diffusion process. Reduction in tensile properties was observed due to the plasticization effect of water. The fiber/matrix bonding becomes weak with increasing moisture content, resulting in interfacial failure.

Stark [86] found that wood flour-polypropylene (PP) composites with 20 wt% wood flour reached equilibrium after 1500 h in a water bath and absorbed only 1.4% moisture while composites with 40 wt% loading reached equilibrium after 1200 h water submersion and absorbed approximately 9.0% moisture. After the analysis, she concluded that the wood flour is inhibited from absorbing moisture due to encapsulation of the wood flour by the PP matrix and that the degree of encapsulation is greater for the 20% wood flour composite than that for the 40% wood flour composite.

Yuan et al. [87] studied the plasma treatment of sisal fibers and its effects on tensile strength and interfacial bonding. They suggested that the interfacial adhesion between the fiber and matrix could be enhanced by cleaned and chemically modified fiber surface. The strong intermolecular fiber-matrix bonding decreases the rate of moisture absorption in bio-composite.

Stamboulis et al. [88] reported that the moisture absorption and swelling of the treated flax fiber polypropylene composites is approximately 30% lower than that of composites based on untreated flax fibers.

Thomas et al. [89], while studying water absorption characteristics of sisal fiber polyester composites found that diffusion coefficient decreases with chemical treatment of fiber. In addition to this the chemical treatment also decreases water absorption capacity of the composite. They also showed that the composite with benzoyl-chloride treated sisal fiber composite exhibited lower water absorption capacity.

For potential application of natural fiber polymer composites a comprehensive study on the moisture absorption characteristic and its effect on mechanical properties are required. In this chapter, the characteristics of moisture sorption kinetics, thickness swelling and effect of moisture absorption on mechanical properties of both untreated and chemically treated Lantana-Camara fiber epoxy composite under different environments (Steam, Saline water and Sub-zero temperature) are investigated.

3.2 CHEMICAL MODIFICATION OF FIBER

Processing of plastic composites using natural fibers as reinforcement has increased dramatically in recent years [41, 63, 90, 91]. A better understanding of the chemical composition and surface adhesive bonding of natural fiber is necessary for developing natural fiber reinforced composites. The interfacial bonding between the reinforcing fibers and the resin matrix is an important element for improving the mechanical properties of the composites. Realizing this, several authors [92-95] have focused their studies on the treatment of fibers to improve the bonding with resin matrix. The mechanical properties of the composites are controlled by the properties and quantities of the individual component and by the character of the interfacial region between matrix and reinforcement. Lack of good interfacial adhesion makes the use of cellular fiber composites less attractive. Often the interfacial properties between the fiber and polymer matrix is low, because of hydrophilic nature of natural fiber which reduces its potential of being used as reinforcing agents. Hence chemical modifications are considered to optimize the interface of fibers. Chemicals may activate hydroxyl groups or introduce new moieties that can effectively interlock with the matrix. There are various chemical treatments available for the fiber surface modification. Chemical treatment including alkali, silane, acetylation, benzoylation, acrylation, isocynates, maleated coupling agents, permanganate treatment are discussed in details in [96].

The chemical treatment of fiber aimed at improving the adhesion between the fiber surface and the polymer matrix by modifying the fiber surface and the fiber strength. It also reduces the water absorption capacity of the fiber and helps in improving the mechanical properties. Out of the available treatments, for the present case to have a good bonding between the fiber and the resin matrix Lantana-Camara fiber have been treated with alkali,

acetone & benzoylation. The subsequent section will elaborate separately the treatment of the fiber surface by these methods, results of fiber modification through XRD, FTIR and SEM, study of mechanical properties of both untreated and treated fiber reinforced polymer composite and environmental effects on mechanical performance of the composite along with moisture absorption characteristics.

3.2.1 Methods of Chemical Modifications

3.2.1.1 Alkaline Treatment

Alkaline treatment or mercerization is one of the most used chemical treatments of natural fibers when used to reinforce thermoplastics and thermosets. The important modification done by alkaline treatment is the disruption of hydrogen bonding in the network structure, thereby increasing surface roughness. This treatment removes a certain amount of lignin, wax and oils covering the external surface of the fiber cell wall, depolymerizes cellulose and exposes the short length crystallites [97]. Addition of aqueous sodium hydroxide (NaOH) to natural fiber promotes the ionization of the hydroxyl group to the alkoxide [98].

$$\textbf{Fiber} - \textbf{OH} + \textbf{NaOH} \rightarrow \textbf{Fiber} - \textbf{O} - \textbf{Na} + \textbf{H}_2\textbf{O}$$

Thus, alkaline processing directly influences the cellulosic fibril, the degree of polymerization and the extraction of lignin and hemicellulosic compounds [99]. It is reported that alkaline treatment has two effects on the fiber:

1) It increases surface roughness resulting in better mechanical interlocking, and
2) It increases the amount of cellulose exposed on the fiber surface, thus increasing the number of possible reaction sites [63].

Consequently, alkaline treatment has a lasting effect on the mechanical behaviour of flax fiber, especially on fiber strength and stiffness.

For alkali treatment, the Lantana-Camara fibers were soaked in a 5% NaOH solution at room temperature maintaining a liquor ratio of 15:1. The fibers were kept immersed in the alkali solution for 4hrs. The fibers were then washed several times with fresh water to

remove any NaOH sticking to the fiber surface, neutralized with dilute acetic acid and finally washed again with distilled water. A final pH of 7 was maintained. The fibers were then dried at room temperature for 48 hrs followed by oven drying at 100°C for 6hrs. The alkali reaction between Lantana-Camara fiber and NaOH is as follows:

$$\mathbf{(Lantana-Camara)-OH+NaOH \Leftrightarrow (Lantana-Camara)-O^{-}Na^{+}+H_2O}$$

3.2.1.2 Acetone Treatment

When the fiber is treated with acetone, the lignin, cellulolignin and other such material get dissolved in acetone. As acetone is a non-polar organic solvent it usually dissolves the non-polar organic component.

The Lantana-Camara fibers were washed in soxhlet extractor (Figure-3.1) with acetone for approximately 1-1.5hrs. The acetone was evaporated (boiled at 63^0C) and condensed back into the volume with the fibers. This process was repeated four times for each batch. The used acetone was discarded before the new batch was cleaned in the same manner. The acetone changed from transparent to light green after treatment due to the presence of waxes and organic materials after the extraction. All the fibers were washed with pressurized water at a temperature of 90^0C for 70 minutes before acetone treatment. The fibers were then dried at room temperature for 24 hrs.

3.2.1.3 Benzoylation Treatment

Benzoylation is an important transformation in organic synthesis [100]. Benzoyl chloride is most often used in fiber treatment. Benzoyl chloride includes benzoyl (C6H5C=O) which is attributed to the decreased hydrophilic nature of the treated fiber and improved interaction with the hydrophobic polymer matrix. The reaction between the cellulosic hydroxyl group of the fiber and benzoyl chloride is given as follows:

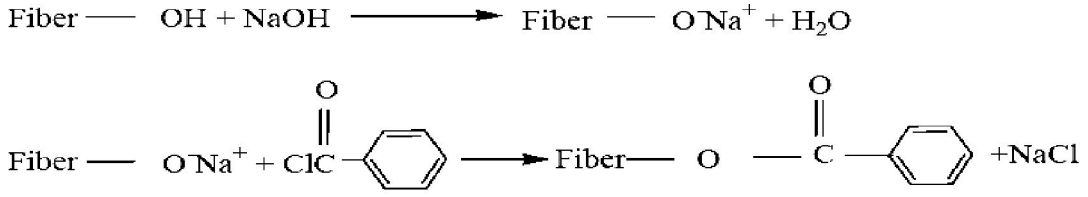

Benzoylation of fiber improves fiber matrix adhesion, thereby considerably increasing the strength of composite, decreasing its water absorption and improving its thermal stability [65, 101, 102].

The pre-treated Lantana-Camara fibers were suspended in 10% NaOH solution and agitated with benzoyl chloride. The mixture was kept for 15 min, filtered, washed thoroughly with water and dried between filter papers. The isolated fibers were then soaked in ethanol for 1 h to remove the benzoyl chloride and finally was washed with water and dried in the oven at 80^0 C for 24 h.

3.2.2 SEM Micrographs of Treated Fibers

The morphology of the untreated and treated fiber surfaces has been studied using scanning electron microscope (SEM) JEOL JSM-6480LV. The sample surfaces were gold coated to make them conductive prior to SEM observation. SEM micrographs of the untreated and treated Lantana-Camara fibers are shown in Figures-3.2. It is well established that the cellulose chains of natural fiber are strongly bound by chemical constituents, lignin, and hemicellulose, resulting in the formation of multi-cellular fiber [103]. The surface of untreated fiber appeared rough due to the presence of lignin, wax, oil, and surface impurities [Figure-3.2(a)], which are partially removed with acetone [Figure-3.2(b)] and further removed with alkali and benzoyl-chloride treatments [Figure-3.2(c) & (d)]. These clean surfaces are expected to provide direct bonding between the fiber cellulose and a matrix such as epoxy resin. By comparing treated fibers with the untreated fibers, it can be seen that the alkali and benzoyl-chloride treatments resulted in separation of the microfibrillar structure (fibrillation) and reduction in thickness of fiber because of the removal of cemented materials (i.e. lignin and hemicellulose) [104, 105]. Moreover these two treatments increase the effective surface area by fibrillation which promotes the mechanical interlocking between the fiber and the matrix. Where as the acetone treatment does not affects the fiber surface very much.

3.2.3 FTIR Spectroscopy

The effect of chemical modifications on the fiber surface was observed by using FTIR spectroscopy. FTIR measurement was performed using an IR-Prestige-21

spectrometer. A total of 100 scans were taken from 400-4000 cm^{-1} with a resolution of 2 cm^{-1} for each sample. The comparison of the representative FTIR spectra of untreated Lantana-Camara before and after chemical treatment (acetone, alkali and benzoyl-chloride treatment) is shown in Figure-3.3. In comparison to the unmodified Lantana-Camara fiber, the alkali treated, acetone treated and benzoylated Lantana-Camara showed a reduction in O-H stretching intensity and shifting of the peak from 3308.5 cm^{-1} to 3384.2, 3334.7, and 3364.2 cm^{-1} respectively, indicating participation of some free hydroxyl groups in these chemical reactions. The point of reaction was probably at the lignin –OH and C_2-OH of the glucopyranose unit in the cellulose component. A strong and sharp band at 1725.3 cm^{-1} is observed due to C=O stretching of carbonyl groups (>C=O) in hemicellulose components for untreated fiber, which disappeared in alkali treated fiber. Alkali treatment of Lantana-Camara destroys the C=O unit of the uronic acid residue in hemicellulose, perhaps arising from the intermolecular addition of the alcoholate ($-CH2-O^-Na^+$) from cellulose and lignin components to the C=O group. The C=O stretching band at 1763.2 cm^{-1} in benzoylated fiber shifts to 1752.7 cm^{-1} in acetone treated fiber. The benzoylation of Lantana-Camara fiber introduces the new absorption peaks at about 1763.2 cm^{-1} owing to the presence of phenyl nucleus [106]. This band in benzoylated fiber is more intense, indicating a combined effect of -O-CO-Ph and $–O-CO-CH_3$ groups arising from benzoylation. The acetone extracted Lantana-Camara fiber spectrum is similar to that of the untreated hemp, although a light green extract was observed during Soxhlet extraction. The band of medium intensity at 831.9 cm^{-1} due to b-glycosidic linkage in the unmodified Lantana-Camara fiber underwent shifting to a lower wave number, except alkali treated fiber accompanied by an increase in the intensity. This relates to the rotation of glucose residue around the glycosidic bond [107] and indicates a slow transition from unmodified to chemically modified Lantana-Camara.

3.2.4 X-ray Diffraction

X-ray diffraction is a useful method for evaluating the crystallographic structure of semi-crystalline materials such as Lantana-Camara fiber. A Philips X-ray diffractometer, employing CuKα ($\lambda = 1.54$) radiation and a graphite monochromator with a current of 40 mA and a voltage of 40 mV was used with a diffraction intensity in the range of 5 to 45^0 (2θ-angle range). The X-ray diffractograms of untreated, alkali treated, acetone treated and benzoyl-chloride treated Lantana-Camara fiber can be seen in Figure-3.4. It is observe that

the major crystalline peak of each profile occurred at around $2\theta=23.7^0$, which represents the cellulose crystallographic plane (002). The X-ray diffractograms show that the intensity of the (002) crystallographic plane was increased significantly as a result of fiber treatments.

The fiber crystallinity index (I_c) of the treated and untreated samples were calculated by using equation:

$$I_c = \left(\frac{I_{002} - I_{am}}{I_{002}} \right) \tag{3.1}$$

where '$I_{00'2}$' is the maximum intensity of diffraction of the (002) lattice peak at a 2θ angle of between 22^0 and 23^0, and 'I_{am}' is the intensity of diffraction of the amorphous material, which is taken at a 2θ angle between 14.5^0 and 16^0 where the intensity is at a minimum [108]. The results are summarized in Table-3.1. It is seen that, the crystallinity index of LC fiber was increased by chemical treatment. As previously mentioned, this is thought to be due to better packing and stress relaxation of cellulose chains as a result of the removal of pectins and other amorphous constituents from the fiber. It can also be seen that fiber treated with benzoyl-chloride has a slightly higher crystallinity index compared to fiber treated with alkali and acetone.

3.3 SINGLE FIBER PULL-OUT TEST

To find out the critical fiber length of Lantana-Camara to be used for preparation of composite, single fiber pull-out test was carried out. Figure-3.5(a) shows the schematic diagram of the sample to be used for test. Single fibers were taken and partially embedded in the mixture of epoxy resin and hardener (ratio 10:1) inside a per-pex sheet mould to prepare the samples. The embedded lengths and diameter of the fiber were measured by electron microscope. The embedded lengths were found to be 1.25 to 15.14mm with fiber free length of 30 mm. The cast samples were shown in Figure-3.5(b). After curing, the specimens were taken out from the mould. Pull-out test was then conducted on an Instron-4204 tensile testing machine at crosshead speed of 1 mm/min and using 5KN-load cell. Five specimens were prepared for each embedded length and average value was taken.

The experiment was conducted as per Tanaka et al. [109] and Valadez et al. [63]. Table-3.2 shows the pull-out load for different embedded fiber length achieved through single fiber pull-out test. The average maximum load at failure (P_{break}) in fiber tensile testing was found to be 8.803 kg. A regression analysis has been done [Figure-3.6] between fiber embedded length and fiber pullout load to find out the effective fiber embedded length for rupture. This was found to be approximately 9.11 mm. Thus for composite preparation we have to consider higher value than 9.11mm. In the present work fiber length of 10mm has been taken for preparation of composite.

3.4 COMPOSITE FABRICATION

For preparation of composite the following materials have been used;

1. Lantana-Camara fiber
2. Epoxy
3. Hardener

3.4.1 Preparation of Lantana-Camara Fiber

Fresh Lantana-Camara stems were collected locally. They were cut to sizes between two nodes. The upper skin was removed by scrapping without damaging the fiber surface. Then they were cut to sizes of 100mm lengthwise. Long fibers were washed with pressurized water to remove unwanted organic materials present on the surface. These fibers were then spread over a water proof sheet and stored in an enclosed shed to reduce the moisture content. After two weeks the long fibers were cut to lengths of 10mm (optimum fiber length found from single fiber pull-out test) and of width 1mm with a pair of scissor. Due to low moisture content of the fibers, no fungus grew during storage. The Lantana-Camara fibers after cutting were again washed with pressurized water to remove the fine particle and other organic material that grew and adhered to the surface of fiber during storage and cutting. The fibers were then dried with compressed air at a pressure of approximately 145 kPa at 108^0C. The required drying time was determined by weighing a

trial sample every 10min. until the measured mass become constant. A drying time of 40min. was established to provide subsequent drying of the fiber.

3.4.2 Epoxy Resin

The type of epoxy resin used in the present investigation is Araldite LY-556 which chemically belongs to epoxide family. Its common name is Bisphinol-A-Diglycidyl-Ether. The hardener with IUPAC name NNO-bis (2aminoethylethane-1,2diamin) has been used with the epoxy designated as HY 951. Both the epoxy and hardener were supplied by Ciba-Geigy of India Ltd.

3.4.3 Composite preparation

A Per-pex sheet mold of dimension 130×100×6 mm was used for casting the composite sheet. The first group of samples were manufactured with 10, 20, 30 and 40% volume fraction by weight of fiber. The usual hand lay-up technique was used for preparation of the samples. For different volume fraction of fibers, a calculated amount of epoxy resin and hardener (ratio of 10:1 by weight) was thoroughly mixed with gentle stirring to minimize air entrapment. For quick and easy removal of composite sheets, a mould release sheet was put over glass plate and mold release agent was applied at the inner surface of the mould. After keeping the mould on glass sheet a thin layer (≈2mm thickness) of mixture was poured. The required amount of fiber was then distributed on the mixture. The remaining mixture was then poured into the mould. Care was taken to avoid formation of air bubbles. Pressure was then applied from the top and the mould was allowed to cure at room temperature for 72 hrs. During application of pressure a small amount of mixture of epoxy and hardener was squeezed out. Care has been taken to consider this loss during manufacturing of composite sheets. After 72 hrs the samples were taken out from the mould, cut in to different sizes and kept in an air tight container for further experimentation.

3.5 STUDY OF MECHANICAL PROPERTIES OF COMPOSITE

The study of mechanical properties such as tensile strength, flexural strength, impact strength and hardness of both untreated and treated Lantana-Camara fiber randomly

distributed in the epoxy matrix have been conducted as per ASTM standards. The results are tabulated in Table-3.3 and 3.4. It is seen that with increase in fiber content, the tensile strength, flexural strength, impact strength and hardness of the composite has been increased considerably in comparison to neat epoxy. The increase in Young's modulus of the developed composite with fiber content is in line with other works, which are well documented [110-112]. It is also observed that the un-notched charpy impact strength of the Lantana-Camara epoxy composite showed an increasing trend with increase in fiber content. Similar type of work [58, 113, 114] showed an increase in impact strength with an increase in fiber content, indicating positive contribution of the fiber. Higher impact strength indicates the capability of the composite to absorb energy. This is because of strong interfacial bonding between the fiber and matrix [115]. It also depends on the nature of the fiber, polymer and fiber–matrix interfacial bonding [116].

From the above investigation, it can be concluded that the composite containing 30 vol% fiber provided the best combination of strength, modulus and work of fracture. Decrease in the mechanical properties is observed at higher fiber loading i.e. 40 vol%. This may be due to poor fiber matrix adhesion which might have promoted micro-crack formation at the interface as well as non-uniform stress transfer due to fiber agglomeration within the matrix [117, 118]. Similar results have been reported by Mohanty et al. [9] and Rana et al. [91] while they worked with jute fiber.

The effect of different chemical modifications of fibers on mechanical properties of the composite have been studied by taking 30 vol% of fiber as an optimum reinforcement as discussed earlier. It is clearly seen from Table-3.4 that, the mechanical properties of the composite enhanced significantly due to chemical modification of fiber surface. This improvement in properties occurs due to rough fiber surface produce by removal of natural and artificial impurities, fibrillation of fiber which facilate the mechanical anchoring between fiber and matrix as explained in Art-3.2.2. In addition to this the increase of crystallinity index of fibers (Art-3.2.4) due to removal of cementing materials also enhanced the properties. Higher increase in properties was observed in the case of benzoyl-chloride treated fiber and alkali treated fiber composite, however acetone treated fiber composite showed a slight improvement in properties. Similar observations were reported by Manikandan et al. [65], Sreenivasan et al. [119] and Britton et al. [120] while working with

benzoylated sisal fibers, alkali treated coir fibers and acetone treated bagasse fibers respectively.

3.6 STUDY OF ENVIRONMENTAL EFFECT

To study the effect of environment on performance of Lantana-Camara fiber epoxy composite, the composite sample with both untreated and chemically treated fibers were subjected to various environments such as:

(a) Steam treatment

(b) Saline treatment

(c) Subzero condition

3.6.1 Moisture absorption test

Moisture absorption and thickness swelling tests were conducted in accordance with ASTM D570-98. Three specimens for each composite system were cut with dimensions of 64 x 12.7mm (length x width) and the experiment was performed using test samples. The specimens prior to testing were dried in an oven at 80^0 C and then were allowed to cool to room temperature and kept in a desiccator. The weight of the samples were taken before subjected to steam, saline water and sub-zero temperature environments. After expose for 10 hr, the specimens were taken out from the moist environment and all surface moisture was removed with a clean dry cloth or tissue paper. The specimens were reweighed to the nearest 0.001 mg within 1 min. of removing them from the environment chamber. The specimens were weighed regularly from 10-80 hrs with a gap of 10hrs of exposure. The moisture absorption was calculated by the weight difference. The percentage weight gain of the samples was measured at different time intervals by using the following equation:

$$\%M_t = \frac{(W_t - W_0) \times 100}{W_0} \tag{3.2}$$

where 'W_0' and 'W_t' denote the oven-dry weight and weight after time 't', respectively. Equilibrium Moisture Content (EMC) of the sample is the moisture content

when the periodic weight change of the sample was less than 0.1% and thus the equilibrium state was assumed to be reached. The thickness swelling (TS) was determined by using the following equation:

$$TS(t) = \frac{H_t - H_0}{H_0} \times 100 \quad (3.3)$$

where 'H_t' and 'H_0' are the composite thickness after and before the water immersion respectively.

3.6.2 Results and discussion

3.6.2.1 Moisture absorption behaviour

The results of both untreated and treated fiber composite samples exposed to different environments are shown in Table-3.5 to 3.10.

Figure-3.7 to 3.9, shows the percentage of moisture absorption characteristics of composite samples with untreated fiber exposed to Steam, Saline water and Sub-Zero temperature environment with time. It is clear from the figure that the initial rate of moisture absorption and the maximum moisture uptake in all environment increases for all composite specimens as fiber content increases. Moisture absorption is maximum for composites made with 40% fiber content, having moisture absorption of 13.72% in steam, 8.90% in saline water and 2.30% in sub-zero temperature environments. It is known that [121], the factors like porosity content, the lumen and fiber–matrix adhesion are somewhat responsible for the moisture absorption behavior of the natural fiber composites. But in this case the hydrophilicity of Lantana-Camara fiber, in addition to poor fiber–matrix adhesion and voids content might have affect the moisture uptake characteristics of the composite.

Again it is observed that, the moisture absorption increases with immersion time, and got saturated after certain time period. Time to reach the saturation point is not same for all the environments. The saturation time is approximately 60 hrs for steam, and 70hrs for saline water and sub-zero temperature treatment for 40% fiber reinforced composite. Environmental conditions also play a significant role in moisture absorption process. Figure-3.10 shows the maximum moisture absorption of composite in all three

environments. In steam environment moisture absorption is maximum as compare to saline water and sub-zero temperature environments irrespective of fiber content. It can be conclude that higher temperatures in case of steam environment seem to accelerate the moisture uptake behavior. The absorption rate in case of saline water is less than that of steam. This happens because of the accumulation of NaCl ions in the fiber's surface immersed in saline water, which increases with time and hinders subsequent moisture diffusion [122]. Again the absorption rate of water in sub-zero temperature is much less in comparison to steam and saline water treatment. This may be due to less intermolecular hydrogen bonding which is responsible for this behavior.

Figure-3.11 to 3.13 shows that the moisture absorption behaviour of the chemically treated fiber reinforced epoxy composites was lower than that of the untreated fiber-based composites when exposed to different environmental treatment. It is clear from these plots that the changes in surface chemistry of the fiber have reduced the affinity of fibers to moisture. Due to surface modification by chemical treatment, the fibers get masked with the epoxy resin with a stronger adhesion, resulting in greater hydrophobicity and less moisture absorption. In comparison to all the chemical treatments, the Benzoyl-Chloride process showed considerable reduction in moisture absorption. In case of Benzoyl-Chloride treated fiber composite the maximum moisture absorption reduced by 61.96% in steam, while it is 54.1% in saline water and 60% in subzero environment.

3.6.2.2 Measurement of Diffusivity

The water sorption kinetics in LCF reinforced epoxy composite has been studied through the diffusion constants k and n. The behaviour of moisture sorption in the composite was studied by the shape of the sorption curve represented by the following equation [123, 124]:

$$\frac{M_t}{M_m} = kt^n \qquad (3.4)$$

where 'M_t' is the moisture content at specific time 't', 'M_m' the equilibrium moisture content (EMC), and 'k' and 'n' are constants. The value of k and n were determined from

the slope and the intercept of M_t /M_m versus 't' in the log plot which was drawn from experimental data of moisture absorption with time. Figure-3.14 to 3.16 and Figure-3.17 to 3.19 showed the typical curve of log (M_t/M_m) as a function of log (t) for both untreated and treated LCF reinforced epoxy composite respectively, used to determine these constants. An example of the fitting of the experimental data for Lantana-Camara epoxy composites under steam environment is given in Figure-3.20 and the values of k and n resulting from the fitting of all formulations are shown in Table-3.11. It was observed that the value of n is close to 0.5 for all of the composites. This confirms that the Fickian diffusion can be used to adequately describe moisture absorption in the composites, which is consistent with previous studies [125, 126]. A higher value of n and k indicates that the composite needs shorter time to attain equilibrium water absorption. The value of k was found to increases with increasing fiber content for LCF reinforced epoxy composite in all environments resulting higher moisture absorption initially. The value of k for untreated fiber composite was higher than that of treated fiber composite, except saline water environment. It might have happened due to the accumulation of NaCl ions in the fiber's surface which delays subsequent moisture diffusion. However, Benzoyl-Chloride treated fiber composites showed higher k value than that of alkali and acetone treated fiber composite, which is probably because of equilibrium moisture content (EMC) was not reached in these composites.

The diffusion coefficient or diffusivity (D_x) of moisture absorption was calculated using the following equation [127]:

$$D_x = \pi \left[\frac{h}{4M_m} \right]^2 \left(\frac{M_2 - M_1}{\sqrt{t_2} - \sqrt{t_1}} \right)^2 \qquad (3.5)$$

where 'M_m' is the maximum percentage of moisture content, 'h' is the sample thickness, 't_1' and 't_2' are the selected points in the initial linear portion of the plot of moisture absorption (M_t) versus $\sqrt{t}$ (Figure-3.21) and 'M_1' and 'M_2' are the respective moisture content.

From the plot of M_t verses square root of time (t) (Figure-3.22 to 3.27) the value of D_x has been evaluated and summarized in Table-3.12. It has been observed D_x value

increases with the LCF content for the composites examined. These results are consistent with previous findings on wood and natural fibers composites [79, 126]. The increase was more pronounced for the specimens subjected to steam than those subjected to saline water and sub-zero environments. The surface modification of fiber decreases the diffusion coefficient (D_x). Benzoyl-Chloride treated fiber exhibits lower diffusion coefficient in all environment except saline water environment. The results obtained here are consistent with the findings by Thomas et al. [89] for sisal fiber/polyester composite.

The direct comparison of the diffusivity obtained from this work with previous studies is difficult due to differences in materials, manufacturing methods and test conditions. In spite of this, the magnitude of the diffusivity obtained in this work is1.2872×10^{-11} to 1.4417×10^{-10} m^2/s as reported by Deo and Acharya [128], which is also similar to the other reported values. Thomas et al. [85] reported the value of diffusivity varies from 0.79×10^{-12} to 4.39×10^{-12} for sisal fiber reinforced polypropylene composites. Espert et al. [79] reported a diffusivity of 1.09×10^{-12} m^2/s for PP composites containing 30 wt. % coir fiber and a diffusivity of 1.83×10^{-12} m^2/s for composites containing 30 wt. % Luffa fiber.

3.6.2.3 Thickness swelling behaviour

The thickness swelling processes for LCF reinforced epoxy composites at different ambient environments has been studied by considering the thickness swelling (TS) and swelling rate parameter (K_{SR}). The value of K_{SR} was evaluated through a non-linear regression curve fitting method to fit the experimental data (Table-3.5 to 3.10) in equation-3.6 [129], using computer software with curve fitting routines.

$$TS(t) = \left(\frac{H_\infty}{H_0 + (H_\infty - H_0)e^{-K_{SR}t}} - 1 \right) \times 100 \qquad (3.6)$$

where *'TS (t)'* is the thickness swelling at specific time (t), *'H_0'* and *'H_∞'* are the initial and equilibrium thickness respectively.

Figure-3.28 to 3.30 shows the thickness swelling behaviour of untreated LCF reinforced epoxy composites at various environments. It was observed that in all

environmental conditions the thickness swelling (TS) increases with an increase in fiber content and immersion time. The results showed that the thickness swelling (TS) found to be highest for the composite with 40 vol% fiber content (27.804% in steam, 23.105% in saline water and 17.303% at sub-zero temperature environments), which corresponds to the highest water absorption. This might have happened because of the increased number of micro voids caused by the larger amount of poorly bonded area between the hydrophilic filler and the hydrophobic matrix polymer.

However, the swelling of LCF reinforced epoxy composites was reduced with chemical treatment as shown in Figure-3.31 to 3.33. The different thickness swelling behavior observed between various composites at the same content i.e. 30% loading of fiber can be attributed to the type their interaction of treated fiber with the matrix. Benzoyl-chloride treated fiber composite shows higher reduction of thickness swelling compare to acetone and alkali treatment. The reduction was 48.848% in case Benzoyl-chloride treatment, 41.227% in case acetone treatment and 45.557% in case of alkali treatment under steam environment. Similar trend was also observed for saline water and subzero temperature environments.

The experimental data was used to obtain the swelling rate parameter (K_{SR}) by using equation-3.6. Table-3.13 summarizes the respective value of K_{SR} obtained through non-linear curve fitting. The swelling parameter, K_{SR}, quantifies the rate of the composites approaching the equilibrium value for thickness swelling after sufficient time of water immersion. The higher value of K_{SR} indicates, the higher rate of swelling along with reaching of equilibrium thickness swelling in a shorter period of time. The swelling rate parameter of the composites increases with increase in fiber content but it reduces significantly with chemical treatment of fiber surface which was due to the improved compatibility between polymer and fiber [130]. Benzoyl-chloride treated fiber composite showed lower K_{SR} value compared to other treatments.

3.6.3 Effect of moisture absorption on Mechanical properties

The moisture absorption has a significant influence on the mechanical properties of the natural fiber polymer composite. Table-3.14 shows the result of mechanical properties of the composite with both treated and untreated fiber reinforced composite after expose to

different moist environment for a period of 80hrs. It has been observed that, both strength and stiffness of all composite decrease after moisture absorption. This reduction in the strength and stiffness is attributed to the changes occurring in the fiber, and the interface between fiber and matrix. When fiber/matrix interface is accessible to moisture from the environment, the cellulosic fibers tend to swell, thereby developing shear stresses at the interface, which favors ultimate debonding of the fibers, which in turn causes a reduction in strength [85]. It is also observed that the reduction in properties was greatly influenced by the fiber loading and nature of environment. The maximum reduction in strength and stiffness happened in case 40 vol% fiber loading at steam environment. The fact has already been discussed in Art-3.4.4. Further it is also noticed that the extent of decrease in mechanical properties is reduced with chemical modification of fiber. The benzoyl-chloride treated fiber composite exhibits the best result in all environments in comparison to other two treated fiber composite. Because the benzoyl-chloride treatments reduces the hydrophilic nature of the fiber to great extend which leads to less moisture absorption as reported in Art-3.6.2.1.

3.7 SEM MICROGRAPH STUDY OF FRACTURE SURFACE

A SEM micrograph (magnified view) of the tensile fracture surface of 30 vol% of untreated Lantana-Camara fiber composites is shown in Figure-3.34. The phenomenon of pull-out fibers was clearly observed, which indicates the poor interfacial bonding between matrix and fiber. But in case of acetone treated and alkali treated based composites (shown in Figure-3.35 & 3.36), the fibers are still embedded in the resin together with some cavities left by pulled-out fibers. However it is interesting to note that there is little evidence of fiber pulled-out in the benzoyl-chloride treated fibers based composites (shown in Figure-3.37), which indirectly indicate better adhesion exists at the inter-phase. Figure-3.38 shows the SEM micrographs of the fracture surface 40 vol% of untreated Lantana-Camara fiber reinforced composites during bending test. Debonding between fiber and matrix, fiber pull-out and an empty space between fibers due to insufficient wetting are observed. This reveals that at higher fiber loading poor fiber wetting occurs due to insufficient matrix material, resulting in a lowering in strength and modulus as discussed earlier. Swelling of fiber occurs due to moisture absorption which lead to debonding at the fiber-matrix interface is clearly seen Figure-3.39. This debonding at the fiber-matrix interface is mainly responsible for degradation in the mechanical properties.

3.8 CONCLUSIONS

Based on experimental results, this study has led to the following conclusions:

- The Lantana-Camara fiber can successfully be used as reinforcing agent to fabricate composite by suitably bonding with epoxy resin.

- The effective fiber length for fabrication of Lantana-Camara epoxy composite as found out from the single fiber pull-out test is approximately 9.11 mm or longer.

- On increasing the fiber content the strength, modulus and work of fracture increases and the best combination is found with 30 vol% of fiber.

- The fiber surface modification by chemical treatments significantly improves the fiber matrix adhesion, which in turn improves the mechanical properties of composite. Benzoyl-chloride treatment shows the highest improvement in comparison to alkali and acetone treatment. These results are confirmed through SEM, FTIR and XRD analysis.

- The moisture uptake and thickness swelling values increases with increase in fiber loading. Both values are found to be higher in steam environment than in saline water and sub-zero temperature environments. However these values are considerably reduced with chemical treatments of the fiber.

- Under all environment conditions, the moisture diffusion process of both treated and untreated Lantana-Camara fiber composites are found to follow the Fick's law.

- Fiber breakages are found to be the predominant mode of failure as ascertained from the morphology of the treated fiber composites.

Table-3.1 Crystallinity index of untreated and treated Lantana-Camara fiber

Types of Fiber	I_{am} ($2\theta=15^0$)	I_{002} ($2\theta=23^0$)	Crystallinity Index
Untreated (UT)	715	5108	86.00
Acetone treated	707	5910	88.03
Alkali treated	782	6372	87.73
Benzoyl-chloride treated	798	6768	88.21

Table- 3.2 Pullout Testing Results

Embedded Fiber Length (mm)	Pullout Load (Kg)
1.25	1.54
1.78	2.05
2.41	3.28
2.84	3.69
3.58	4.56
4.02	3.58
4.51	4.26
5.8	4.97
6.45	6.92
7.28	7.74
8.75	8.55
9.22	8.68
10.42	8.83*
11.25	8.32*
12.05	8.98*
13.34	8.37*
14.05	9.08*
15.14	9.24*

*Note: " * " did not pullout / ruptured*

Table-3.3 Mechanical properties of untreated Lantana-Camara fiber epoxy composite.

Fiber Content (wt%)	Tensile strength (Mpa)	Yong's Modulus (Mpa)	Elongation of Break (%)	Flexural strength (MPa)	Flexural Modulus (MPa)	Impact strength (KJ/m2)	Vickers Hardness (HV)
0%	18.031	521	3.4	45.519	632	25.78	17.894
10%	17.680	821	4.83	39.346	1284	31.73	17.375
20%	18.020	965	4.46	48.082	1356	36.56	18.145
30%	19.080	1132	5.22	55.491	1425	34.69	19.455
40%	18.440	1172	4.12	46.597	1373	30.38	17.315

Table-3.4 Mechanical properties of treated Lantana-Camara fiber epoxy composite.

Fiber Content (%)	Type of fiber	Tensile strength (Mpa)	Yong's Modulus (Mpa)	Elongation of Break (%)	Flexural strength (Mpa)	Flexural Modulus (Mpa)	Impact strength (KJ/m2)
30	Untreated	19.080	1132	5.22	55.491	1425	34.69
30	Acetone treated	20.078	1435	4.98	58.351	1489	36.24
30	Alkali treated	23.451	1542	5.29	69.527	1658	42.36
30	Benzoylated	25.621	1631	5.36	72.047	1785	45.42

Table-3.5 Variation of weight gain and thickness swelling of untreated Lantana-Camara fiber epoxy composite with immersion time expose at steam environment

% of Fiber	Immersion Time 't' (hrs)	Weight of the Sample (w_t)	Percentage of weight gain (% M)	Thickness at time 't' H(t)	Thickness swelling TS (t)
10	0	9.304	0.00	3.152	0.00
	10	9.800	5.33	3.202	1.60
	20	10.018	7.67	3.288	4.30
	30	10.209	9.73	3.373	7.00
	40	10.356	11.31	3.496	10.90
	50	10.417	11.96	3.644	15.60
	60	10.434	12.15	3.719	18.00
	70	10.443	12.24	3.776	19.80
	80	10.443	12.24	3.795	20.40
20	0	14.937	0.00	3.512	0.00
	10	15.889	6.37	3.674	4.60
	20	16.271	8.93	3.821	8.80
	30	16.550	10.80	3.962	12.80
	40	16.710	11.87	4.095	16.60
	50	16.770	12.27	4.197	19.50
	60	16.803	12.49	4.288	22.10
	70	16.828	12.66	4.362	24.20
	80	16.828	12.66	4.379	24.70
30	0	16.304	0.00	4.674	0.00
	10	17.494	7.30	4.945	5.80
	20	17.902	9.80	5.151	10.20
	30	18.154	11.35	5.389	15.30
	40	18.314	12.33	5.571	19.20
	50	18.379	12.73	5.698	21.90
	60	18.424	13.00	5.824	24.60
	70	18.456	13.20	5.913	26.50
	80	18.463	13.24	5.922	26.70
40	0	20.273	0.00	4.895	0.00
	10	21.944	8.24	5.233	6.90
	20	22.453	10.75	5.541	13.20
	30	22.754	12.24	5.771	17.90
	40	22.962	13.26	5.894	20.40
	50	23.003	13.47	6.050	23.60
	60	23.034	13.62	6.197	26.60
	70	23.055	13.72	6.251	27.70
	80	23.065	13.77	6.256	27.80

Table-3.6 Variation of weight gain and thickness swelling of untreated Lantana-Camara fiber epoxy composite with immersion time expose at saline water environment.

% of Fiber	Immersion Time 't' (hrs)	Weight of the Sample (w_t)	Percentage of weight gain (% M)	Thickness at time 't' H(t)	Thickness swelling TS (t)
10	0	10.273	0.00	3.152	0.00
	10	10.487	2.08	3.196	1.40
	20	10.587	3.06	3.281	4.10
	30	10.668	3.85	3.366	6.80
	40	10.722	4.37	3.470	10.10
	50	10.740	4.55	3.562	13.00
	60	10.758	4.72	3.675	16.60
	70	10.749	4.63	3.713	17.80
	80	10.751	4.65	3.732	18.40
20	0	14.932	0.00	3.512	0.00
	10	15.424	3.29	3.582	2.00
	20	15.635	4.71	3.681	4.80
	30	15.759	5.54	3.796	8.10
	40	15.853	6.17	3.898	11.00
	50	15.885	6.38	4.025	14.60
	60	15.888	6.40	4.148	18.10
	70	15.897	6.46	4.207	19.80
	80	15.909	6.54	4.214	20.00
30	0	17.254	0.00	4.674	0.00
	10	17.933	3.94	4.805	2.80
	20	18.183	5.38	4.945	5.80
	30	18.392	6.60	5.081	8.70
	40	18.492	7.18	5.272	12.80
	50	18.531	7.40	5.459	16.80
	60	18.541	7.46	5.571	19.20
	70	18.555	7.54	5.665	21.20
	80	18.552	7.52	5.679	21.50
40	0	20.824	0.00	4.895	0.00
	10	21.805	4.71	5.086	3.90
	20	22.201	6.61	5.252	7.30
	30	22.516	8.12	5.429	10.90
	40	22.667	8.85	5.639	15.20
	50	22.679	8.91	5.845	19.40
	60	22.698	9.00	5.982	22.20
	70	22.706	9.04	6.016	22.90
	80	22.713	9.07	6.026	23.10

Table-3.7 Percentage of weight gain and thickness swelling of untreated Lantana-Camara fiber epoxy composite with immersion time expose at sub-zero temperature environment.

% of Fiber	Immersion Time 't' (hrs)	Weight of the Sample (w_t)	Percentage of weight gain (% M)	Thickness at time 't' H(t)	Thickness swelling TS (t) (%)
10	0	9.862	0.00	3.152	0.000
	10	9.918	0.57	3.177	0.800
	20	9.950	0.89	3.212	1.900
	30	9.967	1.06	3.275	3.900
	40	9.974	1.14	3.351	6.300
	50	9.976	1.16	3.423	8.600
	60	9.980	1.20	3.521	11.700
	70	9.984	1.24	3.578	13.500
	80	9.985	1.25	3.603	14.300
20	0	15.024	0.00	3.512	0.000
	10	15.138	0.76	3.561	1.400
	20	15.182	1.05	3.621	3.100
	30	15.206	1.21	3.674	4.600
	40	15.221	1.31	3.782	7.700
	50	15.233	1.39	3.891	10.800
	60	15.240	1.44	3.990	13.600
	70	15.242	1.45	4.046	15.200
	80	15.246	1.48	4.060	15.600
30	0	16.786	0.00	4.674	0.000
	10	16.930	0.86	4.744	1.500
	20	16.992	1.23	4.833	3.400
	30	17.019	1.39	4.954	6.000
	40	17.039	1.51	5.099	9.100
	50	17.053	1.59	5.240	12.100
	60	17.060	1.63	5.398	15.500
	70	17.068	1.68	5.427	16.100
	80	17.073	1.71	5.431	16.200
40	0	21.043	0.00	4.895	0.000
	10	21.314	1.29	4.993	2.000
	20	21.437	1.87	5.091	4.000
	30	21.495	2.15	5.247	7.200
	40	21.521	2.27	5.401	10.330
	50	21.548	2.40	5.551	13.400
	60	21.562	2.47	5.683	16.100
	70	21.571	2.51	5.732	17.100
	80	21.571	2.51	5.742	17.300

Table-3.8 Percentage of weight gain and thickness swelling of treated Lantana-Camara fiber epoxy composite with immersion time expose at steam environment

Type of Fiber	Immersion Time 't' (hrs)	Weight of the Sample (w_t)	Percentage of weight gain (% M)	Thickness at time 't' H(t)	Thickness swelling TS(t) (%)
Acetone	0	14.745	0.00	5.187	0.00
	10	15.512	5.20	5.318	2.52
	20	15.928	8.02	5.457	5.20
	30	16.077	9.04	5.594	7.85
	40	16.329	10.74	5.718	10.24
	50	16.371	11.03	5.833	12.45
	60	16.429	11.42	5.948	14.67
	70	16.476	11.74	5.993	15.53
	80	16.481	11.78	6.001	15.70
Alkali	0	17.246	0.00	4.552	0.00
	10	17.962	4.15	4.633	1.79
	20	18.301	6.12	4.738	4.09
	30	18.606	7.89	4.843	6.40
	40	18.839	9.24	4.940	8.53
	50	18.897	9.57	5.041	10.75
	60	19.035	10.38	5.135	12.80
	70	19.057	10.50	5.181	13.82
	80	19.057	10.50	5.185	13.91
Benzoyl-Chloride	0	17.635	0.00	4.576	0.00
	10	17.970	1.90	4.668	2.00
	20	18.129	2.80	4.759	4.00
	30	18.226	3.35	4.838	5.72
	40	18.369	4.16	4.931	7.76
	50	18.457	4.66	5.037	10.07
	60	18.523	5.03	5.154	12.63
	70	18.545	5.16	5.198	13.60
	80	18.559	5.24	5.201	13.65

Table-3.9 Percentage of weight gain and thickness swelling of treated Lantana-Camara fiber epoxy composite with immersion time expose at saline water environment.

Type of Fiber	Immersion Time 't' (hrs)	Weight of the Sample (w_t)	Percentage of weight gain (% M)	Thickness at time 't' H(t)	Thickness swelling TS(t) (%)
Acetone	0	15.105	0.00	5.187	0.00
	10	15.555	2.98	5.276	1.71
	20	15.739	4.20	5.358	3.30
	30	15.881	5.14	5.432	4.72
	40	15.944	5.56	5.498	6.00
	50	16.077	6.43	5.560	7.20
	60	16.151	6.93	5.618	8.30
	70	16.163	7.00	5.668	9.27
	80	16.169	7.04	5.683	9.57
Alkali	0	18.241	0.00	4.552	0.00
	10	18.691	2.47	4.609	1.25
	20	18.814	3.14	4.687	2.96
	30	18.894	3.58	4.744	4.21
	40	18.960	3.94	4.796	5.35
	50	19.010	4.22	4.860	6.77
	60	19.054	4.46	4.920	8.08
	70	19.047	4.42	4.958	8.93
	80	19.054	4.46	4.971	9.20
Benzoyl-Chloride	0	17.054	0.00	4.576	0.00
	10	17.368	1.84	4.628	1.14
	20	17.457	2.36	4.678	2.22
	30	17.511	2.68	4.732	3.41
	40	17.559	2.96	4.777	4.40
	50	17.580	3.08	4.829	5.52
	60	17.621	3.32	4.883	6.71
	70	17.634	3.40	4.924	7.60
	80	17.627	3.36	4.938	7.91

Table-3.10 Percentage of weight gain and thickness swelling of treated Lantana-Camara fiber epoxy composite with immersion time expose at sub-zero temperature environment.

Type of Fiber	Immersion Time 't' (hrs)	Weight of the Sample (w_t)	Percentage of weight gain M_t (%)	Thickness at time 't' H(t)	Thickness swelling TS(t) (%)
Acetone	0	14.237	0.00	5.187	0.00
	10	14.313	0.53	5.233	0.88
	20	14.342	0.74	5.289	1.96
	30	14.362	0.88	5.337	2.89
	40	14.379	1.00	5.390	3.91
	50	14.395	1.11	5.450	5.08
	60	14.405	1.18	5.513	6.29
	70	14.410	1.22	5.543	6.86
	80	14.410	1.22	5.557	7.13
Alkali	0	16.558	0.00	4.552	0.00
	10	16.609	0.31	4.588	0.78
	20	16.634	0.46	4.635	1.83
	30	16.649	0.55	4.675	2.70
	40	16.671	0.68	4.711	3.49
	50	16.688	0.78	4.762	4.61
	60	16.704	0.88	4.803	5.52
	70	16.705	0.89	4.842	6.36
	80	16.709	0.91	4.853	6.62
Benzoyl-Chloride	0	16.786	0.00	4.576	0.00
	10	16.827	0.24	4.608	0.69
	20	16.850	0.38	4.639	1.38
	30	16.860	0.44	4.661	1.85
	40	16.873	0.52	4.705	2.82
	50	16.887	0.60	4.751	3.82
	60	16.901	0.68	4.797	4.83
	70	16.901	0.68	4.835	5.65
	80	16.908	0.73	4.845	5.87

Table-3.11 Diffusion case selection parameters

Environment	% of Fiber	Type of Fiber	n	k(h^2)
Steam	10	Untreated	0.5478	0.1233
	20	Untreated	0.5005	0.159
	30	Untreated	0.4376	0.2019
	40	Untreated	0.4066	0.2377
	30	Acetone Treated	0.5455	0.104
	30	Alkali Treated	0.5845	0.1029
	30	Benzoyl-Chloride Treated	0.6251	0.1045
Saline Water	10	Untreated	0.5593	0.1275
	20	Untreated	0.5291	0.1522
	30	Untreated	0.4849	0.1741
	40	Untreated	0.5402	0.1524
	30	Acetone Treated	0.4962	0.1358
	30	Alkali Treated	0.3392	0.251
	30	Benzoyl-Chloride Treated	0.3429	0.2459
Sub-Zero Temperature	10	Untreated	0.6761	0.0992
	20	Untreated	0.4763	0.1715
	30	Untreated	0.5495	0.1489
	40	Untreated	0.6038	0.1285
	30	Acetone Treated	0.4606	0.1513
	30	Alkali Treated	0.5745	0.0902
	30	Benzoyl-Chloride Treated	0.6172	0.0866

Table-3.12 Diffusivity of untreated and treated fiber Lantana-Camara fiber epoxy composites at different environments

Environment	% of Fiber	Type of Fiber	EMC	Diffusivity (D_x) x 10^{-11} (mm2/s)
Steam	10	Untreated	12.24%	1.6977
	20	Untreated	12.70%	2.3996
	30	Untreated	13.20%	7.8262
	40	Untreated	13.72%	14.4170
	30	Acetone Treated	11.70%	5.5237
	30	Alkali Treated	10.50%	1.9680
	30	Benzoyl-Chloride Treated	5.20%	1.8328
Saline Water	10	Untreated	4.50%	1.3044
	20	Untreated	6.40%	3.4697
	30	Untreated	7.40%	5.4658
	40	Untreated	8.90%	10.5710
	30	Acetone Treated	6.90%	6.3520
	30	Alkali Treated	4.50%	2.4905
	30	Benzoyl-Chloride Treated	3.40%	3.6631
Sub-Zero Temperature	10	Untreated	1.20%	1.2872
	20	Untreated	1.30%	2.7408
	30	Untreated	1.70%	5.1626
	40	Untreated	2.30%	6.4176
	30	Acetone Treated	1.22%	3.9599
	30	Alkali Treated	0.88%	2.4700
	30	Benzoyl-Chloride Treated	0.68%	1.0054

Table-3.13 Swelling rate parameter of treated and untreated Lantana-Camara fiber epoxy composite in different environments.

Environment	% of Fiber	Type of Fiber	T_0 (mm)	T_∞ (mm)	TS (%)	Swelling Rate Parameter (K_{SR}) $\times 10^{-3}$ (h^{-1})
Steam	10	Untreated	3.152	3.795	20.400	29.9
	20	Untreated	3.512	4.379	24.687	34.5
	30	Untreated	4.674	5.922	26.701	38.3
	40	Untreated	4.895	6.256	27.804	41.2
	30	Acetone Treated	5.187	6.001	15.693	33.3
	30	Alkali Treated	4.552	5.185	13.906	31.0
	30	Benzoyl-Chloride Treated	4.576	5.201	13.658	27.4
Saline Water	10	Untreated	3.152	3.732	18.401	26.8
	20	Untreated	3.512	4.214	19.989	28.1
	30	Untreated	4.674	5.679	21.502	32.0
	40	Untreated	4.895	6.026	23.105	38.0
	30	Acetone Treated	5.187	5.683	9.562	28.8
	30	Alkali Treated	4.552	4.971	9.205	27.2
	30	Benzoyl-Chloride Treated	4.576	4.938	7.911	24.5
Sub-Zero Temperature	10	Untreated	3.152	3.603	14.308	19.8
	20	Untreated	3.512	4.060	15.604	24.3
	30	Untreated	4.674	5.431	16.196	28.8
	40	Untreated	4.895	5.742	17.303	31.4
	30	Acetone Treated	5.187	5.557	7.133	25.0
	30	Alkali Treated	4.552	4.853	6.612	23.8
	30	Benzoyl-Chloride Treated	4.576	4.845	5.878	20.6

Table-3.14 Mechanical properties of both untreated and treated Lantana-Camara fiber epoxy composite after expose to different environment.

Type of Environment	Fiber content (%)	Type of fiber	Tensile strength (MPa)	Young's Modulus (MPa)	Elongation of Break (%)	Flexural strength (MPa)	Flexural Modulus (MPa)	Impact strength (KJ/m^2)
Steam	10	Untreated	13.200	648	2.05	29.109	765	19.55
	20	Untreated	12.100	675	2.75	35.402	986	12.100
	30	Untreated	13.340	877	3.88	38.312	1005	20.45
	40	Untreated	11.239	742	3.04	33.391	886	19.96
	30	Acetone treated	14.089	966	3.21	41.161	1127	24.47
	30	Alkali treated	19.558	1102	2.94	44.810	1314	27.66
	30	Benzoylated	20.904	1168	3.57	45.860	1208	32.17
Saline Water	10	Untreated	14.140	729	2.64	35.211	844	22.33
	20	Untreated	13.740	763	3.41	39.641	1024	13.740
	30	Untreated	15.116	914	4.25	40.764	1051	26.71
	40	Untreated	13.200	803	4.51	38.182	971	21.87
	30	Acetone treated	15.890	1154	4.06	47.270	1254	31.24
	30	Alkali treated	18.483	1261	3.16	58.211	1378	33.30
	30	Benzoylated	22.728	1332	3.75	55.455	1301	37.40
Sub-zero Temperature	10	Untreated	15.200	795	3.08	37.594	973	24.43
	20	Untreated	16.620	914	4.02	42.308	1089	16.620
	30	Untreated	16.520	1021	4.74	42.451	1142	28.31
	40	Untreated	15.130	947	4.83	39.864	1066	24.01
	30	Acetone treated	18.445	1257	4.12	53.935	1251	34.57
	30	Alkali treated	21.839	1406	3.48	63.396	1426	38.87
	30	Benzoylated	23.583	1463	3.02	66.321	1504	41.78

Figure-3.1 Soxhlet Extractor

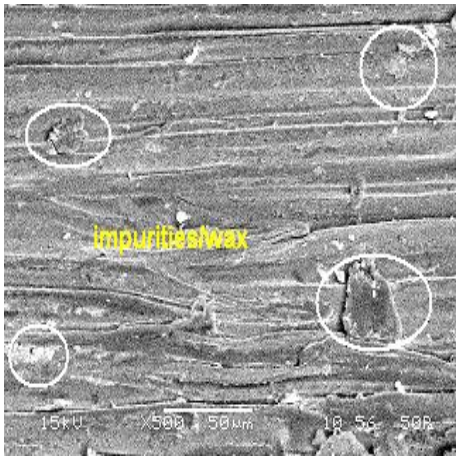

Figure-3.2 (a)

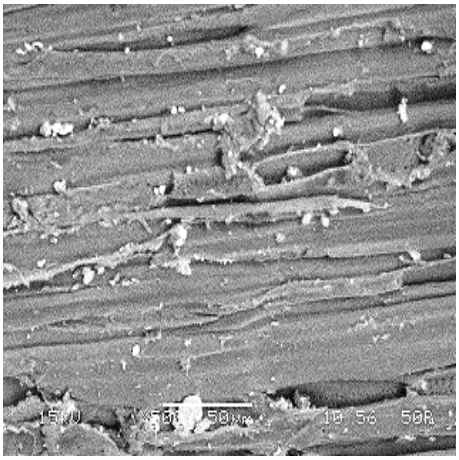

Figure-3.2 (b)

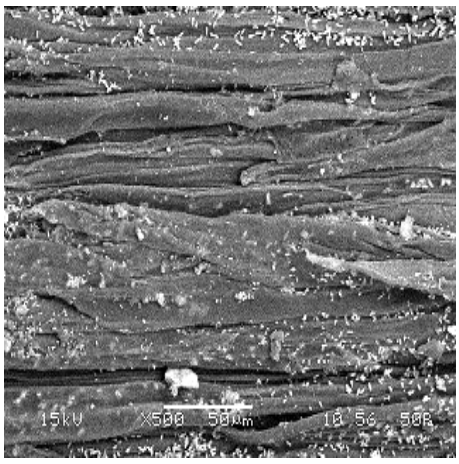

Figure-3.2 (c)

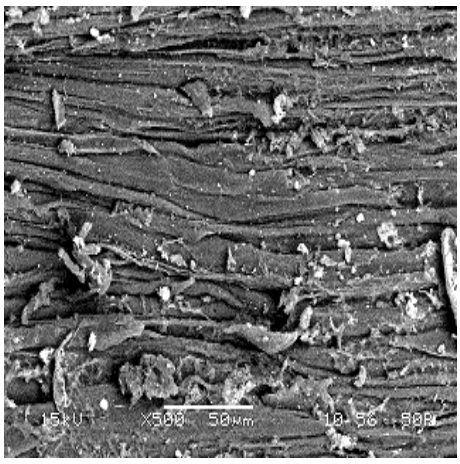

Figure-3.2 (d)

Figure-3.2 SEM micrograph of Lantana-Camara fiber (a)Untreated; (b) Acetone treated; (c) Alkali treated; (d) Benzoyl-Chloride treated

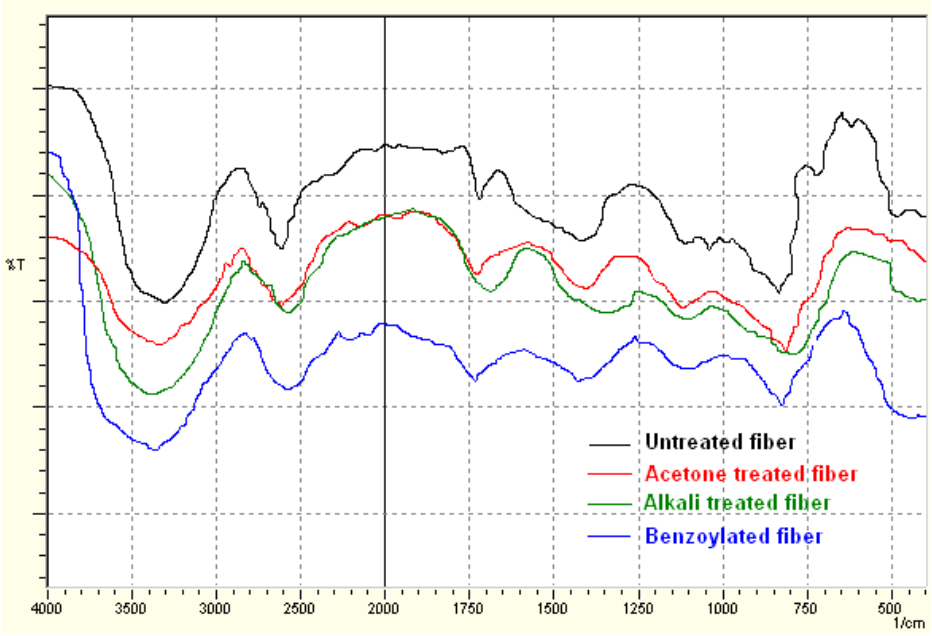

Figure-3.3 FTIR spectra of Lantana-Camara fiber before and after chemical modification

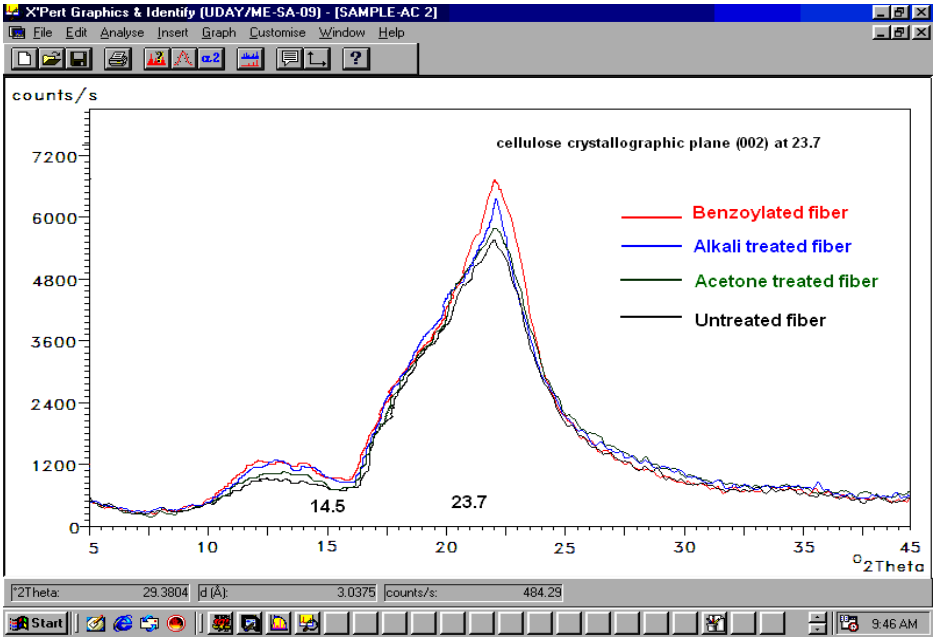

Figure-3.4 XRD pattern of both untreated and treated Lantana-Camara fiber

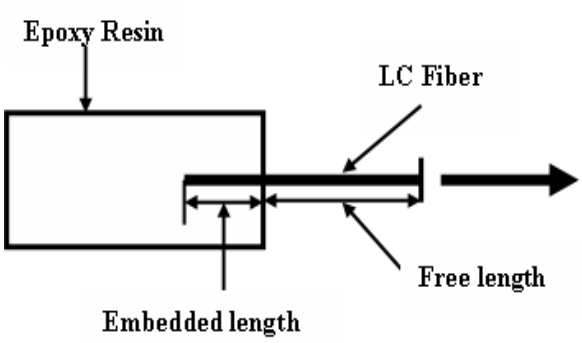

Fig.-3. 5 (a) Schematic diagram for single fiber pull-out test

Fig.-3.5 (b) Cast samples for single fiber pull-out test

Figure-3.5 Sample for single fiber pull-out test

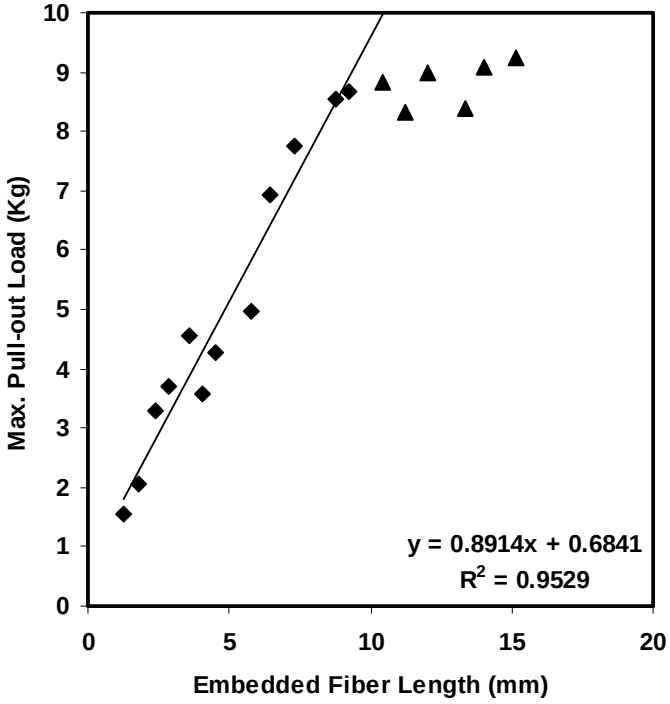

Figure-3.6 Embedded fiber length vs. Pull-out Load

Note: data (▲) not used in regression analysis (fibers did not pullout)

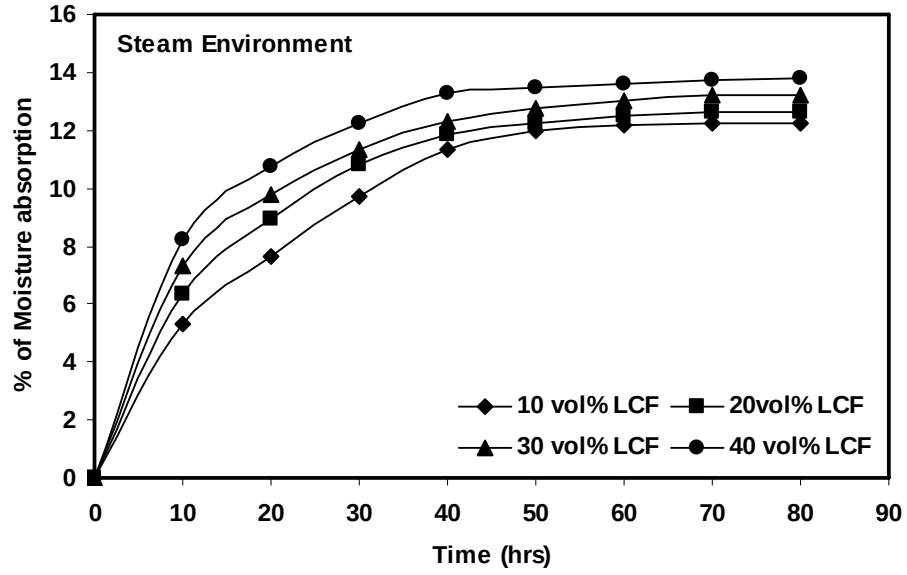

Figure-3.7 **Variation of weight gain of the untreated Lantana-Camara fiber epoxy composites with immersion time at steam environment**

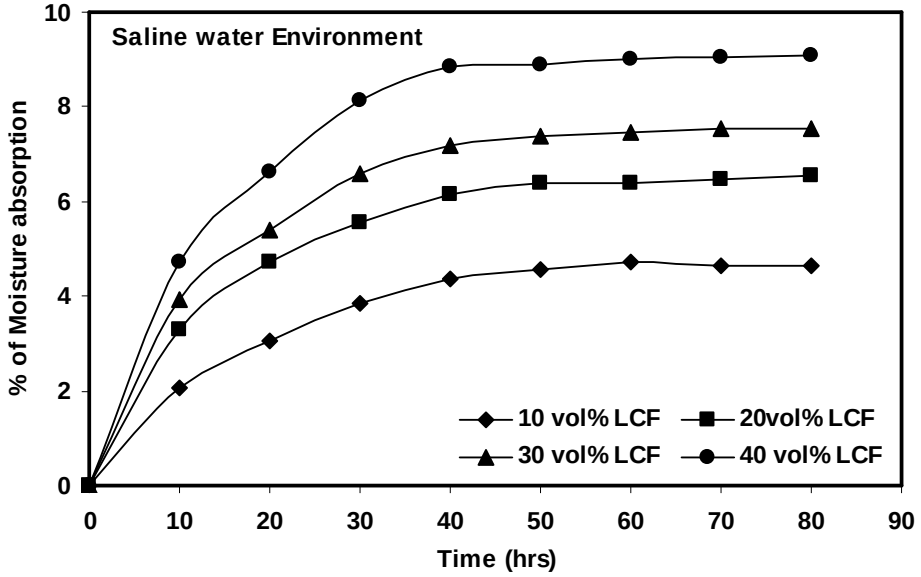

Figure-3.8 **Variation of weight gain of the untreated Lantana-Camara fiber epoxy composites with immersion time at saline water environment**

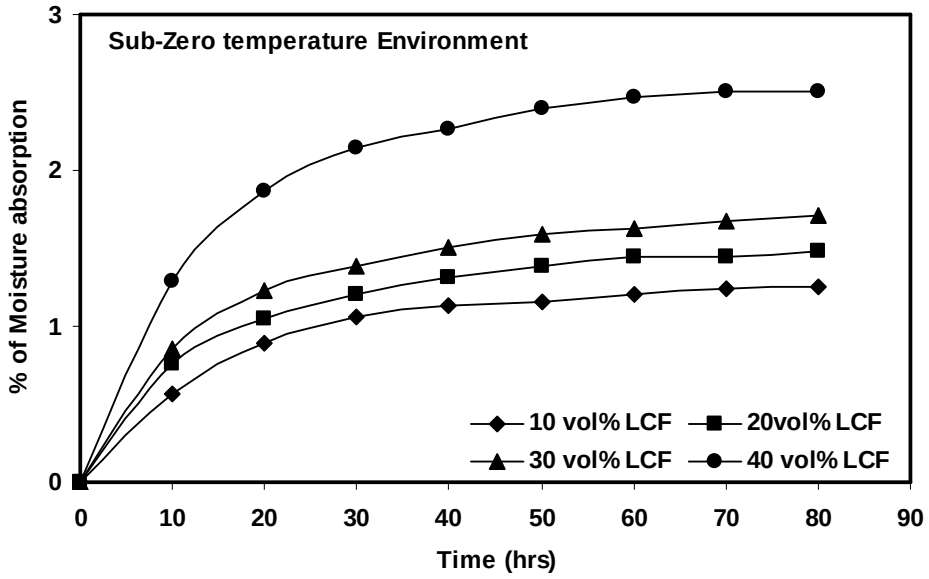

Figure-3.9 **Variation of weight gain of the untreated Lantana-Camara fiber epoxy composites with immersion time at sub-zero temperature environment**

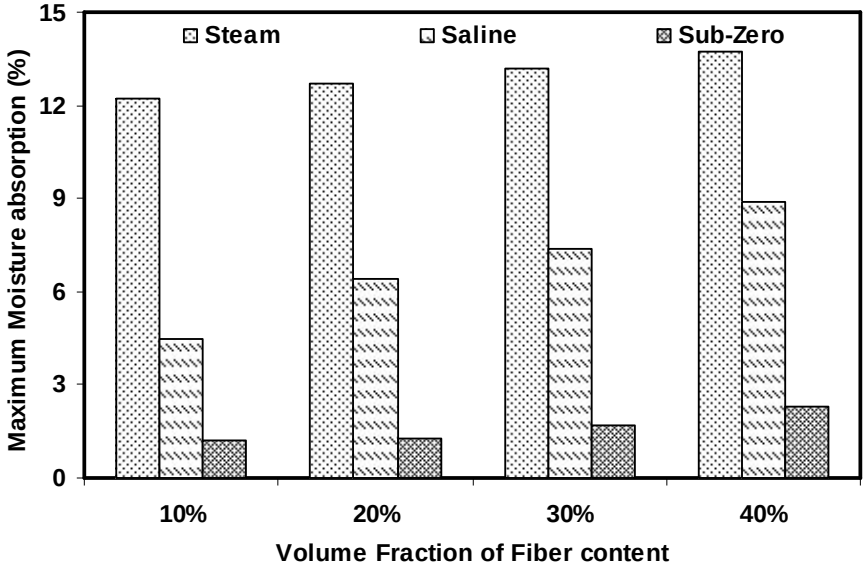

Figure-3.10 **Maximum moisture absorption of untreated Lantana-Camara fiber epoxy composite versus fiber loading in all the three environments**

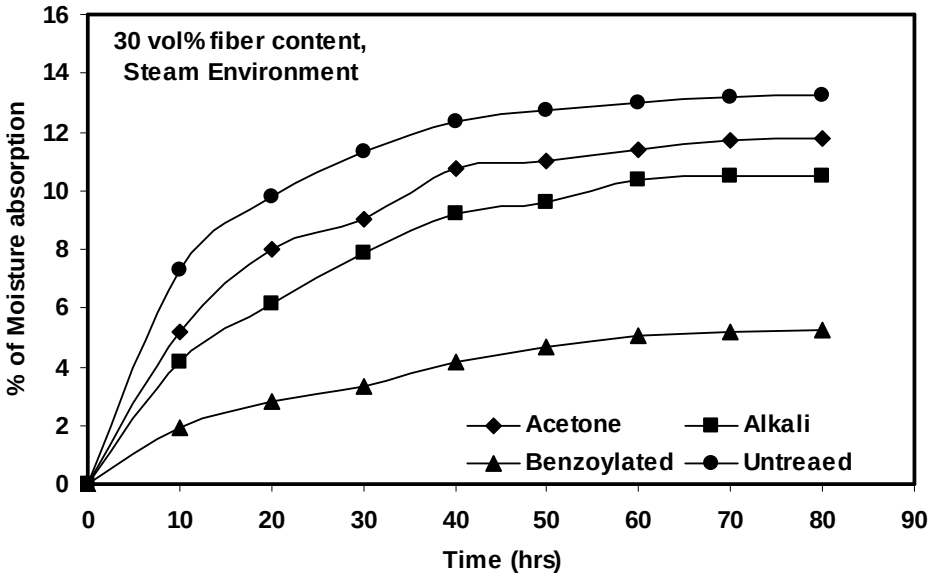

Figure-3.11 Variation of moisture absorption of the treated Lantana-Camara fiber epoxy composites with immersion time at steam environment

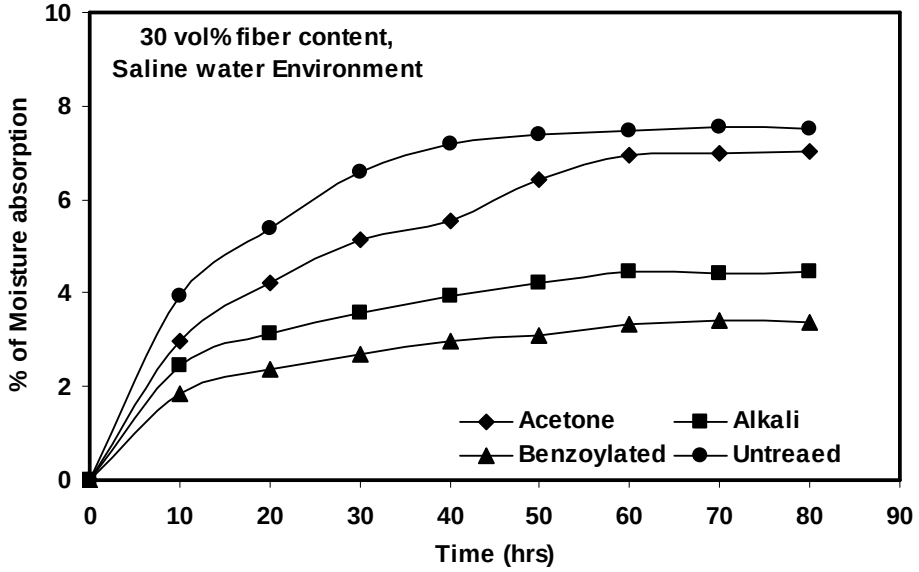

Figure-3.12 Variation of moisture absorption of the treated Lantana-Camara fiber epoxy composites with immersion time at saline water environment

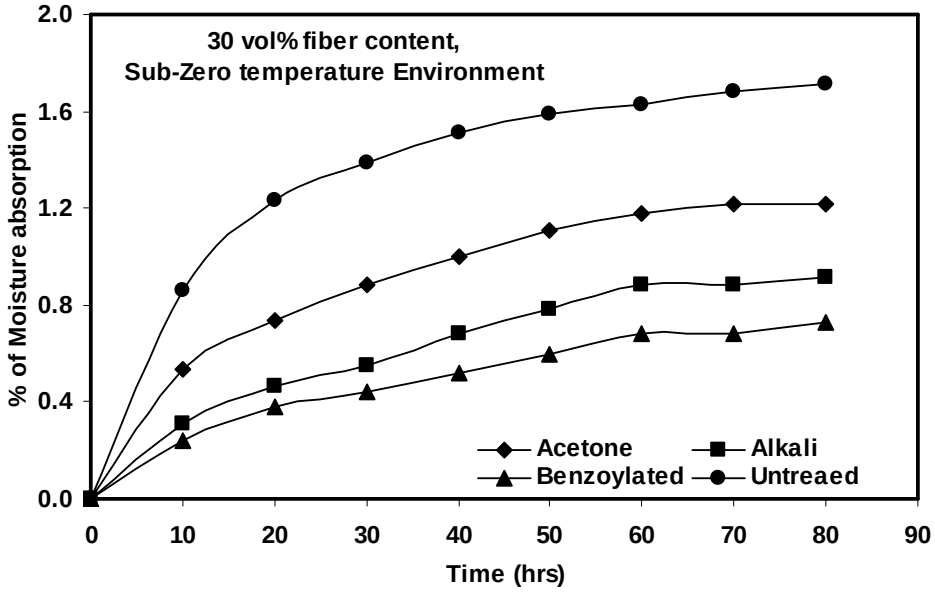

Figure-3.13 Variation of moisture absorption of the treated Lantana-Camara fiber epoxy composites with immersion time at sub-zero temperature environment

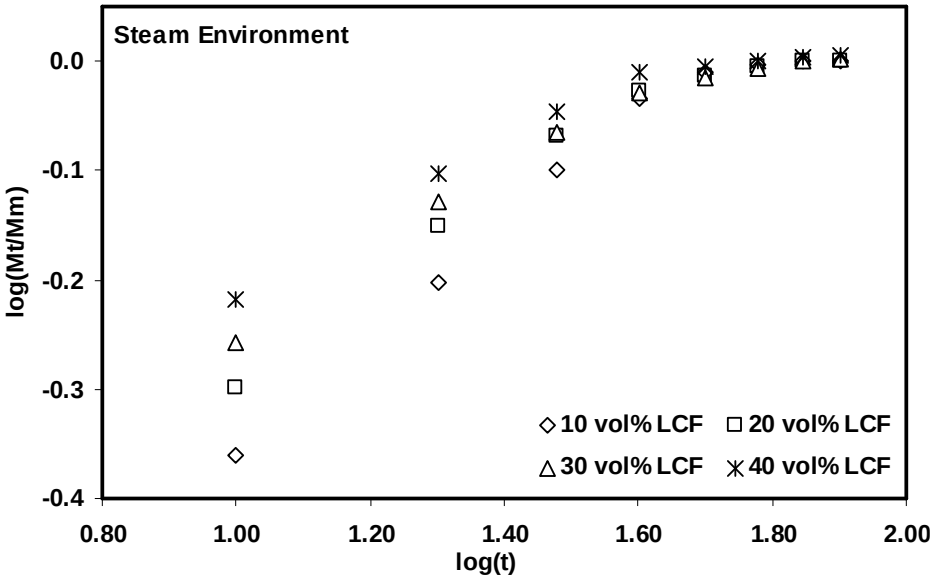

Figure-3.14 Variation of log ($M_t/M_{m)}$ with log (t) for untreated Lantana-Camara fiber epoxy composites at steam environment

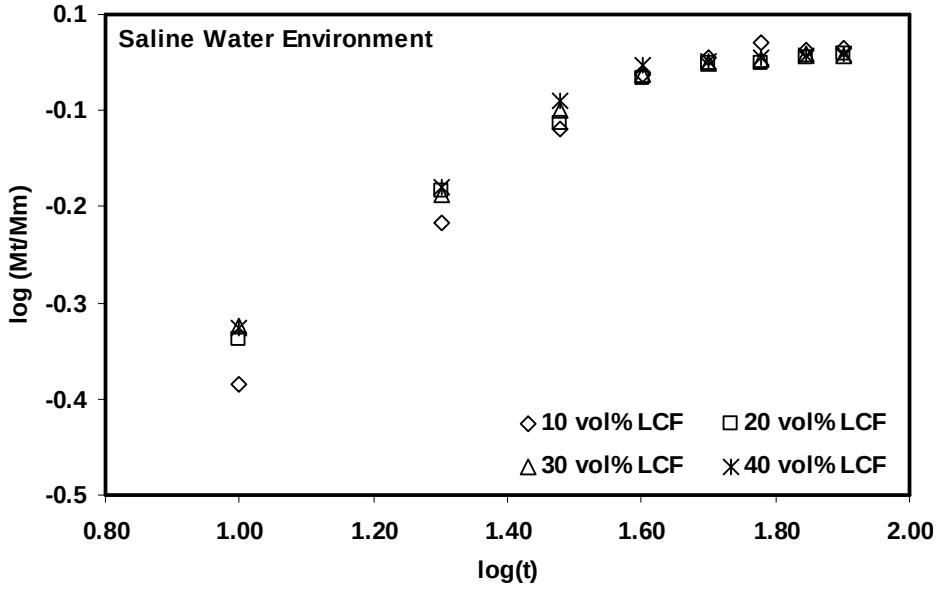

Figure-3.15 Variation of log ($M_t/M_{m)}$ with log (t) for untreated Lantana-Camara fiber epoxy composites at saline water environment

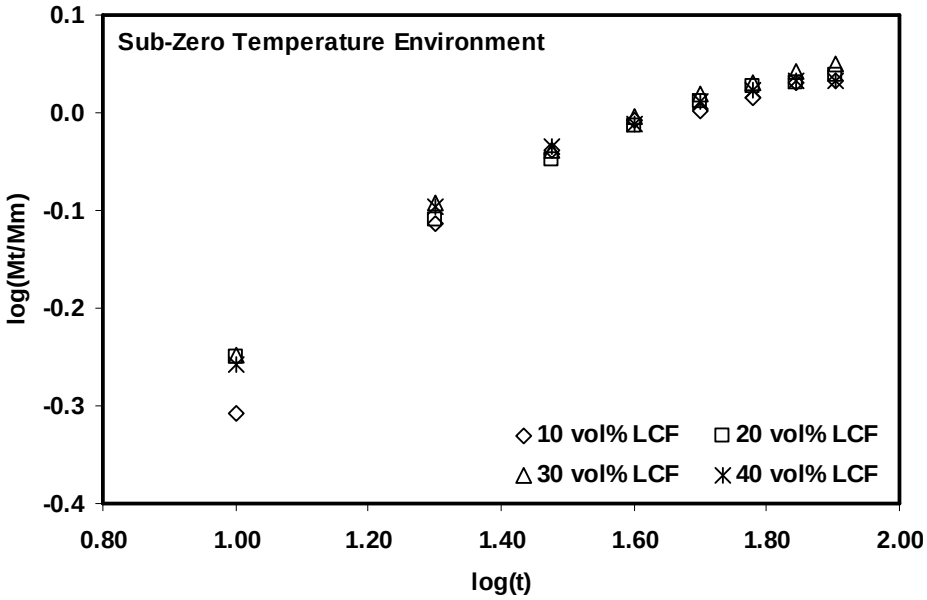

Figure-3.16 Variation of log ($M_t/M_{m)}$ with log (t) for untreated Lantana-Camara fiber epoxy composites at sub-zero temperature environment

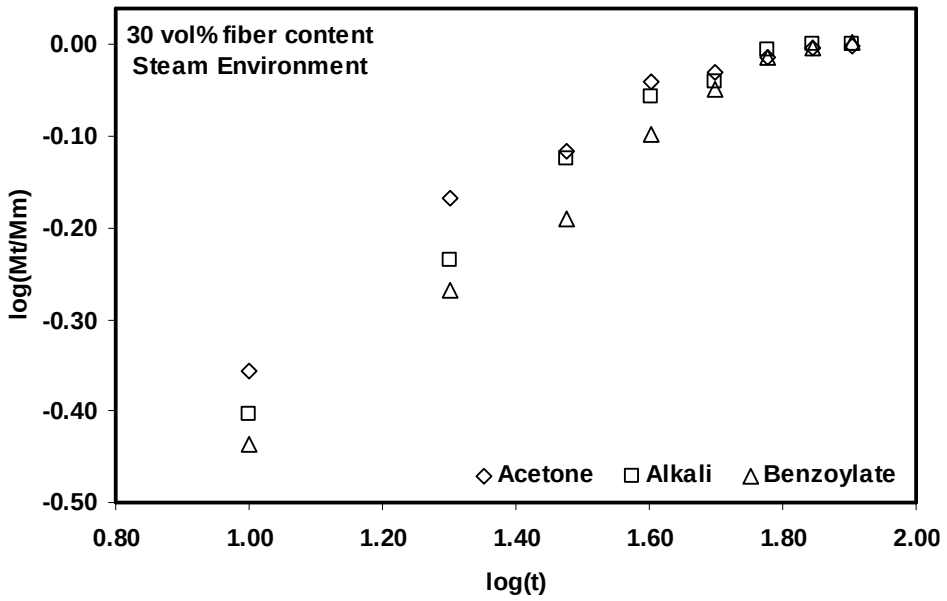

Figure-3.17 Variation of log ($M_t/M_{m)}$ with log (t) for treated Lantana-Camara fiber epoxy composites at steam environment

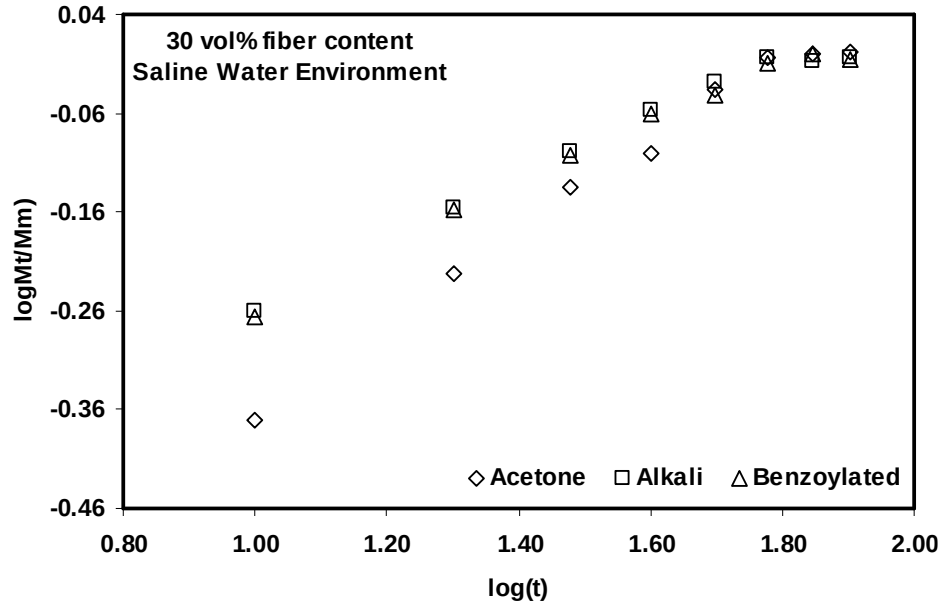

Figure-3.18 Variation of log ($M_t/M_{m)}$ with log (t) for treated Lantana-Camara fiber epoxy composites at saline water environment

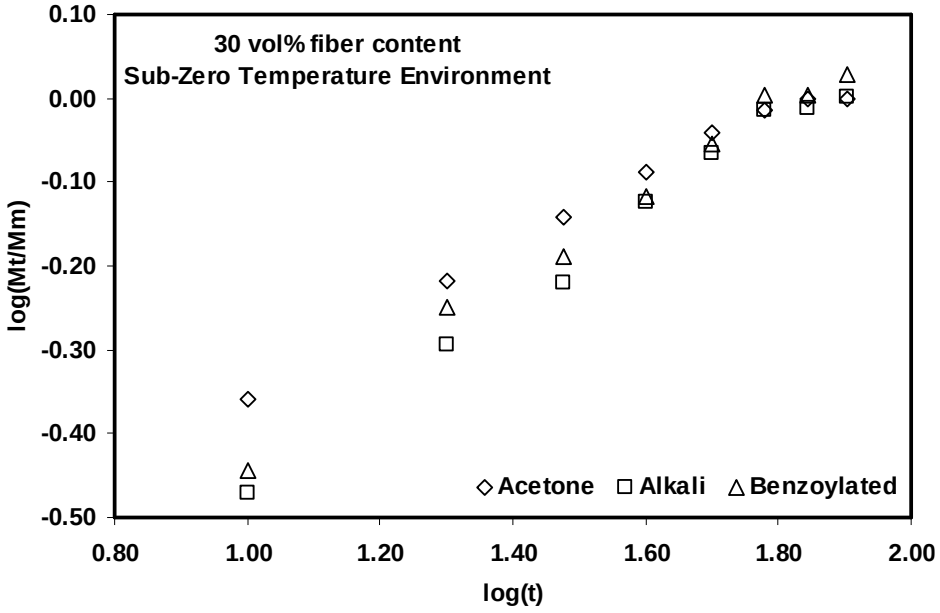

Figure-3.19 **Variation of log ($M_t/M_{m)}$ with log (t) for treated Lantana-Camara fiber epoxy composites at sub-zero temperature environment**

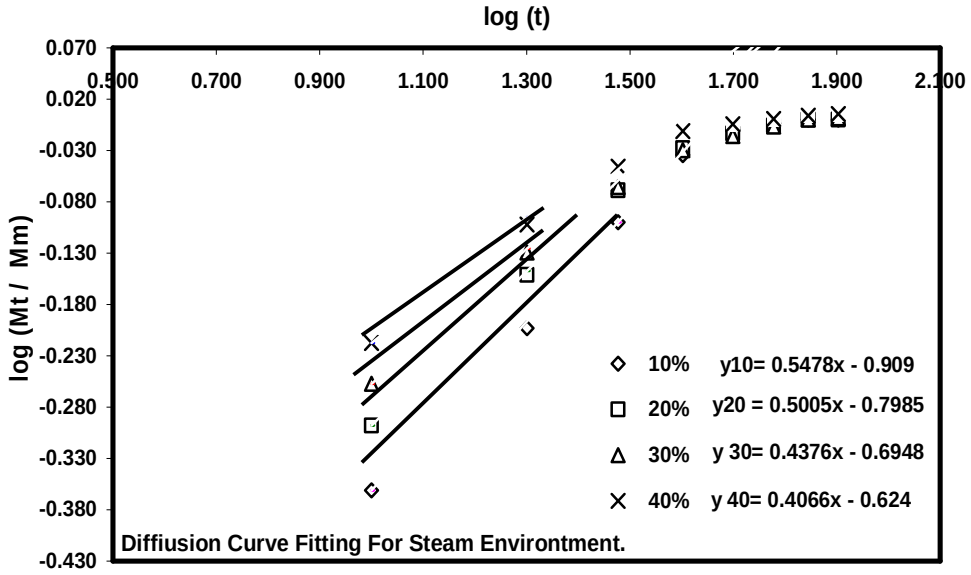

Figure-3.20 **Diffusion curve fitting for untreated Lantana-Camara fiber epoxy composites under Steam environment**

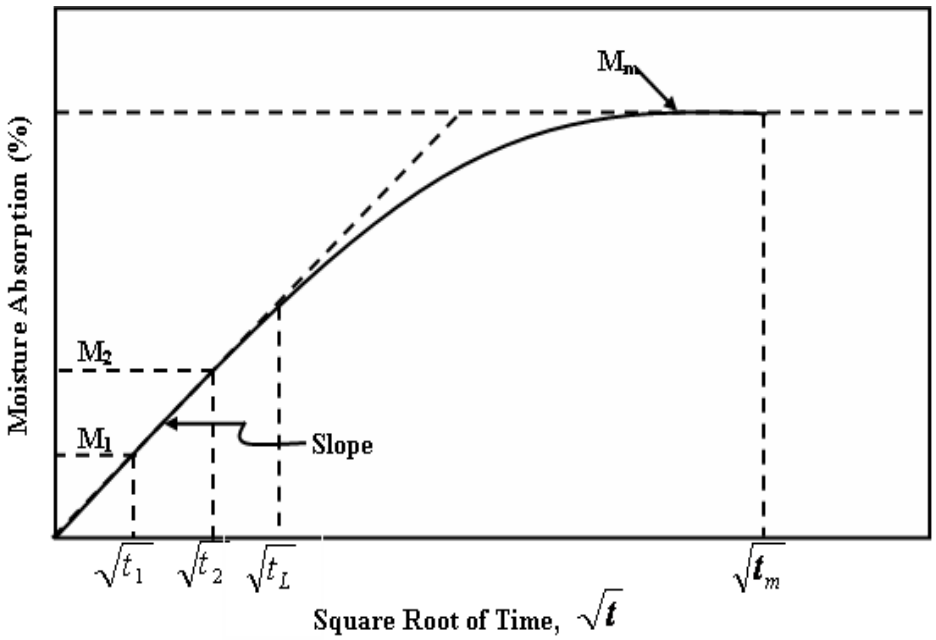

Figure-3.21 Example Plot of percentage of moisture absorption versus square root of time for calculation of Difusivity

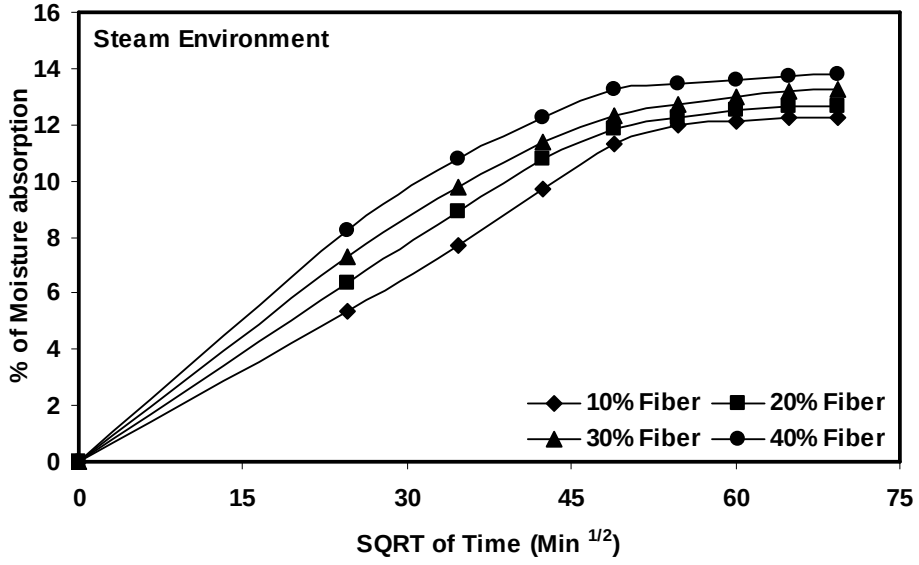

Figure-3.22 Variation of moisture absorption of untreated Lantana-Camara fiber epoxy composites with square root of immersion time at steam environment

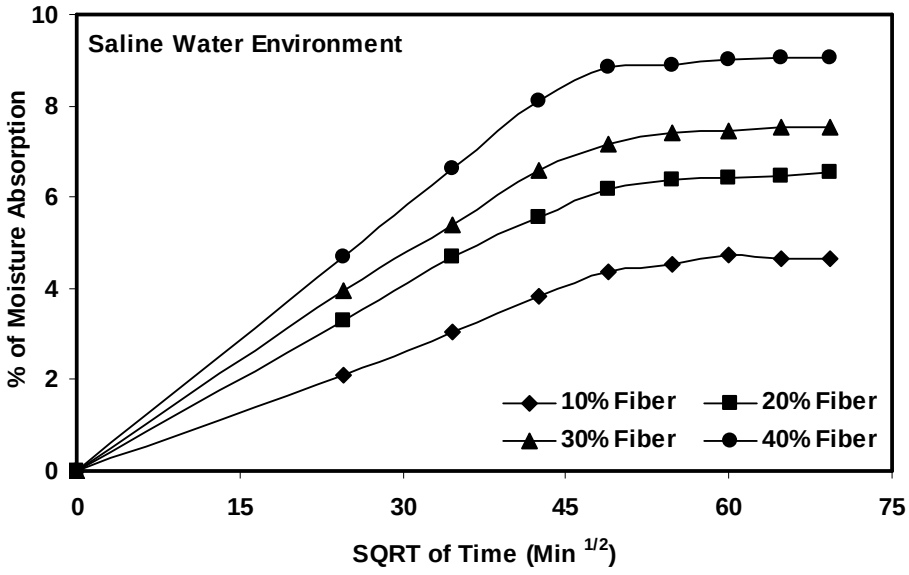

Figure-3.23 Variation of moisture absorption of untreated Lantana-Camara fiber epoxy composites with square root of immersion time at saline water environment

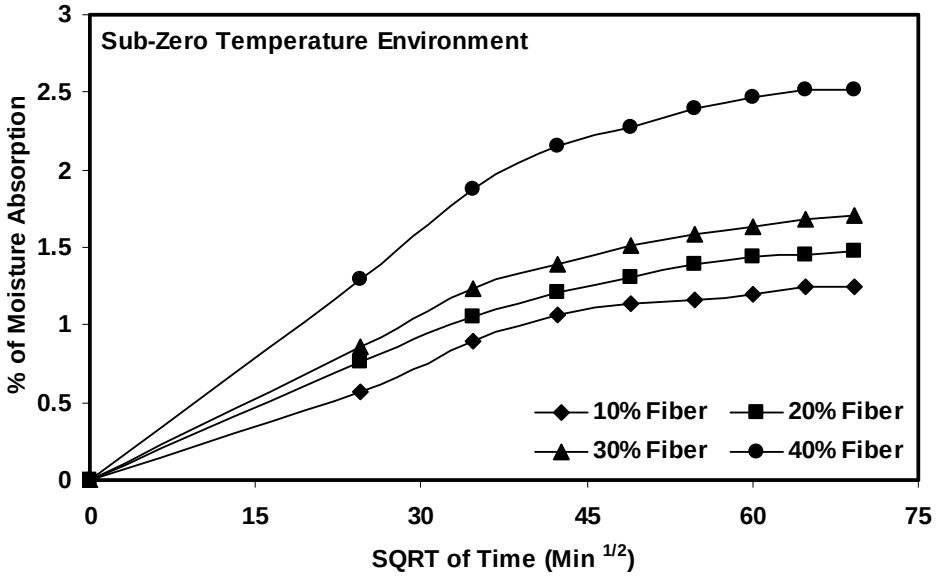

Figure-3.24 Variation of moisture absorption of untreated Lantana-Camara fiber epoxy composites with square root of immersion time at sub-zero temperature environment

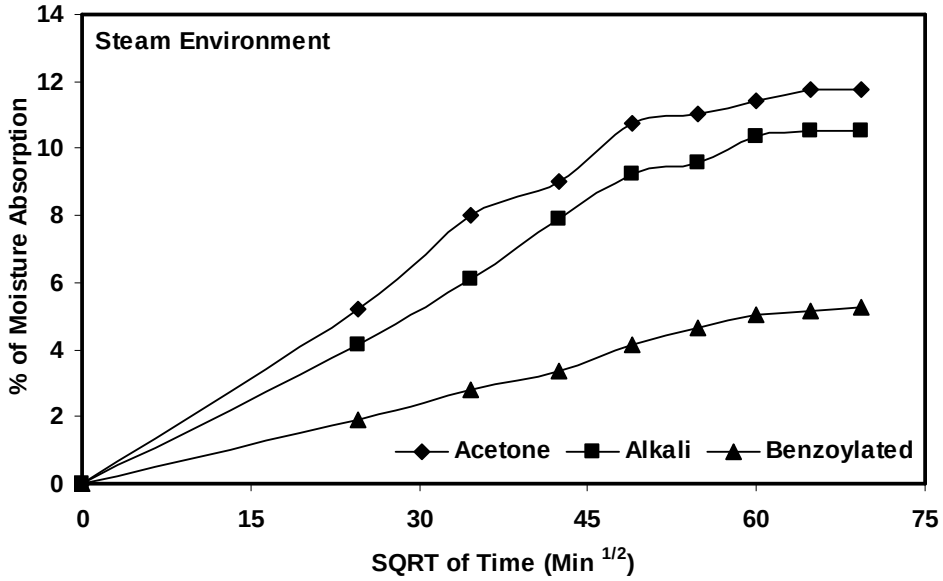

Figure-3.25 Variation of moisture absorption of treated Lantana-Camara fiber epoxy composites with square root of immersion time at steam environment

.

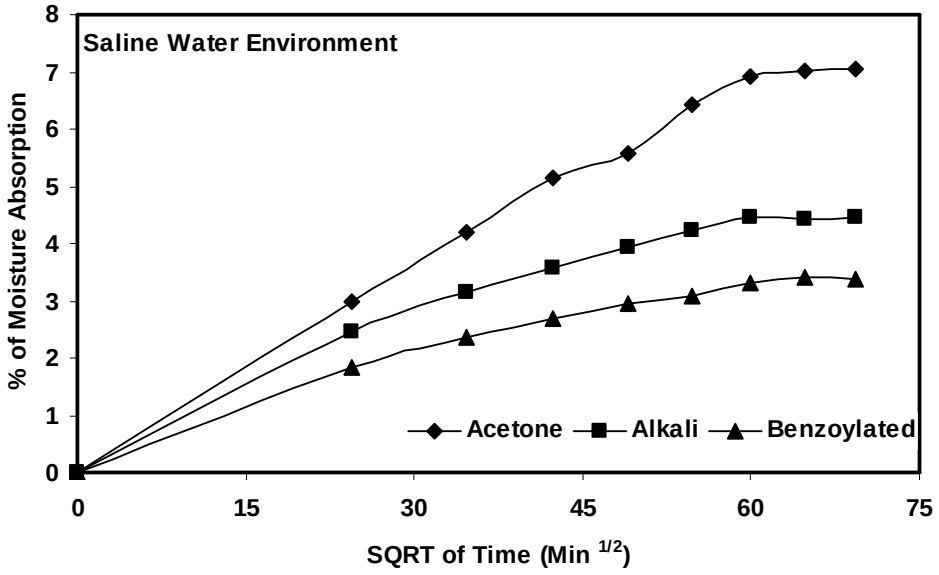

Figure-3.26 Variation of moisture absorption of treated Lantana-Camara fiber epoxy composites with square root of immersion time at saline water environment

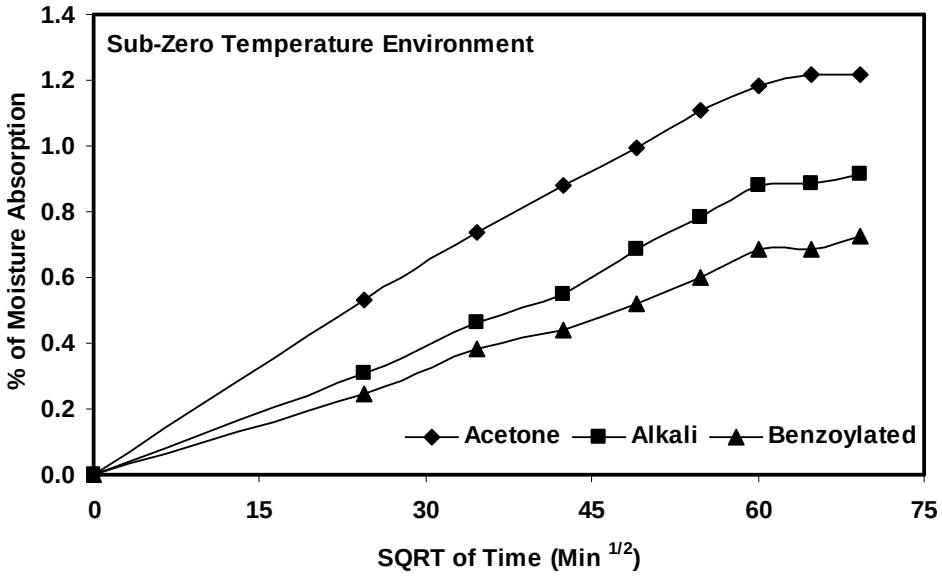

Figure-3.27 Variation of moisture absorption of treated Lantana-Camara fiber epoxy composites with square root of immersion time at sub-zero temperature environment

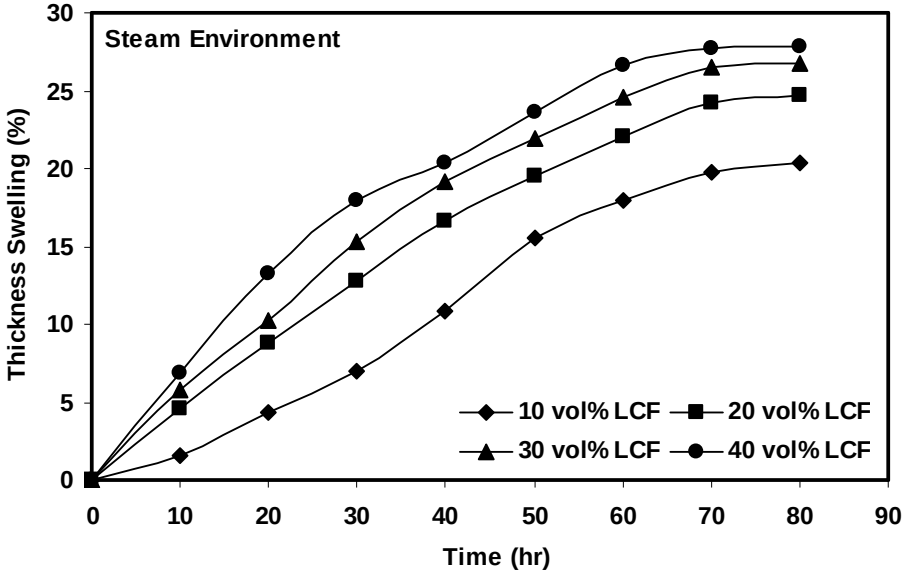

Figure-3.28 Variation of thickness swelling of untreated Lantana-Camara fiber epoxy composites with immersion time at steam environment

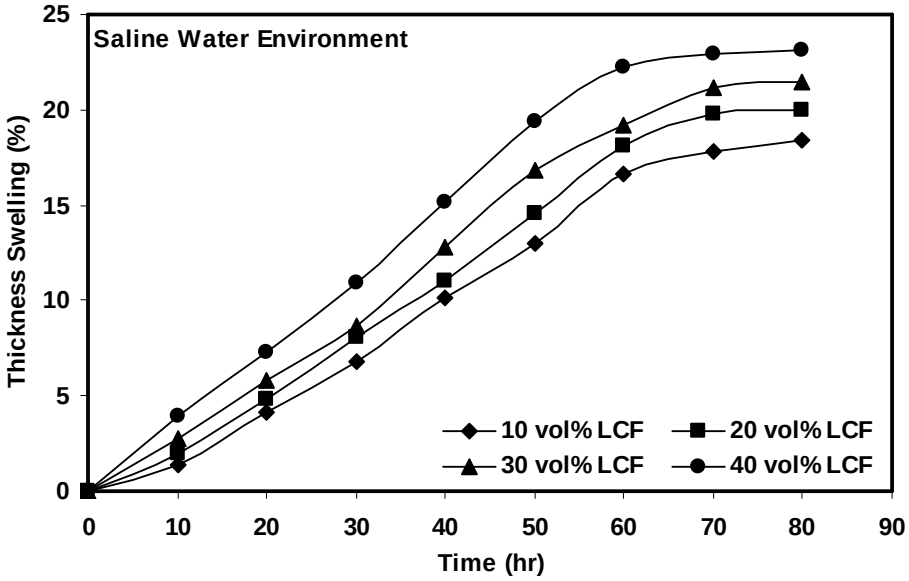

Figure-3.29 Variation of thickness swelling of untreated Lantana-Camara fiber epoxy composites with immersion time at saline water environment

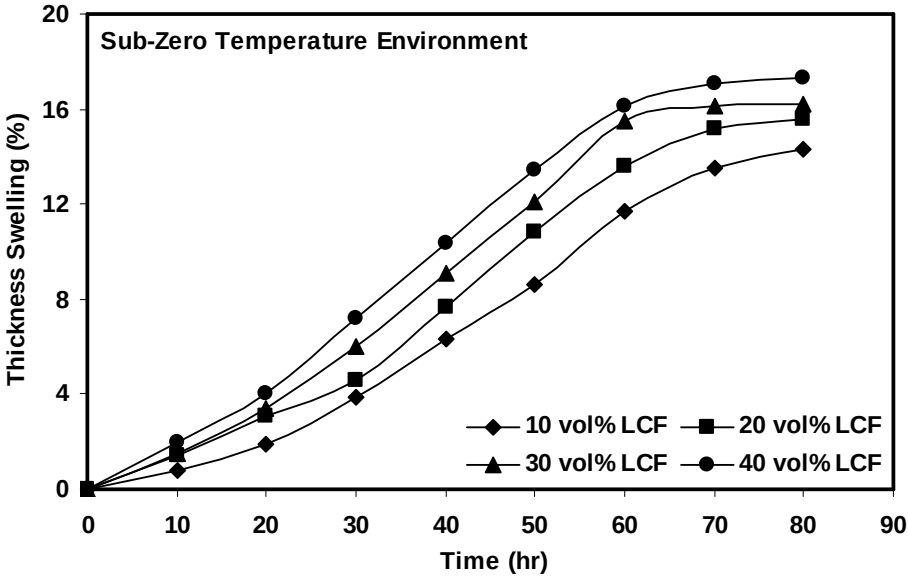

Figure-3.30 Variation of thickness swelling of untreated Lantana-Camara fiber epoxy composites with immersion time at sub-zero temperature environment

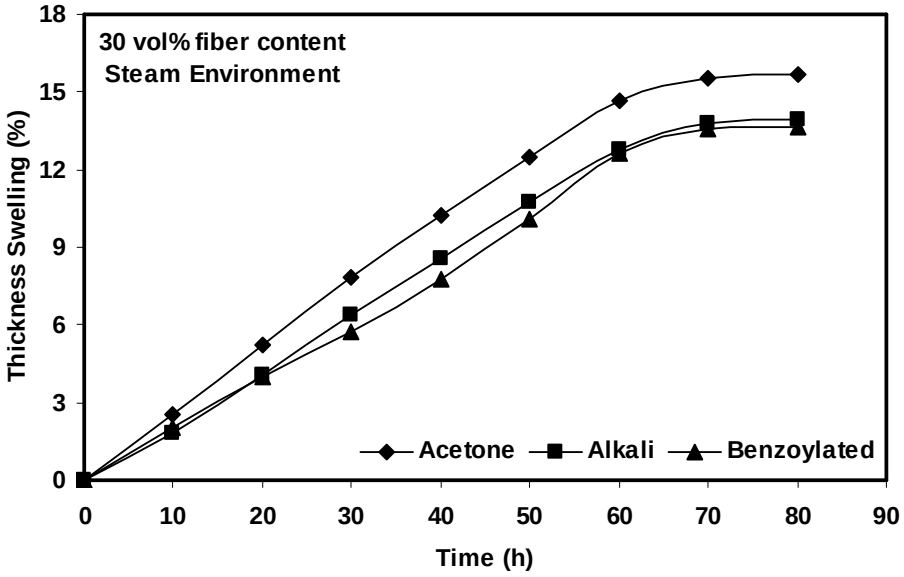

Figure-3.31 Variation of thickness swelling of treated Lantana-Camara fiber epoxy composites with immersion time at steam environment

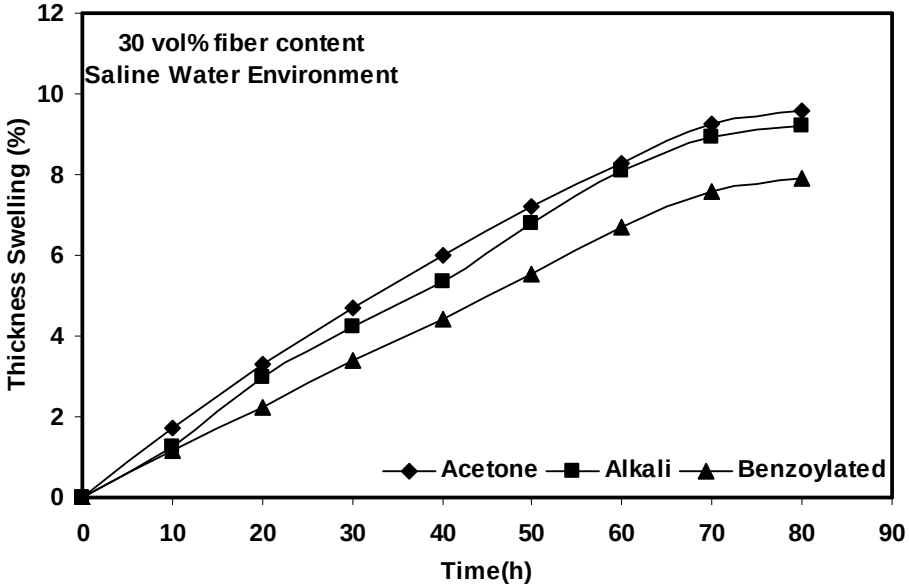

Figure-3.32 Variation of thickness swelling of treated Lantana-Camara fiber epoxy composites with immersion time at saline water environment.

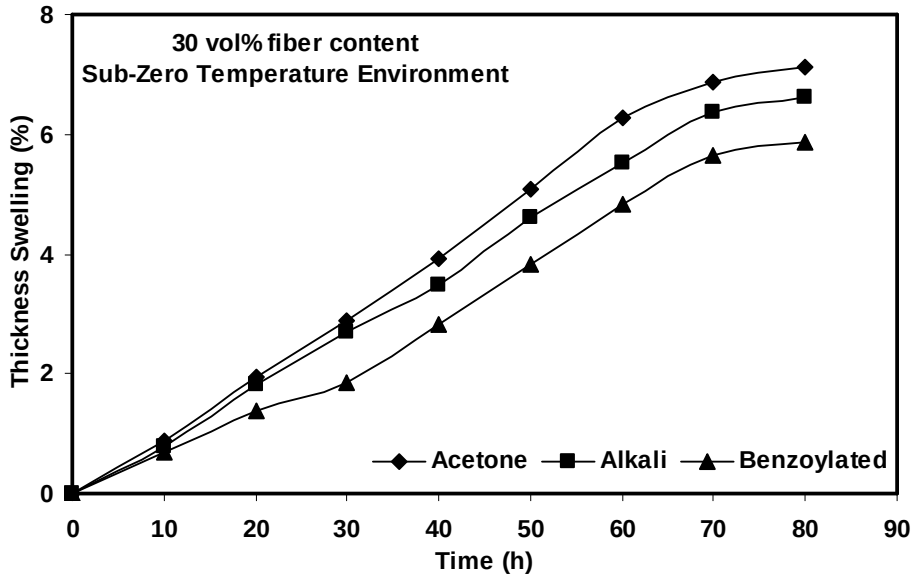

Figure-3.33 Variation of thickness swelling of treated Lantana-Camara fiber epoxy composites with immersion time at sub-zero temperature environment

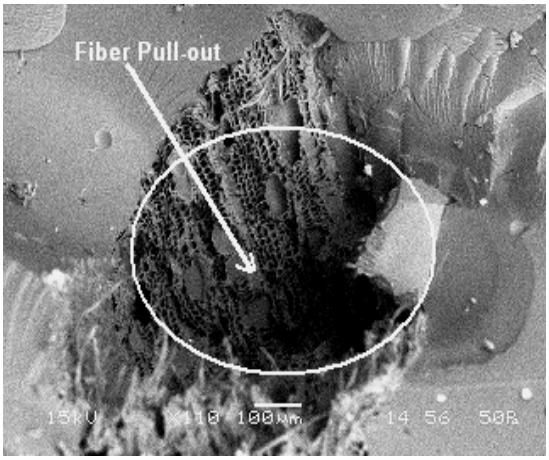

Figure-3.34 Magnified view of SEM micrograph of 30 vol% of untreated Lantana-Camara fiber epoxy composites subjected to tensile loads

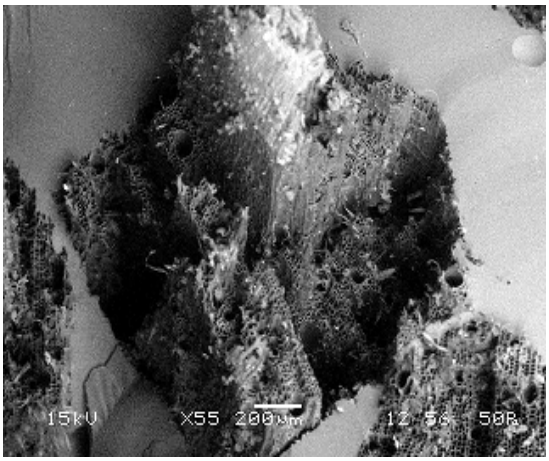

Figure-3.35 Magnified view of SEM micrograph of 30 vol% of acetone treated Lantana-Camara fiber epoxy composites subjected to tensile load

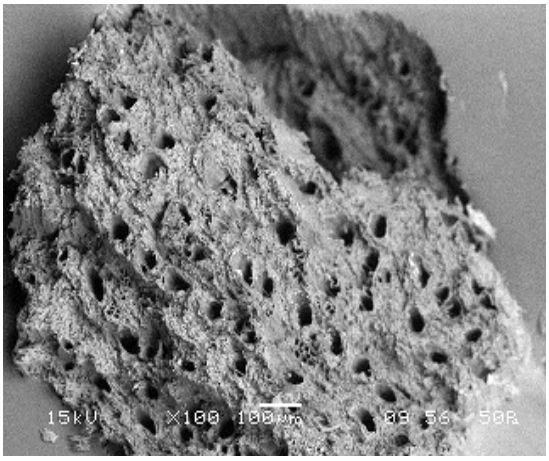

Figure-3.36 Magnified view of SEM micrograph of 30 vol% of alkali treated Lantana-Camara fiber epoxy composites subjected to tensile loads

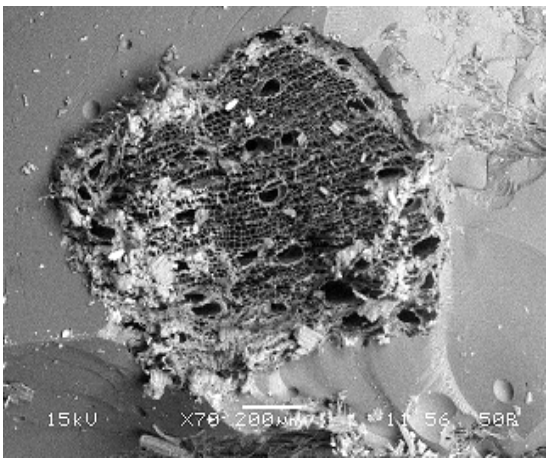

Figure-3.37 Magnified view of SEM micrograph of 30 vol% of benzoyl-chloride treated Lantana-Camara fiber epoxy composites subjected to tensile loads

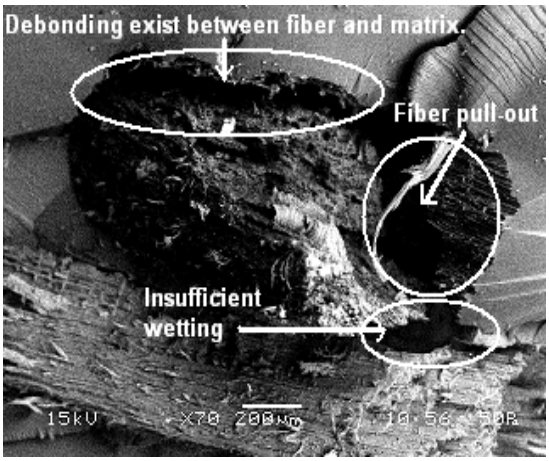

Figure-3.38 SEM micrograph of 40 vol% of untreated Lantana-Camara fiber epoxy composites subjected to three point bend test

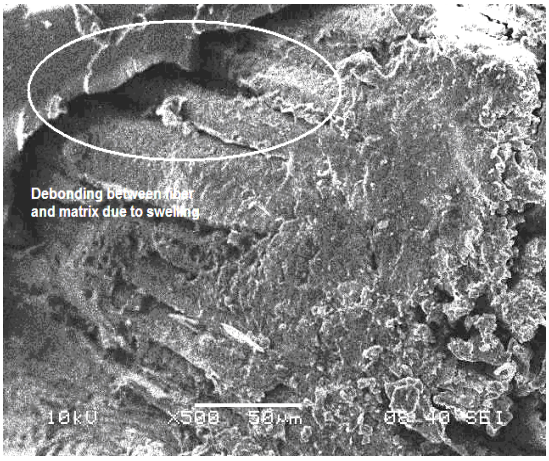

Figure-3.39 SEM micrograph of fracture surface steam exposed 20 vol% Lantana-Camara fiber epoxy composites subjected to three point bend test.

Chapter 4

ABRASIVE WEAR BEHAVIOUR OF LANTANA-CAMARA FIBER EPOXY COMPOSITES

Chapter-4

4.1 INTRODUCTION

Wear is probably the most important yet the least understood aspect of tribology. It is certainly the youngest of the tri of topics, friction, lubrication and wear, to attract scientific attention, although its practical significance has been recognizes throughout the ages. The findings of Guillaume Amontons in 1699 [131] establishing scientific studies of friction are almost of 300 years old, while Petrov [132], Tower [133] and Reynolds [134] brought enlightenment to the subject of lubrication a century ago in the hectic 1880s. Substantial Studies of wear can be associated only with the five decades that have elapsed since R. Holm [135] explored the fundamental aspects of surface interactions encountered in electrical contacts.

One third of our global energy consumption has been devoured wastefully in friction. In addition to the primary saving of energy, very significant additional economics can be made by the reduction of the cost involved in the manufacture and replacement of prematurely worn out components. The dissipation of energy by wear impairs strongly to the national economy and the life style of most of the peoples. So, the effective decrease and control of wear of metals are always desired [136].

Wear causes an enormous annual expenditure by industry and consumers. Most of this is replacing or repairing equipment that has worn to the extent that it no longer performs a useful function. For many machine components, this occurs after a very small percentage of the total volume has been worn away. For some industries, such as agriculture, as many as 40% of the components replaced on equipment have failed by abrasive wear. Other major sources of expenditure are losses of production consequent upon lower efficiency and plant shutdown, the need to invest more frequently in capital equipment and increased energy consumption as equipment wears. Estimates of direct cost of abrasive wear to industrial nations vary from 1 to 4 % of gross national product and Rigney [137] has estimated that about 10% of all energy generated by man is dissipated in various friction processes.

Wear is not an intrinsic material property but characteristics of the engineering system which depends on load, speed, temperature, hardness, presence of foreign material and the environmental condition [138]. Widely varying wear conditions cause wear of materials. It may be due to surface damage or removal of material from one or both of two solid surfaces in a sliding, rolling or impact motion relative to one another. In most cases wear occurs through surface interactions at asperities. During relative motion, material on contacting surface may be removed from a surface, may result in the transfer to the mating surface, or may break loose as a wear particle. The wear resistance of materials is related to its microstructure may take place during the wear process and hence, it seems that in wear research emphasis is placed on microstructure [139]. Wear of material depends on many variables, so a wear research program must be planned systematically. Therefore researchers have normalized some of the data to make them more useful. The wear map proposed by Lim [140] is very useful in this regard to understand the wear mechanism in different sliding conditions as well as the anticipated rates of wear.

4.2 RECENT TRENDS IN WEAR RESEARCH

Numerous wear researches have been carried out in the 1940's and 1950's by mechanical engineers and metallurgists to generate data for the construction of motor drive, trains, brakes, bearings, bushings and other types of moving mechanical assemblies [141].

It became apparent during the survey that wear of materials was a prominent topic in a large number of the responses regarding some future priorities for research in tribology. Some 22 experienced technologists in this field, who attended the 1983 'Wear of Materials Conference' in Reston, prepared a ranking list [142]. Their proposals with top priority were further investigations of the mechanism of wear and this no doubt reflects the judgments that particular effects of wear should be studied against a background of the basic physical and chemical processes involved in surface interactions. The list proposed is shown in Table- 4.1.

Peterson [6] reviewed the development and use of tribo-materials and concluded that metals and their alloys are the most common engineering materials used in wear applications. Grey cast iron for example has been used as early as 1388. Much of the wear

research conducted over the past 50 years is in ceramics, polymers, composite materials and coatings [143].

Table-4.1 Priority in wears research [142]

Ranking	Topics
1.	Mechanism of Wear
2.	Surface Coatings and treatments
3.	Abrasive Wear
4.	Materials
5.	Ceramic Wear
6.	Metallic Wear
7.	Polymer Wear
8.	Wear with Lubrication
9.	Piston ring-cylinder liner Wear
10.	Corrosive Wear
11.	Wear in other Internal Combustion Machine component

Wear of materials encountered in industrial situations can be grouped into different categories as shown in Table-4.2. Though there are situations where one type changes to another or where two or more mechanism plays together.

Table-4.2 Type of wear in industry [141]

Type of wear in Industry	Approximate percentage involved
Abrasive	50
Adhesive	15
Erosion	8
Fretting	8
Chemical	5

4.3 THEORY OF WEAR

Wear occurs as a natural consequence when two surfaces with a relative motion interact with each other. Wear may be defined as the progressive loss of material from contacting surfaces in relative motion. Scientists have developed various wear theories in which the Physico-Mechanical characteristics of the materials and the physical conditions (e.g. the resistance of the rubbing body and the stress state at the contact area) are taken in to consideration. In 1940 Holm [135] starting from the atomic mechanism of wear, calculated the volume of substance worn over unit sliding path.

Barwell and Strang [144] in 1952: Archard [145] in 1953 and Archard and Hirst [146] in 1956 developed the adhesion theory of wear and proposed a theoretical equation identical in structure with Holm's equation. In 1957, Kragelski [147] developed the fatigue theory of wear. This theory of wear has been widely accepted by scientists in different countries. Because of the Asperities in real bodies, their interactions in sliding is discrete, and contact occurs at individual locations, which, taken together, form the real contact area. Under normal force the asperities penetrate into each other or are flattened out and in the region of real contact points corresponding stress and strain rise. In sliding, a fixed volume of material is subjected to the many times repeated action, which weakens the material and leads finally to rupture. In 1973, Fleischer [148] formulated his energy theory of wear. The main concept of this theory is that the separation of wear particles requires that a certain volume of material accumulates a specific critical store of internal energy. It is known that a large part of the work done in sliding is dissipated as heat, and that a small proportion of it accumulates in the material as internal potential energy. When the energy attains a critical value, plastic flow of the material occurs in this volume or a crack is formed. Further theories of wear are found in [147]. Though all the theories are based on different mechanisms of wear, the basic consideration is the frictional work.

In past few decades, numerous research works have been carried out on abrasive wear performance of polymer and polymer based composite in view of their extensive application in the field industry and agricultural sectors where abrasive wear is a predominant mode of failure. Conveyor aids, vanes, gears, bushes, seals, bearings, chute liners etc. are some examples of their applications [149-153]. Since abrasive wear is the

most severe form of wear accounting for 50% of total wear, several researches have been devoted to exploring abrasive wear of polymer composites. Evans et al. [154] studied the abrasion wear behavior for 18 polymers and they noticed that low density polyethylene (LDPE) showed the lowest wear rate in abrasion against rough mild steel, but a higher wear rate in abrasion with coarse corundum paper. Unal et al. [155] studied abrasive wear behaviour of polymeric materials. They concluded that the specific wear rate decreases with the decrease in abrasive surface roughness. They also concluded that, the abrasive wear include micro-cracking, micro-cutting, and micro-ploughing mechanisms. Whereas in another investigation [156] they concluded that the sliding speed has a stronger effect on the specific wear rate. Shipway and Ngao [157] investigated the abrasive behaviour of polymeric materials in micro-scale level. They concluded that the wear behaviour and wear rates of polymers depended critically on the polymer type. Harsha and Tewari [158] investigated the abrasive wear behaviour of polyaryletherketone (PAEK) and its composites against SiC abrasive paper. They concluded that the sliding distance, load, abrasive grit size have a significant influence on abrasive wear performance. Further there are many references that illustrate the influence of fillers and fiber reinforcement on the abrasive wear resistance of polymeric composites. Cirino et al. [159, 160] investigated the sliding and abrasive wear behavior of polyetheretherketone (PEEK) with different continuous fiber types and reported that the wear rate decreases with increase in the fiber content. Chand et al. [161] studied low stress abrasive wear behavior of short E-glass fiber reinforced polymer composites with and without fillers by using rubber wheel abrasion test apparatus. They reported that higher weight fraction of glass fibers (45%) in the composites improves the wear resistance as compared to the composite containing less glass fibers (40%). Bijwe et al. [162] tested polyamide 6, polytetrafluoroethylene (PTFE) and their various composites in abrasive wear under dry and multi-pass conditions against silicon carbide (SiC) paper on pin-on-disc arrangement. They concluded that the polymers without fillers had better abrasive wear resistance than their composites. Liu et al. [163] investigated the abrasive wear behaviour of ultrahigh molecular weight polyethylene (UHMWPE) polymer. They concluded that the applied load is the main parameter and the wear resistance improvement of filler reinforced UHMWPE was attributed to the combination of hard particles which prevent the formation of deep, wide and continuous furrows.

With regards to the usage of natural fiber as reinforcement for tribological application in polymeric composite, few works have been attempted. However, in recent

years, some work has been done on natural fiber like jute [164], cotton [165, 166], sugarcane [16], oil palm [167], coir [168], kenaf [169], betel-nut [170], betel palm [171], wood flour [172] and bamboo powder [173] as reinforcement. In these works, the wear resistance of polymeric composites has been improved when natural fiber introduced as reinforcement.

4.4 TYPES OF WEAR

In most basic wear studies where the problems of wear have been a primary concern, the so-called dry friction has been investigated to avoid the influences of fluid lubricants.

Dry friction is defined as friction under not intentionally lubricated conditions but it is well known that it is friction under lubrication by atmospheric gases, especially by oxygen [174].

A fundamental scheme to classify wear was first outlined by Burwell and Strang [175]. Later Burwell [176] modified the classification to include five distinct types of wear, namely (1) Abrasive (2) Adhesive (3) Erosive (4) Surface fatigue (5) Corrosive.

4.4.1 Abrasive wear

Abrasive wear can be defined as the wear that occurs when a hard surface slides against and cuts groove from a softer surface. It can be account for most failures in practice. Hard particles or asperities that cut or groove one of the rubbing surfaces produce abrasive wear. This hard material may be originated from one of the two rubbing surfaces. In sliding mechanisms, abrasion can arise from the existing asperities on one surface (if it is harder than the other), from the generation of wear fragments which are repeatedly deformed and hence get work hardened for oxidized until they became harder than either or both of the sliding surfaces, or from the adventitious entry of hard particles, such as dirt from outside the system. Two body abrasive wear occurs when one surface (usually harder than the second) cuts material away from the second, although this mechanism very often changes to three body abrasion as the wear debris then acts as an abrasive between the two surfaces. Abrasives can act as in grinding where the abrasive is fixed relative to one surface or as in

lapping where the abrasive tumbles producing a series of indentations as opposed to a scratch. According to the recent tribological survey, abrasive wear is responsible for the largest amount of material loss in industrial practice [177].

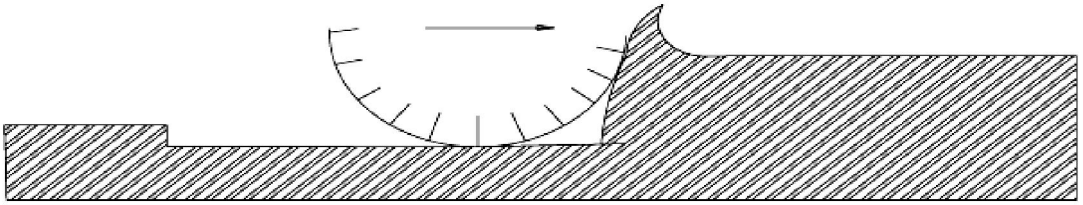

Figure-4.1 Schematic representations of the abrasion wear mechanism

4.4.2 Adhesive wear

Adhesive wear can be defined as the wear due to localized bonding between contacting solid surfaces leading to material transfer between the two surfaces or the loss from either surface. For adhesive wear to occur it is necessary for the surfaces to be in intimate contact with each other. Surfaces, which are held apart by lubricating films, oxide films etc. reduce the tendency for adhesion to occur.

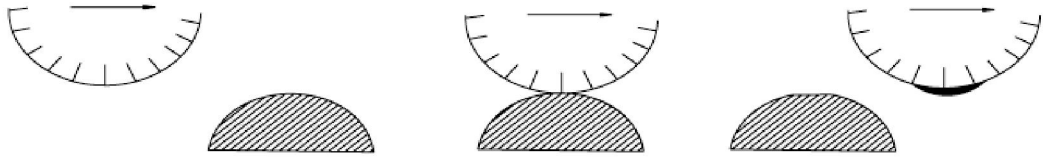

Figure-4.2 Schematic representations of the adhesive wear mechanism

4.4.3 Erosive wear

Erosive wear can be defined as the process of metal removal due to impingement of solid particles on a surface. Erosion is caused by a gas or a liquid, which may or may not carry, entrained solid particles, impinging on a surface. When the angle of impingement is small, the wear produced is closely analogous to abrasion. When the angle of impingement

is normal to the surface, material is displaced by plastic flow or is dislodged by brittle failure.

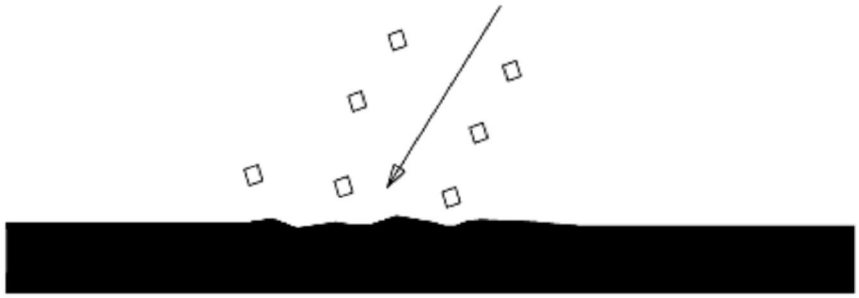

Figure-4.3 Schematic representations of the erosive wear mechanism

4.4.4 Surface fatigue wear

Wear of a solid surface is caused by fracture arising from material fatigue. The term 'fatigue' is broadly applied to the failure phenomenon where a solid is subjected to cyclic loading involving tension and compression above a certain critical stress. Repeated loading causes the generation of micro cracks, usually below the surface, at the site of a pre-existing point of weakness. On subsequent loading and unloading, the micro crack propagates. Once the crack reaches the critical size, it changes its direction to emerge at the surface, and thus flat sheet like particles is detached during wearing. The number of stress cycles required to cause such failure decreases as the corresponding magnitude of stress increases. Vibration is a common cause of fatigue wear.

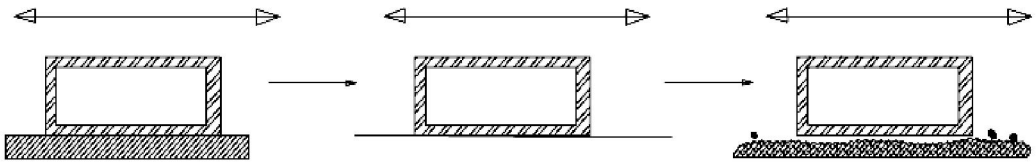

Figure-4.4 Schematic representations of the surface fatigue wear mechanism

4.4.5 Corrosive wear

Most metals are thermodynamically unstable in air and react with oxygen to form an oxide, which usually develop layer or scales on the surface of metal or alloys when their

interfacial bonds are poor. Corrosion wear is the gradual eating away or deterioration of unprotected metal surfaces by the effects of the atmosphere, acids, gases, alkalis, etc. This type of wear creates pits and perforations and may eventually dissolve metal parts.

4.5 SYMPTOMS OF WEAR

A summary of the appearance and symptoms of different wear mechanism is indicated in Table-4.3 and the same is a systematic approach to diagnose the wear mechanisms.

Table-4.3 Symptoms and appearance of different types of wear [178]

Types of wear	**Symptoms**	**Appearance of the worn-out surface**
Abrasive	Presence of clean furrows cut out by abrasive particles.	Grooves
Adhesive	Metal transfer is the prime symptoms.	Seizure, catering rough and torn-out surfaces.
Erosion	Presence of abrasives in the fast moving fluid and short abrasion furrows.	Waves and troughs.
Corrosion	Presence of metal corrosion products.	Rough pits or depressions.
Fatigue	Presence of surface or subsurface cracks accompanied by pits and spalls.	Sharp and angular edges around pits.
Impacts	Surface fatigue, small sub-micron particles or formation of spalls.	Fragmentation, peeling and pitting.
Delamination	Presence of subsurface cracks parallel to the surface with semi-dislodged or loose flakes.	Loose, long and thin sheet like particles
Fretting	Production of voluminous amount of loose debris.	Roughening, seizure and development of oxide ridges
Electric attack	Presence of micro craters or a track with evidence of smooth molten metal.	Smooth holes

Literature available on the rate of controlling abrasive wear mechanism demonstrate that it may change abruptly from one another at certain sliding velocities and contact loads, resulting in abrupt increases in wear rates. The conflicting results in the abrasive wear literature arise partly because of the differences in testing conditions, but they also make clear that a deeper understanding of the abrasive wear mechanism is required if an improvement in the wear resistances of the polymer matrix composites is to be achieved. This in turn requires a systematic study of the wear under different loads and velocities. It is generally recognized that abrasive wear is a characteristic of a system and is influenced by many parameters. Laboratory scale investigation if designed properly allows careful control of the tribo system where by the effects of different variables on wear behaviour of PMCs can be isolated and determined. The data generated through such investigation under controlled conditions may help in correct interpretation of the results.

As new developments are still under way to explore innovative fields for tribo-application of natural fiber base materials, in this chapter an attempt has been made to study the potential of using Lantana-Camara fiber (LCF) for tribological applications. In the current study the effect of fiber loading, sliding velocity and normal load on abrasive wear behaviour of chopped LCF field epoxy composite has been evaluated and possible wear mechanism has been discussed with SEM observation.

4.6 EXPERIMENT

4.6.1 Preparation for the test specimens

The weighted quantity of fibers (10, 20, 30, 40 and 50 vol %) were added to resin with required quantity of hardener. The procedure of mixing the resin, same and as per the procedure explained in chapter-3, Art-3.4.3. A steel mould has been designed and fabricated in the work-shop and used for preparation of cylindrical (pin) type specimen of length 35mm & diameter of 10 mm which is shown in Figure-4.5. The mixture of Lantana-Camara fiber and resin has been poured into the cylindrical cavity present in the mould and then the two halves of the mould are fixed properly. During fixing some of the resin mix may squeezed out. Adequate care has been taken for squeezing out of resin-mix during preparation of composites. After closing of the mould the specimens were allowed to

solidify in the mould at the room temperature for 24 hrs. For the purpose of comparison the matrix material was also cast under similar condition. After curing the samples were taken out from the mould, finished ground to required shape, sizes for wear testing.

4.6.2 Measurement of Density and Voids content

The density and the void content of composite sample have been determined as per ASTM-C 639 and ASTM D-2734-70 standard procedure respectively. The volume fraction of voids (V_v) in the composites was calculated by using equation:

$$V_v = \frac{\rho_t - \rho_a}{\rho_t} \tag{4.1}$$

where ρ_t and ρ_a are the theoretical and actual density of composite respectively.

4.6.3 Dry sliding wear test

Dry sliding wear test has been carried out under multi-pass condition on a pin-on-disc type wear testing machine (As per ASTM G-99 standard) supplied by Magnum Engineers, Bangalore (Figure-4.6). Abrasive paper of 400 grade (grit-23 μm) has been pasted on a rotating disc (EN 31 Steel disc) of 120mm diameter using double-sided adhesive tape. The specimens under tests were fixed to the sample holder. The holder along with the specimen (Pin) was positioned at a particular track diameter. This track diameter is to be changed after each test (i.e.) a fresh track is to be selected for each specimen. A track radius of 100mm was selected for this experiment and was kept constant for the entire investigation. For each test new abrasive paper was used and the sample was abraded for a total sliding distance of 471.25m. During experiment the specimen remains fixed and disc rotates. Load is applied through a dead weight loading system to press the pin against the disc. The speed of the disc or motor rpm can be varied through the controller and interval of time can be set by the help of timer provided at the control panel. The mass loss in the specimen after each test was estimated by measuring the weight of the specimen before and after each test using an electronic balance with an accuracy of ± 0.001 mg. care has been taken that the specimen under test are continuously cleaned woolen cloth to avoid

entrapment of wear debris and achieve uniformity in the experimental procedure. Test pieces are cleaned with acetone prior and after each test. The machine is fixed with data acquisition system with 'MAGVIEW-2007' software from which the frictional force that arises at the contact can be read out/recorded directly. The test under which the experiment has been carried out is given in Table-4.5. For a particular type of composite 25 sets of test pieces were tested.

4.6.4 Calculation for Wear

Wear rate was estimated by measuring the weight loss of the specimen after each test. The weight loss was calculated by taking the weight difference of the sample before and after each test. The weight loss:

$$(\Delta w) = (w_a - w_b) \text{ gm} \tag{4.2}$$

where Δw is the weight loss in gm and w_a and w_b are the weight of the sample after and before the abrasion test in gm. The abrasive wear rate (W) can be calculated by using the following formula:

$$W = \frac{\Delta w}{(\rho \times S_d)} \tag{4.3}$$

where 'W' is the wear rate in cm^3/m, 'ρ' is the density of the composite, Δw *the* weight loss in gm and 'S_d' is the sliding distance in m. The average value of weight loss and wear rate for each batch is listed in Table-4.6 to 4.35. For characterization of the abrasive wear behaviour of composite, the specific wear rate is employed. This is defined as the volume loss of the composite per unit sliding distance and per unit applied load. Often the inverse of the specific wear rate can be expressed in terms of volumetric wear rate. The specific wear rate (k_0) can also be calculated by using equation:

$$k_0 = \frac{\Delta w}{(\rho \times S_d \times L)} \tag{4.4}$$

where 'k_0' is the specific wear rate in m^3/Nm, 'Δw' is the weight loss in grams, 'S_d' is the sliding distance in meter, and 'L' is the applied load in N.

4.7 RESULTS AND DISCUSSION

Based on the experiment and tabulated results, various graphs are plotted and presented in Figure-4.7 to 4.34 for different percentage of reinforcement under different test conditions.

As seen from Table-4.4, the density of the composite has increased with fiber content. The neat epoxy taken for this study possess a density of 1.082 gm/cc which increases to 1.115 gm/cc (with a void fraction of 3.498%) with the reinforcement of 50 vol% of LCF in it. It is also noticed that void fraction of composites increases from 10 vol% to 50 vol% fiber reinforcement.

The influence of normal loads on the abrasive wear rate of the un-reinforced and reinforced composites for different sliding velocities are shown in Figures-4.7 to 4.11. It has been observed that irrespective of sliding velocity the wear rate of all composite samples increases with normal load. This is because at higher load, the frictional thrust increases, which results in increased debonding and fracture. A similar effect of normal load on volumetric wear rate has been observed by Cirino et.al. [159] in the case of carbon epoxy composite and Verma et. al. [179] for GRP composite. It has also been observed that the abrasive wear rate decreases with addition of Lantana-Camara fiber up to 40vol% under all testing condition. Thus it can be conclude, addition of the Lantana-Camara fiber in epoxy is very effective in improving its wear resistance. Further increase in fiber content (50 vol %) wear rate again increases. This increase in wear rate for higher volume fraction of fiber (50 vol %) might have happened due to agglomeration of fibers in the composite, which leads to poor interfacial adhesion between the fiber and the matrix. Similar type of behavior was reported by Wu and Cheng [180], while they studied the tribological properties of Kevlar pulp reinforced epoxy composites.

Figure-4.12 illustrates the effect of sliding velocity on the abrasive wear behaviour of 40 vol% fiber reinforced composite under different normal loads (5N to 25N). It is clear from the plot that the abrasive wear rate of the composite increases with increase in sliding velocity at all normal loads. It is also seen that when the load increases from 5 to 25N the percentage of increase in wear rate is about 48.7%. But when the velocity increases from

0.157m/s to 0.470m/s the percentage increase in wear rate is as high as 126%. Hence it can be conclude that, the abrasive wear of LCF epoxy composite is very much sensitive to the normal load than the sliding velocity. Since similar trend has been observed for all other reinforcement, it has not been presented here for those cases.

The assessments of specific wear rate (k_0) with different sliding distance under the aforesaid testing conditions are reported in Table-4.11 to 4.35. Using these data, Figures-4.13 to 4.17 have been plotted to explain the variation of specific wear rate (k_0) with sliding distance at normal load 25N. It has been observed that the specific wear rate decreases with increasing sliding distance for all the samples under all sliding velocities. Further it has been observed from the tabulated results that, in all case the range of specific wear rate is high at the initial stage of sliding distance and achieved a steady state at a distance of about 282.75 m. In other words, there is less removal of material at longer sliding distances and this could be due to the less penetration of abrasive particle in to the composite sample. Because at initial stage the abrasive paper is fresh and then become smooth due to filling of the space between abrasives by wear debris, which consequently reduce the depth of penetration. It is also observed that the 40vol% LCF reinforced composite shows a minimum specific wear rate under all testing conditions. This again reveals that the addition of Lantana-Camara fiber can improve the wear resistance capacity of epoxy.

Figures-4.18 to 4.22 shows the variation of wear rate with sliding distance for different applied loads (5N to 25N). It is seen from the plots that, with addition of Lantana-Camara fiber the wear rate of epoxy decrease. Also as the sliding distance increases the wear rate first decreases and then almost remains same for the entire test period. Since the trend is same for other sliding velocities, it has not been presented here.

Figures-4.23 to 4.27 shows the variation of specific wear rate with fiber volume fraction i.e. Lantana-Camara fiber. It is clear from the plot that, irrespective of sliding velocity the specific wear rate decreases with increase in fiber volume fraction and after attaining a minimum value at 40%, it then increases with increase in fiber volume fraction up 50%. Thus it can be concluded here that the optimum fiber volume fraction for the composite is 40%, which gives maximum wear resistance to the composite.

Figures-4.28 to 4.32 shows variation of specific wear rate with sliding velocity. The plot shows that the specific wear rate of the composite increases with increase in sliding velocity. It is also clear from the plot that specific wear rate for 40 vol % Lantana-Camara fiber reinforced composite is the lowest. For 50 vol % Lantana-Camara fiber reinforced composite, it is higher than 40 vol %. This is somewhat related to the results projected in Figures-4.23 to 4.27.

With the help of on-line data acquisition system, the variation of coefficient of friction (μ) data with time for all samples has been acquired and analyzed through MAGVIEW-2007 software. The variation of friction coefficient of neat epoxy and 10vol% to 50vol % Lantana-Camara fiber reinforced epoxy composite samples at 25N of applied load and sliding velocity of 0.314m/s are shown in Figure-4.33 & Figure-4.34. From both the figures it has been observed that the friction coefficient increased from a low value to a nearly stabilized value with time. Therefore the initial part of graph has been considered as pre-equilibrium state for a particular set of test parameters. Again reduction in friction coefficient is also noticed with addition of Lantana-Camara fiber. The 40vol% reinforced Lantana-Camara fiber composite shows the best friction performance (minimum coefficient of friction), where as the neat epoxy shows the worst. This attribute to the fact that the incorporation of Lantana-Camara fiber in to epoxy matrix may effectively improve tribo-performance. A similar trend was reported by Chand et al. [166] while studying the tribological properties graphite modified cotton fiber reinforced polyester composites. In all other testing conditions, similar observations are found; hence these are not illustrated here.

4.8 WORN SURFACE MORPHOLOGY

The worn surface morphologies of neat epoxy and its composites have been examined by scanning electron microscopy (SEM). The worn surfaces of neat epoxy samples are shown in Figure-4.35 (a) and (b). The removal of debris of brittle fragmented matrix forms the wear tracks has been observed in Figure-4.35(a). In addition to this plastic deformation and adherence are also noticed at higher load of 25N on the worn surface of neat epoxy [Figure-4.35 (b)]. This might have happened due to thermal softening effect because of generation of high frictional heat at sliding surface under higher normal load. The filling of space between the abrasives by the wear debris formed during abrasion with

consecutive runs can be seen in Figure-4.35 (c). This makes abrasive grits smooth and reduces the penetration of abrasive to composite. The fiber surface detoriation under 20N load of 10vol% reinforcement is clearly illustrated in Figure-4.35 (d). It has been observed from this figure that some of the fiber tissues are sheared and becomes loose. In addition to this the extent of damage and the fiber stripping are more pronounced without any fiber pullout. This reveals a good interaction between matrix and fiber. Figure-4.35 (e) shows the worn surface of Lantana-Camara fiber epoxy composite sample with 40 vol% fiber under 15N load. There is no indication of plastic deformation and adherence, whereas the worn surface is characterized by furrows. This indicates that the applied load is mainly borne by Lantana-Camara fiber and the wear resistance has been greatly improved with fibers reinforcement. Further appearance of deep wear grooves on the worn surface of 50 vol% of fiber composite sample under 15N load due to relatively poorer interfacial has also been noticed [Figure-4.35 (f)]. Along with this drawing out of fiber bundles from the worn surface is also observed. This might be the main cause for resulting maximum wear at higher fiber content.

4.9 CONCLUSIONS

Based on experimental results of abrasive wear of Lantana-Camara fiber epoxy composite tested under different normal loads, sliding velocity and sliding distances, the following conclusions have been drawn:

- Lantana-Camara fiber reinforced epoxy composite have been successfully fabricated with fairly uniform distribution of fibers.

- Dispersion of fibers in the matrix improves the hardness of matrix material and also the wear behaviour of composite. The effect is increases in interfacial area between the matrix and the fiber leading to increase in strength.

- The abrasive wear rate is found more sensitive to normal load in comparison to sliding velocity and it also increase marginally with increase in sliding velocity.

- The specific wear rate of composite decreases with addition of fiber. In this present study, the optimum volume fraction which gives maximum wear resistance to the composite is found to be 40 volume percent.

- Coefficient of friction decreases as the fiber volume fraction increases.

- Fragmentation, adherence and plastic deformation are primary wear mechanisms for the neat epoxy. However the addition of Lantana-Camara fiber reduces this adherence and plastic deformation to a great extent. The worn surface of Lantana-Camara fiber epoxy composite is characterized by furrows.

Table-4.4 Density and voids content of neat epoxy and LCF reinforced composite samples

Fiber content (%)	Measured Density (gm/cm^3)	Theoretical Density (gm/cm^3)	Volume fraction of voids (%)
0	1.082	1.100	1.636
10	1.086	1.110	2.190
20	1.093	1.121	2.546
30	1.101	1.132	2.775
40	1.107	1.142	3.204
50	1.115	1.154	3.498

Table-4.5 Test parameter for Dry Sliding wear test

Test Parameters	Units	Values
Load (L)	N	5, 10, 15, 20, and 25
Sliding Velocity (v)	m/s	0.157 (interval of time is 10 minutes), 0.235 ((interval of time is 6 minutes 40seconds), 0.314 (interval of time is 5 minutes), 0.392 (interval of time is 4 minutes) and 0.470 (interval of time is 3minutes 20seconds)
Track radius (r)	mm	50
Temperature	^0C	20

Table-4.6 Weight loss (Δw), Wear rate (*W*) and Specific wear rate (k_0) of tested composite samples for Sliding velocity =0.157m/s, Sliding distance =471.25m

Fiber content (vol %)	Load (N)	(Δw) (gm)	$W \times 10^{-10}$ (m^3/m)	$k_0 \times 10^{-11}$ ($m^3/N.m$)
0	5	0.206	4.045	8.090
	10	0.265	5.201	5.201
	15	0.285	5.585	3.723
	20	0.296	5.801	2.901
	25	0.336	6.585	2.634
10	5	0.167	3.263	6.526
	10	0.211	4.123	4.123
	15	0.220	4.299	2.866
	20	0.225	4.396	2.198
	25	0.234	4.572	1.829
20	5	0.099	1.922	3.844
	10	0.126	2.446	2.446
	15	0.160	3.106	2.071
	20	0.177	3.436	1.718
	25	0.189	3.669	1.468
30	5	0.083	1.600	3.199
	10	0.096	1.850	1.850
	15	0.110	2.120	1.413
	20	0.126	2.428	1.214
	25	0.147	2.833	1.133
40	5	0.055	1.054	2.109
	10	0.060	1.150	1.150
	15	0.083	1.591	1.061
	20	0.098	1.879	0.939
	25	0.119	2.281	0.912
50	5	0.093	1.770	3.540
	10	0.117	2.227	2.227
	15	0.152	2.893	1.929
	20	0.171	3.254	1.627
	25	0.195	3.711	1.484

Table-4.7 Weight loss (Δw), Wear rate (*W*) and Specific wear rate (k_0) of tested composite samples for Sliding velocity =0.235, Sliding distance =471.25m

Fiber content (vol %)	Load (N)	(Δw) (gm)	$W\times 10^{-10}$ (m^3/m)	$k_0\times 10^{-11}$ ($m^3/N.m$)
0	5	0.227	4.452	8.904
	10	0.274	5.374	5.374
	15	0.296	5.805	3.870
	20	0.313	6.139	3.069
	25	0.352	6.903	2.761
10	5	0.208	4.064	8.129
	10	0.265	5.178	5.178
	15	0.206	4.025	2.683
	20	0.248	4.846	2.423
	25	0.233	4.553	1.821
20	5	0.111	2.155	4.310
	10	0.138	2.679	2.679
	15	0.189	3.669	2.446
	20	0.177	3.436	1.718
	25	0.212	4.116	1.646
30	5	0.087	1.677	3.354
	10	0.088	1.696	1.696
	15	0.125	2.409	1.606
	20	0.127	2.448	1.224
	25	0.141	2.718	1.087
40	5	0.063	1.208	2.415
	10	0.078	1.495	1.495
	15	0.104	1.994	1.329
	20	0.121	2.319	1.160
	25	0.118	2.262	0.905
50	5	0.087	1.656	3.311
	10	0.123	2.341	2.341
	15	0.172	3.273	2.182
	20	0.174	3.311	1.656
	25	0.232	4.415	1.766

Table-4.8 Weight loss (Δw), Wear rate (*W*) and Specific wear rate (k_0) of tested composite samples for Sliding velocity =0.314m/s, Sliding distance =471.25m

Fiber content (vol %)	Load (N)	(Δw) (gm)	$W\times 10^{-10}$ (m^3/m)	$k_0\times 10^{-11}$ ($m^3/N.m$)
0	5	0.240	4.707	9.414
	10	0.280	5.491	5.491
	15	0.300	5.884	3.922
	20	0.307	6.021	3.010
	25	0.365	7.158	2.863
10	5	0.200	3.908	7.816
	10	0.263	5.139	5.139
	15	0.284	5.549	3.700
	20	0.278	5.432	2.716
	25	0.298	5.823	2.329
20	5	0.120	2.330	4.660
	10	0.140	2.718	2.718
	15	0.220	4.271	2.847
	20	0.210	4.077	2.039
	25	0.230	4.465	1.786
30	5	0.090	1.735	3.469
	10	0.112	2.159	2.159
	15	0.170	3.277	2.184
	20	0.175	3.373	1.686
	25	0.196	3.778	1.511
40	5	0.060	1.150	2.300
	10	0.080	1.534	1.534
	15	0.122	2.339	1.559
	20	0.133	2.549	1.275
	25	0.160	3.067	1.227
50	5	0.104	1.979	3.959
	10	0.153	2.912	2.912
	15	0.230	4.377	2.918
	20	0.252	4.796	2.398
	25	0.270	5.139	2.055

Table-4.9 Weight loss (Δw), Wear rate (*W*) and Specific wear rate (k_0) of tested composite samples for Sliding velocity =0.392m/s, Sliding distance =471.25m

Fiber content (vol %)	Load (N)	(Δw) (gm)	$W\times 10^{-10}$ (m^3/m)	$k_0\times 10^{-11}$ ($m^3/N.m$)
0	5	0.248	4.864	9.728
	10	0.274	5.374	5.374
	15	0.309	6.060	4.040
	20	0.331	6.492	3.246
	25	0.371	7.276	2.910
10	5	0.212	4.142	8.285
	10	0.244	4.768	4.768
	15	0.260	5.080	3.387
	20	0.264	5.158	2.579
	25	0.281	5.491	2.196
20	5	0.115	2.233	4.465
	10	0.138	2.679	2.679
	15	0.238	4.621	3.080
	20	0.243	4.718	2.359
	25	0.242	4.698	1.879
30	5	0.093	1.792	3.585
	10	0.127	2.448	2.448
	15	0.175	3.373	2.249
	20	0.165	3.180	1.590
	25	0.192	3.701	1.480
40	5	0.081	1.553	3.105
	10	0.093	1.783	1.783
	15	0.118	2.262	1.508
	20	0.122	2.339	1.169
	25	0.153	2.933	1.173
50	5	0.131	2.493	4.986
	10	0.147	2.798	2.798
	15	0.195	3.711	2.474
	20	0.225	4.282	2.141
	25	0.261	4.967	1.987

Table-4.10 Weight loss (Δw), Wear rate (*W*) and Specific wear rate (k_0) of tested composite samples for Sliding velocity =0.470m/s, Sliding distance =471.25m

Fiber content (vol %)	Load (N)	(Δw) (gm)	$W\times 10^{-10}$ (m^3/m)	$k_0\times 10^{-11}$ ($m^3/N.m$)
0	5	0.254	4.981	9.963
	10	0.292	5.727	5.727
	15	0.320	6.276	4.184
	20	0.325	6.374	3.187
	25	0.375	7.354	2.942
10	5	0.216	4.221	8.441
	10	0.278	5.432	5.432
	15	0.295	5.764	3.843
	20	0.284	5.549	2.775
	25	0.314	6.135	2.454
20	5	0.132	2.563	5.125
	10	0.152	2.951	2.951
	15	0.235	4.562	3.042
	20	0.248	4.815	2.407
	25	0.253	4.912	1.965
30	5	0.112	2.159	4.317
	10	0.135	2.602	2.602
	15	0.191	3.681	2.454
	20	0.167	3.219	1.609
	25	0.205	3.951	1.580
40	5	0.078	1.495	2.990
	10	0.102	1.955	1.955
	15	0.137	2.626	1.751
	20	0.147	2.818	1.409
	25	0.177	3.393	1.357
50	5	0.133	2.531	5.062
	10	0.167	3.178	3.178
	15	0.214	4.073	2.715
	20	0.236	4.491	2.246
	25	0.271	5.158	2.063

Table-4.11 Weight loss (Δw), Wear rate (*W*) and Specific wear rate (k_0) of tested composite samples at different Sliding distance for Sliding velocity =0.157m/s, Normal load =5N

Fiber content (vol %)	Sliding Distance (m)	(Δw) (gm)	$W\times 10^{-10}$ (m^3/m)	$k_0\times 10^{-11}$ ($m^3/N.m$)
0	94.25	0.081	7.943	15.886
	188.50	0.049	4.805	9.610
	282.75	0.032	3.138	6.276
	377.00	0.024	2.353	4.707
	471.25	0.020	1.961	3.922
10	94.25	0.064	6.253	12.505
	188.50	0.044	4.299	8.597
	282.75	0.027	2.638	5.276
	377.00	0.018	1.759	3.517
	471.25	0.014	1.368	2.736
20	94.25	0.042	4.077	8.154
	188.50	0.025	2.427	4.854
	282.75	0.014	1.359	2.718
	377.00	0.010	0.971	1.941
	471.25	0.008	0.777	1.553
30	94.25	0.036	3.469	6.938
	188.50	0.019	1.831	3.662
	282.75	0.013	1.253	2.506
	377.00	0.008	0.771	1.542
	471.25	0.007	0.675	1.349
40	94.25	0.025	2.396	4.792
	188.50	0.012	1.150	2.300
	282.75	0.007	0.671	1.342
	377.00	0.006	0.575	1.150
	471.25	0.005	0.479	0.958
50	94.25	0.037	3.521	7.042
	188.50	0.023	2.144	4.289
	282.75	0.015	1.399	2.797
	377.00	0.010	0.932	1.865
	471.25	0.008	0.746	1.492

Table-4.12 Weight loss (Δw), Wear rate (*W*) and Specific wear rate (k_0) of tested composite samples at different Sliding distance for Sliding velocity =0.157m/s, Normal load =10N

Fiber content (vol %)	Sliding Distance (m)	(Δw) (gm)	$W\times 10^{-10}$ (m^3/m)	$k_0\times 10^{-11}$ ($m^3/N.m$)
0	94.25	0.090	8.825	8.825
	188.50	0.059	5.786	5.786
	282.75	0.048	4.707	4.707
	377.00	0.037	3.628	3.628
	471.25	0.031	3.040	3.040
10	94.25	0.076	7.425	7.425
	188.50	0.047	4.592	4.592
	282.75	0.036	3.517	3.517
	377.00	0.029	2.833	2.833
	471.25	0.023	2.247	2.247
20	94.25	0.049	4.757	4.757
	188.50	0.032	3.106	3.106
	282.75	0.020	1.941	1.941
	377.00	0.014	1.359	1.359
	471.25	0.011	1.068	1.068
30	94.25	0.041	3.951	3.951
	188.50	0.023	2.216	2.216
	282.75	0.014	1.349	1.349
	377.00	0.011	1.060	1.060
	471.25	0.007	0.675	0.675
40	94.25	0.027	2.588	2.588
	188.50	0.015	1.438	1.438
	282.75	0.008	0.767	0.767
	377.00	0.005	0.479	0.479
	471.25	0.005	0.479	0.479
50	94.25	0.042	3.997	3.997
	188.50	0.029	2.760	2.760
	282.75	0.021	1.998	1.998
	377.00	0.015	1.427	1.427
	471.25	0.010	0.952	0.952

Table-4.13 Weight loss (Δw), Wear rate (*W*) and Specific wear rate (k_0) of tested composite samples at different Sliding distance for Sliding velocity =0.157m/s, Normal load =15N

Fiber content (vol %)	Sliding Distance (m)	(Δw) (gm)	$W\times 10^{-10}$ (m^3/m)	$k_0\times 10^{-11}$ ($m^3/N.m$)
0	94.25	0.103	10.100	6.733
	188.50	0.062	6.080	4.053
	282.75	0.047	4.609	3.073
	377.00	0.039	3.824	2.550
	471.25	0.034	3.334	2.223
10	94.25	0.082	8.011	5.341
	188.50	0.051	4.983	3.322
	282.75	0.037	3.615	2.410
	377.00	0.028	2.736	1.824
	471.25	0.022	2.149	1.433
20	94.25	0.061	5.921	3.948
	188.50	0.042	4.077	2.718
	282.75	0.026	2.524	1.683
	377.00	0.018	1.747	1.165
	471.25	0.013	1.262	0.841
30	94.25	0.048	4.626	3.084
	188.50	0.028	2.698	1.799
	282.75	0.016	1.542	1.028
	377.00	0.010	0.964	0.642
	471.25	0.008	0.771	0.514
40	94.25	0.036	3.450	2.300
	188.50	0.020	1.917	1.278
	282.75	0.013	1.246	0.831
	377.00	0.008	0.767	0.511
	471.25	0.006	0.575	0.383
50	94.25	0.063	5.995	3.997
	188.50	0.037	3.521	2.347
	282.75	0.022	2.093	1.396
	377.00	0.016	1.523	1.015
	471.25	0.014	1.332	0.888

Table-4.14 Weight loss (Δw), Wear rate (*W*) and Specific wear rate (k_0) of tested composite samples at different Sliding distance for Sliding velocity =0.157m/s, Normal load =20N

Fiber content (vol %)	Sliding Distance (m)	(Δw) (gm)	$W\times 10^{-10}$ (m^3/m)	$k_0\times 10^{-11}$ ($m^3/N.m$)
0	94.25	0.088	8.629	4.315
	188.50	0.066	6.472	3.236
	282.75	0.055	5.393	2.697
	377.00	0.046	4.511	2.255
	471.25	0.041	4.020	2.010
10	94.25	0.072	7.034	3.517
	188.50	0.051	4.983	2.491
	282.75	0.040	3.908	1.954
	377.00	0.034	3.322	1.661
	471.25	0.028	2.736	1.368
20	94.25	0.061	5.921	2.961
	188.50	0.042	4.077	2.039
	282.75	0.031	3.009	1.505
	377.00	0.023	2.233	1.116
	471.25	0.020	1.941	0.971
30	94.25	0.044	4.240	2.120
	188.50	0.030	2.891	1.446
	282.75	0.021	2.024	1.012
	377.00	0.018	1.735	0.867
	471.25	0.013	1.253	0.626
40	94.25	0.036	3.450	1.725
	188.50	0.021	2.013	1.006
	282.75	0.016	1.534	0.767
	377.00	0.014	1.342	0.671
	471.25	0.011	1.054	0.527
50	94.25	0.056	5.329	2.664
	188.50	0.037	3.521	1.760
	282.75	0.029	2.760	1.380
	377.00	0.025	2.379	1.189
	471.25	0.024	2.284	1.142

Table-4.15 Weight loss (Δw), Wear rate (*W*) and Specific wear rate (k_0) of tested composite samples at different Sliding distance for Sliding velocity =0.157m/s, Normal load =25N

Fiber content (vol %)	Sliding Distance (m)	(Δw) (gm)	$W\times 10^{-10}$ (m^3/m)	$k_0\times 10^{-11}$ ($m^3/N.m$)
0	94.25	0.110	10.787	4.315
	188.50	0.074	7.256	2.903
	282.75	0.059	5.786	2.314
	377.00	0.050	4.903	1.961
	471.25	0.043	4.217	1.687
10	94.25	0.082	8.011	3.205
	188.50	0.053	5.178	2.071
	282.75	0.041	4.006	1.602
	377.00	0.032	3.126	1.251
	471.25	0.026	2.540	1.016
20	94.25	0.065	6.310	2.524
	188.50	0.044	4.271	1.708
	282.75	0.032	3.106	1.243
	377.00	0.026	2.524	1.010
	471.25	0.022	2.136	0.854
30	94.25	0.064	6.168	2.467
	188.50	0.044	4.240	1.696
	282.75	0.035	3.373	1.349
	377.00	0.028	2.698	1.079
	471.25	0.025	2.409	0.964
40	94.25	0.051	4.888	1.955
	188.50	0.035	3.355	1.342
	282.75	0.029	2.780	1.112
	377.00	0.025	2.396	0.958
	471.25	0.020	1.917	0.767
50	94.25	0.078	7.422	2.969
	188.50	0.065	6.185	2.474
	282.75	0.050	4.758	1.903
	377.00	0.043	4.092	1.637
	471.25	0.034	3.235	1.294

Table-4.16 Weight loss (Δw), Wear rate (*W*) and Specific wear rate (k_0) of tested composite samples at different Sliding distance for Sliding velocity =0.235m/s, Normal load =5N

Fiber content (vol %)	Sliding Distance (m)	(Δw) (gm)	$W\times 10^{-10}$ (m^3/m)	$k_0\times 10^{-11}$ ($m^3/N.m$)
0	94.25	0.080	7.845	15.690
	188.50	0.047	4.609	9.218
	282.75	0.038	3.726	7.453
	377.00	0.033	3.236	6.472
	471.25	0.029	2.844	5.687
10	94.25	0.071	6.937	13.873
	188.50	0.048	4.690	9.379
	282.75	0.035	3.419	6.839
	377.00	0.028	2.736	5.471
	471.25	0.026	2.540	5.080
20	94.25	0.044	4.271	8.542
	188.50	0.025	2.427	4.854
	282.75	0.016	1.553	3.106
	377.00	0.014	1.359	2.718
	471.25	0.012	1.165	2.330
30	94.25	0.033	3.180	6.360
	188.50	0.021	2.024	4.047
	282.75	0.016	1.542	3.084
	377.00	0.010	0.964	1.927
	471.25	0.007	0.675	1.349
40	94.25	0.026	2.492	4.984
	188.50	0.013	1.246	2.492
	282.75	0.010	0.958	1.917
	377.00	0.008	0.767	1.534
	471.25	0.006	0.575	1.150
50	94.25	0.036	3.426	6.851
	188.50	0.020	1.865	3.729
	282.75	0.012	1.119	2.238
	377.00	0.011	1.026	2.051
	471.25	0.008	0.746	1.492

Table-4.17 Weight loss (Δw), Wear rate (*W*) and Specific wear rate (k_0) of tested composite samples at different Sliding distance for Sliding velocity =0.235m/s, Normal load =10N

Fiber content (vol %)	Sliding Distance (m)	(Δw) (gm)	$W\times 10^{-10}$ (m^3/m)	$k_0\times 10^{-11}$ ($m^3/N.m$)
0	94.25	0.090	8.825	8.825
	188.50	0.060	5.884	5.884
	282.75	0.048	4.707	4.707
	377.00	0.041	4.020	4.020
	471.25	0.035	3.432	3.432
10	94.25	0.085	8.304	8.304
	188.50	0.059	5.764	5.764
	282.75	0.047	4.592	4.592
	377.00	0.039	3.810	3.810
	471.25	0.035	3.419	3.419
20	94.25	0.050	4.854	4.854
	188.50	0.036	3.495	3.495
	282.75	0.022	2.136	2.136
	377.00	0.016	1.553	1.553
	471.25	0.014	1.359	1.359
30	94.25	0.034	3.277	3.277
	188.50	0.021	2.024	2.024
	282.75	0.015	1.446	1.446
	377.00	0.011	1.060	1.060
	471.25	0.007	0.675	0.675
40	94.25	0.029	2.780	2.780
	188.50	0.019	1.821	1.821
	282.75	0.014	1.342	1.342
	377.00	0.010	0.958	0.958
	471.25	0.006	0.575	0.575
50	94.25	0.055	5.234	5.234
	188.50	0.039	3.711	3.711
	282.75	0.027	2.569	2.569
	377.00	0.018	1.713	1.713
	471.25	0.014	1.332	1.332

Table-4.18 Weight loss (Δw), Wear rate (*W*) and Specific wear rate (k_0) of tested composite samples at different Sliding distance for Sliding velocity =0.235m/s, Normal load =15N

Fiber content (vol %)	Sliding Distance (m)	(Δw) (gm)	$W\times 10^{-10}$ (m^3/m)	$k_0\times 10^{-11}$ ($m^3/N.m$)
0	94.25	0.104	10.198	6.799
	188.50	0.062	6.080	4.053
	282.75	0.052	5.099	3.399
	377.00	0.045	4.413	2.942
	471.25	0.033	3.236	2.157
10	94.25	0.074	7.230	4.820
	188.50	0.043	4.201	2.801
	282.75	0.034	3.322	2.215
	377.00	0.030	2.931	1.954
	471.25	0.025	2.442	1.628
20	94.25	0.072	6.989	4.660
	188.50	0.046	4.465	2.977
	282.75	0.031	3.009	2.006
	377.00	0.024	2.330	1.553
	471.25	0.016	1.553	1.035
30	94.25	0.054	5.204	3.469
	188.50	0.027	2.602	1.735
	282.75	0.022	2.120	1.413
	377.00	0.014	1.349	0.899
	471.25	0.008	0.771	0.514
40	94.25	0.042	4.026	2.684
	188.50	0.025	2.396	1.597
	282.75	0.020	1.917	1.278
	377.00	0.012	1.150	0.767
	471.25	0.005	0.479	0.319
50	94.25	0.068	6.471	4.314
	188.50	0.041	3.901	2.601
	282.75	0.026	2.474	1.649
	377.00	0.021	1.998	1.332
	471.25	0.016	1.523	1.015

Table-4.19 Weight loss (Δw), Wear rate (*W*) and Specific wear rate (k_0) of tested composite samples at different Sliding distance for Sliding velocity =0.235m/s, Normal load =20N

Fiber content (vol %)	Sliding Distance (m)	(Δw) (gm)	$W\times 10^{-10}$ (m^3/m)	$k_0\times 10^{-11}$ ($m^3/N.m$)
0	94.25	0.094	9.218	4.609
	188.50	0.071	6.962	3.481
	282.75	0.058	5.687	2.844
	377.00	0.049	4.805	2.402
	471.25	0.041	4.020	2.010
10	94.25	0.075	7.327	3.664
	188.50	0.054	5.276	2.638
	282.75	0.046	4.494	2.247
	377.00	0.040	3.908	1.954
	471.25	0.033	3.224	1.612
20	94.25	0.062	6.019	3.009
	188.50	0.040	3.883	1.941
	282.75	0.030	2.912	1.456
	377.00	0.024	2.330	1.165
	471.25	0.021	2.039	1.019
30	94.25	0.042	4.047	2.024
	188.50	0.029	2.795	1.397
	282.75	0.021	2.024	1.012
	377.00	0.019	1.831	0.915
	471.25	0.016	1.542	0.771
40	94.25	0.044	4.217	2.109
	188.50	0.028	2.684	1.342
	282.75	0.022	2.109	1.054
	377.00	0.015	1.438	0.719
	471.25	0.012	1.150	0.575
50	94.25	0.054	5.139	2.569
	188.50	0.038	3.616	1.808
	282.75	0.032	3.045	1.523
	377.00	0.027	2.569	1.285
	471.25	0.023	2.189	1.094

Table-4.20 Weight loss (Δw), Wear rate (*W*) and Specific wear rate (k_0) of tested composite samples at different Sliding distance for Sliding velocity =0.235m/s, Normal load =25N

Fiber content (vol %)	Sliding Distance (m)	(Δw) (gm)	$W\times 10^{-10}$ (m^3/m)	$k_0\times 10^{-11}$ ($m^3/N.m$)
0	94.25	0.112	10.983	4.393
	188.50	0.077	7.551	3.020
	282.75	0.061	5.982	2.393
	377.00	0.053	5.197	2.079
	471.25	0.049	4.805	1.922
10	94.25	0.076	7.425	2.970
	188.50	0.048	4.690	1.876
	282.75	0.041	4.006	1.602
	377.00	0.036	3.517	1.407
	471.25	0.032	3.126	1.251
20	94.25	0.071	6.892	2.757
	188.50	0.045	4.368	1.747
	282.75	0.037	3.592	1.437
	377.00	0.032	3.106	1.243
	471.25	0.027	2.621	1.048
30	94.25	0.055	5.300	2.120
	188.50	0.032	3.084	1.234
	282.75	0.021	2.024	0.809
	377.00	0.018	1.735	0.694
	471.25	0.015	1.446	0.578
40	94.25	0.046	4.409	1.764
	188.50	0.026	2.492	0.997
	282.75	0.018	1.725	0.690
	377.00	0.015	1.438	0.575
	471.25	0.013	1.246	0.498
50	94.25	0.073	6.947	2.779
	188.50	0.049	4.663	1.865
	282.75	0.045	4.282	1.713
	377.00	0.035	3.331	1.332
	471.25	0.030	2.855	1.142

Table-4.21 Weight loss (Δw), Wear rate (*W*) and Specific wear rate (k_0) of tested composite samples at different Sliding distance for Sliding velocity =0.314m/s, Normal load =5N

Fiber content (vol %)	Sliding Distance (m)	(Δw) (gm)	$W\times 10^{-10}$ (m^3/m)	$k_0\times 10^{-11}$ ($m^3/N.m$)
0	94.25	0.088	8.629	17.259
	188.50	0.049	4.805	9.610
	282.75	0.041	4.020	8.041
	377.00	0.033	3.236	6.472
	471.25	0.029	2.844	5.687
10	94.25	0.068	6.644	13.287
	188.50	0.047	4.592	9.184
	282.75	0.033	3.224	6.448
	377.00	0.027	2.638	5.276
	471.25	0.025	2.442	4.885
20	94.25	0.047	4.562	9.125
	188.50	0.029	2.815	5.630
	282.75	0.018	1.747	3.495
	377.00	0.014	1.359	2.718
	471.25	0.012	1.165	2.330
30	94.25	0.036	3.469	6.938
	188.50	0.021	2.024	4.047
	282.75	0.016	1.542	3.084
	377.00	0.01	0.964	1.927
	471.25	0.007	0.675	1.349
40	94.25	0.026	2.492	4.984
	188.50	0.013	1.246	2.492
	282.75	0.008	0.767	1.534
	377.00	0.007	0.671	1.342
	471.25	0.006	0.575	1.150
50	94.25	0.042	3.997	7.993
	188.50	0.025	2.331	4.662
	282.75	0.016	1.492	2.984
	377.00	0.012	1.119	2.238
	471.25	0.009	0.839	1.678

Table-4.22 Weight loss (Δw), Wear rate (*W*) and Specific wear rate (k_0) of tested composite samples at different Sliding distance for Sliding velocity =0.314m/s, Normal load =10N

Fiber content (vol %)	Sliding Distance (m)	(Δw) (gm)	$W\times 10^{-10}$ (m^3/m)	$k_0\times 10^{-11}$ ($m^3/N.m$)
0	94.25	0.093	9.120	9.120
	188.50	0.060	5.884	5.884
	282.75	0.050	4.903	4.903
	377.00	0.041	4.020	4.020
	471.25	0.036	3.530	3.530
10	94.25	0.083	8.109	8.109
	188.50	0.059	5.764	5.764
	282.75	0.046	4.494	4.494
	377.00	0.039	3.810	3.810
	471.25	0.036	3.517	3.517
20	94.25	0.051	4.951	4.951
	188.50	0.037	3.592	3.592
	282.75	0.022	2.136	2.136
	377.00	0.016	1.553	1.553
	471.25	0.014	1.359	1.359
30	94.25	0.045	4.337	4.337
	188.50	0.028	2.698	2.698
	282.75	0.017	1.638	1.638
	377.00	0.012	1.156	1.156
	471.25	0.010	0.964	0.964
40	94.25	0.032	3.067	3.067
	188.50	0.019	1.821	1.821
	282.75	0.014	1.342	1.342
	377.00	0.009	0.863	0.863
	471.25	0.006	0.575	0.575
50	94.25	0.055	5.234	5.234
	188.50	0.039	3.711	3.711
	282.75	0.027	2.569	2.569
	377.00	0.018	1.713	1.713
	471.25	0.014	1.332	1.332

Table-4.23 Weight loss (Δw), Wear rate (*W*) and Specific wear rate (k_0) of tested composite samples at different Sliding distance for Sliding velocity =0.314m/s, Normal load =15N

Fiber content (vol %)	Sliding Distance (m)	(Δw) (gm)	$W\times 10^{-10}$ (m^3/m)	$k_0\times 10^{-11}$ ($m^3/N.m$)
0	94.25	0.108	10.590	7.060
	188.50	0.062	6.080	4.053
	282.75	0.055	5.393	3.596
	377.00	0.045	4.413	2.942
	471.25	0.030	2.942	1.961
10	94.25	0.093	9.086	6.057
	188.50	0.063	6.155	4.103
	282.75	0.051	4.983	3.322
	377.00	0.040	3.908	2.605
	471.25	0.037	3.615	2.410
20	94.25	0.072	6.989	4.660
	188.50	0.057	5.533	3.689
	282.75	0.041	3.980	2.653
	377.00	0.027	2.621	1.747
	471.25	0.023	2.233	1.488
30	94.25	0.062	5.975	3.983
	188.50	0.042	4.047	2.698
	282.75	0.029	2.795	1.863
	377.00	0.020	1.927	1.285
	471.25	0.017	1.638	1.092
40	94.25	0.048	4.601	3.067
	188.50	0.032	3.067	2.045
	282.75	0.020	1.917	1.278
	377.00	0.012	1.150	0.767
	471.25	0.010	0.958	0.639
50	94.25	0.077	7.327	4.885
	188.50	0.061	5.805	3.870
	282.75	0.038	3.616	2.411
	377.00	0.029	2.760	1.840
	471.25	0.025	2.379	1.586

Table-4.24 Weight loss (Δw), Wear rate (*W*) and Specific wear rate (k_0) of tested composite samples at different Sliding distance for Sliding velocity =0.314m/s, Normal load =20N

Fiber content (vol %)	Sliding Distance (m)	(Δw) (gm)	$W\times 10^{-10}$ (m^3/m)	$k_0\times 10^{-11}$ ($m^3/N.m$)
0	94.25	0.095	9.316	4.658
	188.50	0.068	6.668	3.334
	282.75	0.055	5.393	2.697
	377.00	0.048	4.707	2.353
	471.25	0.041	4.020	2.010
10	94.25	0.080	7.816	3.908
	188.50	0.065	6.350	3.175
	282.75	0.054	5.276	2.638
	377.00	0.043	4.201	2.101
	471.25	0.036	3.517	1.759
20	94.25	0.069	6.698	3.349
	188.50	0.048	4.660	2.330
	282.75	0.035	3.398	1.699
	377.00	0.031	3.009	1.505
	471.25	0.027	2.621	1.310
30	94.25	0.057	5.493	2.746
	188.50	0.041	3.951	1.976
	282.75	0.031	2.987	1.494
	377.00	0.024	2.313	1.156
	471.25	0.022	2.120	1.060
40	94.25	0.045	4.313	2.157
	188.50	0.032	3.067	1.534
	282.75	0.025	2.396	1.198
	377.00	0.018	1.725	0.863
	471.25	0.013	1.246	0.623
50	94.25	0.075	7.137	3.568
	188.50	0.065	6.185	3.093
	282.75	0.047	4.472	2.236
	377.00	0.036	3.426	1.713
	471.25	0.029	2.760	1.380

Table-4.25 Weight loss (Δw), Wear rate (*W*) and Specific wear rate (k_0) of tested composite samples at different Sliding distance for Sliding velocity =0.314m/s, Normal load =25N

Fiber content (vol %)	Sliding Distance (m)	(Δw) (gm)	$W\times 10^{-10}$ (m^3/m)	$k_0\times 10^{-11}$ ($m^3/N.m$)
0	94.25	0.112	10.983	4.393
	188.50	0.081	7.943	3.177
	282.75	0.065	6.374	2.550
	377.00	0.058	5.687	2.275
	471.25	0.049	4.805	1.922
10	94.25	0.095	9.281	3.713
	188.50	0.068	6.644	2.657
	282.75	0.055	5.373	2.149
	377.00	0.042	4.103	1.641
	471.25	0.038	3.713	1.485
20	94.25	0.071	6.892	2.757
	188.50	0.051	4.951	1.980
	282.75	0.044	4.271	1.708
	377.00	0.035	3.398	1.359
	471.25	0.029	2.815	1.126
30	94.25	0.064	6.168	2.467
	188.50	0.044	4.240	1.696
	282.75	0.035	3.373	1.349
	377.00	0.028	2.698	1.079
	471.25	0.025	2.409	0.964
40	94.25	0.051	4.888	1.955
	188.50	0.035	3.355	1.342
	282.75	0.029	2.780	1.112
	377.00	0.025	2.396	0.958
	471.25	0.020	1.917	0.767
50	94.25	0.078	7.422	2.969
	188.50	0.065	6.185	2.474
	282.75	0.050	4.758	1.903
	377.00	0.043	4.092	1.637
	471.25	0.034	3.235	1.294

Table-4.26 Weight loss (Δw), Wear rate (*W*) and Specific wear rate (k_0) of tested composite samples at different Sliding distance for Sliding velocity =0.392m/s, Normal load =5N

Fiber content (vol %)	Sliding Distance (m)	(Δw) (gm)	$W\times 10^{-10}$ (m^3/m)	$k_0\times 10^{-11}$ ($m^3/N.m$)
0	94.25	0.084	8.237	16.474
	188.50	0.053	5.197	10.394
	282.75	0.042	4.119	8.237
	377.00	0.036	3.530	7.060
	471.25	0.033	3.236	6.472
10	94.25	0.071	6.937	13.873
	188.50	0.049	4.787	9.574
	282.75	0.036	3.517	7.034
	377.00	0.030	2.931	5.862
	471.25	0.026	2.540	5.080
20	94.25	0.047	4.562	9.125
	188.50	0.024	2.330	4.660
	282.75	0.018	1.747	3.495
	377.00	0.014	1.359	2.718
	471.25	0.012	1.165	2.330
30	94.25	0.038	3.662	7.324
	188.50	0.021	2.024	4.047
	282.75	0.016	1.542	3.084
	377.00	0.011	1.060	2.120
	471.25	0.007	3.662	1.349
40	94.25	0.032	3.067	6.134
	188.50	0.019	1.821	3.642
	282.75	0.014	1.342	2.684
	377.00	0.009	0.863	1.725
	471.25	0.007	0.671	1.342
50	94.25	0.049	4.663	9.325
	188.50	0.030	2.797	5.594
	282.75	0.022	2.051	4.102
	377.00	0.016	1.492	2.984
	471.25	0.014	1.305	2.611

Table-4.27 Weight loss (Δw), Wear rate (*W*) and Specific wear rate (k_0) of tested composite samples at different Sliding distance for Sliding velocity =0.392m/s, Normal load =10N

Fiber content (vol %)	Sliding Distance (m)	(Δw) (gm)	$W\times 10^{-10}$ (m^3/m)	$k_0\times 10^{-11}$ ($m^3/N.m$)
0	94.25	0.087	8.531	8.531
	188.50	0.060	5.884	5.884
	282.75	0.050	4.903	4.903
	377.00	0.041	4.020	4.020
	471.25	0.036	3.530	3.530
10	94.25	0.073	7.132	7.132
	188.50	0.054	5.276	5.276
	282.75	0.044	4.299	4.299
	377.00	0.039	3.810	3.810
	471.25	0.034	3.322	3.322
20	94.25	0.051	4.951	4.951
	188.50	0.035	3.398	3.398
	282.75	0.022	2.136	2.136
	377.00	0.016	1.553	1.553
	471.25	0.014	1.359	1.359
30	94.25	0.047	4.529	4.529
	188.50	0.033	3.180	3.180
	282.75	0.021	2.024	2.024
	377.00	0.014	1.349	1.349
	471.25	0.012	1.156	1.156
40	94.25	0.037	3.546	3.546
	188.50	0.022	2.109	2.109
	282.75	0.016	1.534	1.534
	377.00	0.011	1.054	1.054
	471.25	0.007	0.671	0.671
50	94.25	0.054	5.139	5.139
	188.50	0.035	3.331	3.331
	282.75	0.025	2.379	2.379
	377.00	0.018	1.713	1.713
	471.25	0.015	1.427	1.427

Table-4.28 Weight loss (Δw), Wear rate (*W*) and Specific wear rate (k_0) of tested composite samples at different Sliding distance for Sliding velocity =0.392m/s, Normal load =15N

Fiber content (vol %)	Sliding Distance (m)	(Δw) (gm)	$W\times 10^{-10}$ (m^3/m)	$k_0\times 10^{-11}$ ($m^3/N.m$)
0	94.25	0.112	10.983	7.322
	188.50	0.063	6.178	4.119
	282.75	0.054	5.295	3.530
	377.00	0.044	4.315	2.876
	471.25	0.036	3.530	2.353
10	94.25	0.087	8.500	5.667
	188.50	0.062	6.057	4.038
	282.75	0.044	4.299	2.866
	377.00	0.036	3.517	2.345
	471.25	0.031	3.029	2.019
20	94.25	0.079	7.669	5.113
	188.50	0.054	5.242	3.495
	282.75	0.041	3.980	2.653
	377.00	0.035	3.398	2.265
	471.25	0.029	2.815	1.877
30	94.25	0.062	5.975	3.983
	188.50	0.042	4.047	2.698
	282.75	0.030	2.891	1.927
	377.00	0.022	2.120	1.413
	471.25	0.019	1.831	1.221
40	94.25	0.048	4.601	3.067
	188.50	0.028	2.684	1.789
	282.75	0.020	1.917	1.278
	377.00	0.012	1.150	0.767
	471.25	0.010	0.958	0.639
50	94.25	0.070	6.661	4.441
	188.50	0.045	4.282	2.855
	282.75	0.032	3.045	2.030
	377.00	0.027	2.569	1.713
	471.25	0.021	1.998	1.332

Table-4.29 Weight loss (Δw), Wear rate (*W*) and Specific wear rate (k_0) of tested composite samples at different Sliding distance for Sliding velocity =0.392m/s, Normal load =20N

Fiber content (vol %)	Sliding Distance (m)	(Δw) (gm)	$W\times 10^{-10}$ (m^3/m)	$k_0\times 10^{-11}$ ($m^3/N.m$)
0	94.25	0.101	9.904	4.952
	188.50	0.080	7.845	3.922
	282.75	0.062	6.080	3.040
	377.00	0.040	3.922	1.961
	471.25	0.048	4.707	2.353
10	94.25	0.075	7.327	3.664
	188.50	0.061	5.960	2.980
	282.75	0.051	4.983	2.491
	377.00	0.038	3.713	1.856
	471.25	0.039	3.810	1.905
20	94.25	0.072	6.989	3.495
	188.50	0.058	5.630	2.815
	282.75	0.045	4.368	2.184
	377.00	0.035	3.398	1.699
	471.25	0.033	3.203	1.602
30	94.25	0.053	5.107	2.554
	188.50	0.038	3.662	1.831
	282.75	0.031	2.987	1.494
	377.00	0.023	2.216	1.108
	471.25	0.020	1.927	0.964
40	94.25	0.041	3.930	1.965
	188.50	0.031	2.971	1.486
	282.75	0.021	2.013	1.006
	377.00	0.016	1.534	0.767
	471.25	0.013	1.246	0.623
50	94.25	0.065	6.185	3.093
	188.50	0.055	5.234	2.617
	282.75	0.042	3.997	1.998
	377.00	0.034	3.235	1.618
	471.25	0.029	2.760	1.380

Table-4.30 Weight loss (Δw), Wear rate (*W*) and Specific wear rate (k_0) of tested composite samples at different Sliding distance for Sliding velocity =0.392m/s, Normal load =25N

Fiber content (vol %)	Sliding Distance (m)	(Δw) (gm)	$W\times 10^{-10}$ (m^3/m)	$k_0\times 10^{-11}$ ($m^3/N.m$)
0	94.25	0.112	10.983	4.393
	188.50	0.081	7.943	3.177
	282.75	0.069	6.766	2.706
	377.00	0.059	5.786	2.314
	471.25	0.050	4.903	1.961
10	94.25	0.089	8.695	3.478
	188.50	0.062	6.057	2.423
	282.75	0.052	5.080	2.032
	377.00	0.041	4.006	1.602
	471.25	0.037	3.615	1.446
20	94.25	0.074	7.183	2.873
	188.50	0.053	5.145	2.058
	282.75	0.045	4.368	1.747
	377.00	0.037	3.592	1.437
	471.25	0.033	3.203	1.281
30	94.25	0.061	5.878	2.351
	188.50	0.044	4.240	1.696
	282.75	0.033	3.180	1.272
	377.00	0.029	2.795	1.118
	471.25	0.025	2.409	0.964
40	94.25	0.051	4.888	1.955
	188.50	0.035	3.355	1.342
	282.75	0.026	2.492	0.997
	377.00	0.022	2.109	0.843
	471.25	0.019	1.821	0.728
50	94.25	0.078	7.422	2.969
	188.50	0.057	5.424	2.170
	282.75	0.050	4.758	1.903
	377.00	0.043	4.092	1.637
	471.25	0.033	3.140	1.256

Table-4.31 Weight loss (Δw), Wear rate (*W*) and Specific wear rate (k_0) of tested composite samples at different Sliding distance for Sliding velocity =0.470m/s, Normal load =5N

Fiber content (vol %)	Sliding Distance (m)	(Δw) (gm)	$W\times 10^{-10}$ (m^3/m)	$k_0\times 10^{-11}$ ($m^3/N.m$)
0	94.25	0.091	8.923	17.847
	188.50	0.056	5.491	10.983
	282.75	0.042	4.119	8.237
	377.00	0.036	3.530	7.060
	471.25	0.029	2.844	5.687
10	94.25	0.083	8.139	16.278
	188.50	0.050	4.903	9.806
	282.75	0.037	3.628	7.256
	377.00	0.028	2.746	5.491
	471.25	0.018	1.765	3.530
20	94.25	0.060	5.884	11.767
	188.50	0.033	3.236	6.472
	282.75	0.019	1.863	3.726
	377.00	0.012	1.177	2.353
	471.25	0.008	0.784	1.569
30	94.25	0.049	4.805	9.610
	188.50	0.030	2.942	5.884
	282.75	0.016	1.569	3.138
	377.00	0.010	0.981	1.961
	471.25	0.007	0.686	1.373
40	94.25	0.038	3.726	7.453
	188.50	0.018	1.765	3.530
	282.75	0.010	0.981	1.961
	377.00	0.007	0.686	1.373
	471.25	0.005	0.490	0.981
50	94.25	0.052	5.099	10.198
	188.50	0.029	2.844	5.687
	282.75	0.023	2.255	4.511
	377.00	0.018	1.765	3.530
	471.25	0.011	1.079	2.157

Table-4.32 Weight loss (Δw), Wear rate (*W*) and Specific wear rate (k_0) of tested composite samples at different Sliding distance for Sliding velocity =0.470m/s, Normal load =10N

Fiber content (vol %)	Sliding Distance (m)	(Δw) (gm)	$W\times 10^{-10}$ (m^3/m)	$k_0\times 10^{-11}$ ($m^3/N.m$)
0	94.25	0.105	10.296	10.296
	188.50	0.067	6.570	6.570
	282.75	0.05	4.903	4.903
	377.00	0.039	3.824	3.824
	471.25	0.031	3.040	3.040
10	94.25	0.101	9.868	9.868
	188.50	0.063	6.155	6.155
	282.75	0.048	4.690	4.690
	377.00	0.038	3.713	3.713
	471.25	0.028	2.736	2.736
20	94.25	0.062	6.019	6.019
	188.50	0.033	3.203	3.203
	282.75	0.025	2.427	2.427
	377.00	0.019	1.844	1.844
	471.25	0.013	1.262	1.262
30	94.25	0.057	5.493	5.493
	188.50	0.03	2.891	2.891
	282.75	0.021	2.024	2.024
	377.00	0.016	1.542	1.542
	471.25	0.011	1.060	1.060
40	94.25	0.046	4.409	4.409
	188.50	0.023	2.204	2.204
	282.75	0.015	1.438	1.438
	377.00	0.011	1.054	1.054
	471.25	0.007	0.671	0.671
50	94.25	0.063	5.995	5.995
	188.50	0.036	3.426	3.426
	282.75	0.028	2.664	2.664
	377.00	0.021	1.998	1.998
	471.25	0.019	1.808	1.808

Table-4.33 Weight loss (Δw), Wear rate (*W*) and Specific wear rate (k_0) of tested composite samples at different Sliding distance for Sliding velocity =0.470m/s, Normal load =15N

Fiber content (vol %)	Sliding Distance (m)	(Δw) (gm)	$W\times 10^{-10}$ (m^3/m)	$k_0\times 10^{-11}$ ($m^3/N.m$)
0	94.25	0.111	10.885	7.256
	188.50	0.071	6.962	4.642
	282.75	0.054	5.295	3.530
	377.00	0.046	4.511	3.007
	471.25	0.038	3.726	2.484
10	94.25	0.103	10.063	6.709
	188.50	0.063	6.155	4.103
	282.75	0.052	5.080	3.387
	377.00	0.042	4.103	2.736
	471.25	0.035	3.419	2.280
20	94.25	0.079	7.669	5.113
	188.50	0.054	5.242	3.495
	282.75	0.041	3.980	2.653
	377.00	0.033	3.203	2.136
	471.25	0.028	2.718	1.812
30	94.25	0.073	7.035	4.690
	188.50	0.041	3.951	2.634
	282.75	0.032	3.084	2.056
	377.00	0.026	2.506	1.670
	471.25	0.019	1.831	1.221
40	94.25	0.052	4.984	3.323
	188.50	0.03	2.875	1.917
	282.75	0.023	2.204	1.470
	377.00	0.017	1.629	1.086
	471.25	0.015	1.438	0.958
50	94.25	0.067	6.376	4.250
	188.50	0.05	4.758	3.172
	282.75	0.039	3.711	2.474
	377.00	0.032	3.045	2.030
	471.25	0.026	2.474	1.649

Table-4.34 Weight loss (Δw), Wear rate (*W*) and Specific wear rate (k_0) of tested composite samples at different Sliding distance for Sliding velocity =0.470m/s, Normal load =20N

Fiber content (vol %)	Sliding Distance (m)	(Δw) (gm)	$W\times 10^{-10}$ (m^3/m)	$k_0\times 10^{-11}$ ($m^3/N.m$)
0	94.25	0.099	9.708	4.854
	188.50	0.068	6.668	3.334
	282.75	0.057	5.589	2.795
	377.00	0.053	5.197	2.599
	471.25	0.048	4.707	2.353
10	94.25	0.086	8.402	4.201
	188.50	0.060	5.862	2.931
	282.75	0.051	4.983	2.491
	377.00	0.046	4.494	2.247
	471.25	0.041	4.006	2.003
20	94.25	0.081	7.863	3.931
	188.50	0.052	5.048	2.524
	282.75	0.042	4.077	2.039
	377.00	0.039	3.786	1.893
	471.25	0.034	3.300	1.650
30	94.25	0.059	5.686	2.843
	188.50	0.037	3.566	1.783
	282.75	0.028	2.698	1.349
	377.00	0.024	2.313	1.156
	471.25	0.019	1.831	0.915
40	94.25	0.052	4.984	2.492
	188.50	0.033	3.163	1.581
	282.75	0.025	2.396	1.198
	377.00	0.021	2.013	1.006
	471.25	0.016	1.534	0.767
50	94.25	0.074	7.042	3.521
	188.50	0.054	5.139	2.569
	282.75	0.044	4.187	2.093
	377.00	0.035	3.331	1.665
	471.25	0.029	2.760	1.380

Table-4.35 Weight loss (Δw), Wear rate (*W*) and Specific wear rate (k_0) of tested composite samples at different Sliding distance for Sliding velocity =0.470m/s, Normal load =25N

Fiber content (vol %)	Sliding Distance (m)	(Δw) (gm)	$W\times 10^{-10}$ (m^3/m)	$k_0\times 10^{-11}$ ($m^3/N.m$)
0	94.25	0.127	12.454	4.981
	188.50	0.085	8.335	3.334
	282.75	0.062	6.080	2.432
	377.00	0.054	5.295	2.118
	471.25	0.047	4.609	1.844
10	94.25	0.106	10.356	4.142
	188.50	0.068	6.644	2.657
	282.75	0.054	5.276	2.110
	377.00	0.046	4.494	1.798
	471.25	0.040	3.908	1.563
20	94.25	0.086	8.348	3.339
	188.50	0.052	5.048	2.019
	282.75	0.044	4.271	1.708
	377.00	0.038	3.689	1.476
	471.25	0.033	3.203	1.281
30	94.25	0.072	6.938	2.775
	188.50	0.043	4.144	1.658
	282.75	0.035	3.373	1.349
	377.00	0.031	2.987	1.195
	471.25	0.024	2.313	0.925
40	94.25	0.064	6.134	2.454
	188.50	0.038	3.642	1.457
	282.75	0.029	2.780	1.112
	377.00	0.026	2.492	0.997
	471.25	0.020	1.917	0.767
50	94.25	0.082	7.803	3.121
	188.50	0.058	5.519	2.208
	282.75	0.049	4.663	1.865
	377.00	0.044	4.187	1.675
	471.25	0.038	3.616	1.446

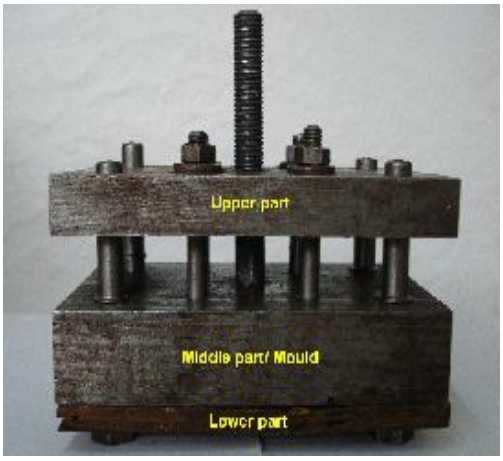

Figure-4.5 (a)

Figure-4.5 (b)

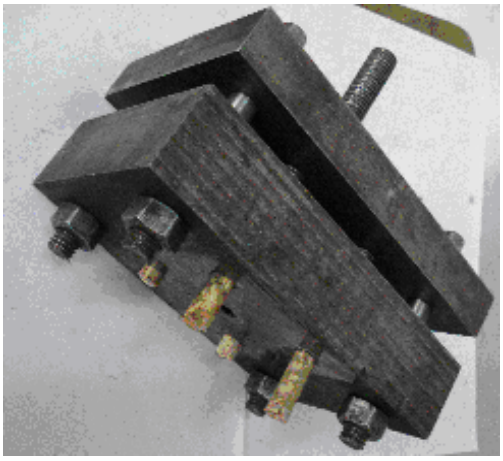

Figure-4.5 (c)

Figure-4.5 (d)

Figure-4.5. Steel Mould and prepared pin type composite samples; (a) Mould used for preparing samples, (b) Two halves of the mould, (c) Mould with Pin types composite samples, (d) Fabricated Composite Pins

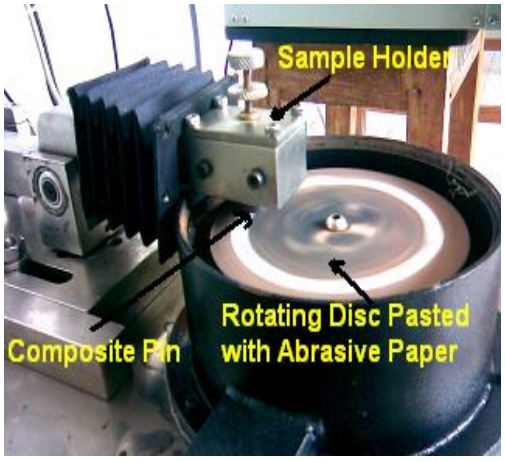

Figure-4.6 (a) **Figure-4.6 (b)**

Figure-4.6 **Experimental set-up; (a) Pin-on-disc type wear testing machine, (b) Composite sample under abrasive wear test**

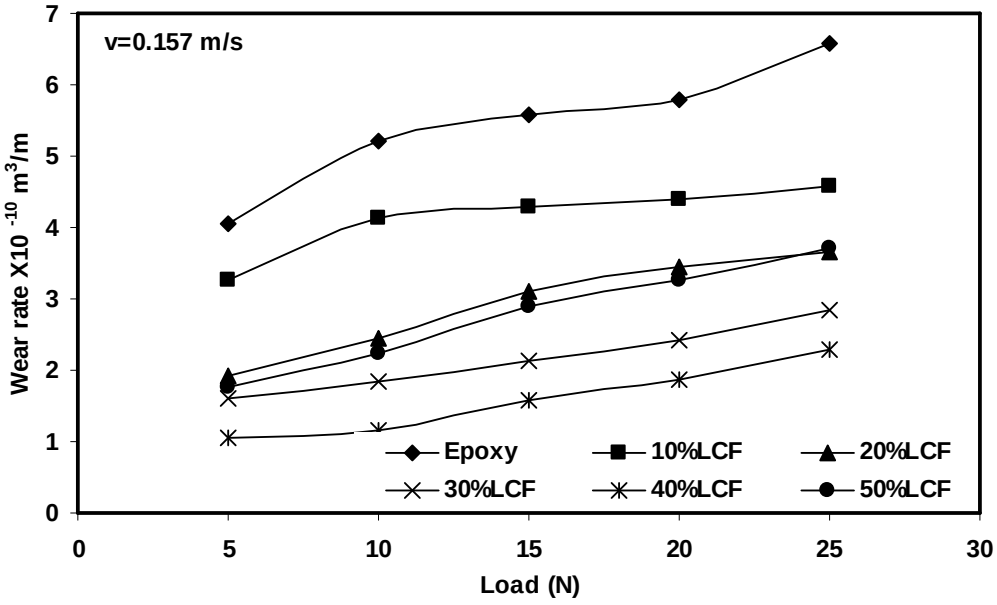

Figure-4.7 **Variation of wear rate with normal load at sliding velocity of 0.157m/s**

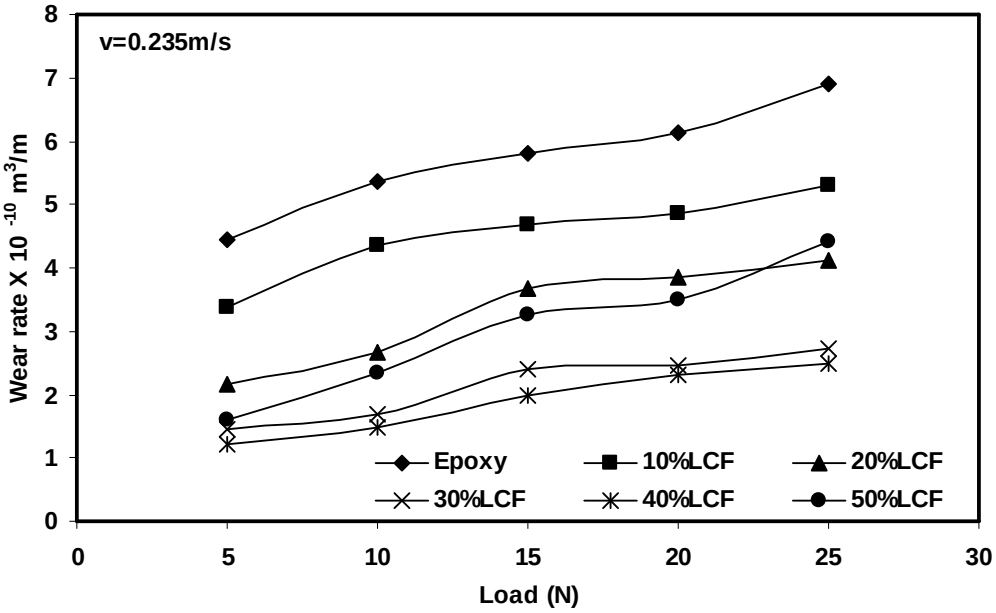

Figure-4.8 **Variation of wear rate with normal load at sliding velocity of 0.235m/s**

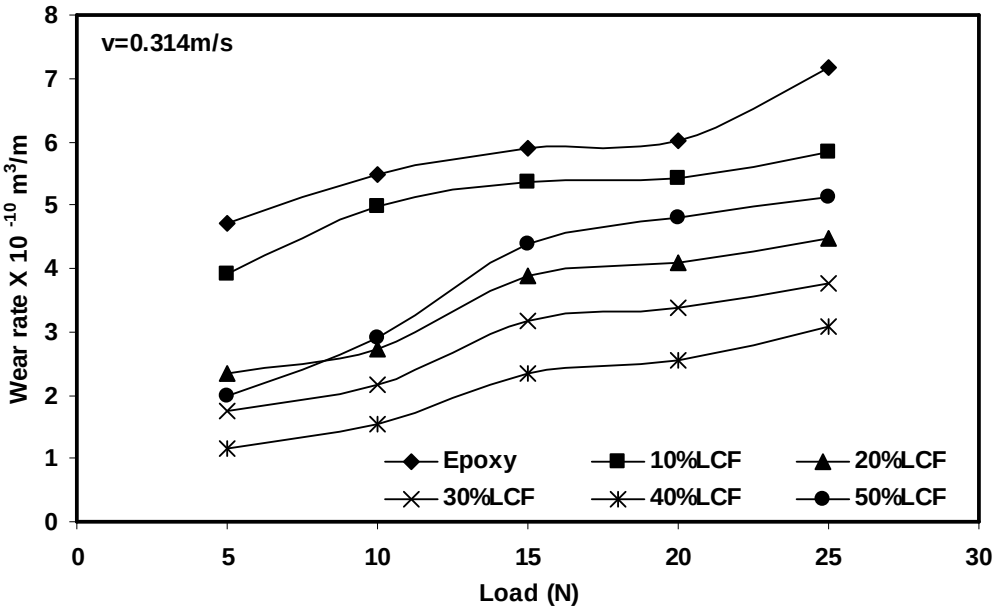

Figure-4.9 **Variation of wear rate with normal load at sliding velocity of 0.314m/s**

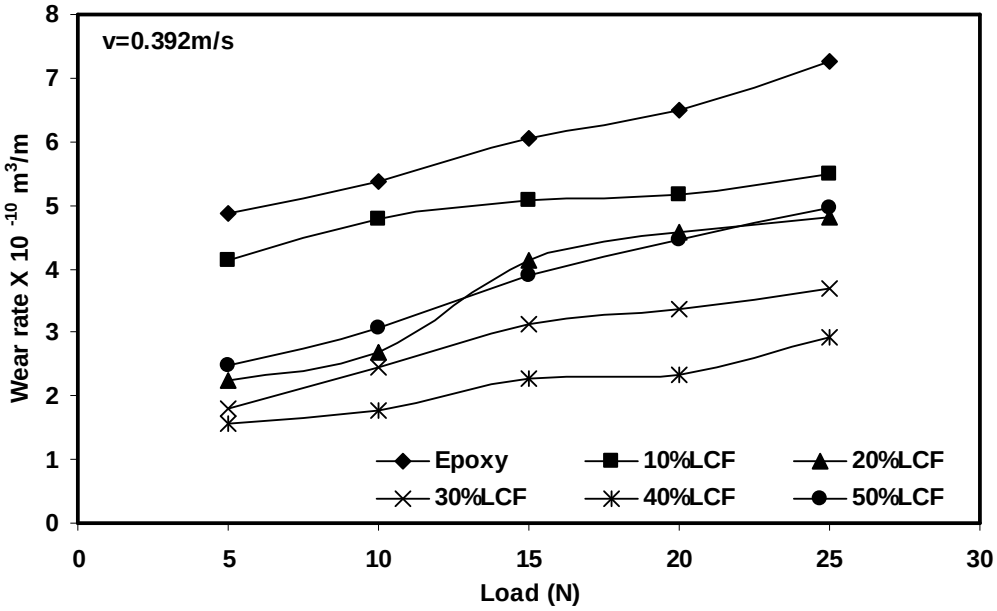

Figure-4.10 Variation of wear rate with normal load at sliding velocity of 0.392m/s

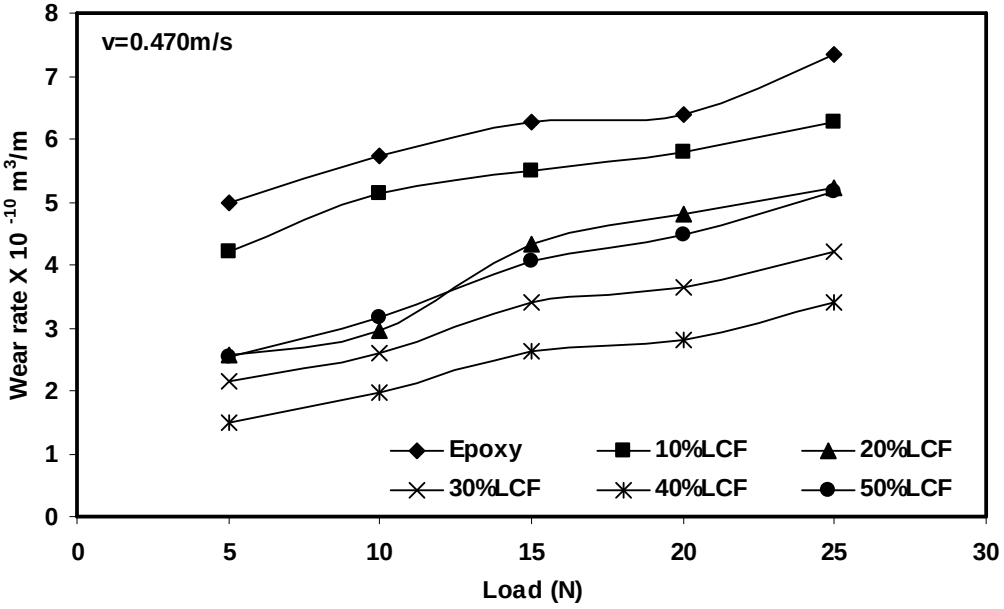

Figure-4.11 Variation of wear rate with normal load at sliding velocity of 0.470m/s

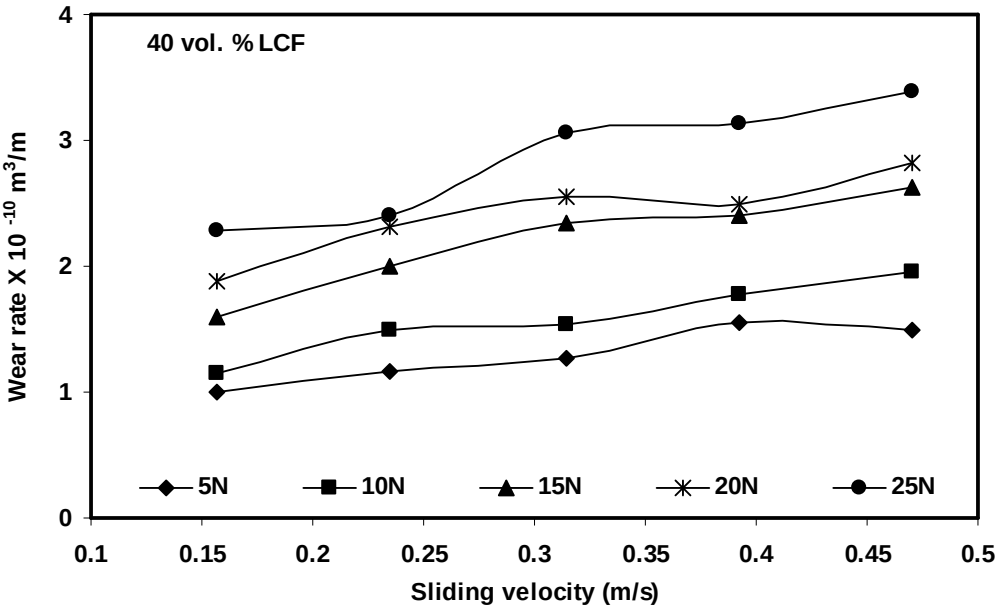

Figure-4.12 Variation of wear rate as function of sliding velocity for 40vol % composite under different loads (5N to 25N)

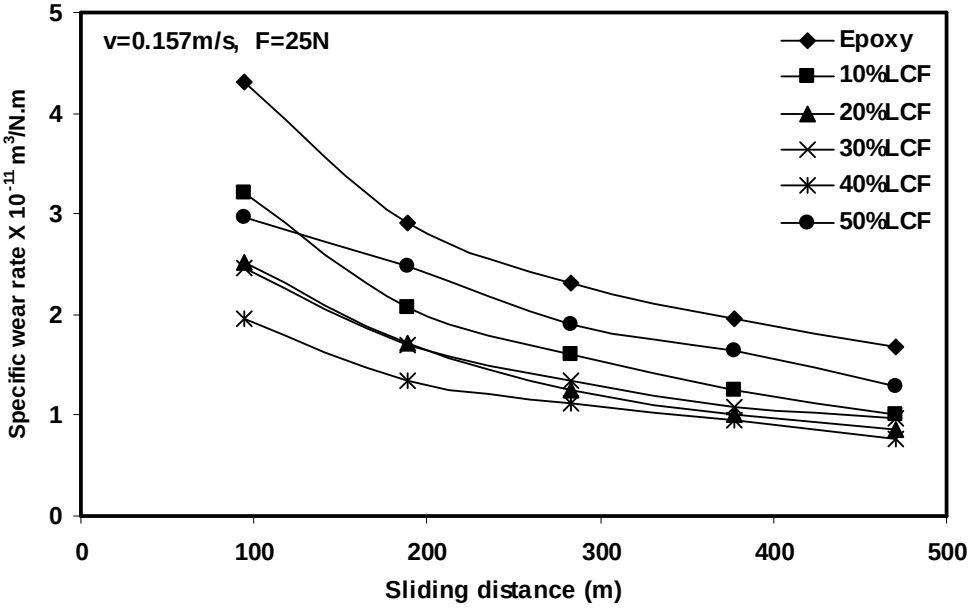

Figure-4.13 Variation of Specific wear rate with sliding distance for all composites at Sliding velocity= 0.157 m/s and Normal load=25N.

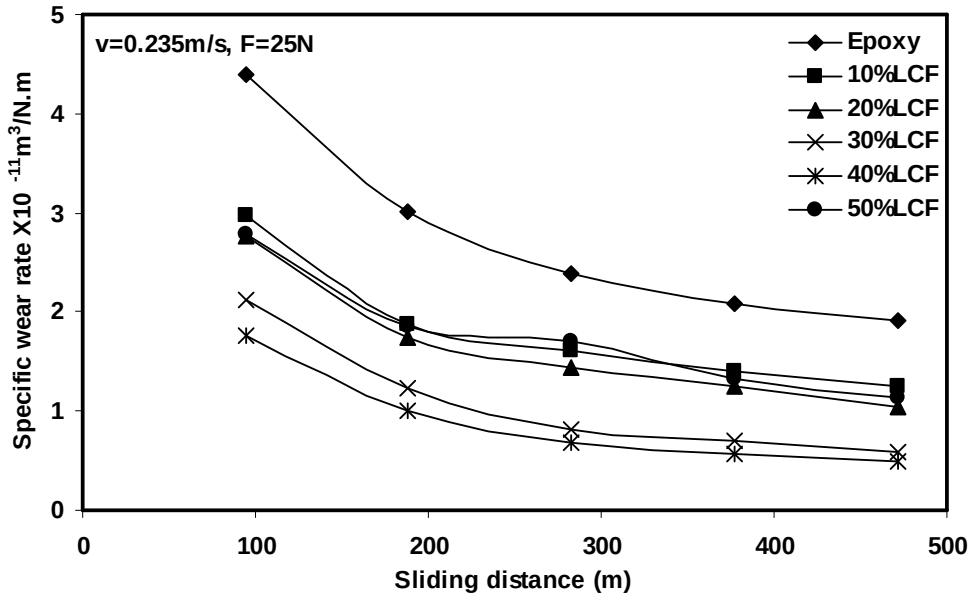

Figure-4.14 Variation of Specific wear rate with sliding distance for all composites at Sliding velocity= 0.235 m/s and Normal load =25N

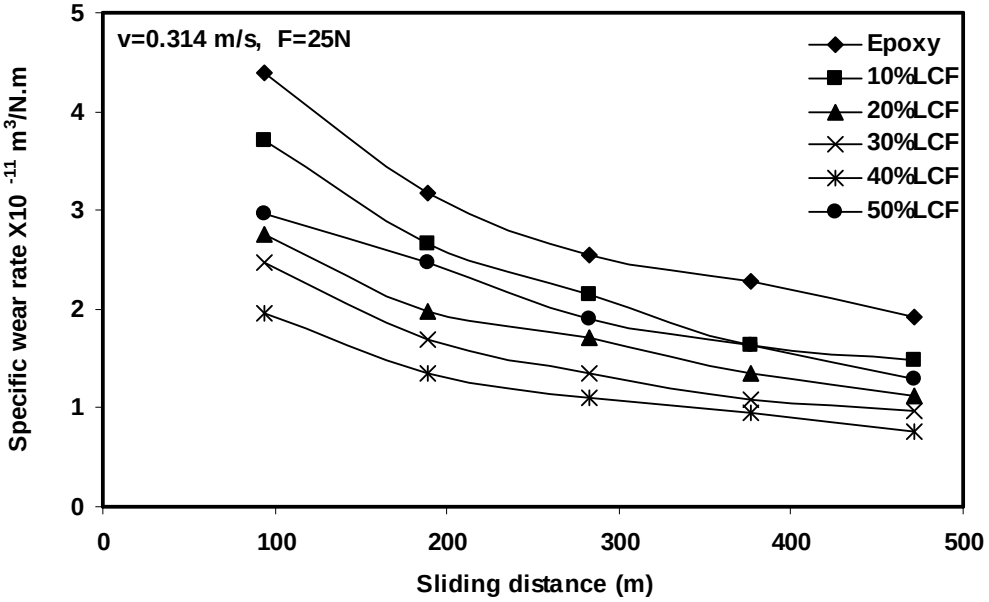

Figure-4.15 Variation of Specific wear rate with sliding distance for all composites at Sliding velocity= 0.314 m/s and Normal load=25N

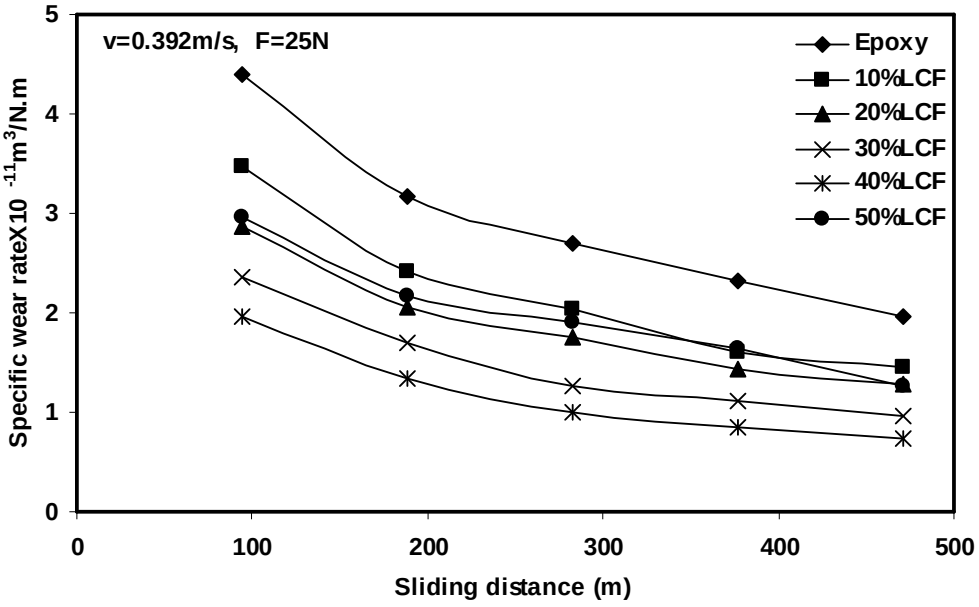

Figure-4.16 Variation of Specific wear rate with sliding distance for all composites at Sliding velocity= 0.392 m/s and Normal load= 25N.

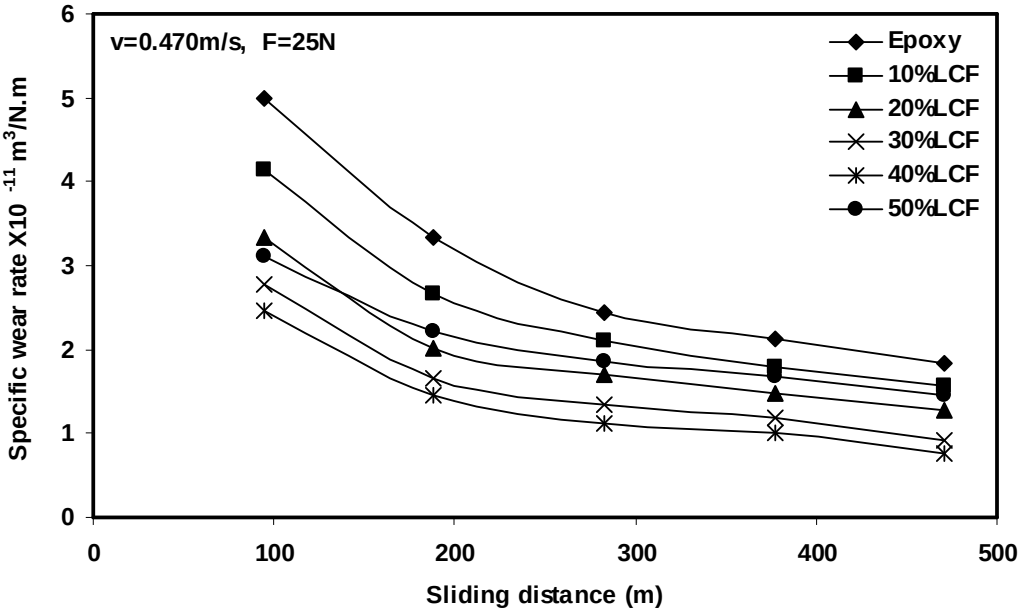

Figure-4.17 Variation of Specific wear rate with sliding distance for all composites at Sliding velocity = 0.470 m/s and Normal load=25N.

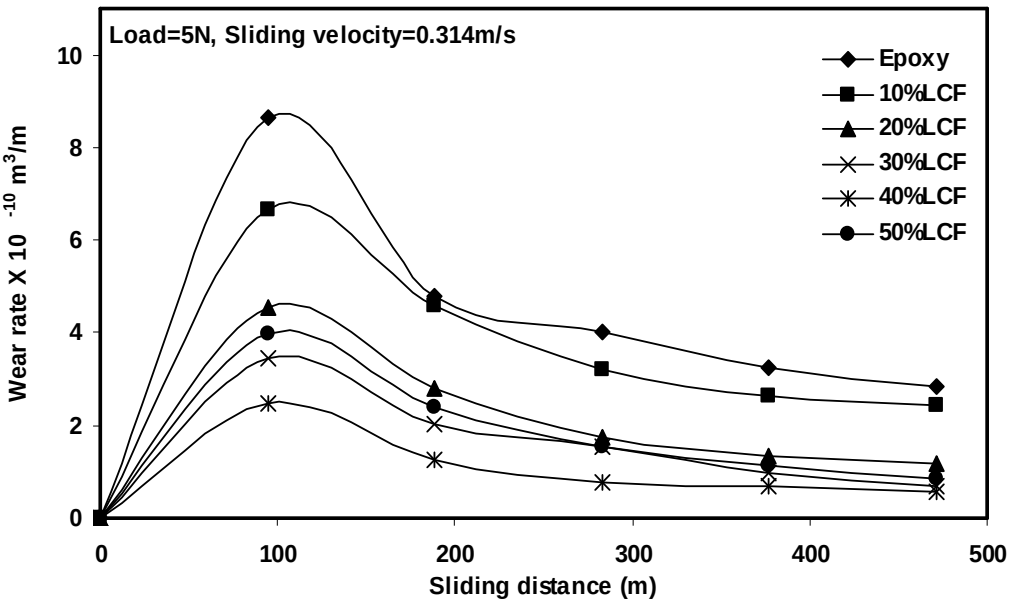

Figure-4.18 Variation of wear rate with sliding distance under the applied Normal load of 5N

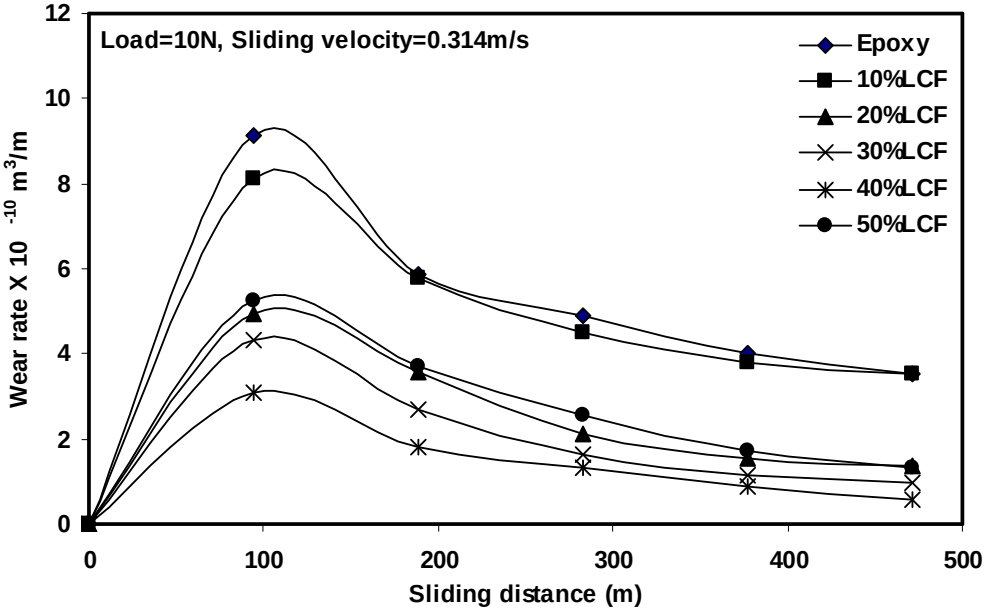

Figure-4.19 Variation of wear rate with sliding distance under the applied Normal load of 10N

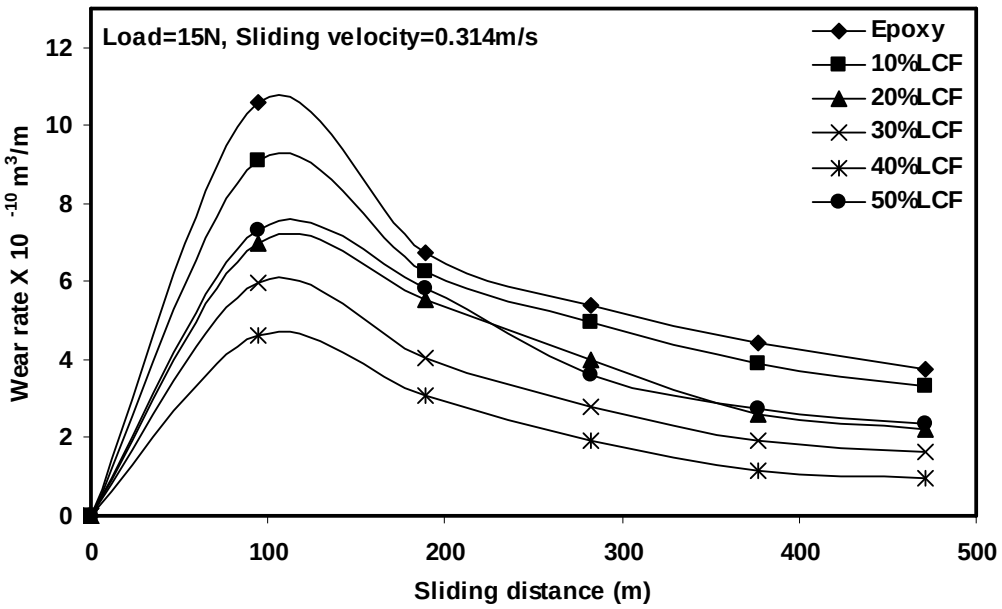

Figure-4.20 Variation of wear rate with sliding distance under the applied Normal load of 15N

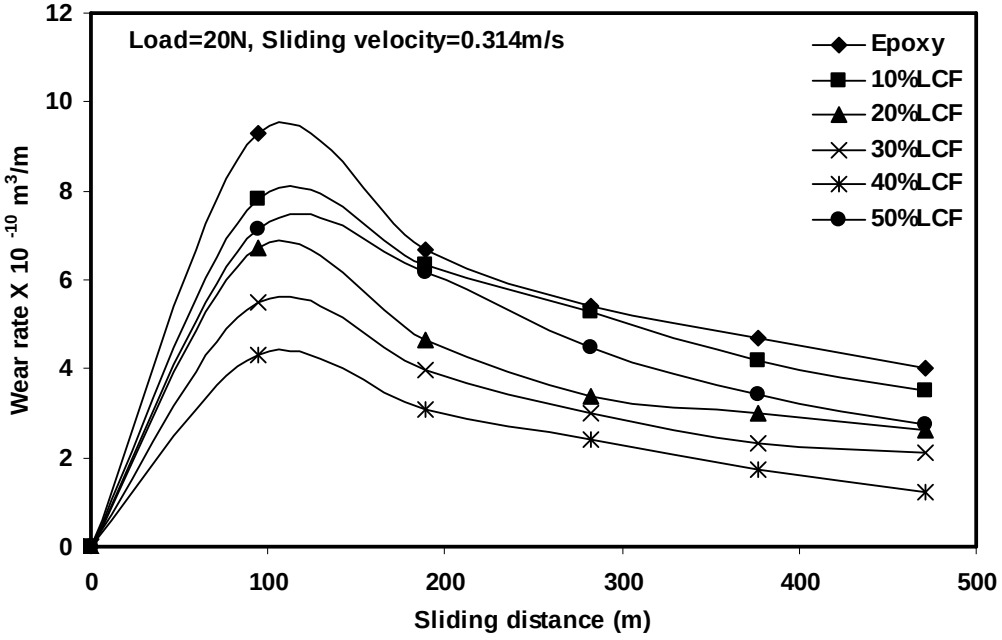

Figure-4.21 Variation of wear rate with sliding distance under the applied Normal load of 20N

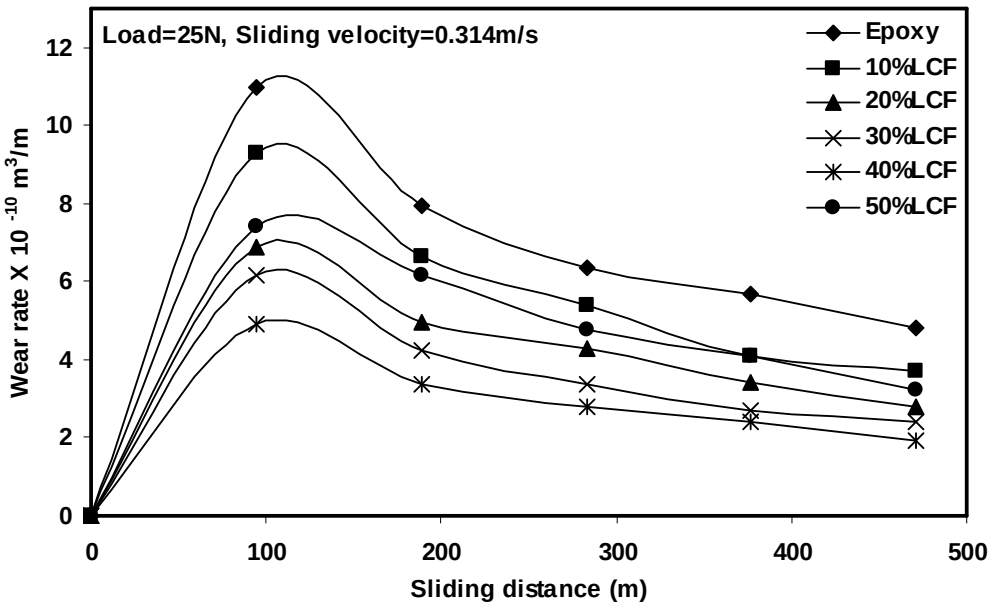

Figure-4.22 Variation of wear rate with sliding distance under the applied Normal load of 25N

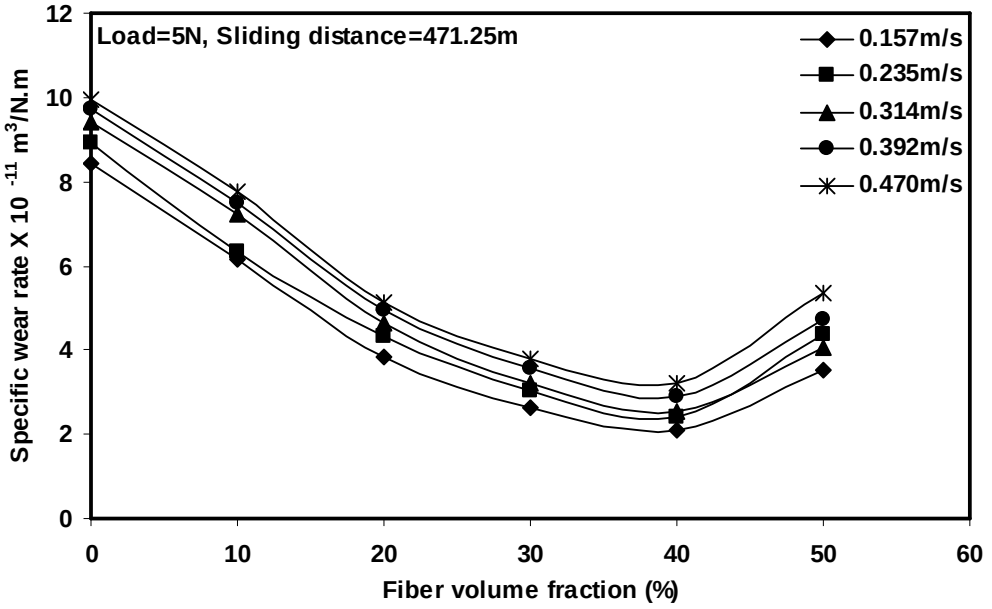

Figure-4.23 Variation of specific wear rate with fiber volume fraction under Normal load of 5N

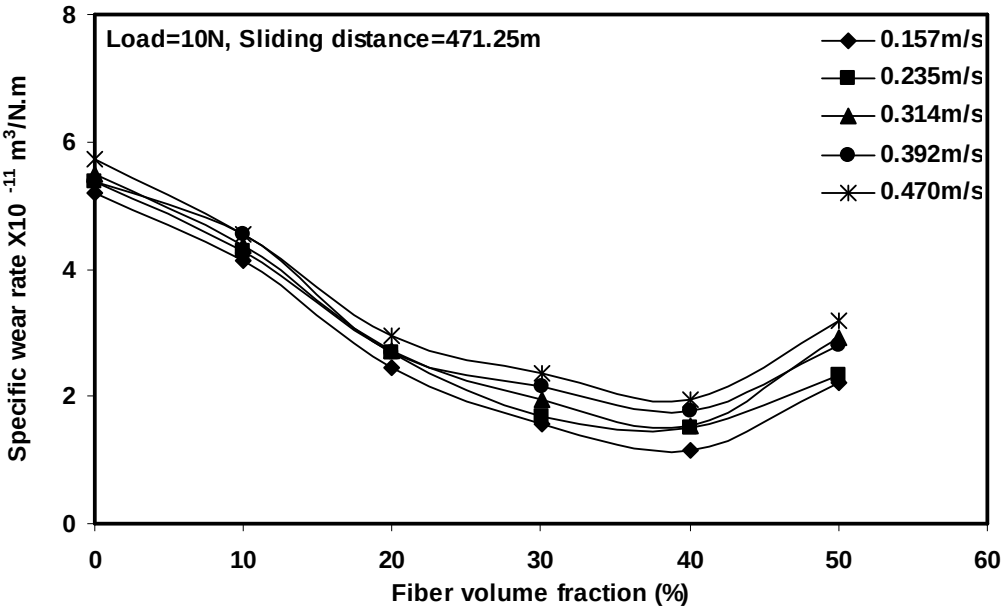

Figure-4.24 Variation of specific wear rate with fiber volume fraction under Normal load of 10N

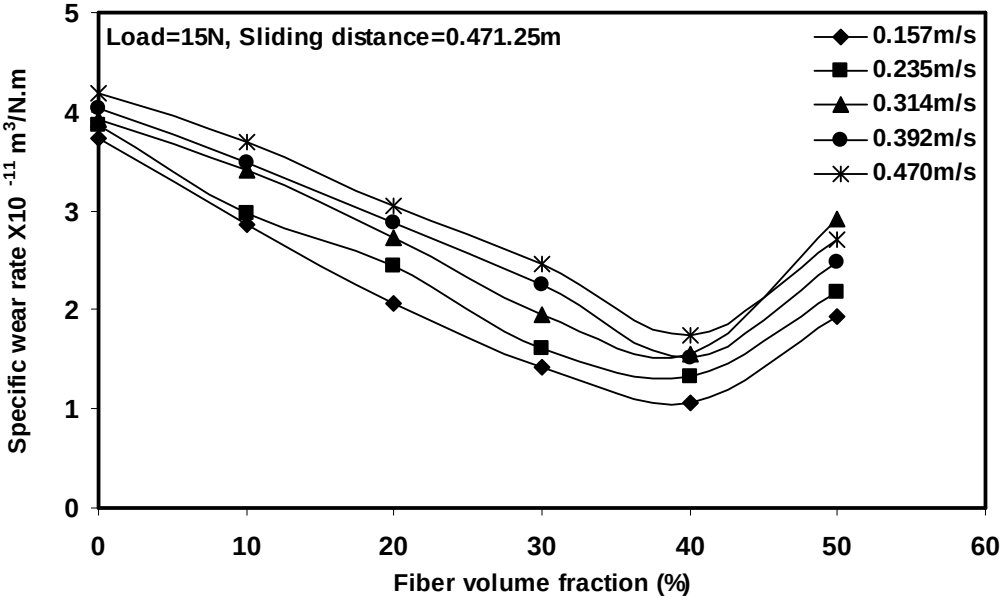

Figure-4.25 Variation of specific wear rate with fiber volume fraction under Normal load of 15N

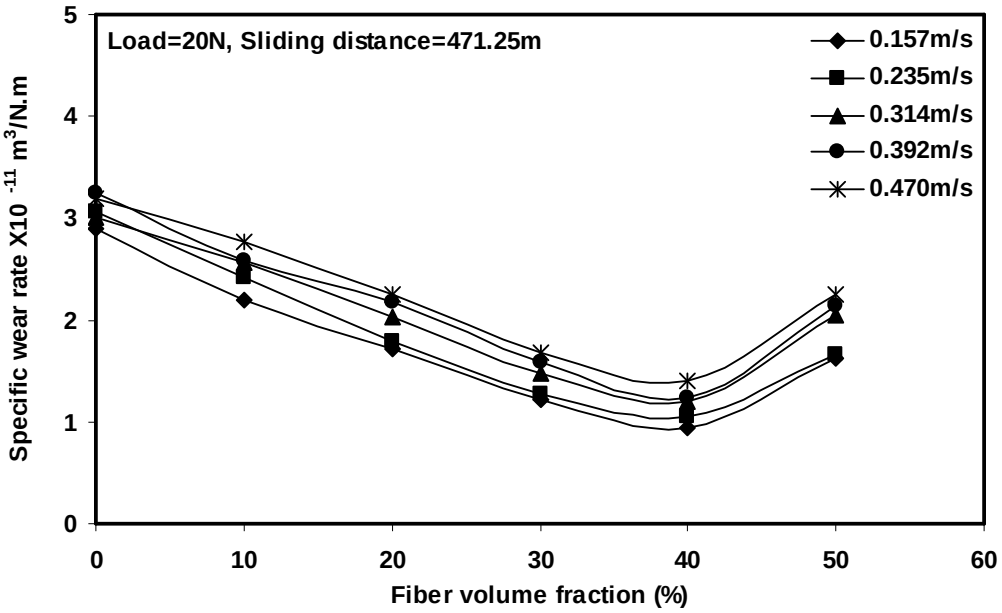

Figure-4.26 Variation of specific wear rate with fiber volume fraction under Normal load of 20N

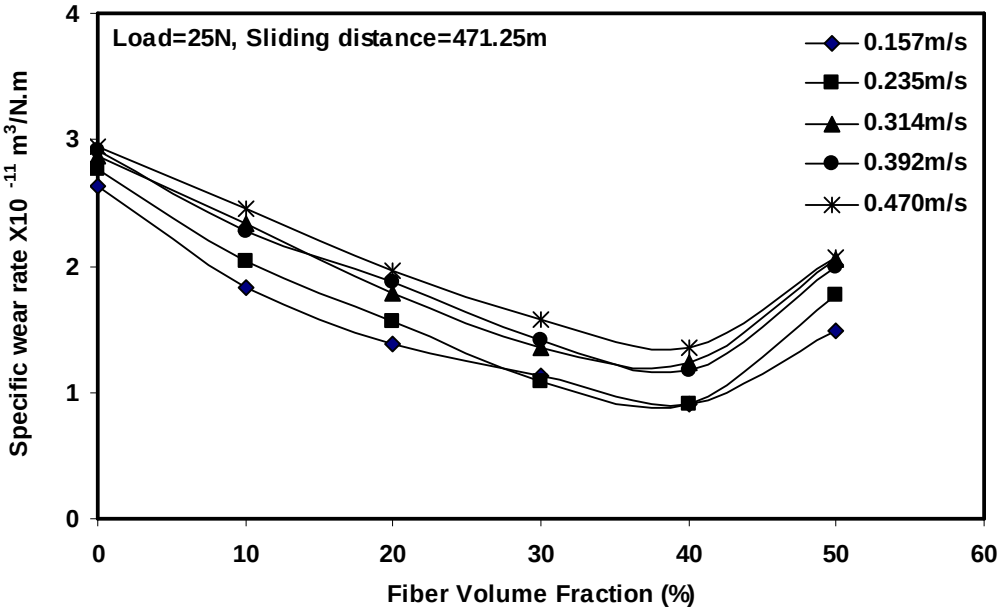

Figure-4.27 Variation of specific wear rate with fiber volume fraction under Normal load of 25N

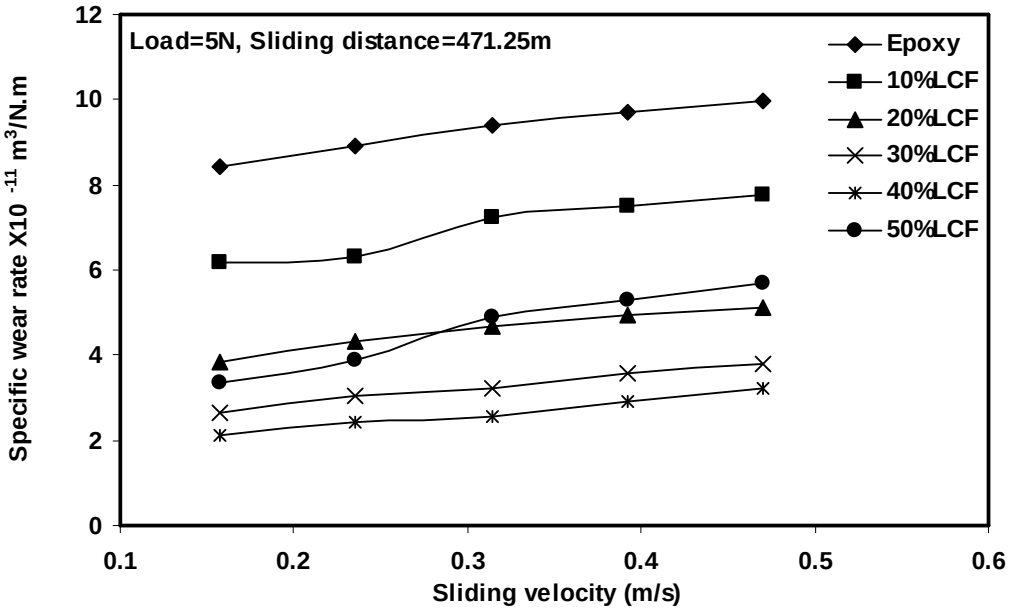

Figure-4.28 Variation of specific wear rate with sliding velocity under Normal load of 5N

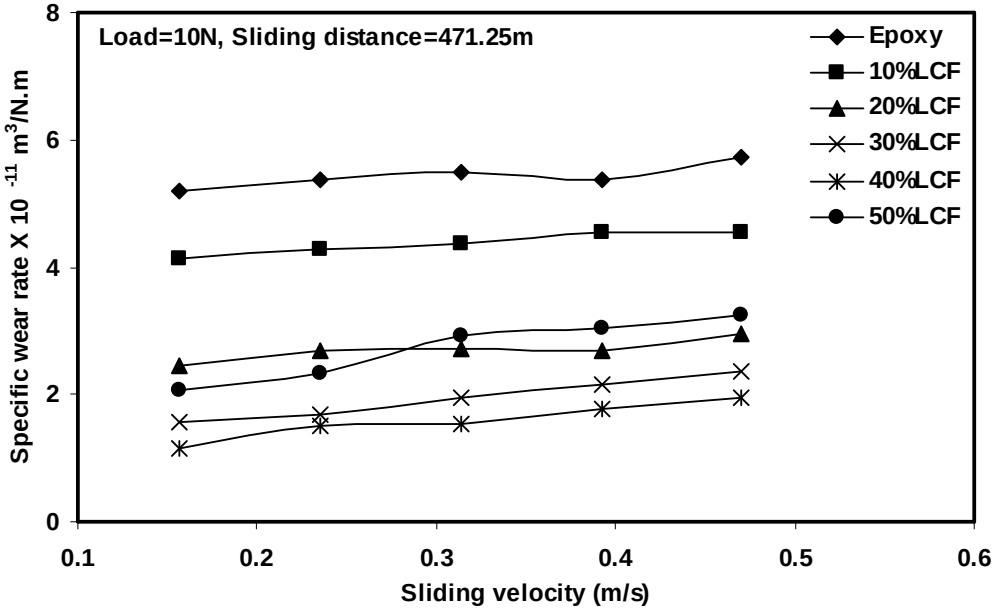

Figure-4.29 Variation of specific wear rate with sliding velocity under Normal load of 10N

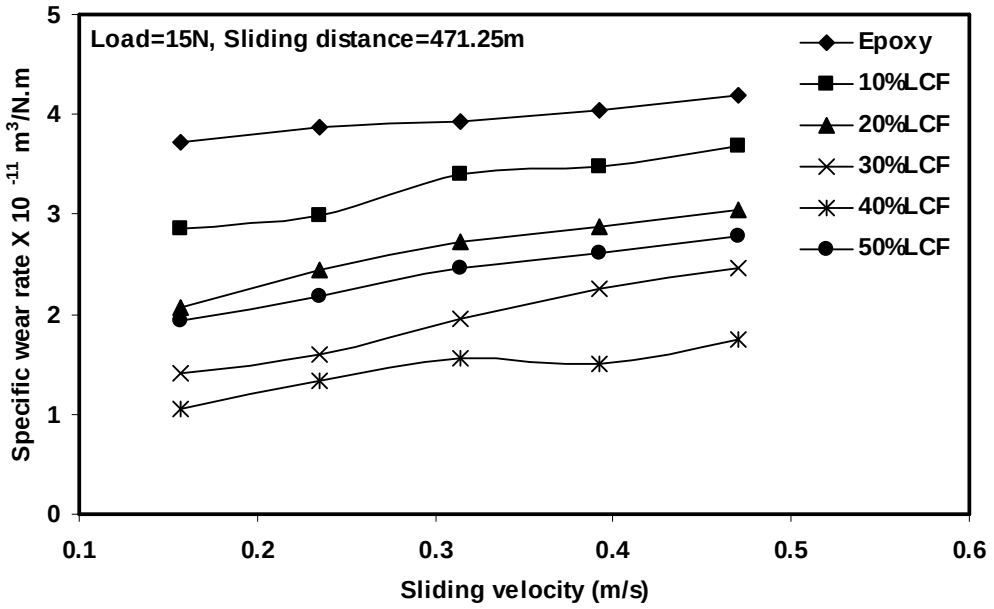

Figure-4.30 Variation of specific wear rate with sliding velocity under Normal load of 15N

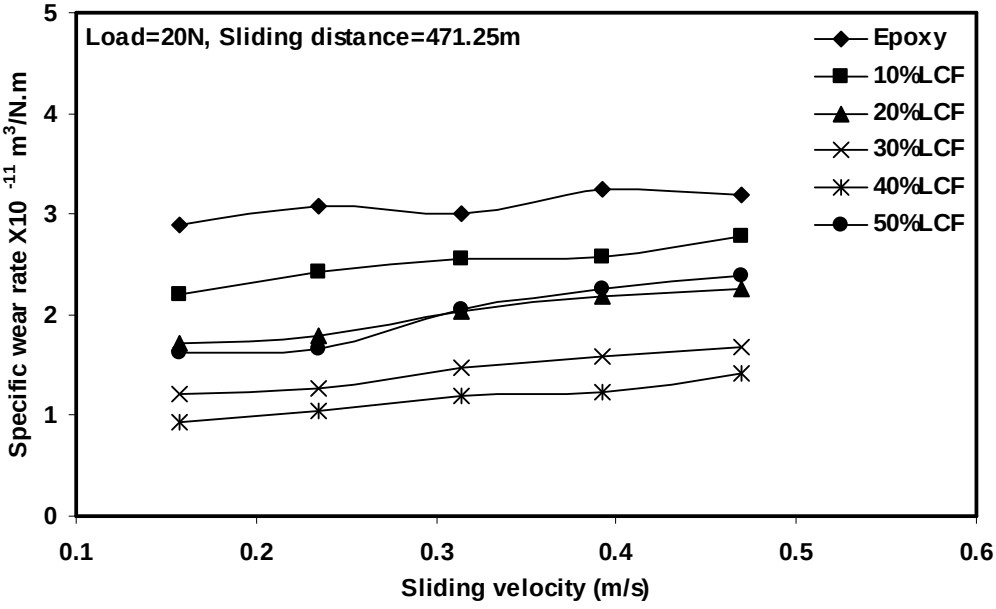

Figure-4.31 Variation of specific wear rate with sliding velocity under Normal load of 20N

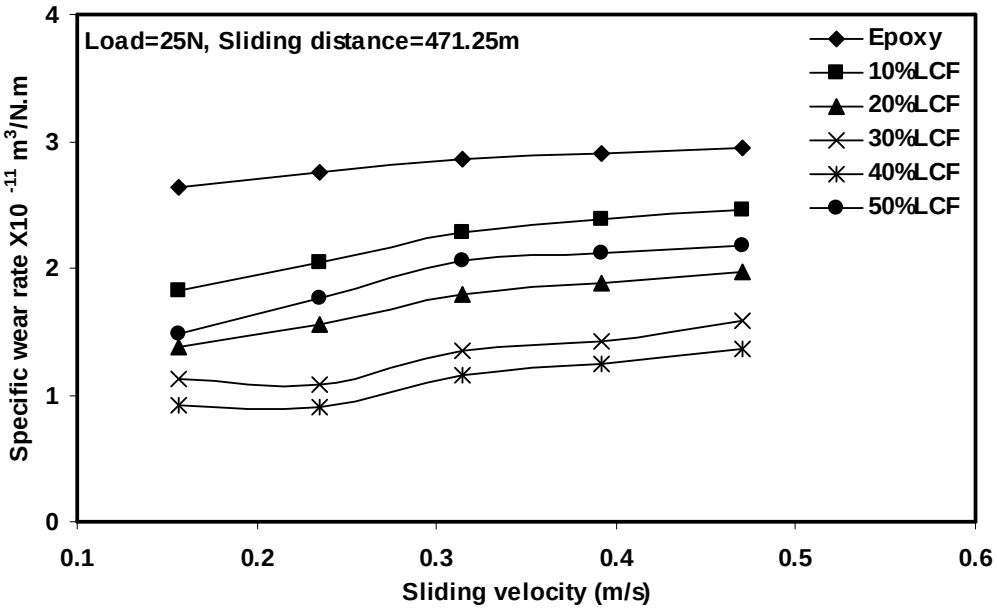

Figure-4.32 Variation of specific wear rate with sliding velocity under Normal load of 25N

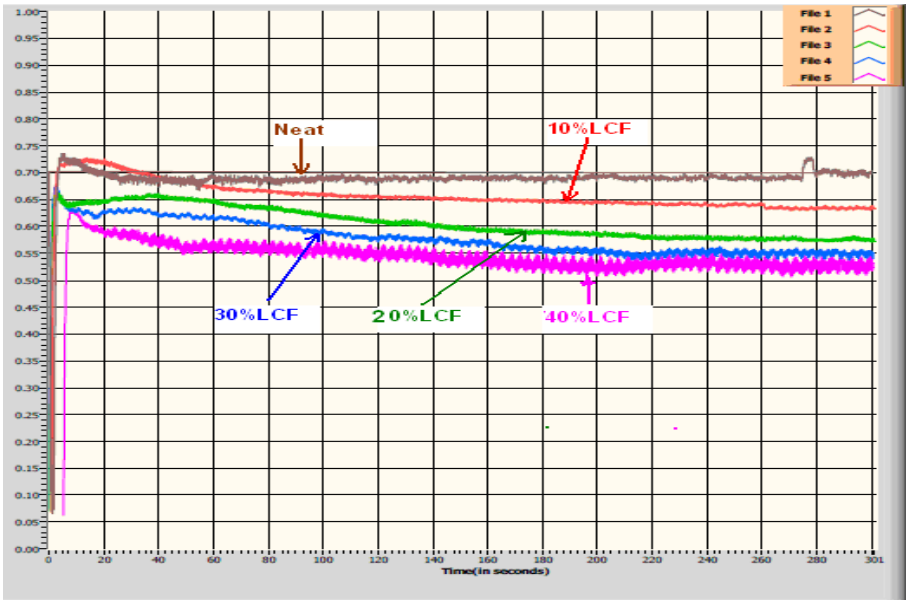

Figure-4.33 Plots between the friction coefficients and time for different composites (neat epoxy and 10vol% to 40vol% fiber reinforced epoxy composite) at 25N applied normal load and 0.314m/s sliding velocity.

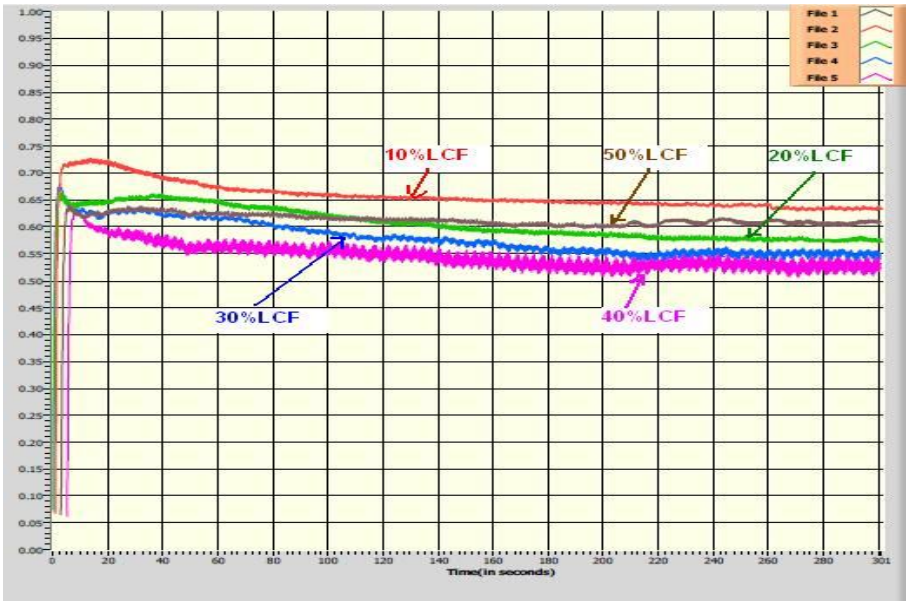

Figure-4.34 Plots between the friction coefficients and time for different composites (10vol% to 50vol% fiber reinforced epoxy composite) at 25N applied normal load and 0.314m/s sliding velocity.

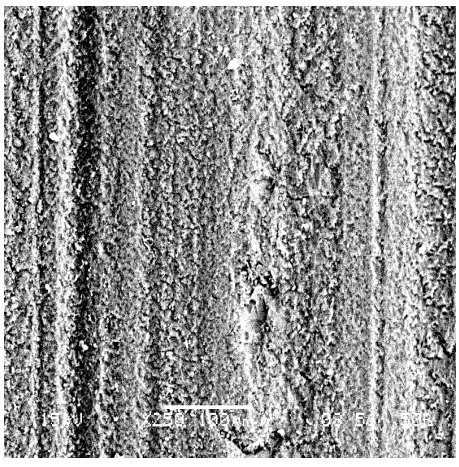

Figure-4.35 (a)

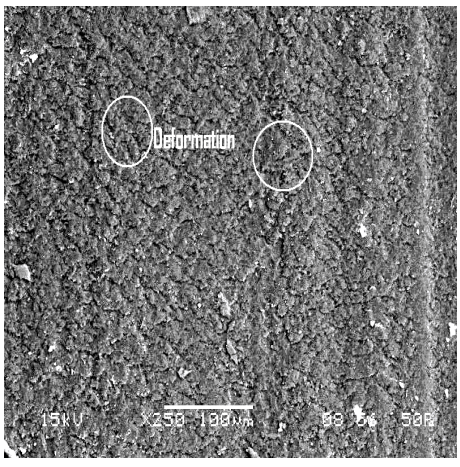

Figure-4.35 (b)

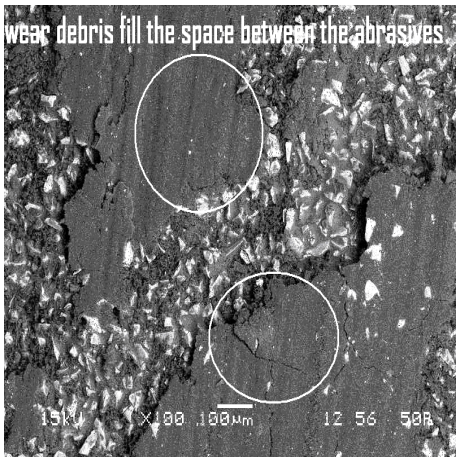

Figure-4.35 (c)

Figure-4.35 (d)

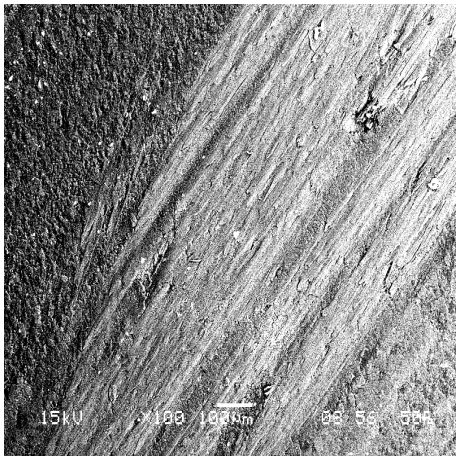

Figure-4.35 (e)

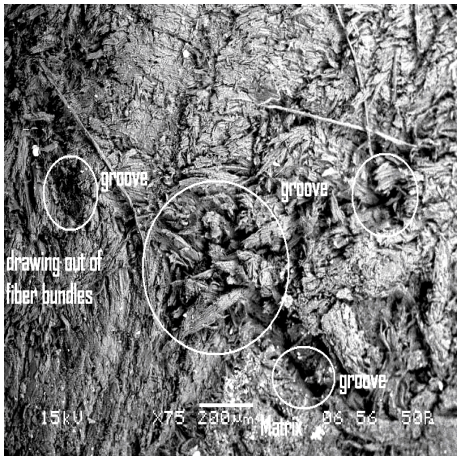

Figure-4.35 (f)

Figure-4.35 **Scanning electron micrograph of worn surface of tested composite samples; (a) Neat epoxy under 15N load, (b) Neat epoxy under 25N load, (c) abrasive surface after test (d) 10vol% LCF reinforced composite under 15N load, (e) 40vol% LCF reinforced composite under 15N load, (f) 50vol% LCF reinforced composite under 15N load.**

Chapter 5

WEAR ANISOTROPY OF LANTANA-CAMARA FIBER REINFORCED EPOXY COMPOSITE

Chapter-5

5.1 INTRODUCTION

Unidirectional continuous fiber-reinforced polymer composites exhibit significant tribological anisotropy due to their heterogeneity. As described in the literature [181-185] fiber orientation with respect to sliding direction is one of the most important parameters affecting properties of composites including friction and wear behaviour of FRP composite. It is also said that properties of natural fiber composites are influenced by fiber loading, dispersion, orientation, and fiber to matrix interface [186]. Natural fibers such as sisal and jute are naturally occurring composites containing cellulose fibrils embedded in lignin matrix. These cellulosic fibrils are aligned along the length of the fiber irrespective of its origin. Such an alignment leads to maximum tensile strength and provides rigidity in that direction of the fiber. Experimental investigation has shown that the largest wear resistance in FRP composites occurred when the sliding was normal to the fiber orientation, while the lowest wear resistance occurred when the fiber orientation was in the transverse direction. Experiments have also shown that the coefficient of friction and the wear in FRP composites depend on several factors including the material combination, the fiber orientation, and the surface roughness.

Cirino et al. [183] studied the dry abrasive wear behaviour of continuous aramid fiber reinforced epoxy composite and found that among three orientations of aramid fiber in epoxy matrix i.e. normal, parallel and anti-parallel directions, normal orientation produces optimum wear resistance. Shim et al. [185] reported the effect of fiber orientation on friction and wear properties of graphite fiber composites and discovered that the differences in friction and wear behaviour of specimens with different fiber orientation are mainly due to the anisotropic properties caused by the microstructure of fiber orientation in the matrix. Lhymn [182] investigated the tribological properties of unidirectional polyphenylene sulfide-carbon fiber laminate composites and reports that fibers that are oriented normal to sliding surface exhibits better wear resistance. He also attempted to qualitatively explain the effect of fiber orientation in terms of the difference in the inter-laminar shear strength and

the fracture strain of the three principal fiber orientations. Sung et al. [181] reported the same type of result while they worked for Kevlar-epoxy composites. Whereas results of Friedrich et al. [187] for with unidirectional carbon fiber-glass matrix composite showed maximum wear resistance in case of anti-parallel orientation.

Though extensive work on wear anisotropy of synthetic fiber has already been done, the wear anisotropic of natural fiber composite is meager. Recently some attempt has been taken to study the wear anisotropy of on natural fibers like cotton [188], bamboo [189-190], sisal [191], jute [192], and kenaf [193]. Amin [188] reported the effect of unidirectional cotton fiber reinforcement on the friction and sliding wear characteristics of polyester with varying sliding speed, fiber volume fraction, and fiber orientation. Chand et al. [189-190] studied the wear behaviour of bamboo in different orientations such as LL, LT and TT, and observed that in bamboo the wear rate follows the trend $W_{TT} < W_{LT} < W_{LL}$. Tong et. al. [191] reported the three-body abrasive wear (low stress) results of bamboo against a free abrasive consisting of quartz sand and bentonite in the past on a rotary-disk type abrasive wear tester. Chand et al. [192] while working on influence of fiber orientation on high stress wear behaviour of sisal fiber reinforced epoxy composites, reported that the wear rate for sisal fiber follows the trend; $W_{TT} < W_{LT} < W_{LL}$. Similar results also observed while they worked with jute fiber reinforced polyester composite [193]. Chin et al. [194] investigated wear and friction performance of kenaf fibers reinforced epoxy composite in three different fiber orientations with respect to the sliding direction and reported that the composite exhibited better wear performance in normal (N-O) compared to parallel (P-O), anti-parallel (AP-O) orientations.

Acceptance of Lantana-Camara fiber epoxy composite in various engineering application is possible if tribological properties of these materials are thoroughly investigated. There is no evidence in the litreture on abrasive wear performance of LCF composites in different directions. Wear properties of Lantana-Camara fiber-reinforced composite in different directions would have an advantage in utilization of Lantana-Camara fiber epoxy composites. Hence in this chapter the effect of Lantana-Camara fiber orientation, sliding distance, and applied load on the abrasive wear properties of Lantana-Camara fiber-reinforced epoxy composite has been determined and discussed.

5.2 EXPERIMENT

5.2.1 Sample preparation

The thermosetting resin used in this study was a Araldite LY-556, which was obtained from Ciba-Geigy of India Ltd. Lantana-Camara fibers used in this study were locally collected. Composites were prepared by using a resin to hardener ratio as 10:1. Lantana-Camara fiber fibers were arranged in the desired direction with epoxy in a mold to prepare the desired direction composites. A hand-layup technique was used to prepare samples. The weight ratio of epoxy to fiber in the composite was from 40 to 60. The density of the composite was found to be 1.107 gm/cm^3. A schematic diagram of composites showing different fiber orientations and sliding direction with designations of samples is shown in Figure-5.1. Samples were cut in a standard size of 30×30×30mm^3 and polished before testing on a Two-Body Abrasion Tester. The cast samples of Lantana-Camara fiber epoxy composite with different fiber orientation are shown in Figure-5.2.

5.2.2 Two-body Abrasive wear test (Single-pass condition)

Two-body Abrasion wear studies in the single-pass condition have been conducted on a Two-body abrasion wear tester (Figure-5.3), supplied by Magnum Engineers, Bangalore, India. The specimens are abraded against water-proof silicon carbide (SiC) abrasive papers of different grades (100, 220, 320, and 400) suitably fixed on the machine bed. The samples were finished ground to have a uniform contact on the abrasive paper. The specimen was mounted on a sample holder which is fixed on the reciprocating ram and then loaded as per requirement by placing a dead weight on the load pan. The experiment was conducted at a selected constant speed of 1 m/min, with different loads (1, 4, 7 and 10 N) and different sliding distances (6.75, 13.5, 20.25, and 27 m) corresponding to 30, 60, 90 and 120 numbers of strokes respectively. After each test the specimen was removed from the holder and cleaned with a brush to remove any wear debris/particle which might have attached to the specimen. The specimen was again cleaned with acetone prior to weighing. The weight loss was measured by precision electronics weighing machine with an accuracy of ± 0.001gm. The wear rate was calculated as discussed in chapter-4, Art-4.6.3, for dry sliding wear rate. For each test five samples were tested and average value was calculated. The results thus achieved from this test are tabulated and shown in Table-5.1 to 5.4.

5.3 RESULT AND DISCUSSION

Variation of wear rate with applied load for different directionally oriented (PO, APO and NO) Lantana-Camara fiber reinforced epoxy composites are shown in Figure-5.4 to 5.7. It is clear from these figures that wear rate of the composite increases with the increase in normal load for different directionally oriented fibers. However the magnitude of the wear rate is not the same. Minimum wear rate has been observed for NO sample, whereas PO sample exhibits maximum wear rate. The wear rate follows the trend; $W_{NO} < W_{APO} < W_{PO}$ which indicate an-isotropic wear behaviour. In case of NO-type sample the long fibers are well embedded in the matrix and only the cross sections of the vascular bundles come in contact with abrasive particle which oppose the movement of the abrading particles, as a result minimum wear occurred. There is a possibility of maximum real contact area with fibers in the sliding direction in the case of the PO-type sample, which leads to maximum wear in comparison to APO-type and NO-type sample. In this case the abrasion in the composite might have taken place due to the removal of a complete layer of fiber, microcutting of the cell, delamination of fibers leading to micro-cutting and breaking of resin. This in turn leads to formation of debris. In APO-type sample the exposed area of fiber is less in comparison to PO-type but higher than that in NO-type. The removal of complete fiber is restricted due to phase discontinuity i.e. because of the presence of matrix phase present between the fibers. Chand et al. [190] reports the same type of results when they studied the abrasive wear behaviour of bamboo.

Figure-5.8 shows the increase in abrasive grit size from 400 to 100 grit size increase the weight loss of the above three different oriented Lantana-Camara fiber epoxy composite. The wear rate is primarily dependent on the depth and width of the groove made by the abrasives. Using coarser abrasives, the depth of penetration of the abrasive particle is high therefore material removal from the specimen surface is increased. If the applied load is fixed, then the effective stress on individual abrasives increases with coarser abrasive particles, as the load is shared by a lower number of abrasive particles. When the abrasive particles are finer in size, they make only elastic contact with the test specimen surface, as the effective stress in individual abrasive is less. However, at higher load regime, the effective stress on each individual abrasive particles reach to a level where the abrasives make plastic contact with the specimen surface and causing more surface damage even at finer abrasive size.

An attempt has been made in this study to introduce an anisotropy coefficient as explained by Chand et al. [189] in their study for bamboo. Anisotropy coefficient is defined as the ratio of the wear loss value in perpendicular to parallel fiber direction in unidirectional fiber reinforced composites. Physical significance of anisotropy coefficient is to show the anisotropy magnitude of material property in the composites. Anisotropy coefficient can be written as:

$$\text{Anisotropy coefficient } (n) = \frac{W_{NO}}{W_{PO}} \text{ (if property } W \text{ is less in NO case than PO case)}$$

$$\text{or} \qquad n = \frac{W_{PO}}{W_{NO}} \text{ (if property } W \text{ is less in PO case than NO case)}$$

n = 1 for isotropic composites; n = 0, for ideal anisotropic composites (or Infinite anisotropic composites); $0 < n < 1$ for anisotropic composites.

Generally the value of the anisotropy coefficient will lie between 0 and 1. Here the magnitude of wear rate is at a minimum in the case of NO rather than PO, so n =W_{NO}/W_{PO}.

The dependency of wear anisotropy coefficient for different loads and different abrasive grit size for unidirectional Lantana-Camara epoxy composite has also been determined in this study. Figure-5.9 shows the variation of wear anisotropy coefficient with applied loads ranging from 1 to 10N for 27m sliding distance. It is clear from the figure that the increase of load from 1N to 7N, the value of anisotropic coefficient increases. Again further increase of load from 7N to 10N the value of anisotropic coefficient decreases. The minimum anisotropic coefficient occurred at the 7N load.

The relationship for the wear anisotropy for all unidirectional fiber reinforced composite is $n = f(L)$, as proposed by Chand et al [190]. The following equation is drawn for the present case i.e. $\frac{W_{NO}}{W_{PO}} = -aL^2 + bL - c$

where 'W_{PO}' and 'W_{NO}' are the wear in parallel and perpendicular directions of fibers orientations and 'L' is the applied load. Constants a, b and c for Lantana-Camara fiber-reinforced epoxy composites are 0.0063, 0.1002, and 0.1357, respectively.

Similarly figure-5.10 shows the variation of wear anisotropy coefficient with different abrasive grit size. On increasing the grit size removal of material was found to be more due to the deep ploughing action. But this experimental study exhibited the decreasing trend of wear anisotropy coefficient with increasing abrasive grit size (GS). This behaviour of wear anisotropy coefficient is represented as a function of GS for Lantana-Camara fiber-reinforced epoxy composites.

$$n = f(GS)$$

where GS is the abrasive grit size.

Figure 5.11 shows the comparison of weight loss with sliding distance at different applied loads for different direction oriented Lantana-Camara fiber-reinforced epoxy composites. A steady increase in weight loss with increasing sliding distance and load in all the cases has been observed. It might have happened due to exposure of the material to fresh abrading surface every time. There is a marked difference in increase in weight loss of different fiber orientated samples with increase in sliding distance and normal load has also been noticed. This again supplements wear anisotropic behaviour of Lantana-Camara fiber epoxy composite which was shown in Figure-5.4. A similar trend has been found when abraded against all other grade abrasive paper.

5.4 WORN SURFACE MORPHOLOGY

Figure 5.12 (a) to (c) show the SEM micrographs of worn surfaces of PO, APO and NO samples respectively. In PO sample, fiber orientation supports the flow of asperities. First the fiber's surface and cells delaminated by these hard asperities, bent, and then the removal of the debris occurred from composite surface. Whereas the remaining attached fiber became fibrillated, this is clearly visible in Figure.5.12 (a). In this case delamination of fiber's cell and microploughing mechanism dominated in the wear process. Figure.5.12 (b) shows worn surface of the APO sample where, the abrasive particles have slid perpendicular to the fiber alignment. Due to this transverse motion, the abrasives cut the fibers and bend them in the direction of sliding motion. The wear process in this case is mainly due to the micro-cutting of fiber. In case of TT sample, cells of fiber are oriented

normal to the sliding direction. This fiber geometry resists the flow of asperities and removal of debris. Figure.5.12 (c) shows the unworn surface of NO sample, which illustrates the fibrillated cross-section without fiber pullout. In this case micro-cutting of the fiber cross-section was mainly responsible for formation of fine wear debris.

5.5 CONCLUSIONS

From the experiment and observation made on the surface morphology of the tested samples, the following conclusions are drawn:

- Maximum wear resistance (minimum wear rate) is observed in NO-Type sample and the wear rate under sliding mode follows the trend; $W_{NO} < W_{APO} < W_{PO}$ which indicates an anisotropic wear behaviour.

- The wear anisotropy of unidirectional Lantana-Camara fiber-reinforced epoxy composites depends on load and abrasive grit size.

- An equation between abrasive wear anisotropy and load for unidirectional Lantana-Camara fiber-reinforced epoxy composites is proposed. Another relationship between abrasive wear anisotropy with abrasive grit is also suggested.

- Abrasive grit size and normal load have a significant influence on abrasive wear loss, irrespective of fiber orientations.

- In PO-Type sample, the abrasion taking place is due to micro-ploughing and delamination of fiber's cell. Whereas in APO and NO-Type samples, micro-cutting is found to be responsible for the wear process.

Table-5.1 Weight loss and wear rate of PO, APO and NO type samples at sliding distance of 27m for different grit size abrasive paper

Abrasive Grit Size	Load (N)	PO Type Sample		APO Type Sample		NO Type Sample	
		Δw (gm)	$W \times 10^{-9}$ (m^3/m)	Δw (gm)	$W \times 10^{-9}$ (m^3/m)	Δw (gm)	$W \times 10^{-9}$ (m^3/m)
100	1	0.076	2.543	0.042	1.405	0.021	0.703
	4	0.135	4.517	0.098	3.279	0.070	2.342
	7	0.202	6.758	0.165	5.520	0.115	3.848
	10	0.263	8.799	0.218	7.294	0.152	5.085
220	1	0.058	1.941	0.028	0.937	0.011	0.368
	4	0.110	3.680	0.087	2.911	0.065	2.175
	7	0.158	5.286	0.124	4.149	0.094	3.145
	10	0.215	7.193	0.160	5.353	0.138	4.617
320	1	0.043	1.439	0.015	0.502	0.008	0.268
	4	0.091	3.045	0.067	2.242	0.047	1.572
	7	0.138	4.617	0.115	3.841	0.095	3.178
	10	0.170	5.688	0.139	4.651	0.119	3.981
400	1	0.028	0.937	0.015	0.502	0.005	0.167
	4	0.088	2.944	0.065	2.175	0.043	1.439
	7	0.133	4.450	0.094	3.145	0.081	2.710
	10	0.166	5.554	0.120	4.015	0.107	3.563

Table-5.2 Weight loss of PO type sample with sliding distance under different loads

Abrasive Grit Size	Sliding Distance (m)	Weight loss (Δw) in gm, under load			
		1N	4N	7N	10N
100	6.75	0.020	0.036	0.052	0.078
	13.50	0.033	0.061	0.090	0.139
	20.25	0.053	0.095	0.138	0.204
	27.00	0.076	0.135	0.202	0.263
220	6.75	0.015	0.026	0.043	0.052
	13.50	0.028	0.051	0.080	0.097
	20.25	0.041	0.081	0.118	0.152
	27.00	0.058	0.110	0.158	0.215
320	6.75	0.012	0.022	0.041	0.049
	13.50	0.020	0.044	0.075	0.087
	20.25	0.030	0.072	0.108	0.134
	27.00	0.043	0.091	0.138	0.170
400	6.75	0.009	0.018	0.035	0.044
	13.50	0.016	0.04	0.076	0.085
	20.25	0.022	0.07	0.105	0.134
	27.00	0.028	0.088	0.133	0.166

Table-5.3 Weight loss of APO type sample with sliding distance under different loads

Abrasive Grit Size	Sliding Distance (m)	Weight loss (Δw) in gm, under load			
		1N	4N	7N	10N
100	6.75	0.010	0.022	0.029	0.045
	13.50	0.016	0.041	0.061	0.082
	20.25	0.024	0.065	0.108	0.142
	27.00	0.042	0.098	0.165	0.218
220	6.75	0.006	0.015	0.023	0.030
	13.50	0.010	0.035	0.050	0.066
	20.25	0.014	0.055	0.082	0.108
	27.00	0.028	0.087	0.124	0.160
320	6.75	0.004	0.014	0.020	0.027
	13.50	0.008	0.028	0.046	0.057
	20.25	0.012	0.046	0.078	0.098
	27.00	0.015	0.067	0.115	0.139
400	6.75	0.003	0.012	0.02	0.023
	13.50	0.007	0.026	0.041	0.05
	20.25	0.011	0.043	0.068	0.088
	27.00	0.015	0.065	0.094	0.120

Table-5.4 Weight loss of NO type sample with sliding distance under different loads

Abrasive Grit Size	Sliding Distance	Weight loss (Δw) in gm, under load			
		1N	4N	7N	10N
100	6.75	0.004	0.012	0.024	0.038
	13.50	0.007	0.029	0.048	0.070
	20.25	0.012	0.047	0.076	0.109
	27.00	0.021	0.070	0.115	0.152
220	6.75	0.002	0.008	0.019	0.033
	13.50	0.005	0.024	0.040	0.064
	20.25	0.008	0.040	0.066	0.100
	27.00	0.011	0.065	0.094	0.138
320	6.75	0.002	0.008	0.016	0.026
	13.50	0.004	0.019	0.037	0.060
	20.25	0.006	0.033	0.060	0.091
	27.00	0.008	0.047	0.095	0.119
400	6.75	0.001	0.008	0.015	0.022
	13.50	0.002	0.015	0.033	0.058
	20.25	0.004	0.032	0.054	0.085
	27.00	0.005	0.043	0.081	0.107

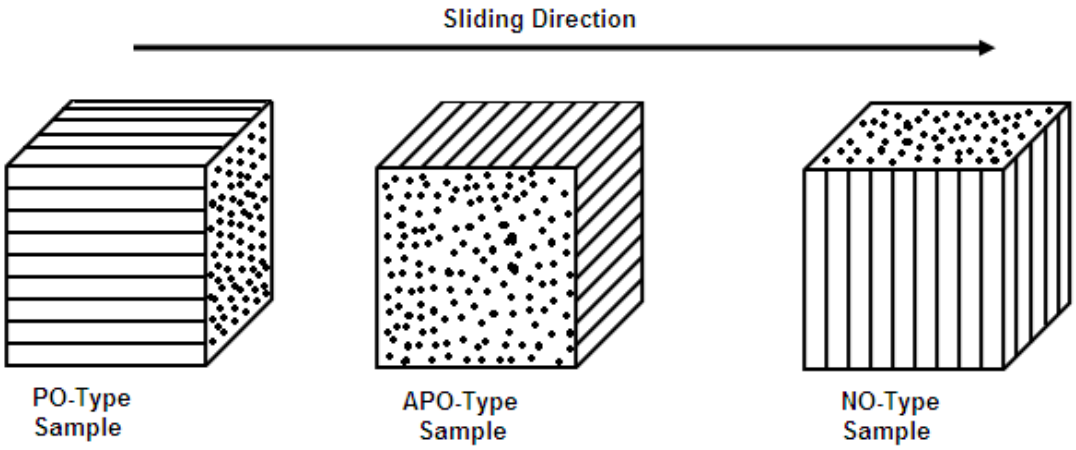

Figure-5.1 **Schematic diagram of different fiber oriented composite with respect to sliding direction**

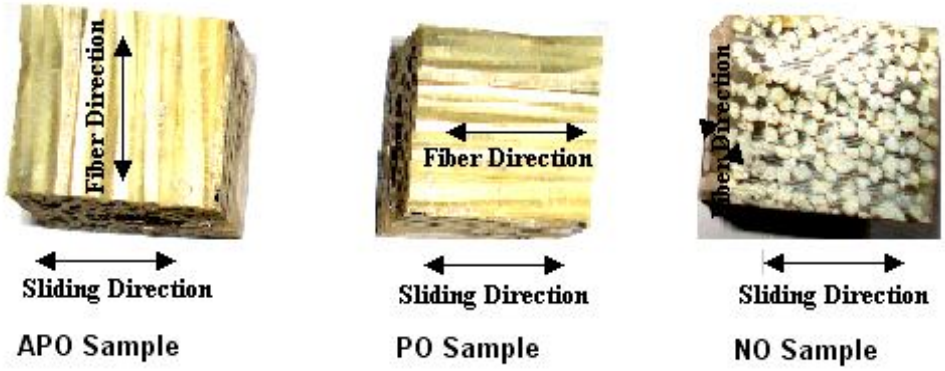

Figure-5.2 **Lantana-Camara fibers reinforced epoxy Composite with three different fiber orientations with respect to sliding direction (APO, PO and NO)**

Figure-5.3 Two-body Abrasion wear tester

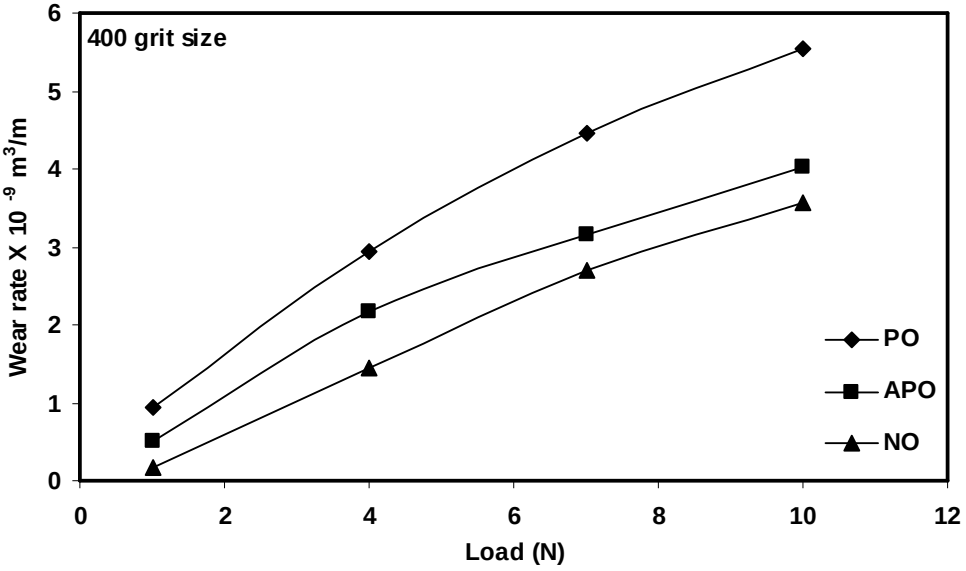

Figure-5.4 Plot between wear rates versus applied load for different oriented composites at 27 m sliding distance and 400 grit size abrasive paper

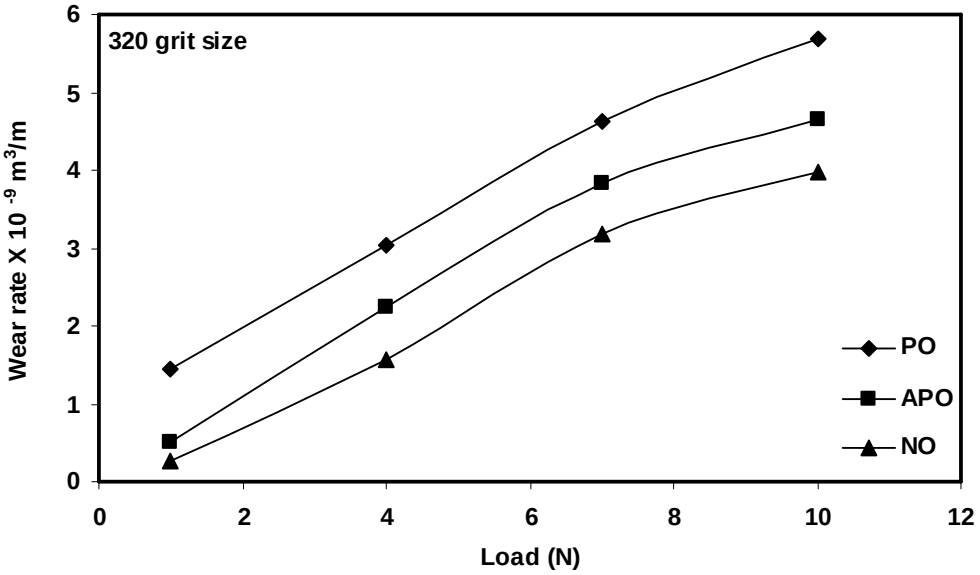

Figure-5.5 **Plot between wear rates versus applied load for different oriented composites at 27 m sliding distance and 320 grit size abrasive paper**

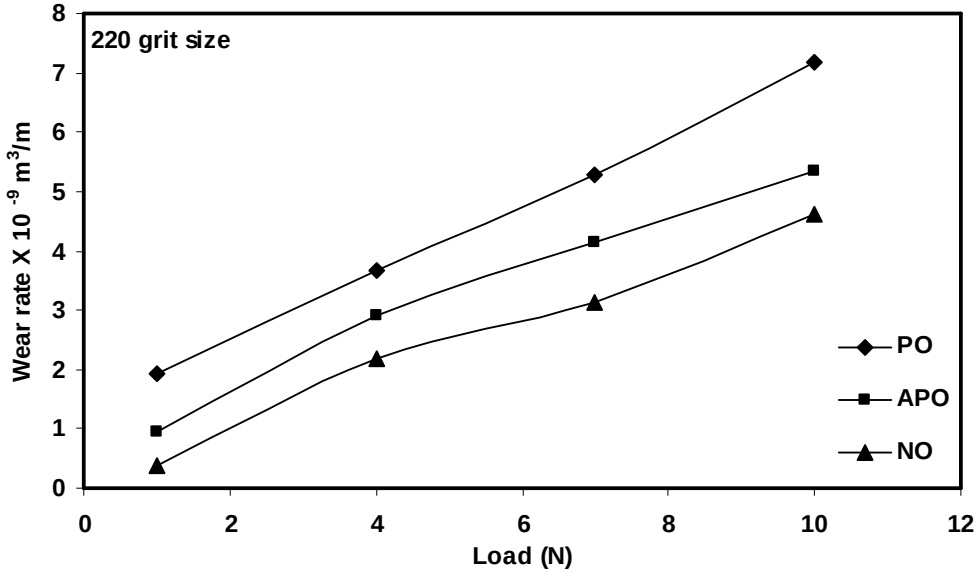

Figure-5.6 **Plot between wear rates versus applied load for different oriented composites at 27 m sliding distance and 220 grit size abrasive paper**

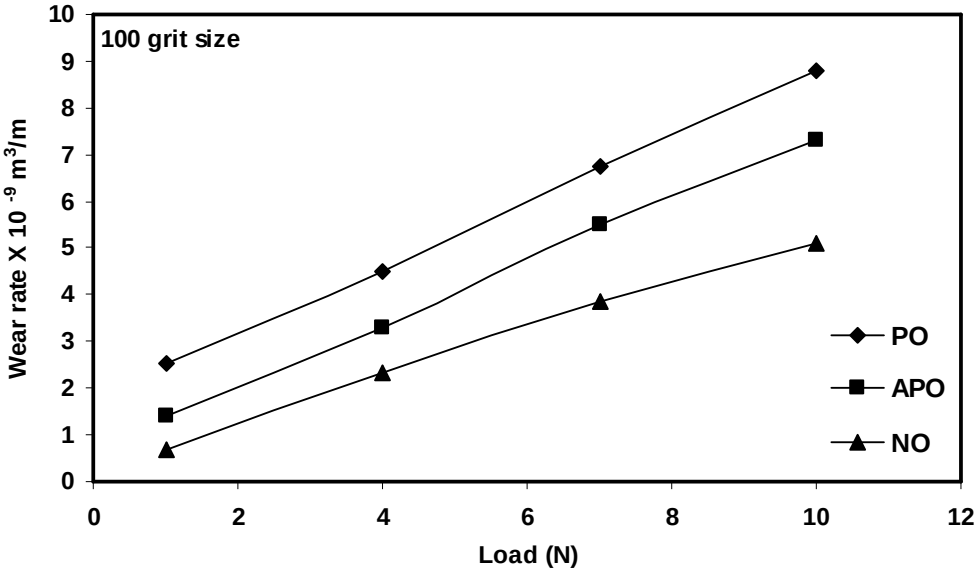

Figure-5.7 **Plot between wear rates versus applied load for different oriented composites at 27 m sliding distance and 100 grit size abrasive paper**

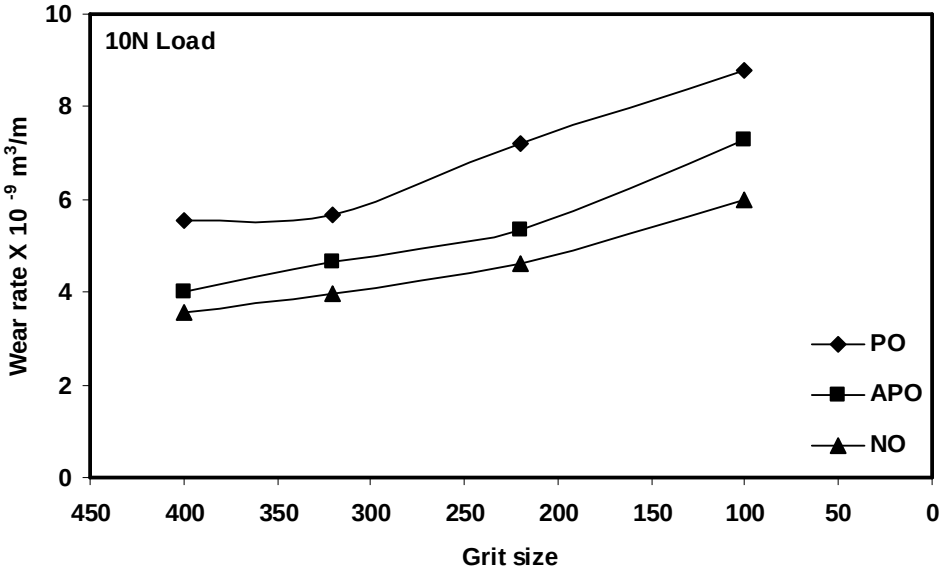

Figure-5.8 **Plot between wear rate vs. grit size for PO, APO and NO samples for applied Load of=10N, Sliding distance = 27 m**

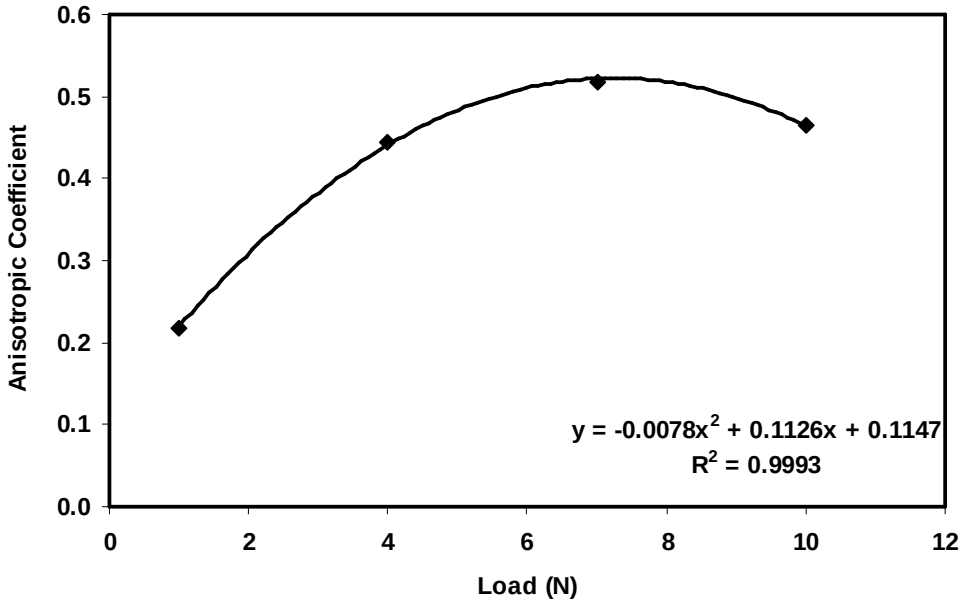

Figure-5.9 **Plot between anisotropy coefficients vs. applied load for unidirectional Lantana-Camara fiber-reinforced epoxy composite**

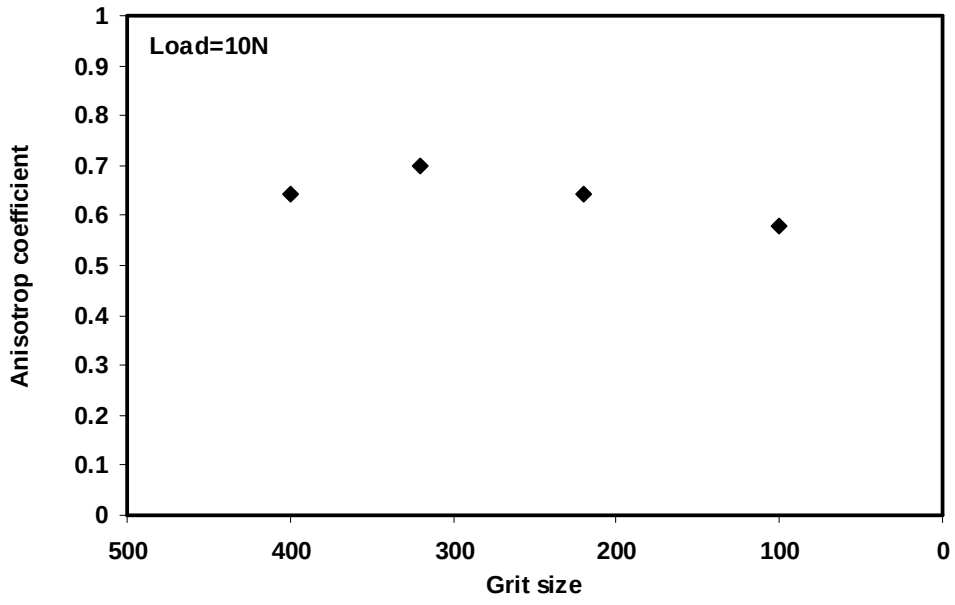

Figure-5.10 **Plot between anisotropy coefficients vs. grit size for unidirectional Lantana-Camara fiber-reinforced epoxy composite**

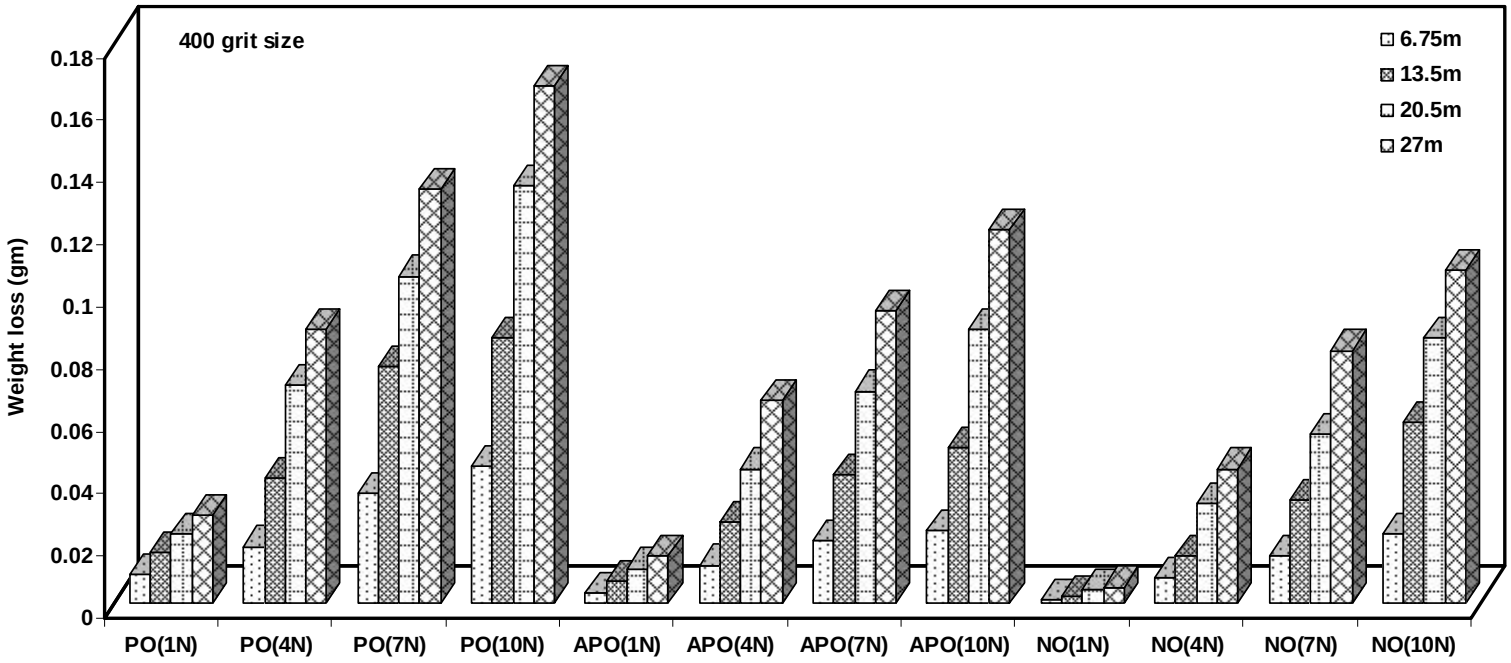

Figure-5.11 **Histogram comparing weight loss at sliding distances 6.75, 13.5, 20.25 and 27 m at different applied loads for differently oriented composites abraded against 400 grit size abrasive paper.**

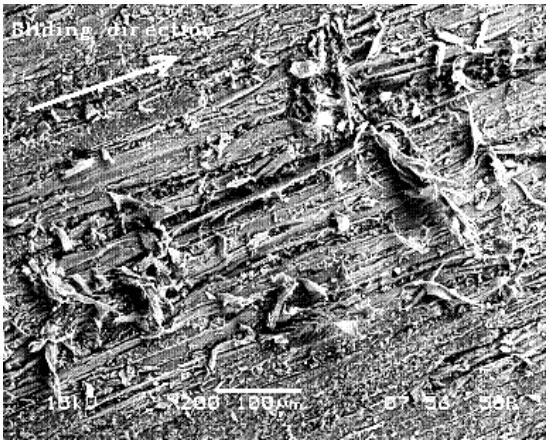

Fig.-5.12 (a)

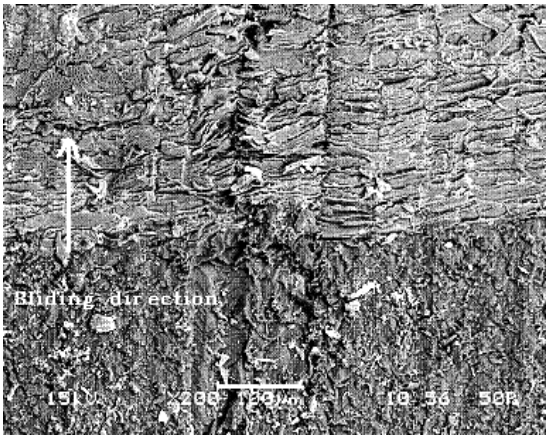

Fig.-5.12 (b)

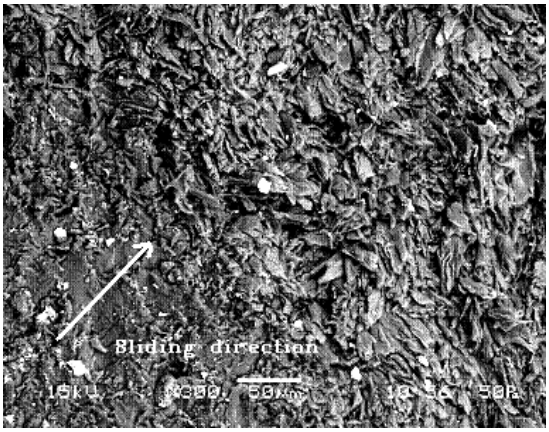

Fig.-5.12 (c)

Figure-5.12 SEM photographs of worn surface of different composites at 10 N load; (a) worn surface of PO-Type sample, (b) worn surface of APO-Type sample, (c) worn surface of NO-Type sample

Chapter 6

SOLID PARTICLE EROSION STUDIES OF LANTANA-CAMARA FIBER EPOXY COMPOSITES

Chapter-6

6.1 INTRODUCTION

Solid particle erosion manifests itself in thinning of components, surface roughening, surface degradation, macroscopic scooping appearance and reduction in functional life of the structure. Hence, solid particle erosion has been considered as a serious problem as it is responsible for many failures in engineering applications. Several attempts to understand the basic mechanisms of the erosion were started in the last half of the 20^{th} century and have been continued to the present. In the year of 1995 an article on the past and the future of erosion was presented by Finnie [195]. In this article, the influencing parameters and dominating mechanisms during solid particle erosion were reviewed on the erosion response of metals and ceramic materials. In the same year another article was published by Meng et al. [196] to provide information about the existing wear models and prediction equations.

6.2 DEFINITION

According to Bitter [197], erosion is a material damage caused by the attack of particles entrained in a fluid system impacting the surface at high speed. Hutchings [198] defines it as an abrasive wear process in which the repeated impact of small particles entrained in a moving fluid against a surface result in the removal of material from the surface. Erosion due to the impact of solid particles can either be constructive (material removal desirable) or destructive (material removal undesirable), and therefore, it can be desirable to either minimize or maximize erosion, depending on the application. The constructive applications include sand blasting, high-speed water-jet cutting, blast stripping of paint from aircraft and automobiles, blasting to remove the adhesive flash from bonded parts, erosive drilling of hard materials. Whereas the solid particle erosion is destructive in industrial applications such as erosion of machine parts, surface degradation of steam turbine blades, erosion of pipelines carrying slurries and particle erosion in fluidized bed combustion systems. In most erosion processes, target material removal typically occurs as

the result of a large number of impacts of irregular angular particles, usually carried in pressurized fluid streams.

6.3 SOLID PARTICLE EROSION OF POLYMER COMPOSITES

The subject of erosion wear of polymer composite has received substantial attention in the past decades. Interest in this area is commensurate with the increasing utilization of polymer based composites in aerospace, transportation and processing industries, where they can be subjected to multiple solid or liquid particle impact. Examples of such applications are pipe lines carrying sand slurries in petroleum refining, helicopter rotor blades , pump impeller blades, high speed vehicles and aircraft operating in desert environments, radomes, surfing boats where the component encounter impact of lot of abrasives like dust, sand, splinters of materials, slurry of solid particle and consequently the materials undergo erosive wear [199-201].

Many researchers have evaluated the resistance of various types of polymers like nylon, epoxy, polypropylene, bismileimide, etc and their composites to solid particle erosion. Harsha et al. [202] has summarized the work done by some of the investigators on solid particle erosion of polymer composites. Roy et al. while working on erosive wear of polymer composite revealed that the composite materials present a rather poor erosion resistance as compared to metallic materials [203].

The most important factors influencing the erosion rate of the composite materials can be summarized under four categories; (i) The properties of the target materials (matrix material properties and morphology, reinforcement type, amount and orientation, interface properties between the matrices and reinforcements, etc.), (ii) Environment and testing conditions (temperature, chemical interaction of erodent with the target), (iii) Operating parameters (angle of impingement, impinging velocity, particle flux–mass per unit time, etc.) and (iv) The properties of the erodent (size, shape, type, hardness, etc.) [201, 204-206]. Thus it seems that the erosion resistance of the material can be evaluated after investigating the combination of above parameters. In general, erosive behaviour of materials can be grouped into ductile and brittle when erosion rate is evaluated as a function of impact angle. The ductile behaviour is characterized by maximum erosion at low impact angle in the

range of 15^0–30°. On the other hand, if maximum erosion occurs at 90°, then the behaviour can be termed as brittle. Reinforced composites have also been some time found to exhibit an intermediate behaviour known as semi-ductile with maximum erosion occurring at an angle in the range of 45^0–60° [207]. However, the above classification is not absolute as the erosion behaviour of a material has a strong dependence on erosion conditions such as impact angle, impact velocity and erodent properties such as shape, hardness, size etc. In the literature, the erosion behaviour of polymers and its composites has also been characterized by the value of the velocity exponent, '*n*' ($E \alpha v^n$) [199].

Visualizing the importance of polymeric composites, much work has been done to evaluate various types of polymers and their composites to solid particle erosion [205, 208-210]. Most of these workers have carried out a wide range of thermoset and thermoplastic PMCs having glass, carbon, graphite and Kevlar fibers in the form of tape, fabric and chopped mat as reinforcement. However there is no information available on the erosion wear behaviour of natural fiber composite. Hence, in this work an attempt has been made to study the erosive wear behaviors of Lantana-Camara fiber (LFC) reinforced epoxy composite. As an initial investigation in the present work the influence of impinging velocity, impingement angle and fiber loading on erosive wear has been carried out and results of these investigations are presented in the subsequent sections.

6.4 EXPERIMENT

6.4.1 Preparation for the test specimens

The preparation of the test specimens were carried out as per the procedure discussed in chapter-3, Art-3.4.3. Specimens of dimension 30 x 30 x 3.0 mm were cut from the composite slabs. Adequate care has been taken to keep the thickness constant (3mm) for all the samples.

6.4.2 Test apparatus & Experiment

The schematic figure of the erosion test apparatus used for the present investigation designed as per ASTM-G76 standard is shown in Figure-6.1. The rig consists of an air

compressor, a particle feeder, and an air particle mixing and accelerating chamber. The compressed dry air is mixed with the erodent particles, which are fed at a constant rate from a conveyor belt-type feeder in to the mixing chamber and then accelerated by passing the mixture through a tungsten carbide converging nozzle of 4 mm diameter. These accelerated particles impact the specimen, and the specimen could be held at various angles with respect to the impacting particles using an adjustable sample holder. The test apparatus has also been fitted with a rotating double disc to measure the velocity of the erodent particle. The impact velocities of the erodent particles has been evaluated experimentally using this rotating double disc method developed as explained by Ives and Ruff [211]. The velocities obtained from this method for various pressures are given in Table-6.1.

The conditions under which the erosion test has been carried out are given in Table 6.2. A standard test procedure is employed for each erosion test. The samples are cleaned in acetone, dried and weighed to an accuracy of 1×10^{-3} gm using an electronic balance, prior and after each test. The test samples after loading in the test rig were eroded for 3 min. at a given impingement angle and then weighed again to determine weight loss (Δw). The erosion rate (E_r) is then calculated by using the following equation:

$$E_r = \frac{\Delta w}{w_e} \tag{6.1}$$

where Δw is the mass loss of test sample in gm and w_e is the mass of eroding particles (i.e., testing time × particle feed rate). This procedure has been repeated until the erosion rate attains a constant steady-state value. In the present study the same procedure is repeated for 5 times (i.e. expose time was 15min).

The erosion efficiency (η) for the process was obtained by using the equation:

$$\eta = \frac{2E_r H}{\rho \times v^2} \tag{6.2}$$

where 'E_r' is erosion rate (kg/kg), 'H' is hardness of eroding material (Pa) and 'v' is velocity of impact (m/s), proposed by Sundararajan et al. [212]. Experimental results of the

erosion test for different volume fraction of Lantana-Camara fiber reinforced epoxy composites with different impingement angle and velocities are tabulated and presented in table 6.3-6.11.

6.5 RESULT AND DISCUSSION

Based on the tabulated results various graphs were plotted and presented in Figure-6.2 to 6.13 for different percentage of reinforcement under different test conditions.

Figure-6.2 to 6.5 illustrate the erosion wear rates of both neat epoxy and LCF reinforced epoxy composite as a function of impingement angle under different impact velocities (48m/s to 109m/s). It is observed that Lantana-Camara fiber epoxy composite shows peak erosion rate ($E_{r\ max}$) at 45^0 impact angle and minimum erosion rate ($E_{r\ min}$) at normal incidence (90^0) under all velocity of impact. Whereas the neat epoxy shows maximum erosion at an angle 90^0. Generally, it has been recognized that peak erosion exists at low impact angles (15^0–30^0) for ductile materials and at a high impact angle (90^0) for brittle materials [213]. However the maximum erosion occurring in the angular range 45^0–60^0 indicates the pseudo semi-ductile behaviour of the material [214]. From the experimental results it is clear that LCF reinforced composites respond to solid particle impact neither behaves in a purely ductile nor in a purely brittle manner. This behaviour can be termed as semi-ductile in nature which may be attributed by the incorporation of Lantana-Camara fibers within the epoxy body. The same type of behavior was also reported by Biswas et al. [215] while studying the erosive behaviour of red mud filled Bamboo-epoxy composite. It is further noticed that irrespective of impact velocity and impact angle, the erosion rate is lowest for neat epoxy and the highest for 40 vol% Lantana-Camara fiber reinforced epoxy composite. Whereas 10vol% to 30 vol% Lantana-Camara fibers reinforced epoxy composites exhibited an intermediate erosion rate under all experimental condition.

The variation of steady-state erosion rate of all composite samples with impact velocity at different impact angles are shown in the form of a histogram in Figure-6.6 to 6.9. It can be observed from these histograms that erosion rate of all composite samples increases with increase in the impact velocity. However, neat epoxy shows least variation in

the erosion rate with increase in the impact velocity at low impact angle ($\alpha = 30^0$). Also, it is clear from the plot that the best erosion resistance under all impact conditions is achieved for the composite made of neat epoxy. Irrespective of impingement angle and impact velocity, there is a steady increase in erosion rate with increase in fiber content has also observed. This indicates that the erosion rate of composites is dominated only by the volume fraction of fiber content. Similar type of observation was reported by Miyazaki et al. [216], while worked with glass and carbon fiber reinforced polyetheretherketon composites.

In the solid particle impact experiments the impact velocity of the erosive particles has a very strong effect on erosion rate. For any material, once steady state conditions have reached, the erosion rate 'E_r' can be expressed as a simple power function of impact velocity (v) [199]:

$$\boldsymbol{E_r = kv^n} \tag{6.3}$$

where *k* is the constant of proportionality includes the effect of all the other variables. The value of '*n*' and '*k*' are found by least-square fitting of the data points in plots which represent the erosion rate dependence on impact velocity by using the power law. The value of '*n*', the velocity exponent, is typically between 2 and 3, although much higher exponent is seen under some circumstances [203]. According to Pool et al. [199], for polymeric materials behaving in ductile manner, the velocity exponent '*n*' varies in the range 2-3 while for polymer composites behaving in brittle fashion the value of '*n*' should be in the range of 3-5. Figure 6.10 to 6.13 illustrates the variation erosion rate with impact velocity at different impingement angle for neat epoxy and its composites. The least-square fits to data point were obtained by using power law and the values of '*n*' and '*k*' are summarized in Table-6.12. The velocity exponents found for 30^0, 45^0, 60^0 and 90^0 impingement angles are in the range of 1.1134–1.9711, 1.1691-1.9505, 1.2882-1.8501 and 1.2046–1.6913 respectively. This velocity exponent at various impingement angles are in conformity with Harsha et al. [208].

It has been reported by Sundararajan et al. [203, 212] that the erosion efficiency (η), can be used to characterize the nature and mechanism of erosion. They also showed that the

ductile material possesses very low erosion efficiency i.e. is very $\eta<<<100\%$, where as the brittle material exhibits an erosion efficiency even greater than 100%. The values of erosion efficiencies of composites under this study are calculated using equation-6.2 and are listed in Table-6.13 along with their hardness values and operating conditions. According to the categorization made by Roy et al. [203], it has been observed that the erosion efficiencies of Lantana-Camara fiber epoxy composite varies from 2.76% to 28.71% for different impact velocities, indicating a semi-ductile erosion response. Further it is noticed that the erosion efficiency of all tests sample slightly decreases with increase in impact velocity. Similar observations are also reported by Srivastava et al. [217] for glass fiber epoxy composite. Thus it can be conclude that the erosion efficiency is not exclusively a material property; but also depends on other operational variables such as impact velocity and impingement angle. The data shown in Table-6.13 are also indicates that the erosion efficiency of Lantana-Camara fiber epoxy composite increase with increase in fiber content whereas the neat epoxy exhibits a lower value under all testing condition. This lower erosion efficiency of neat epoxy indicates a better erosion resistance in comparison to Lantana-Camara fiber epoxy composite.

6.6 SURFACE MORPHOLOGY

To characterize the morphology of eroded surfaces the eroded samples were observed under a scanning electron microscope. Figure 6.14(a) shows the surface of 30 vol% of Lantana-Camara epoxy composite eroded at 60^0 impingement angle. It can be seen from the surface of the samples that material removal is mainly due to micro-cutting and micro-ploughing. Figure 6.14(b) shows the micrograph of surfaces of 30 vol% of Lantana-Camara epoxy composite eroded at an impingement angle of 45^0 with higher particle speed. It is seen that the fiber in composite subjected to particle erosion, encountered intensive debonding and breakage of the fibers, which were not supported enough by the matrix. The continuous impingement of silica sand on the fiber breaks the fiber because of the formation of cracks perpendicular to their length. Also the bending of fibers becomes possible because of softening of the surrounding matrix, which in turn lowers the strength of the surrounding fibers. Same type of behaviour has also been reported by Sari et al. [218] while they worked with carbon fiber reinforced polyetherimide composites under low particle speed.

6.7 CONCLUSIONS

The solid particle erosion study of Lantana-Camara fiber reinforced epoxy composites for various impingement angles and impact velocities led to the following conclusions:

- The influence of impingement angle on erosive wear of composites under consideration exhibits pseudo semi-ductile erosive wear behaviour with maximum wear rate at 45^0 impingement angle.

- The erosion rate of composites increases with increase in fiber content and velocity of impact.

- In LCF epoxy composites the erosion rate (E_r) displays power law behaviour with particle velocity (v), $E_r \alpha v^n$, where 'n' varies from 1.1134 to 1.9711.

- The erosion efficiency (η) values obtained experimentally also indicate that the Lantana-Camara fiber reinforced epoxy composites exhibit semi-ductile erosion response (2.76%-28.71%).

- The morphologies of eroded surface of the samples observed by SEM indicate that, material removal is mainly due to micro-cutting and micro-ploughing.

Table-6.1 Particle velocity under different air pressure

Sl. No.	Air Pressure (Bar)	Particle velocity (m/s)
1	1	48
2	2	70
3	3	82
4	4	109

Table-6.2 Experimental condition for the erosion test

Test parameters	
Erodent:	Silica sand
Erodent size (μm):	200±50
Erodent shape:	Angular
Hardness of silica particles (HV):	1420±50
Impingement angle (α^0):	30, 45, 60 and 90
Impact velocity (m/s):	48, 70, 82 and 109.
Erodent feed rate (gm/min):	1.467±0.02
Test temperature:	(27 ^{0}C)
Nozzle to sample distance (mm):	10

Table-6.3 Cumulative weight loss of 10% LCF epoxy composites with respect to time at different impact angle and velocity

Velocity (m/s)	Time (sec)	Cumulative weight loss 'ŵ' for different Impact Angle (gm)			
		$\alpha=30^0$	$\alpha=45^0$	$\alpha=60^0$	$\alpha=90^0$
48	180	0.001	0.001	0.001	0.001
	360	0.002	0.003	0.003	0.002
	540	0.003	0.004	0.004	0.003
	720	0.005	0.006	0.006	0.005
	900	0.006	0.009	0.008	0.006
70	180	0.003	0.004	0.002	0.002
	360	0.005	0.010	0.005	0.004
	540	0.008	0.015	0.010	0.006
	720	0.012	0.020	0.014	0.009
	900	0.016	0.025	0.018	0.013
82	180	0.004	0.005	0.004	0.003
	360	0.008	0.014	0.010	0.006
	540	0.011	0.023	0.016	0.010
	720	0.016	0.033	0.023	0.014
	900	0.022	0.048	0.028	0.018
109	180	0.005	0.007	0.005	0.004
	360	0.012	0.018	0.014	0.008
	540	0.017	0.033	0.022	0.013
	720	0.023	0.043	0.029	0.018
	900	0.032	0.057	0.035	0.023

Table-6.4 Cumulative weight loss of 20% LCF epoxy composites with respect to time at different impact angle and velocity

Velocity (m/s)	Time (sec)	Cumulative weight loss 'ŵ' for different Impact Angle (gm)			
		$\alpha=30^0$	$\alpha=45^0$	$\alpha=60^0$	$\alpha=90^0$
48	180	0.001	0.001	0.002	0.001
	360	0.003	0.006	0.004	0.003
	540	0.006	0.010	0.008	0.006
	720	0.008	0.017	0.012	0.008
	900	0.010	0.025	0.016	0.010
70	180	0.003	0.003	0.003	0.002
	360	0.007	0.009	0.007	0.004
	540	0.010	0.016	0.012	0.007
	720	0.014	0.024	0.018	0.010
	900	0.019	0.037	0.024	0.013
82	180	0.005	0.005	0.005	0.004
	360	0.011	0.014	0.012	0.007
	540	0.016	0.023	0.021	0.011
	720	0.022	0.035	0.029	0.016
	900	0.030	0.057	0.035	0.021
109	180	0.009	0.009	0.009	0.006
	360	0.017	0.017	0.019	0.011
	540	0.026	0.033	0.031	0.016
	720	0.039	0.045	0.044	0.022
	900	0.049	0.065	0.052	0.029

Table-6.5 Cumulative weight loss of 30% LCF epoxy composites with respect to time at different impact angle and velocity

Velocity (m/s)	Time (sec)	Cumulative weight loss 'ŵ' for different Impact Angle (gm)			
		$\alpha=30^0$	$\alpha=45^0$	$\alpha=60^0$	$\alpha=90^0$
48	180	0.002	0.003	0.001	0.001
	360	0.005	0.010	0.007	0.003
	540	0.009	0.016	0.014	0.004
	720	0.014	0.027	0.022	0.006
	900	0.022	0.041	0.029	0.007
70	180	0.003	0.005	0.003	0.002
	360	0.008	0.014	0.011	0.007
	540	0.013	0.021	0.018	0.011
	720	0.020	0.034	0.024	0.015
	900	0.027	0.049	0.030	0.021
82	180	0.005	0.006	0.004	0.003
	360	0.013	0.018	0.018	0.008
	540	0.021	0.028	0.028	0.013
	720	0.030	0.048	0.038	0.019
	900	0.043	0.065	0.048	0.026
109	180	0.006	0.008	0.006	0.004
	360	0.018	0.025	0.023	0.012
	540	0.029	0.040	0.034	0.018
	720	0.040	0.058	0.049	0.024
	900	0.059	0.075	0.058	0.031

Table-6.6 Cumulative weight loss of 40% LCF epoxy composites with respect to time at different impact angle and velocity

Velocity (m/s)	Time (sec)	Cumulative weight loss 'ŵ' for different Impact Angle (gm)			
		$\alpha=30^0$	$\alpha=45^0$	$\alpha=60^0$	$\alpha=90^0$
48	180	0.002	0.003	0.003	0.001
	360	0.007	0.012	0.010	0.004
	540	0.011	0.020	0.016	0.007
	720	0.016	0.033	0.024	0.010
	900	0.025	0.044	0.032	0.014
70	180	0.004	0.005	0.004	0.003
	360	0.009	0.016	0.015	0.009
	540	0.014	0.024	0.023	0.014
	720	0.021	0.037	0.031	0.019
	900	0.030	0.051	0.037	0.025
82	180	0.004	0.007	0.004	0.004
	360	0.015	0.022	0.020	0.010
	540	0.024	0.034	0.029	0.018
	720	0.032	0.049	0.043	0.022
	900	0.043	0.074	0.052	0.028
109	180	0.006	0.009	0.005	0.004
	360	0.022	0.027	0.024	0.013
	540	0.034	0.044	0.040	0.020
	720	0.049	0.064	0.059	0.027
	900	0.062	0.082	0.070	0.036

Table-6.7 Weight loss and Erosion rate of Neat epoxy composites with respect to impingement angle due to erosion for a period of 15min

Velocity (m/s)	Impact Angle (°)	Weight loss '∆w' (gm)	Erosion Rate × 10^{-4} (gm/gm)
48	30^0	0.0036	1.650
	45^0	0.0049	2.230
	60^0	0.0055	2.510
	90^0	0.0060	2.720
70	30^0	0.0062	2.840
	45^0	0.0084	3.810
	60^0	0.0108	4.930
	90^0	0.0120	5.460
82	30^0	0.0060	2.730
	45^0	0.0108	4.930
	60^0	0.0131	5.940
	90^0	0.0204	9.270
109	30^0	0.0070	3.180
	45^0	0.0130	5.890
	60^0	0.0174	7.920
	90^0	0.0222	10.090

Table-6.8 Weight loss and Erosion rate of 10% LCF epoxy composites with respect to impingement angle due to erosion for a period of 15min

Velocity (m/s)	Impact Angle (°)	Weight loss 'Δw' (gm)	Erosion Rate × 10^{-4} (gm/gm)
48	30^0	0.0072	3.282
	45^0	0.0090	4.100
	60^0	0.0080	3.636
	90^0	0.0060	2.727
70	30^0	0.0162	7.364
	45^0	0.0248	11.273
	60^0	0.0180	8.182
	90^0	0.0125	5.700
82	30^0	0.0220	10.000
	45^0	0.0480	21.818
	60^0	0.0280	12.727
	90^0	0.0180	8.182
109	30^0	0.0320	14.545
	45^0	0.0566	25.727
	60^0	0.0346	15.727
	90^0	0.0230	10.455

Table-6.9 Weight loss and Erosion rate of 20% LCF epoxy composites with respect to impingement angle due to erosion for a period of 15min

Velocity (m/s)	Impact Angle (°)	Weight loss 'Δw' (gm)	Erosion Rate × 10^{-4} (gm/gm)
48	30^0	0.0100	4.545
	45^0	0.0250	11.364
	60^0	0.0165	7.482
	90^0	0.0100	4.545
70	30^0	0.0190	8.636
	45^0	0.0370	16.818
	60^0	0.0244	11.091
	90^0	0.0130	5.909
82	30^0	0.0300	13.636
	45^0	0.0570	25.909
	60^0	0.0350	15.909
	90^0	0.0210	9.545
109	30^0	0.0491	22.300
	45^0	0.0655	29.769
	60^0	0.0520	23.636
	90^0	0.0290	13.182

Table-6.10 Weight loss and Erosion rate of 30% LCF epoxy composites with respect to impingement angle due to erosion for a period of 15min

Velocity (m/s)	Impact Angle (°)	Weight loss 'Δw' (gm)	Erosion Rate × 10^{-4} (gm/gm)
48	30^0	0.0220	10.000
	45^0	0.0412	18.727
	60^0	0.0286	13.000
	90^0	0.0112	5.100
70	30^0	0.0272	12.367
	45^0	0.0490	22.273
	60^0	0.0300	13.636
	90^0	0.0210	9.545
82	30^0	0.0430	19.545
	45^0	0.0650	29.545
	60^0	0.0480	21.818
	90^0	0.0260	11.818
109	30^0	0.0593	26.969
	45^0	0.0752	34.200
	60^0	0.0576	26.195
	90^0	0.0310	14.082

Table-6.11 Weight loss and Erosion rate of 40% LCF epoxy composites with respect to impingement angle due to erosion for a period of 15min

Velocity (m/s)	Impact Angle (°)	Weight loss '∆w' (gm)	Erosion Rate × 10^{-4} (gm/gm)
48	30^0	0.0246	11.200
	45^0	0.0440	20.000
	60^0	0.0319	14.500
	90^0	0.0140	6.364
70	30^0	0.0300	13.636
	45^0	0.0512	23.291
	60^0	0.0370	16.818
	90^0	0.0250	11.364
82	30^0	0.0450	20.455
	45^0	0.0740	33.636
	60^0	0.0520	23.636
	90^0	0.0350	15.909
109	30^0	0.0621	28.227
	45^0	0.0824	37.473
	60^0	0.0702	31.909
	90^0	0.0356	16.200

Table-6.12 Parameters characterizing the velocity dependence of erosion rate of neat epoxy and its composites

Fiber content (%)	Impact Angle	$k \times 10^{-6}$	n	R^2
0 (Neat epoxy)	30^0	9.00	1.1134	0.8477
	45^0	2.00	1.2165	0.9674
	60^0	1.00	1.4101	0.9760
	90^0	0.40	1.6913	0.9186
10	30^0	0.30	1.8371	0.9854
	45^0	0.05	1.9505	0.9306
	60^0	0.30	1.8501	0.9537
	90^0	0.40	1.6839	0.9675
20	30^0	0.20	1.9711	0.9919
	45^0	9.00	1.2393	0.9406
	60^0	3.00	1.4251	0.9810
	90^0	2.00	1.3481	0.9343
30	30^0	7.00	1.2551	0.9216
	45^0	90.00	1.1691	0.9375
	60^0	30.00	1.3156	0.8163
	90^0	4.00	1.2646	0.9520
40	30^0	10.00	1.1631	0.9249
	45^0	80.00	1.2194	0.8887
	60^0	30.00	1.2882	0.9147
	90^0	7.00	1.2046	0.8904

Table-6.13 Erosion efficiency (η) of various composite samples

Impact Velocity 'v' (m/s)	Impact angle 'α'	Erosion efficiency (η)				
		Neat Epoxy	10%LCF	20%LCF	30%LCF	40%LCF
		H=175.5 (Pa)	H=170.4 (Pa)	H=178.0 (Pa)	H=190.8 (Pa)	H=169.8 (Pa)
48	30^0	2.32	4.47	6.43	15.04	14.91
	45^0	3.14	5.58	16.06	28.17	26.63
	60^0	3.53	4.95	10.58	19.56	19.31
	90^0	3.83	3.71	6.43	7.67	8.47
70	30^0	1.88	4.72	5.74	8.75	8.54
	45^0	2.52	7.22	11.18	15.75	14.58
	60^0	3.26	5.24	7.37	9.65	10.53
	90^0	3.61	3.65	3.93	6.75	7.11
82	30^0	1.32	4.67	6.61	10.07	9.33
	45^0	2.38	10.18	12.55	15.23	15.35
	60^0	2.87	5.94	7.71	11.25	10.78
	90^0	3.80	3.82	4.62	6.09	7.26
109	30^0	0.87	3.84	6.11	7.87	7.29
	45^0	1.61	6.80	8.16	9.98	9.68
	60^0	2.16	4.15	6.48	7.64	8.24
	90^0	2.75	2.76	3.61	4.11	4.18

Figure-6.1 **Details of erosion test rig. (1) Sand hopper, (2) Conveyor belt system for sand flow, (3) Pressure transducer, (4) Particle-air mixing chamber, (5) Nozzle, (6) X–Y and h axes assembly, (7) Sample holder**.

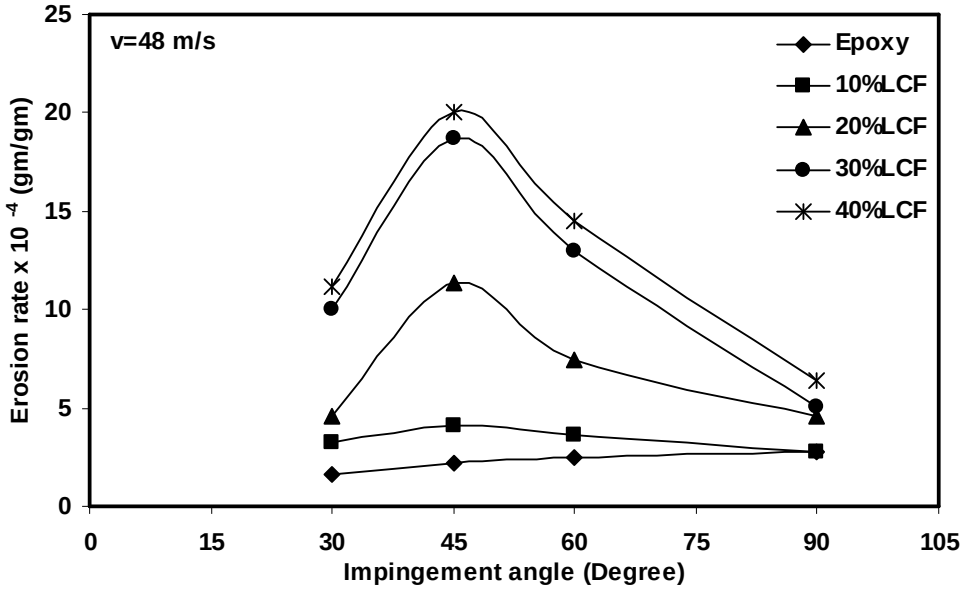

Figure-6.2 **Variation of erosion rate with impingement angle of various Lantana-Camara epoxy composite at impact velocity of 48 m/s**

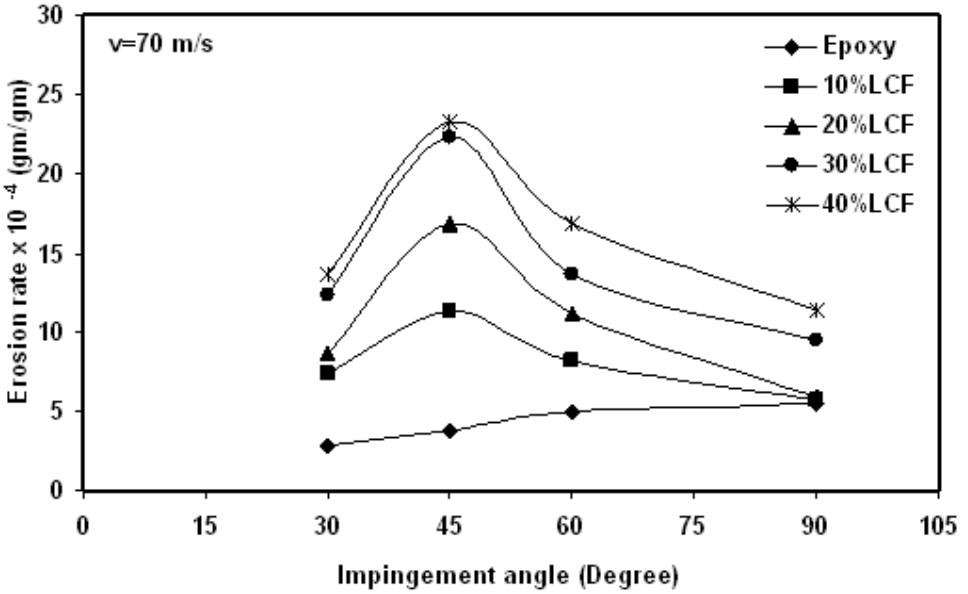

Figure-6.3 **Variation of erosion rate with impingement angle of various Lantana-Camara epoxy composite at impact velocity of 70 m/s**

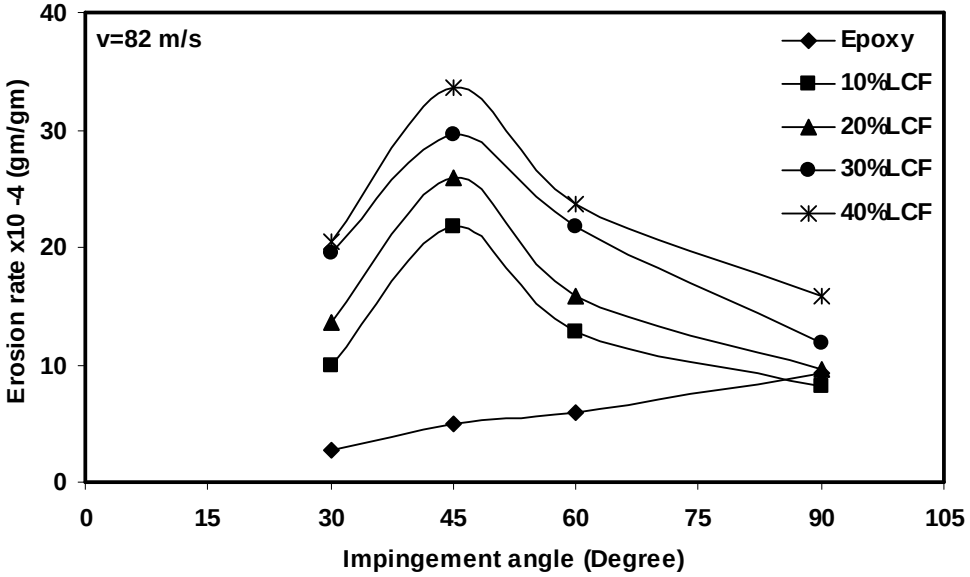

Figure-6.4 **Variation of erosion rate with impingement angle of various Lantana-Camara epoxy composite at impact velocity of 82 m/s**

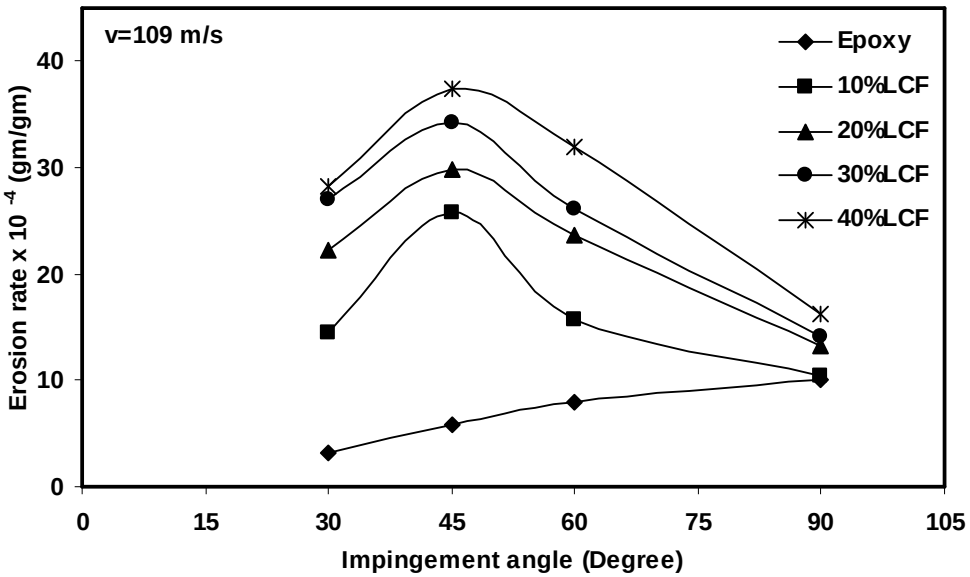

Figure-6.5 **Variation of erosion rate with impingement at impact velocity of 109 m/s**

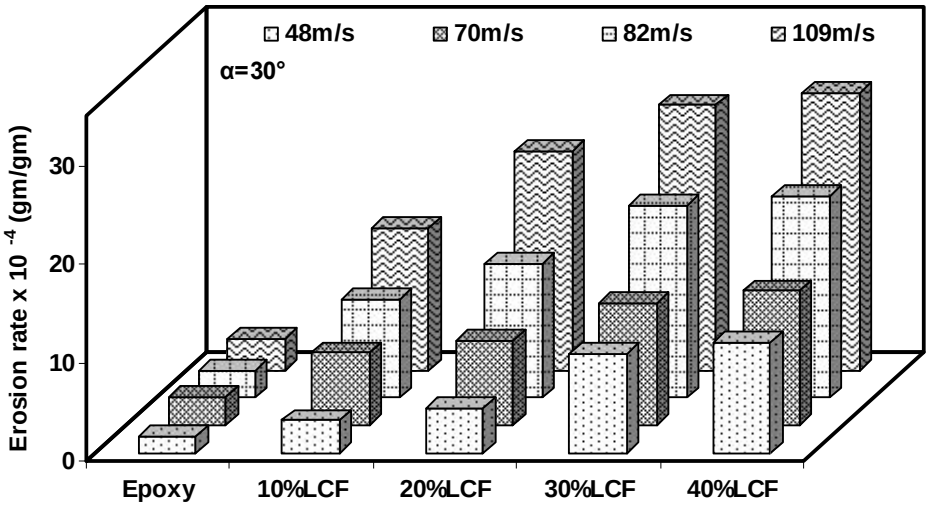

Figure-6.6 **Histogram showing the steady state erosive wear rates of all the composites at four impact velocities (i.e. at 48, 70, 82 and 109 m/s) for 30° impact angle**

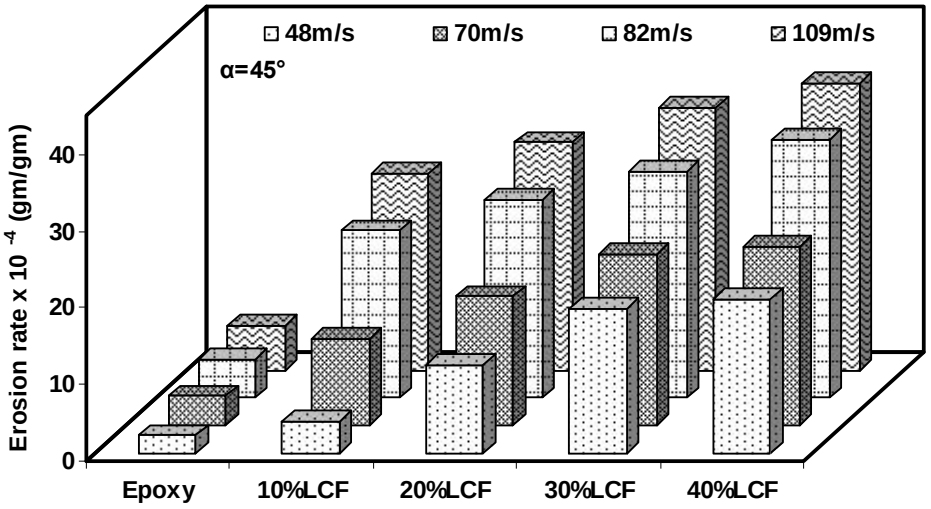

Figure-6.7 **Histogram showing the steady state erosive wear rates of all the composites at four impact velocities (i.e. at 48, 70, 82 and 109 m/s) for 45° impact angle**.

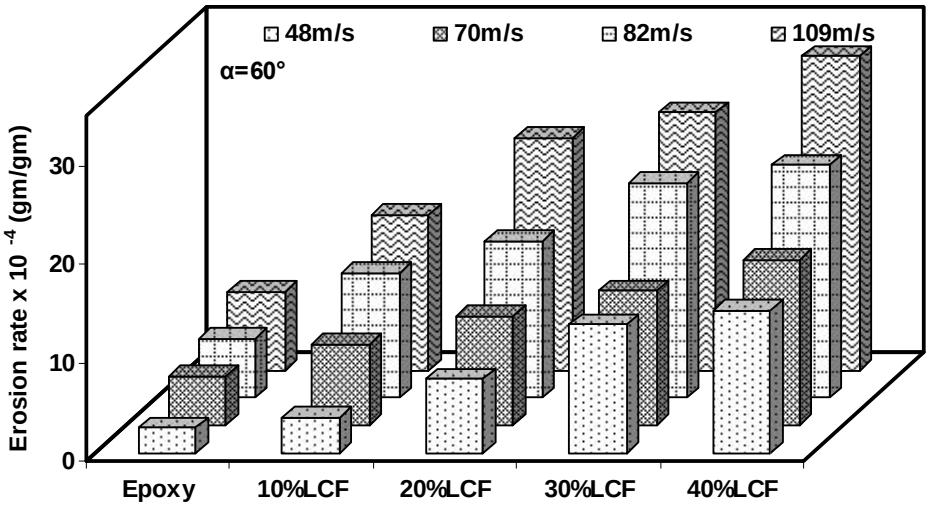

Figure-6.8 **Histogram showing the steady state erosive wear rates of all the composites at four impact velocities (i.e. at 48, 70, 82 and 109 m/s) for 60° impact angle**.

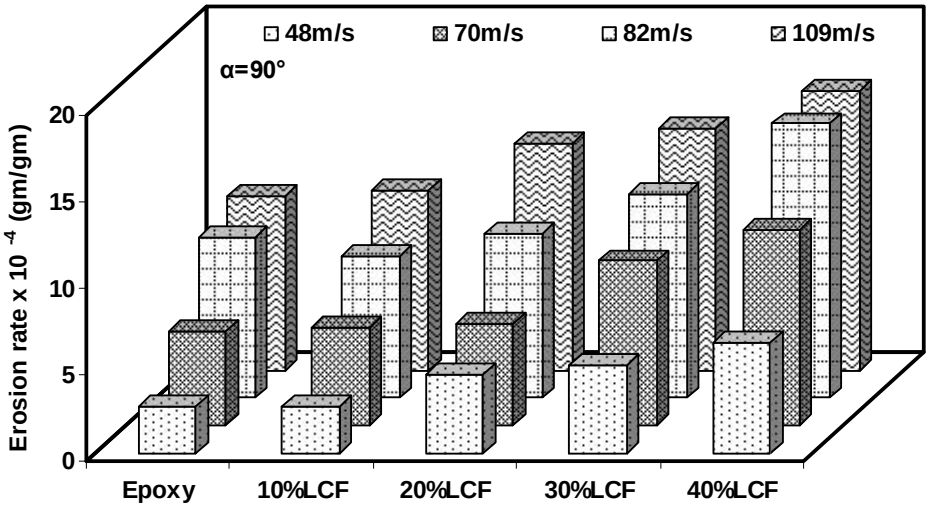

Figure-6.9 **Histogram showing the steady state erosive wear rates of all the composites at four impact velocities (i.e. at 48, 70, 82 and 109 m/s) for 90° impact angle**.

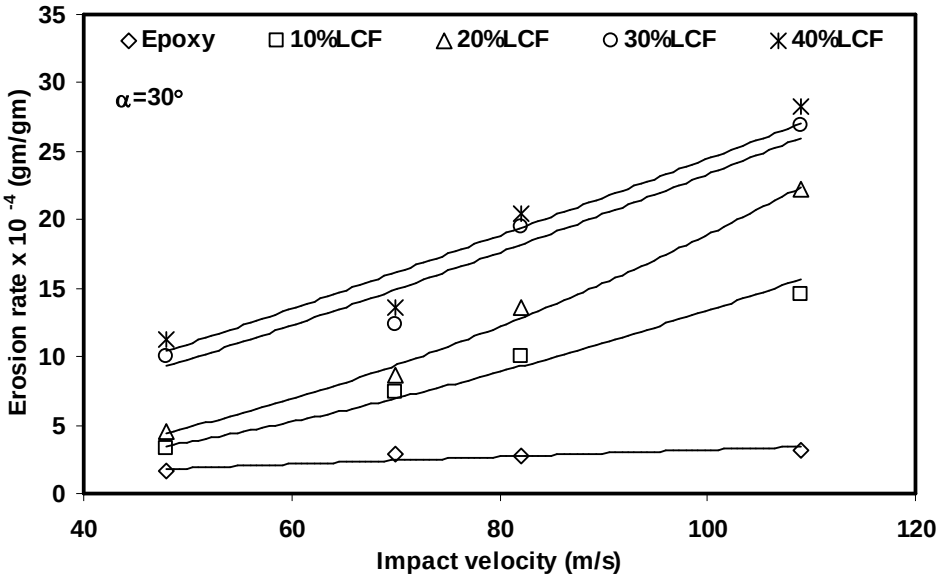

Figure-6.10 Variation of steady-state erosion rate of various composites as a function of impact velocity for 30^0 impact angle

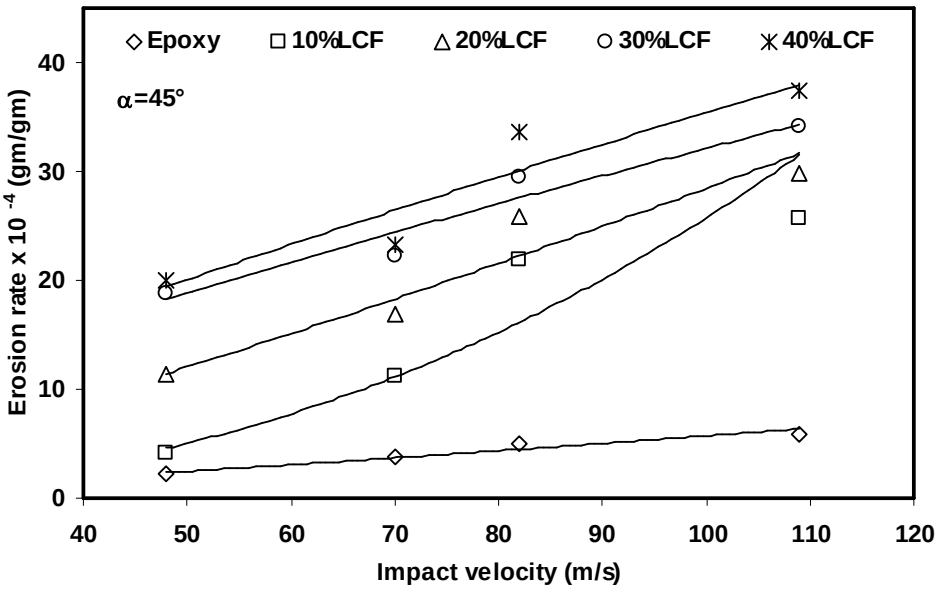

Figure-6.11 Variation of steady-state erosion rate of various composites as a function of impact velocity for 45^0 impact angle

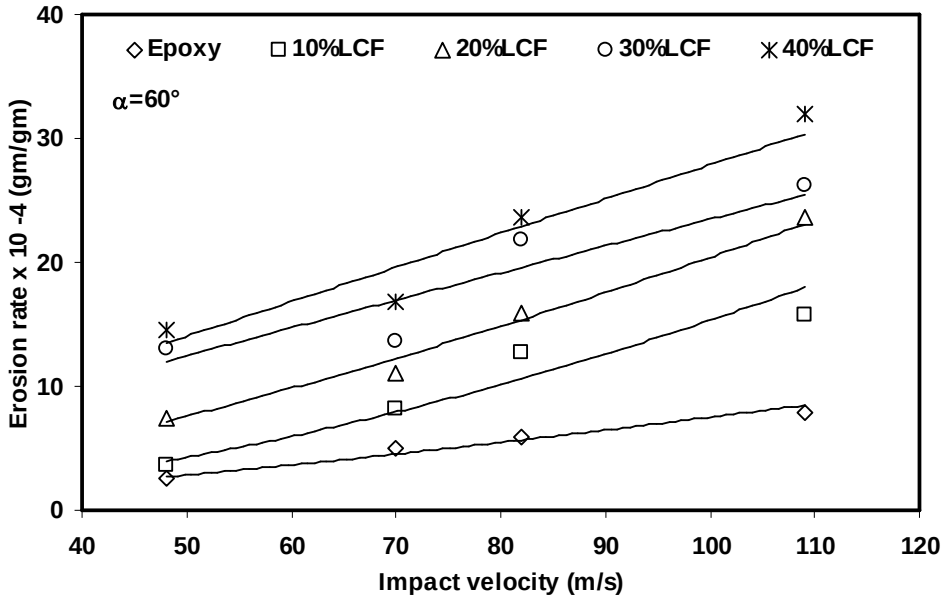

Figgure-6.12 Variation of steady-state erosion rate of various composites as a function of impact velocity for 60^0 impact angle

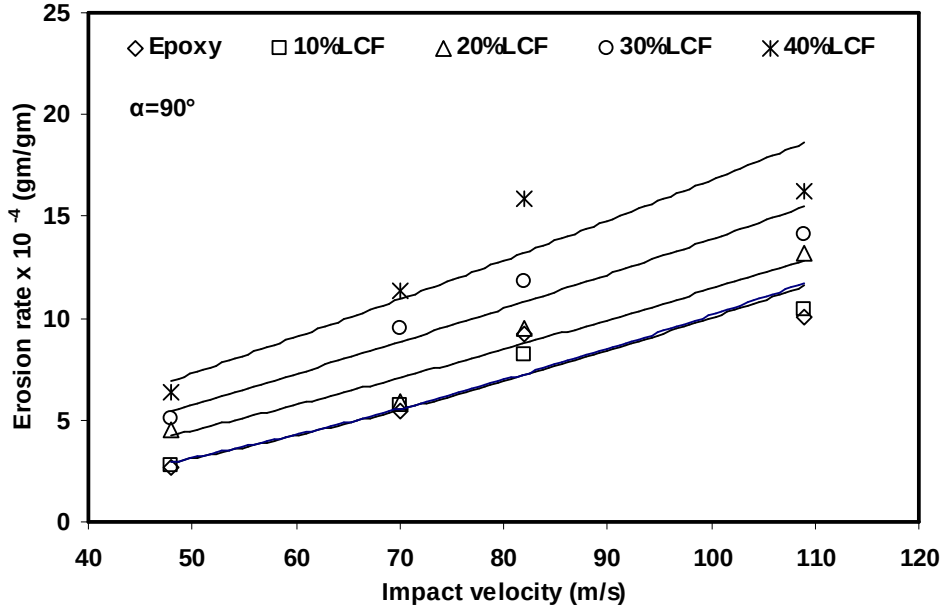

Figure-6.13 Variation of steady-state erosion rate of various composites as a function of impact velocity for 90^0 impact angle

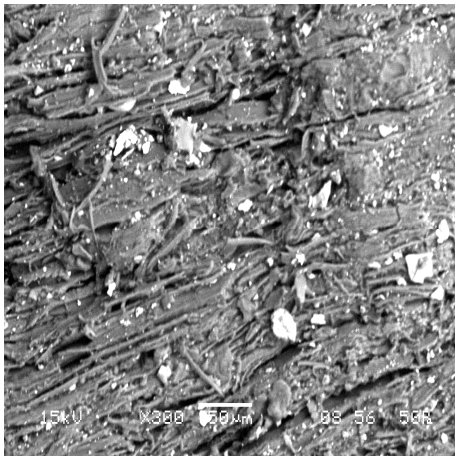

Fig. 6.14 (a)

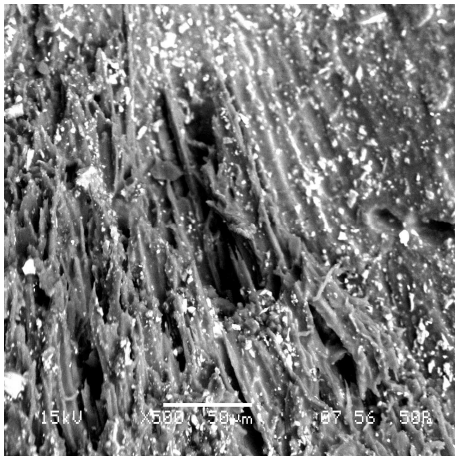

Fig. 6.14 (b)

Figure-6.14 SEM micrographs of eroded surface of 30 vol% of Lantana-Camara epoxy composite at different impact angle; (a) 60° (b) 45°

Chapter 7

MODELING OF ABRASIVE AND EROSIVE WEAR BEHAVIOUR OF LANTANA-CAMARA FIBER EPOXY COMPOSITES BY RESPONSE SURFACE METHODOLOGY

Chapter-7

7.1 INTRODUCTION

Response Surface Methodology (*RSM)* is a practical and useful tool for designing, formulating, developing, and analyzing scientific phenomenon related to any process and product. It is also efficient in the improvement of existing studies on processes and products. The most extensive applications of RSM are found in the industrial world, particularly in situations where several input variables potentially influence some performance measures or quality characteristics of the product or process. The most common applications of *RSM* are in Industrial, Biological and Clinical Sciences, Social Sciences, Food Sciences, and Engineering Sciences. Also, in recent years more emphasis has been imposed by the chemical and processing field for finding regions where there is an improvement in response instead of finding the optimum response [219]. RSM was introduced by G. E. P. Box and K. B. Wilson in 1951 with an idea to use a set of designed experiments to obtain an optimal response [220]. However according to Mead and Pike, the origin of RSM started in 1930 with use of Response Curves [219]. Box and Wilson suggested using a first-degree polynomial model to do this. They acknowledged that this model was only an approximation, but can be used because such a model was easy to estimate and apply, even when little was known about the process.

In the past few decades RSM has been used by several researchers for prediction of tool life, surface roughness, wear resistance, etc. [221-224]. A considerable amount of these works were based on Metal Matrix composites (MMCs). However the modeling and prediction of wear performance of polymeric material and their composite are very limited. Shipway and Ngao [157] investigated the abrasive behaviour of polymeric materials in micro-scale level by using RSM. Similarly, in another study Sagbas et al. [225] used this method for modeling and predicting the abrasive wear behaviour of polyoxy-methylenes. It has been found that literature is almost nil on studying of erosive wear behaviour of polymeric composite. In view of the above literature, it is felt that enough scope of work exists on the use of RSM technique to predict the wear performance of natural fiber composite. Therefore, in the present work, an attempt has been made to develop predictive

models for abrasive wear and erosive wear behaviour of Lantana-Camara fiber reinforced epoxy composite under various testing conditions by using Response Surface Methodology.

7.2 RESPONSE SURFACE METHODOLOGY (RSM)

The Response Surface Methodology is a collection of mathematical and statistical techniques useful for the modeling and the analysis of problems in which a response of interest is influenced by several process variables and the objective is to optimize this response [220]. It consists of a group of techniques used in the empirical study of relationships between one or more measured responses and a number of input factors (process parameters). It comprises (1) designing a set of experiments, (2) determining a mathematical model, (3) testing of adequacy of the model developed (statistical significance) and (4) determining the optimal value of the response, in such a manner that, at least, a better understanding of the overall system behavior is obtained. The empirical relationship is frequently obtained by fitting polynomial models. First-order and second-order experiment designs are set up with the purpose of collecting data for fitting such models [226, 227].

In this chapter, a second-order (quadratic) polynomial response surface mathematical model is employed to analyze the parametric influences on various response criteria. The second-order model helps to understand main effect as well as the quadratic effect of each factors separately and the two-way interaction amongst these factors combined. This second-order mathematical model can be represented as follows:

$$y = \beta_0 + \sum_{i=1}^{k} \beta_i x_i + \sum_{i=1}^{k} \beta_i x_i^2 + \sum_{i=1}^{k} \sum_{j=1}^{k} \beta_{ij} x_i x_j + \varepsilon \qquad \text{for } i<j \qquad (7.1)$$

where β_0, β_i (i = 1, 2, . . . , k) and β_{ij} (i = 1, 2, . . . , k, j = 1, 2, . . . , k) are the unknown as regression coefficients to be estimated by using the method of least squares. In this equations ε are experimentally random errors and x_1, $x_{2.....}$ x_k are the input variables that influence the response y, k is the number of input factors. The least square technique is being used to fit a model equation containing the said regressors or input variables by minimizing the residual error measured by the sum of square deviations between the actual and the estimated responses. This involves the calculation of estimates for the regression

coefficients, i.e. the coefficients of the model variables including the intercept or constant term. The dimensions of the regression coefficients and the constant are evaluated such that, the model equation maintains dimension similarity. However calculated coefficients and model adequacy need to be tested for statistical significance. In this respect, the statistical test named ANOVA (Analysis of Variance) has been performed.

Analysis of variance (ANOVA) is used to check the adequacy of the model for the responses in the experimentation. ANOVA calculates the Fishers F-ratio, which is the ratio between the regression mean square and the mean square error. If the calculated value of F-value is higher than the tabulated F-value, then the model is said to be adequate at desired significance level α. In the current work the α-level is set at 0.05, i.e. the confidence level is set at 95%.

For testing the significance of individual model coefficients, the model is refined by adding or deleting coefficients through backward elimination, forward addition or stepwise elimination or addition algorithms. It involves the determination of P- value or probability of significance that relates the risk of falsely rejecting a given hypothesis. If the P-value is less or equal to the selected α-level, then the effect of presence of the variable term is significant. If the P-value is greater than the selected α-value, then it is considered that the presence of the variable term in the model is not significant. Sometimes the individual variables may not be significant. If the effect of interaction terms is significant, then the effect of each factor is different at different levels of the other factors.

The computation part of ANOVA can be made easily using available statistical soft-wear packages like MINITAB, DESIGN EXPERT, etc. In the present study, MINITAB RELEASE-14 soft-wear has been used.

Additional checks are also needed in order to determine the goodness of fit of the mathematical models by determining the coefficient of determination (R^2) and adjusted coefficient of determination (R^2_{adj}). The R^2 is the proportion of the variation in the dependent variable explained by the regression model. On the other hand, R^2_{adj} is the coefficient of determination adjusted for the number of independent variables in the regression model. For a good model, values of R^2 and R^2_{adj} should be close to each other and also they should be close to 1.

To have an assessment of pure error and model fitting error, some of the experimental trials are replicated. The adequacy of the models is also investigated by the examination of residuals. The residuals, which are the difference between the respective observed responses and the predicted responses, are examined using the normal probability plots of the residuals and the plots of the residuals versus the predicted response. If the model is adequate, the points on the normal probability plots of the residuals should form a straight line. On the other hand, the plots of the residuals versus the predicted response should be structure-less, i.e., they should contain no obvious pattern.

After analyzing all the statistical significance, the response surface analysis is then done in terms of the fitted surface. If the fitted surface is an adequate approximation of the true response function, then analysis of the fitted surface will be approximately equivalent to analysis of the actual system.

The objective of using RSM is not only to investigate the response over the entire factor space but also to locate the region of interest where the response reaches its optimum or near optimal value. By studying carefully the response surface model, the combination of factors, which gives the best response, can be established. This process can be summarized as shown in Figure-7.1.

7.3 MODELING OF ABRASIVE WEAR OF LANTANA-CAMARA FIBER REINFORCED EPOXY COMPOSITE

Basically the abrasive wear of polymer matrix composite (PMC) is influenced by several factors like abrasive grain size, type of reinforcement, type of polymer, size of reinforcement, amount of reinforcement or volume fraction of reinforcement, sliding distance, sliding velocity, applied normal load, etc. In this field statistical tools play an important role to develop mathematical models to predict the wear loss in terms of different factors and analyze the effects of different factors and their interaction on the abrasive wear behaviour. Keeping this in view, an attempt has been made to obtain an empirical model of wear loss as a function of volume fraction of fiber, sliding velocity and normal load by using RSM. In this study, the experimental wear loss data have been taken from chapter-4.

7.3.1 Design of Experiment (DOE)

The design of experiments technique permits us to carry out the modeling and the analysis of the influence of process variables (process input) on the response variables (process output). In the present study volume fraction of fiber (R_e, vol%), sliding velocity (V, m/s) and normal load (L, N) have been selected as design factors while other parameters (abrasive grit size and sliding distance) have been assumed to be constant over the experimental domain. A full factorial design (FFD) has been selected with three design factors of each of five levels to describe response of the wear loss and to estimate the parameters in the second-order model. Thus overall $5^3 = 125$ set of combinations of abrasive wear experimental data are required. In this work the set of combinations of abrasive wear experimental data are taken from chapter-4 (Table-4.5). For the convenience of recording and processing the experimental data, the upper and lower level of the factors have been coded as +1 and -1, respectively and the coded values of any intermediate levels can be calculated using the expression given below [228].

$$X_i = \frac{2X - (X_{max} + X_{min})}{(X_{max} - X_{min})/2} \tag{7.2}$$

where X_i is the required coded value of a factor of any value X from X_{min} to X_{max}, X_{min} the lower level of the factor and X_{max} is the upper level of the factor. The important factors and their levels for the abrasive wear test are shown in Table-7.1.

The FFD design of experiment runs with independent control variables in coded, un-coded forms and response are shown in Table-7.2. In the wear loss (Δw) values are taken from Table-4.6 to 4.10, chapter-4.

7.3.2 Development of the response surface model for the wear loss (Δw)

The results (data in Table-7.2) have been explored to the Minitab 14 software for further analysis following the steps outlined in Section-7.2. The second order regression equation has been developed for predicting wear loss (Δw) within selected experimental conditions using RSM. This second order equation in terms of the coded values of the independent variables can be expressed as:

$$\Delta w = 0.138432 - 0.041584 \times R_e + 0.047568 \times L + 0.027360 \times V + 0.084114 \times R_e^{\,2} - 0.012914 \times L^2 - 0.007520 \times V^2 + 0.011608 \times R_e \times L - 0.001280 \times R_e \times V + 0.008952 \times L \times V \quad (7.3)$$

ANOVA has been performed at a confidence level of 95% to check the adequacy of the proposed full model of wear loss i.e. equation-7.3, and the significance of the individual model coefficients. The results of ANOVA performed are listed in Table-7.3 & 7.4.

Table-7.3 presents the ANOVA table for the proposed second order model for wear loss given in equation-7.3. It can be appreciated that the P-value is less than 0.05 which means that the model is significant at 95% confidence level. Also the calculated value of the F-ratio is more than the standard value of the F-ratio (obtained from F-table) for wear loss. It means the model is adequate at 95% confidence level to represent the relationship between the wear loss (response) and process variables (inputs factors) of the abrasive wear process. Furthermore, the significance of presence each coefficient in the full model has been examined by the P-values. If the P-value is less than 0.05 then the corresponding coefficient is statistically significant for a confidence level of 95% [229].The ANOVA results of statistical significance of each coefficient are represented in Table-7.4. In this case two terms i.e. $R_e \times V$ and V^2 are found insignificant. The backward elimination procedure has been selected to automatically eliminate the insignificant model terms. By doing so, the reduced improved model for the wear loss can be presented as:

$$\Delta w = 0.134672 - 0.041584 \times R_e + 0.047568 \times L + 0.027360 \times V + 0.084114 \times R_e^{\,2} - 0.012914 \times L^2 + 0.011608 \times R_e \times L + 0.008952 \times L \times V \quad (7.4)$$

Again ANOVA has been performed on the reduced model and the results are presented in Table-7.5. From this table, it has been noticed that, the reduced improved model for wear loss is still significant. The response regression coefficients of the terms in the reduced model of wear loss i.e. equation-4, are also shown in Table- 7.6. The value of R^2 and R^2_{adj} of the proposed reduced models are found 0.893 and 0.887 respectively. The value of R^2 indicates that the model as fitted explains 89.3% of the variability in wear loss.

Figure-7.2 depicts the main effect plots for the wear loss considered in the present study. It is thus very much clear from the plot the volume fraction of fiber and normal load

rate are significant for wear loss while sliding velocity on wear loss is very less which reveals the statement as discussed in chapter-4.

7.3.3 Adequacy Checking of Abrasive Wear Loss Model

Though experiments have been conducted using full factorial design, replication of the experiments with each combination could not be carried out due to limitation of experimental resources. To have an assessment of pure error and model fitting error, 20% of the experiments, i.e. 25 experiments were chosen at random for replication .Table-7.7 shows the results for wear loss (Δw) for the replication trails. Then ANOVA has been performed on these replication trails. The results of performed ANOVA (Table-7.8) shows that lack-of-fit error is insignificant (Value of P>0.05 and calculated value of the F-ratio is less than the standard value of the F-ratio), indicating that the fitted model is accurate enough to predict the response.

The normal probability plots of the residuals and the plots of the residuals versus the predicted response for wear loss 'Δw' are shown in Figure-7.3 and 7.4. A check on the plot in the Figure-7.4 shows that the residuals generally fall on a straight line implying that the errors are distributed normally. Also Figure-7.4 revealed that it has no obvious pattern and unusual structure. This implies the model proposed is adequate and there is no reason to suspect any violation of the independence or constant variance assumption.

7.4 MODELING OF EROSION WEAR OF LANTANA-CAMARA FIBER REINFORCED EPOXY COMPOSITE

The influence of volume fraction of fiber, impact velocity and impingement angle on erosive wear behaviour of Lantana-Camara fiber epoxy composite has already been studied independently keeping all parameters at fixed levels in chapter-5. But in actual practice the resultant erosion rate is the combined effect of impact of more than one interacting variables. However, the impact of above parameters in an interacting environment becomes difficult. To this end, an attempt has been made to analyze the influence of more than one parameter on solid particle erosion of Lantana-Camara fiber epoxy composite by using Response Surface Methodology (RSM).

7.4.1 Design of experiment (DOE)

In the current study volume fraction of fiber (R_e, vol %), impact velocity (V, m/s) and impingement angle (α) has been selected as design factors while other parameters (Abrasive shape and size, and Stand-up-distance) are assumed to be constant over the experimental domain. Full factorial design (FFD) has been used with three design factors of each of four levels to describe response of the erosion rate (E_r). Total 4^3 = 64 sets of combination of experimental data have been taken from chapter-6 (Table-6.7 to 6.11). The important factors and their levels for the erosive wear test are shown in Table-7.9 and the design of experiment runs along with test results (response) are illustrated in Table-7.10.

7.4.2 Development of the response surface model for the erosion rate (E_r)

Similar to the procedure as explained in section 7.3.2**,** the full models for erosion rate was developed by taking the data from Table-7.10. The second order regression equation for erosion rate (E_r) can be expressed as:

$$E_r = -0.004345 + 0.000060 \times R_e + 0.000037 \times V + 0.006020 \times \alpha - 0.002483 \times \alpha^2 - 0.000017 \times R_e \times \alpha - 0.000013 \times V \times \alpha \quad (7.5)$$

Similarly ANOVA has been carried out on the full model at a confidence level of 95% and the results in Table-7.11 & 7.12. The proposed second order model for erosion rate is found significant (Table-7.11). The significance of individual coefficient in the full model are also observed through Table-7.12 and it has been noticed that the terms R_e^2, V^2, $R_e \times \alpha$, and $R_e \times V$ are insignificant. The reduced model for erosion rate is then obtained after eliminating the insignificant terms through MINITAB's backward elimination procedure. The reduced improved model for erosion rate (E_r) can be represented as:

$$E_r = -0.003909 + 0.000034 \times R_e + 0.000038 \times V + 0.005596 \times \alpha - 0.002483 \times \alpha^2 - 0.000013 \times V \times \alpha \quad (7.6)$$

To check the significance of reduced model and regression coefficients, again ANOVA has been performed and the results are listed in Table-7.13 & 7.14. The reduced improved model and regression coefficients present in reduced model are found significant. Also the R^2 value is found high, close to 1, which is desirable.

The main effect plots for the erosion rate have been illustrated in Figure 7.5. This figure clearly indicates that impingement angle has significant influence on wear rate in comparison to fiber volume fraction and impact velocity.

7.4.3 Adequacy Checking of Erosion Wear Rate Model

For assessment of pure error and model fitting error, 20% of the experiments, i.e. 16 experiments were chosen at random for replication, which are shown in Table-7.15. Again ANOVA has been performed on these replication trails and results are listed in Table-7.16. The lack-of-fit error is found insignificant, this indicating accuracy of the fitted model to predict the response.

The residuals, which are the difference between the respective, observe responses and the predicted responses have been examined by using the normal probability plots of the residuals and the plots of the residuals (Figure-7.6 & 7.7). It has been observed that residuals are falling on a straight line, which indicating normal distribution of error. Whereas the plot of residuals versus the predicted response for erosion wear rate has no obvious pattern.

7.5 CONCLUSIONS

The full factorial design experimentation followed by RSM approach in this study has been intended to model the abrasive and erosive wear response of Lantana-Camara fiber reinforced epoxy composite with respect to different processing parameters. This has been done by performing statistically designed experiments, estimating the coefficients in the mathematical models, predicting the response, checking for adequacy of the model and assessment of pure error and model fitting error. The mathematical models which are developed to predict the abrasive and erosive wear characteristics are found statistically valid and sound within the range of the factors. The results of the main effect plot (influence of individual process variables on response) are conformity with the findings of the chapet-4 and chapter-6.

Table-7.1 Important factors and their levels for abrasive wear

Sl. No.	Factor	Unit	Levels				
			(-1)	(-0.5)	(0)	(+0.5)	(+1)
1	Fiber volume fraction (R_e)	vol%	10	20	30	40	50
2	Sliding Velocity (V)	m/s	0.157	0.235	0.314	0.392	0.470
3	Applied Load (L)	N	5	10	15	20	25

Table-7.2 Experimental results along with design matrix for Abrasive wear of LCF reinforced epoxy composite

Runs	Factorial value (original)			Factorial value			Response
	R_e (vol %)	L (N)	V (m/s)	R_e	L	V	Δw(gm)
1	10	5	0.157	-1	-1	-1	0.167
2	10	5	0.235	-1	-1	-0.5	0.208
3	10	5	0.314	-1	-1	0	0.200
4	10	5	0.392	-1	-1	0.5	0.212
5	10	5	0.47	-1	-1	1	0.216
6	10	10	0.157	-1	-0.5	-1	0.211
7	10	10	0.235	-1	-0.5	-0.5	0.265
8	10	10	0.314	-1	-0.5	0	0.263
9	10	10	0.392	-1	-0.5	0.5	0.244
10	10	10	0.47	-1	-0.5	1	0.278
11	10	15	0.157	-1	0	-1	0.220
12	10	15	0.235	-1	0	-0.5	0.206
13	10	15	0.314	-1	0	0	0.284
14	10	15	0.392	-1	0	0.5	0.260
15	10	15	0.47	-1	0	1	0.295
16	10	20	0.157	-1	0.5	-1	0.225
17	10	20	0.235	-1	0.5	-0.5	0.248

Table-7.2 Contd.

Runs	Factorial value (original)			Factorial value			Response
	R_e (vol %)	L (N)	V (m/s)	R_e	L	V	$\Delta w(gm)$
18	10	20	0.314	-1	0.5	0	0.278
19	10	20	0.392	-1	0.5	0.5	0.264
20	10	20	0.47	-1	0.5	1	0.284
21	10	25	0.157	-1	1	-1	0.234
22	10	25	0.235	-1	1	-0.5	0.233
23	10	25	0.314	-1	1	0	0.298
24	10	25	0.392	-1	1	0.5	0.281
25	10	25	0.47	-1	1	1	0.314
26	20	5	0.157	-0.5	-1	-1	0.099
27	20	5	0.235	-0.5	-1	-0.5	0.111
28	20	5	0.314	-0.5	-1	0	0.120
29	20	5	0.392	-0.5	-1	0.5	0.115
30	20	5	0.47	-0.5	-1	1	0.132
31	20	10	0.157	-0.5	-0.5	-1	0.126
32	20	10	0.235	-0.5	-0.5	-0.5	0.138
33	20	10	0.314	-0.5	-0.5	0	0.140
34	20	10	0.392	-0.5	-0.5	0.5	0.138
35	20	10	0.47	-0.5	-0.5	1	0.152
36	20	15	0.157	-0.5	0	-1	0.160
37	20	15	0.235	-0.5	0	-0.5	0.189
38	20	15	0.314	-0.5	0	0	0.220
39	20	15	0.392	-0.5	0	0.5	0.238
40	20	15	0.47	-0.5	0	1	0.235
41	20	20	0.157	-0.5	0.5	-1	0.177
42	20	20	0.235	-0.5	0.5	-0.5	0.177
43	20	20	0.314	-0.5	0.5	0	0.210
44	20	20	0.392	-0.5	0.5	0.5	0.243

Table-7.2 Contd.

Runs	Factorial value (original)			Factorial value			Response
	R_e (vol %)	L (N)	V (m/s)	R_e	L	V	$\Delta w(gm)$
45	20	20	0.47	-0.5	0.5	1	0.248
46	20	25	0.157	-0.5	1	-1	0.189
47	20	25	0.235	-0.5	1	-0.5	0.212
48	20	25	0.314	-0.5	1	0	0.230
49	20	25	0.392	-0.5	1	0.5	0.242
50	20	25	0.47	-0.5	1	1	0.253
51	30	5	0.157	0	-1	-1	0.083
52	30	5	0.235	0	-1	-0.5	0.087
53	30	5	0.314	0	-1	0	0.090
54	30	5	0.392	0	-1	0.5	0.093
55	30	5	0.47	0	-1	1	0.112
56	30	10	0.157	0	-0.5	-1	0.096
57	30	10	0.235	0	-0.5	-0.5	0.088
58	30	10	0.314	0	-0.5	0	0.112
59	30	10	0.392	0	-0.5	0.5	0.127
60	30	10	0.47	0	-0.5	1	0.135
61	30	15	0.157	0	0	-1	0.110
62	30	15	0.235	0	0	-0.5	0.125
63	30	15	0.314	0	0	0	0.170
64	30	15	0.392	0	0	0.5	0.175
65	30	15	0.47	0	0	1	0.191
66	30	20	0.157	0	0.5	-1	0.126
67	30	20	0.235	0	0.5	-0.5	0.127
68	30	20	0.314	0	0.5	0	0.175
69	30	20	0.392	0	0.5	0.5	0.165
70	30	20	0.47	0	0.5	1	0.167
71	30	25	0.157	0	1	-1	0.147
72	30	25	0.235	0	1	-0.5	0.141

Table-7.2 Contd.

Runs	Factorial value (original)			Factorial value (coded)			Response
	R_e (vol %)	L (N)	V (m/s)	R_e	L	V	Δw(gm)
73	30	25	0.314	0	1	0	0.196
74	30	25	0.392	0	1	0.5	0.192
75	30	25	0.47	0	1	1	0.205
76	40	5	0.157	0.5	-1	-1	0.055
77	40	5	0.235	0.5	-1	-0.5	0.063
78	40	5	0.314	0.5	-1	0	0.060
79	40	5	0.392	0.5	-1	0.5	0.081
80	40	5	0.47	0.5	-1	1	0.078
81	40	10	0.157	0.5	-0.5	-1	0.060
82	40	10	0.235	0.5	-0.5	-0.5	0.078
83	40	10	0.314	0.5	-0.5	0	0.080
84	40	10	0.392	0.5	-0.5	0.5	0.093
85	40	10	0.47	0.5	-0.5	1	0.102
86	40	15	0.157	0.5	0	-1	0.083
87	40	15	0.235	0.5	0	-0.5	0.104
88	40	15	0.314	0.5	0	0	0.122
89	40	15	0.392	0.5	0	0.5	0.118
90	40	15	0.47	0.5	0	1	0.137
91	40	20	0.157	0.5	0.5	-1	0.098
92	40	20	0.235	0.5	0.5	-0.5	0.121
93	40	20	0.314	0.5	0.5	0	0.133
94	40	20	0.392	0.5	0.5	0.5	0.122
95	40	20	0.47	0.5	0.5	1	0.147
96	40	25	0.157	0.5	1	-1	0.119
97	40	25	0.235	0.5	1	-0.5	0.118
98	40	25	0.314	0.5	1	0	0.160
99	40	25	0.392	0.5	1	0.5	0.153
100	40	25	0.47	0.5	1	1	0.177

Table-7.2 Contd.

Runs	Factorial value (original)			Factorial value (coded)			Response
	R_e (vol %)	L (N)	V (m/s)	R_e	L	V	$\Delta w(gm)$
101	50	5	0.157	1	-1	-1	0.093
102	50	5	0.235	1	-1	-0.5	0.087
100	40	25	0.47	0.5	1	1	0.177
101	50	5	0.157	1	-1	-1	0.093
102	50	5	0.235	1	-1	-0.5	0.087
103	50	5	0.314	1	-1	0	0.104
104	50	5	0.392	1	-1	0.5	0.131
105	50	5	0.47	1	-1	1	0.133
106	50	10	0.157	1	-0.5	-1	0.117
107	50	10	0.235	1	-0.5	-0.5	0.123
108	50	10	0.314	1	-0.5	0	0.153
109	50	10	0.392	1	-0.5	0.5	0.147
110	50	10	0.47	1	-0.5	1	0.167
111	50	15	0.157	1	0	-1	0.152
112	50	15	0.235	1	0	-0.5	0.172
113	50	15	0.314	1	0	0	0.230
114	50	15	0.392	1	0	0.5	0.195
115	50	15	0.47	1	0	1	0.214
116	50	20	0.157	1	0.5	-1	0.171
117	50	20	0.235	1	0.5	-0.5	0.174
118	50	20	0.314	1	0.5	0	0.252
119	50	20	0.392	1	0.5	0.5	0.225
120	50	20	0.47	1	0.5	1	0.236
121	50	25	0.157	1	1	-1	0.195
122	50	25	0.235	1	1	-0.5	0.232
123	50	25	0.314	1	1	0	0.270
124	50	25	0.392	1	1	0.5	0.261
125	50	25	0.47	1	1	1	0.271

Table-7.3. ANOVA for wear loss '∆w' (Full model)

Source	DF	Seq. SS	Adj. SS	Adj. MS	$F_{calculated}$	$F_{0.05}$	P
Regression	9	0.462704	0.462704	0.051412	109.61	1.962	0.000
Linear	3	0.296282	0.296282	0.098761	210.56	2.684	0.000
Square	3	0.159656	0.159656	0.053219	113.46	2.684	0.000
Interaction	3	0.006766	0.006766	0.002255	4.81	2.684	0.003
Residual Error	115	0.053939	0.053939	0.000469			
Total	124	0.516643					

Seq. SS = Sequential sums of squares, Adj. SS = Adjusted sums of squares, Adj. MS = Adjusted mean squares.

Table-7.4. Estimated regression coefficients for wear loss '∆w' (Full model)

Term	Coef.	SE Coef.	P	
Constant	0.138432	0.004453	0.000	
R_e	-0.041584	0.002739	0.000	
L	0.047568	0.002739	0.000	
V	0.027360	0.002739	0.000	
$R_e \times R_e$	0.084114	0.004630	0.000	
$L \times L$	-0.012914	0.004630	0.006	
$V \times V$	-0.007520	0.004630	0.107	(Insignificant)
$R_e \times L$	0.011608	0.003874	0.003	
$R_e \times V$	-0.001280	0.003874	0.742	(Insignificant)
$R_e \times V$	0.008952	0.003874	0.023	
R^2 = 89.6%,		$R^2_{adj.}$ = 88.7%		

Coef. =Coefficient, SE Coef. =Standard error for the estimated coefficient, R2 = Coefficient of determination and $R^2_{adj.}$ = Adjusted R^2.

Table-7.5 ANOVA for wear loss 'Δw' (Reduced model)

Source	DF	Seq. SS	Adj. SS	Adj. MS	$F_{calculated}$	$F_{0.05}$	P
Regression	7	0.461416	0.461416	0.065917	139.65	2.084	0.000
Linear	3	0.296282	0.296282	0.098761	209.23	2.682	0.000
Square	2	0.158419	0.158419	0.079209	167.81	3.074	0.000
Interaction	2	0.006715	0.006715	0.003358	7.11	3.074	0.001
Residual Error	117	0.055227	0.055227	0.000472			
Total	124	0.516643					

Table-7.6 Estimated regression coefficients for wear loss 'Δw' (Reduced model)

Term	Coef.	SE Coef.	P
Constant	0.134672	0.003816	0.000
R_e	-0.041584	0.002748	0.000
L	0.047568	0.002748	0.000
V	0.027360	0.002748	0.000
$R_e \times R_e$	0.084114	0.004645	0.000
$L \times L$	-0.012914	0.004645	0.006
$R_e \times L$	0.011608	0.003886	0.003
$L \times V$	0.008952	0.003886	0.023
R^2= 89.3%,	$R^2_{adj.}$ = 88.7%		

Table-7.7 Replication results for wear loss on Abrasive wear of LCF reinforced epoxy composite

Runs	Factorial value			Factorial value (coded)			Response	
	R_e (vol %)	L (N)	V (m/s)	R_e	L	V	*Replication* Δw_1	*Replication* Δw_2
1	10	5	0.157	-1	-1	-1	0.167	0.153
2	10	5	0.392	-1	-1	0.5	0.212	0.265
3	10	10	0.47	-1	-0.5	1	0.278	0.257
4	10	15	0.47	-1	0	1	0.295	0.314
5	10	25	0.314	-1	1	0	0.298	0.311
6	20	5	0.392	-0.5	-1	0.5	0.115	0.154
7	20	10	0.47	-0.5	-0.5	1	0.152	0.192
8	20	15	0.392	-0.5	0	0.5	0.238	0.167
9	20	25	0.392	-0.5	1	0.5	0.242	0.276
10	30	5	0.157	0	-1	-1	0.083	0.113
11	30	5	0.47	0	-1	1	0.112	0.128
12	30	15	0.235	0	0	-0.5	0.125	0.166
13	30	20	0.314	0	0.5	0	0.175	0.205
14	40	5	0.157	0.5	-1	-1	0.055	0.063
15	40	5	0.392	0.5	-1	0.5	0.081	0.108
16	40	10	0.235	0.5	-0.5	-0.5	0.078	0.114
17	40	10	0.314	0.5	-0.5	0	0.080	0.089
18	40	20	0.235	0.5	0.5	-0.5	0.121	0.174
19	40	25	0.314	0.5	1	0	0.160	0.168
20	50	5	0.392	1	-1	0.5	0.131	0.134
21	50	5	0.157	1	-1	-1	0.093	0.145
22	50	5	0.47	1	-1	1	0.133	0.138
23	50	10	0.314	1	-0.5	0	0.153	0.218
24	50	20	0.314	1	0.5	0	0.252	0.305
25	50	25	0.47	1	1	1	0.271	0.265

Table –7.8 ANOVA for replication of experiments for Wear Loss (Δw)

Source	DF	Seq. SS	Adj. SS	Adj. MS	$F_{calculated}$	$F_{0.05}$	P
Regression	7	0.234445	0.234445	0.033492	39.46	2.237	0.000
Linear	3	0.167596	0.125708	0.041903	49.37	2.827	0.000
Square	2	0.066001	0.060326	0.030163	35.54	3.220	0.000
Interaction	2	0.000847	0.000847	0.000424	0.50	3.220	0.611
Residual Error	42	0.035648	0.035648	0.000849			
Lack-of-Fit	17	0.019707	0.019707	0.001159	1.82	1.872	0.085
Pure Error	25	0.015941	0.015941	0.000638			
Total	49	0.270092					

Table-7.9 Important factors and their levels for erosive wear

SL. No.	Factor	Unit	Levels			
1	Fiber volume fraction (R_e)	vol%	10	20	30	40
2	Impact Velocity (V)	m/s	48	70	82	109
3	Impingement Angle (α)	Degree	30	45	60	90

Table-7.10. Experimental results along with design matrix for Erosive wear of LCF reinforced epoxy composite

Runs	Factors			Response
	R_e (vol %)	V (m/s)	α (Degree)	$E_r \times 10^{-4}$ (gm/gm)
1	10	48	30	3.280
2	10	48	45	4.100
3	10	48	60	3.640
4	10	48	90	2.730
5	10	70	30	7.360
6	10	70	45	11.300

Table.7.10. Contd.

Runs	Factors			Response
	R_e (vol %)	V (m/s)	α *(Degree)*	$E_r \times 10^{-4}$ *(gm/gm)*
7	10	70	60	8.180
8	10	70	90	5.700
9	10	82	30	10.000
10	10	82	45	21.800
11	10	82	60	12.700
12	10	82	90	8.180
13	10	109	30	14.500
14	10	109	45	25.700
15	10	109	60	15.700
16	10	109	90	10.500
17	20	48	30	4.550
18	20	48	45	11.400
19	20	48	60	7.480
20	20	48	90	4.550
21	20	70	30	8.640
22	20	70	45	16.800
23	20	70	60	11.100
24	20	70	90	5.910
25	20	82	30	13.600
26	20	82	45	25.900
27	20	82	60	15.900
28	20	82	90	9.550
29	20	109	30	22.300
30	20	109	45	29.800
31	20	109	60	23.600
32	20	109	90	13.200
33	30	48	30	10.000

Table.7.10. Contd.

Runs	Factors			Response
	R_e (vol %)	V (m/s)	α *(Degree)*	$E_r \times 10^{-4}$ *(gm/gm)*
34	30	48	45	18.700
35	30	48	60	13.000
36	30	48	90	5.100
37	30	70	30	12.400
38	30	70	45	22.300
39	30	70	60	13.600
40	30	70	90	9.550
41	30	82	30	19.500
42	30	82	45	29.500
43	30	82	60	21.800
44	30	82	90	11.800
45	30	109	30	27.000
46	30	109	45	34.200
47	30	109	60	26.200
48	30	109	90	14.100
49	40	48	30	11.200
50	40	48	45	20.000
51	40	48	60	14.500
52	40	48	90	6.360
53	40	70	30	13.600
54	40	70	45	23.300
55	40	70	60	16.800
56	40	70	90	11.400
57	40	82	30	20.500
58	40	82	45	33.600
59	40	82	60	23.600
60	40	82	90	15.900

Table.7.10. Contd.

Runs	Factors			Response
	R_e (vol %)	V (m/s)	α *(Degree)*	$E_r \times 10^{-4}$ *(gm/gm)*
61	40	109	30	28.200
62	40	109	45	37.500
63	40	109	60	31.900
64	40	109	90	16.600

Table-7.11. Analysis of Variance for Erosion Rate 'E_r' (Full model)

Source	DF	Seq. SS	Adj. SS	Adj. MS	$F_{calculated}$	$F_{0.05}$	P
Regression	9	0.000040	0.000040	0.000004	36.38	2.058	0.000
Linear	3	0.000033	0.000006	0.000002	5.82	2.776	0.000
Square	3	0.000006	0.000006	0.000002	16.08	2.776	0.000
Interaction	3	0.000001	0.000001	0.000000	3.31	2.776	0.027
Residual Error	54	0.000007	0.000007	0.000000			
Total	63	0.000047					

Table-7.12 Estimated Regression Coefficients for Erosion Rate 'E_r' (Full model)

Term	Coef	SE Coef	P	
Constant	-0.004345	0.000934	0.000	
R_e	0.000060	0.000028	0.038	
V	0.000037	0.000017	0.037	
α	0.006020	0.000908	0.000	
R_e * R_e	-0.000000	0.000000	0.421	(Insignificant)
V*V	-0.000000	0.000000	0.911	(Insignificant)
α * α	-0.002483	0.000360	0.000	
R_e*V	0.000000	0.000000	0.523	(Insignificant)
R_e*α	-0.000017	0.000010	0.099	(Insignificant)
V* α	-0.000013	0.000005	0.012	

Table-7.13 Analysis of Variance for Erosion Rate 'E_r' (Reduced model)

Source	DF	Seq. SS	Adj. SS	Adj. MS	$F_{calculated}$	$F_{0.05}$	P
Regression	5	0.000040	0.000040	0.000008	64.80	2.374	0.000
Linear	3	0.000033	0.000017	0.000006	46.12	2.764	0.000
Square	1	0.000006	0.000006	0.000006	47.64	4.007	0.000
Interaction	1	0.000001	0.000001	0.000001	6.70	4.007	0.012
Residual Error	58	0.000007	0.000007	0.000000			
Total	63	0.000047					

Table-7.14 Estimated Regression Coefficients for Erosion Rate 'E_r' (Reduced model)

Term	Coef.	SE Coef.	P
Constant	-0.003909	0.000568	0.000
R_e	0.000034	0.000004	0.000
V	0.000038	0.000005	0.000
α	0.005596	0.000871	0.000
α * α	-0.002483	0.000360	0.000
V* α	-0.000013	0.000005	0.012

Table-7.15 Replication results for Erosion rate on Erosive wear of LCF reinforced epoxy composite.

Runs	Factors			Response	
	R_e (vol %)	L (N)	α(Degree)	*Replication* $E_{r1} \times 10^{-4}$(gm/gm)	*Replication* $E_{r2} \times 10^{-4}$(gm/gm)
1	10	70	30	8.180	8.210
2	10	82	45	12.700	13.300
3	10	82	60	21.800	24.800

Table-7.15 Contd.

Runs	Factors			Response	
	R_e (vol %)	L (N)	α(Degree)	Replication $E_{r1} \times 10^{-4}$(gm/gm)	Replication $E_{r2} \times 10^{-4}$(gm/gm)
4	10	109	90	10.500	12.500
5	20	70	30	8.640	8.530
6	20	70	45	5.910	5.710
7	20	82	60	15.900	19.900
8	20	109	90	29.800	28.800
9	30	48	30	13.000	17.800
10	30	70	45	22.300	22.200
11	30	82	60	19.500	25.100
12	30	82	90	11.800	21.400
13	40	48	30	11.200	18.200
14	40	70	45	13.600	27.600
15	40	82	60	20.500	26.500
16	40	109	90	28.200	34.200

Table-7.16 ANOVA for replication of experiments for Erosion Rate 'E_r'

Source	DF	Seq SS	Adj SS	Adj MS	$F_{calculated}$	$F_{0.05}$	P
Regression	5	0.000014	0.000014	0.000003	14.59	2.587	0.000
Linear	3	0.000011	0.000006	0.000002	10.82	2.975	0.000
Square	1	0.000003	0.000002	0.000002	10.41	4.225	0.003
Interaction	1	0.000000	0.000000	0.000000	0.07	4.225	0.792
Residual Error	26	0.000005	0.000005	0.000000			
Lack-of-Fit	10	0.000003	0.000003	0.000000	1.62	2.220	0.187
Pure Error	16	0.000002	0.000002	0.000000			
Total	31	0.000019					

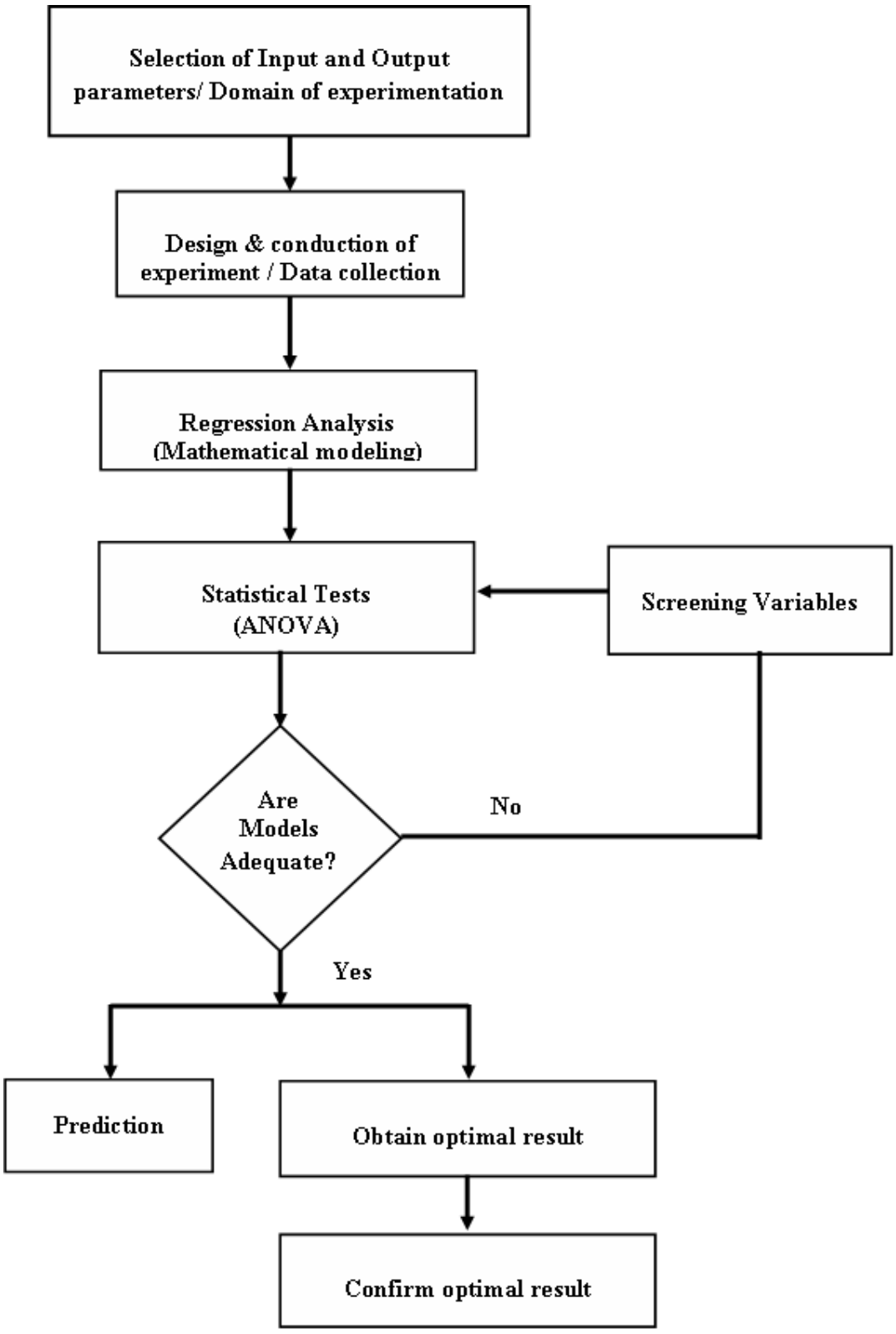

Figure-7.1 Procedure of Response Surface Methodology

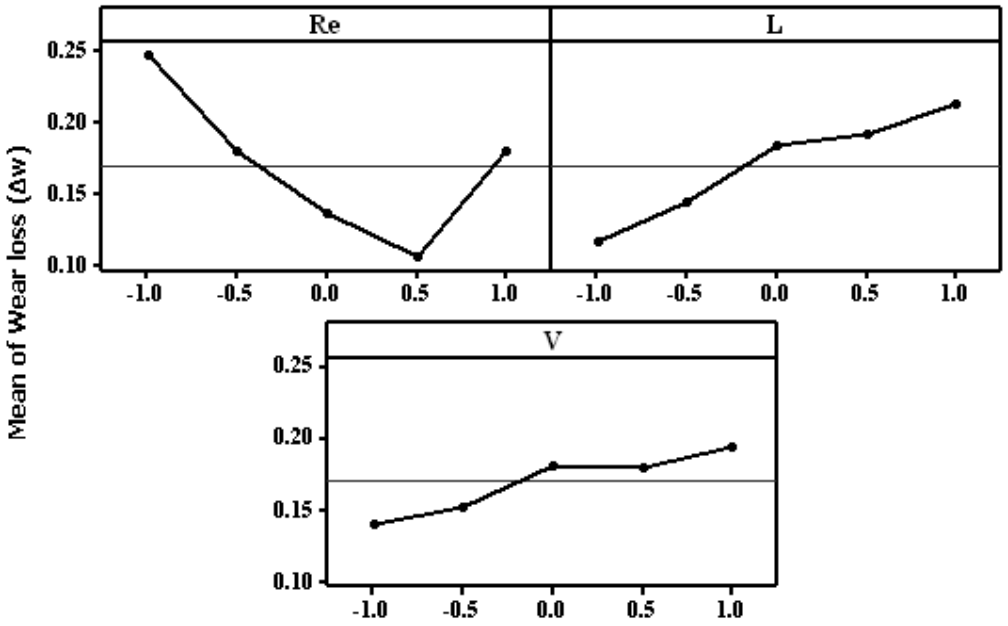

Figure-7.2 Main effect plot of wear loss 'Δw'

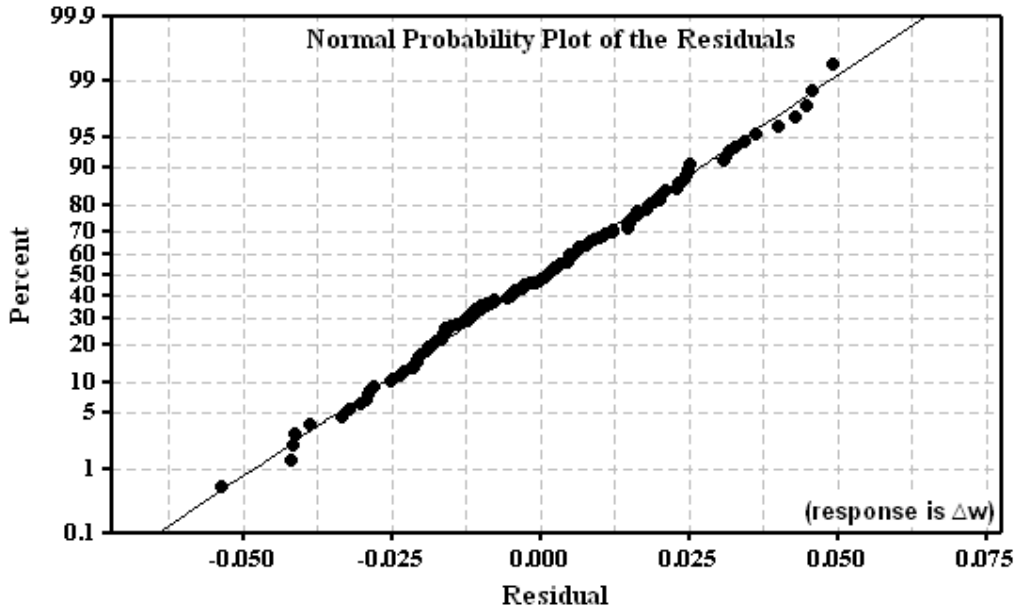

Figure-7.3 Normal probability plot of the residuals (Response is Δ*w*)

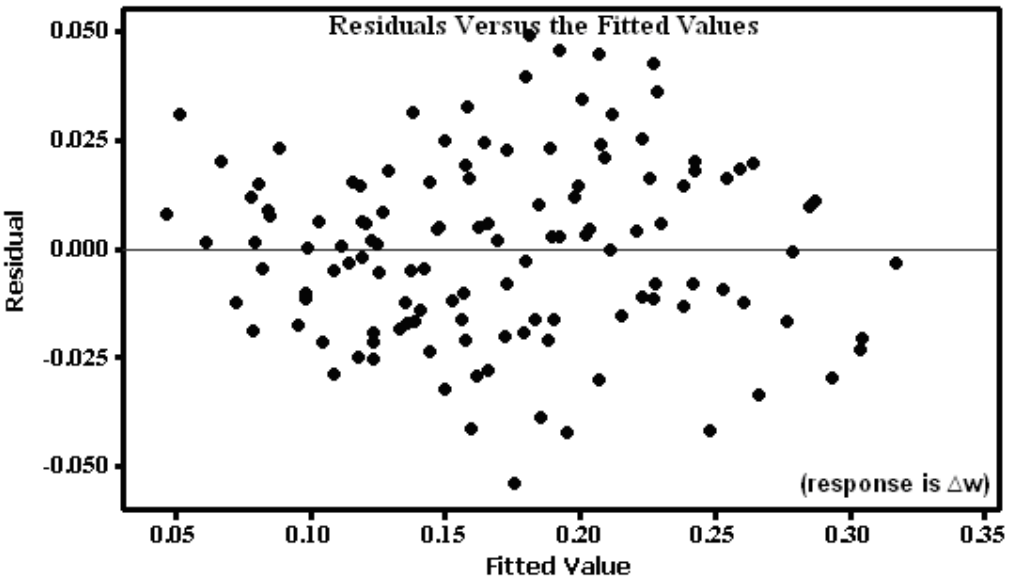

Figure-7.4 Plot of Residuals versus predicted response for wear loss 'Δw'

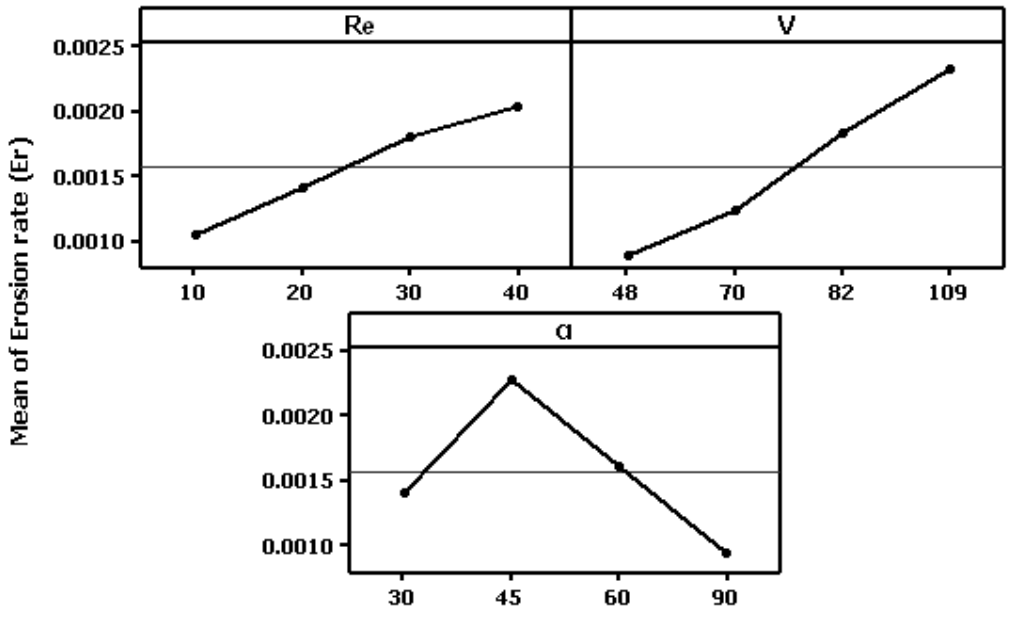

Figure-7.5 Main effect plot of Erosion rate 'E_r'

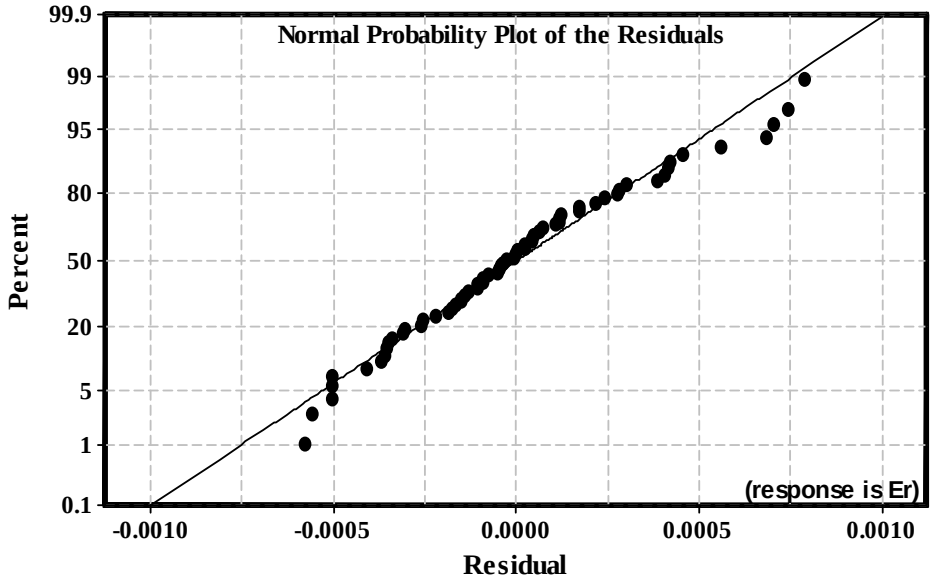

Figure-7.6 Normal probability plot of the residuals (Response is E_r)

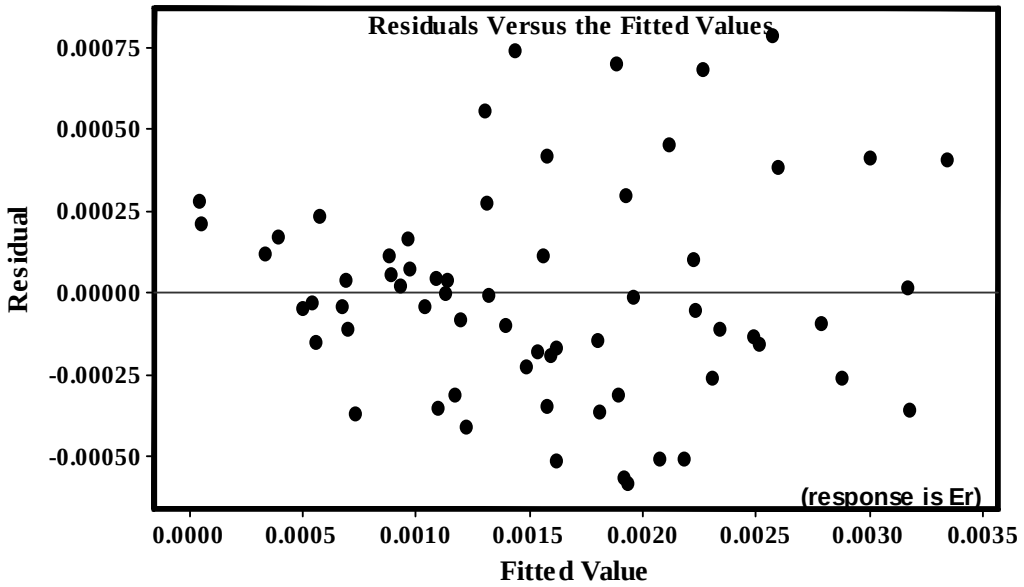

Figure-7.7 Plot of Residuals versus predicted response for Erosion rate 'E_r'

Chapter 8

CONCLUSIONS & FUTURE WORKS

Chapter-8

8.1 CONCLUSIONS

The conclusions drawn from the present investigations are as follows:

1. Lantana-Camara a known worst weed, which creates problem in plantation forestry, can successfully be utilized to produce composite by suitably bonding with resin for the development of value added products.

2. There is a good dispersibility of Lantana-Camara fiber (effective length being 9.11 mm) in the matrix, which improves the hardness, strength, modulus and work fracture of the composite. Thirty volume percent of reinforcement fiber gives the best combination among the tested composites.

3. The surface modification of fiber significantly improves the fiber matrix adhesion which in turn enhances the mechanical properties of the composite. The benzoyl-chloride treatment provides the highest improvement in strength and modulus in-comparison to alkali and acetone treatment.

4. Fickian's diffusion can be used to describe the moisture absorption behaviour of both treated and untreated Lantana-Camara fiber reinforced epoxy composite.

5. The abrasive wear resistance of neat epoxy is appreciably enhanced by incorporation of Lantana-Camara fiber. The specific wear rate of the composite also decreases with addition of fiber. In this present study the optimum fiber volume fraction which gives maximum wear resistance to the composite is found to be 40 vol%.

6. The abrasive wear rate of the Lantana-Camara fiber epoxy composite is influenced by several parameters e.g. sliding velocity, sliding distance and normal load. The wear rate of the composite is found to be more sensitive to normal load in comparison to sliding velocity. The coefficient friction of the composites decreases with addition of Lantana-Camara fiber which confirms that the addition of this fiber is beneficial in reducing the wear of neat epoxy.

7. The trend $W_{NO} < W_{APO} < W_{PO,}$ for Lantana-Camara fiber epoxy composite confirms the an-isotropic wear behaviour.

8. Lantana-Camara fiber epoxy composite shows a pseudo semi-ductile behaviour to solid particle erosion. From the experimental result the erosion efficiency (η) is found in the range of 2.76% to 28.71%.

9. The predictive models for abrasive and erosive wear behaviour of developed composite under various testing conditions have been performed through Response Surface Methodology. The models developed are found statistically valid and sound within the range of factors.

8.2 RECOMMENDATION FOR FURTHER RESEARCH

1. In the present investigation a hand-lay-up technique was used to fabricate the composite. However there exists other manufacturing process for polymer matrix composite. They could be tried and analyzed, so that a final conclusion can be drawn there from. However the results provided in this thesis can act as a base for the utilization of this fiber.

2. From this work it is found that chemical modification of the fiber with alkali, acetone and benzoyl-chloride significantly improves the mechanical performance of the composite. Other chemical modification methods such as silane treatment, acetylation treatment, acrylation treatment isocynates treatment, Permanganate treatment, Maleated coupling agents could be tried and a final conclusion can be drawn there after.

3. In the current study different tribological tests has been carried out on the untreated Lantana-Camara fiber epoxy composite. The same work could be extended to treated fiber composite.

4. In the erosion test sand particle of 200±50 microns only have been used. This work can be further extended to other particle size and types of particle like glass bead etc, to study the effect of particle size and type of particles on wear behaviour of the composite.

REFERENCES

[1] Jartiz, A.E., 1965, “Design,” pp. 18.

[2] Kelly, A., 1967, Sci. American, 217, (B), pp. 161.

[3] Berghezan, A., 1966, “Non-ferrous Materials,” Nucleus, 8: pp. 5–11.

[4] Van Suchtelen., 1972, "Product properties: a new application of composite materials," Philips Res. Reports, Vol. 27, pp. 28.

[5] Agarwal, B.D. and Broutman, L.J., 1980, “Analysis and performance of fiber composites,” John Wiley & Sons, New York, pp.3-12.

[6] Outwater J.O., “The Mechanics of Plastics Reinforcement Tension,” Mod. Plast: March- 1956.

[7] Wetter, R., 1970, “Kunststoffe in der Luft-und Raumfahrt,” Kunststoffe, 60, Heft-10.

[8] Schmidt, K. A. F., 1967, Verstarkungsfasern in Glasfaserverstärkte Kunstoffe, Ed. P. H. Selden, Springer-Verlag, Berlin, pp.159-221.

[9] Hinrichsen, G., Khan, M.A. and Mohanty, A.K., 2000, “Composites”: Part A, Elsevier Science Ltd, 31:pp.143–150.

[10] Joseph, P.V., Kuruvilla J, Thomas S., 1999, “Composites Science And Technology”; 59(11): pp.1625-1640.

[11] Mukherjee, P. S. & Satyanarayana, K. G., 1986, “Structure and properties of some vegetable fibers-II. Pineapple leaf fiber,” J. Material Science 21 (January), pp. 51–56.

[12] Jain, S., Kumar, R., Jindal, U. C., 1992, “Mechanical Behavior of Bamboo and Bamboo Composites,” J. Mater. Sci., **27**, pp. 4598-4604.

[13] Hirao, K., Inagaki, H., Nakamae, K., Kotera, M. and Nishino, T. K., 2003, “Kenaf Reinforced Biodegradable Composite,” Composites Science and Technology, 63: pp.1281-1286.

[14] Vazquez, A., Dominguez V. A., Kenny J. M., 1999, “Bagasse Fiber-Polypropylene Based. Composites.” Journal of Thermoplastic Composite Materials.” Volume 12, (6): pp. 477-497.

[15] Clemons, Craig M., Caulfield, Daniel F., 2005, “Ntural Fibers, Functional fillers for plastics,” Weinheim: Wiley-VCH: pp.195-206.

[16] Ei-Tayeb N.S.M., 2008, “A study on the potential of sugarcane fibers/polyester composite for tribological applications,” Wear, Vol. 265, pp. 223-235.

[17] Swarbrick, J.T., 1986, “History of the lantanas in Australia and origins of the weedy biotypes,” Plant Protection Quarterly 1, 115-121.

[18] Munir, A. A., 1996, “A taxonomic review of Lantana camara and L. montevidensis (Spreng.) Briq. (Verbenaceae) in Australia,” J. Adelaide Bot. Gard. 17: 1-27.

[19] Inada, A., Nakanishi, T., Tokuda, H., & Sharma, O. P., 1997, “Antitumor activities of lantadenes on mouse skin tumors and mouse hepatic tumors”, Planta Medica, 63, pp. 476–478.

[20] Sharma, S, 2004, “Lantana-whose weed any way! developing strategic directions for integrated utilization and control,” In: Workshop on Lantana camara: Problems and prospects (Volume of abstracts), organized by IIT, Delhi, HESCO, Dehra Dun and Department of Science and Technology (DST), Govt. of India, Dehra Dun from Feb. 10–11,

[21] Sharma, O. P. and Sharma, P. D., 1989, “Natural products of lantana plantthe present and prospects,” Journal of Scientific and Industrial Research, 48; pp.471–478.

[22] Gujral G.S. and Vasudevan P., 1983, “Lantana camara L., a problem weed,” J. Sci. Indust. Res. 42, pp. 281–286.

[23] Franck, R.R., 2005, “Bast and Other Plant Fibers,” Cambridge: Woodhead Publishing Limited.

[24] Robson D. and Hague J.A., 1995, “Comparison of wood and plant fibre properties,” in Third International Conference on Wood-fiber-plastic composites, Madison, Wisconsin, USA: Forest Products Society.

[25] Rong, M.Z., Zhang, M.Q., Liu, Y., Yang, G.C. and Zeng, H.M., 2001, “The effect of fiber treatment on the mechanical properties of unidirectional sisal-reinforced epoxy composites,” Compos. Sci. Technol., 61; pp. 1437–1447.

[26] Haigler, C. H., 1985, ‘The Functions and Biogenesis of Native Cellulose,” Cellulose Chemistry and Its Applications. T. P. Nevell and S. H. Zeronian. West Sussex, Ellis Horwood Limited: pp.30-83.

[27] Thygesen, A. et al., 2006, “Comparison of composites made from fungal de-fibrated hemp with composites of traditional hemp yarn”, Industrial Crops and Products.

[28] Rowell, R.M., Young, R.A., and Rowell, J.K., 1997, "Chemical Composition of Fibers: Paper and Composites from Agro-based Resources,"Lewis Publishers, CRC Press, pp.85-91.

[29] Bjerre, A.B. and Schmidt, A.S., 1997, "Development of chemical and biological processes for production of bioethanol: Optimization of the wet oxidation process and characterization of products," Riso-R-967(EN), Riso National Laboratory. pp. 5-9.

[30] Morvan, C., Jauneau, A., Flaman, A., Millet, J. and Demarty, M., "Degradation of flax polysaccharides with purified endo-polygalacturonase", Carbohydrate Polymers, 1990, 13(2): pp.149-163.

[31] Madsen, B., 2004, "Properties of plant fibre yarn polymer composites – An experimental study," 2004, PhD Thesis, Department of civil Engineering, Technical University of Denmark.

[32] Sakakibara, A. and Shiraishi, N., 1991, "Wood and Cellulose Chemistry," New York: Marcel Dekker.

[33] Rowell, R.M., 1995, "A new generation of composite materials from agro-based fibre," in The Third International Conference on Frontiers of Polymers and Advanced Materials, Kuala Lumpur, Malaysia.

[34] Outwater J.O., 1956, "The mechanics of plastics reinforcement in tension," Modern Plastics; 33 (7).

[35] Robson, D. et al., 1996, "Survey of natural materials for use in structural composites as reinforcement and matrices," Woodland Publishing Ltd, Abingdon.

[36] Kohler, R. and Wedler, M., 1994, Techtextil-Symposium, pp. 1.

[37] Joseph, K., Varghese, S., Kalaprasad, G., Thomas, S., Prasannakumari, L., Koshy, P., Pavithran, C., 1996, "Influence of interfacial adhesion on the mechanical properties and fracture behaviour of short sisal fiber reinforced polymer composites," European Polymer Journal, 32: pp. 1243-1250.

[38] Patel, R.D., Patel, R.G. and Patel, V.S., 1988, J. Therm. Anal., 34: pp. 1283.

[39] Yu, L., Dean, K. and Li, L. 2006, "Polymer blends and composites from renewable resources," Prog. Polym. Sci., 31: pp. 576-602.

[40] Bax, B. and Mussig, J., 2008, "Impact and tensile properties of PLA/Cordenka and PLA/flax composites", Composites Science and Technology, 68: pp. 1601-1607.

[41] Oksman, K., M. Skrifvars, and J.F.Selin, 2003, “Natural fibres as reinforcement in polylactic acid (PLA) composites,” Composites Science and Technology, 2003. 63: pp. 1317-1324.

[42] Meinander, K., et al., 1997, “Polylactides-degradable polymers for fibers and films”, Macromolecular Symp, 123: pp. 147-154.

[43] Jiang, L. and Hinrichsen, G., 1999, “Flax and cotton fiber reinforced biodegradable polyester amide composites,” 2. Die Angewandte Makromolekulare Chemie, 268: pp. 18-21.

[44] Riedel, U. and Nickel, J., 1999, “Natural fiber-reinforced biopolymers as construction materials - new discoveries,” Die Angewandte Makromolekulare Chemie, 272: pp. 34-40.

[45] Keller, A., et al., 2000, “Degradation kinetics of biodegradable fiber composites,” Journal of Polymers and the Environment, 8(2): pp. 91-96.

[46] Leaversuch, R.D., 2000, “Modern Plastics,” 77(12): pp. 56-60.

[47] Holbery, J., Houston, D., 2006, “Natural-Fiber-Reinforced Polymer Composites in Automotive Applications”, JOM, 58(11): pp.80-6.

[48] Burgueno, R., Quagliata, M.J., Mehta, G.M., Mohanty, A.K., Misra, M. and Drzal, L.T. 2005, “Sustainable Cellular Biocomposites from Natural Fibers and Unsaturated Polyester Resin for Housing Panel Applications”, Journal of Polymers and the Environment, 13(2): pp.139-149.

[49] Rials, T.G., Wolcott, M.P. and Nassar, J.M., 2001, “Interfacial Contributions in Lignocellulosic Fiber-Reinforced Polyurethane Composites”, Journal of Applied Polymer Science, 80(4): pp.546-555.

[50] Mueller, D.H. and Krobjilowski, A., 2003, “New Discovery in the Properties of Composites Reinforced with Natural Fibers”, Journal of Industrial Textiles, 33(2): pp.111-129.

[51] Bledzki, A.K. and Gassan, J.,1999, “Composites Reinforced with Cellulose Based Fibres”, Progress in Polymer Science, 24(2): pp.221-274.

[52] Eichhorn, S.J., Baillie, C.A., Zafeiropoulos, N., Mwaikambo, L.Y., Ansell, M.P., Dufresne, A., Entwistle, K.M., Herrera-Franco, P.J., Escamilla, G.C., Groom, L.H., Hughes, M., Hill, C., Rials, T.G. and Wild, P.M., 2001, “Review: Current international research into cellulosic fibres and composites”, Journal of Materials Science, 36(9): pp.2107-2131.

[53] Brouwer, W.D., 2000, "Natural Fibre Composites in Structural Components: Alternative Applications for Sisal," FAO, Common Fund for Commodities– Alternative Applications for Sisal and Henequen – Technical Paper No. 14.

[54] Bodros, E., Pillin, I., Montrelay, N., Baley, C., 2007, "Could biopolymers reinforced by randomly scattered flax fiber be used in structural applications", Composites Science and Technology, 67(3-4): pp.462-470.

[55] Pal, P.K., 1984, "Plastics Rubber Process Appl," 4: pp. 215-219.

[56] Bledzki, A.K. and Gassan, J., 1999, "Composites reinforced with cellulose based fibre," Prog. Polym. Sci. 24: pp. 221–274.

[57] Mohanty, A.K., Misra, M. and Drzal, L.T., 2002, "Sustainable bio-composites from renewable resources: opportunities and challenges in the green materials world," J. Polym. Environ. 10: pp. 19–26.

[58] Joseph, S., Sreekalab, M.S., Oommena, Z., Koshyc, P. and Thomas, S., 2002, "A comparison of the mechanical properties of phenol formaldehyde composites reinforced with banana fibres and glass fibres", Compos. Sci. Technol. 62: pp.1857–1868.

[59] Roe, P.J. and Ansel, M.P., 1985, "Jute reinforced polyester composites", J. Mater. Sci. 20: pp.4015.

[60] Qiu Zhang, X. M., Zhi Rong, M., Shia, G. and Cheng Yang, G., 2003, "Self reinforced melt processable composites of sisal", Compos. Sci. Technol. 63 : pp.177–186.

[61] Baiardo, M., Zini, E. and Scandola, M., 2004, 'Flax fibre–polyester composites', J.Compos.: Part A 35 : pp.703–710.

[62] George, J., Sreekala, M.S., and Thomas, S., 2002, "A review on interface modification and characterization of natural fibre reinforced plastic composites", Ploym. Eng. Sci. 41 (9): pp.1471–1485.

[63] Valadez-Gonzales, A., Cetvantes-Uc, J.M., Olayo, R. and Herrera Franco, P.J., 1999, "Effect of fibre surface treatment on the fibre-matrix bond strength of natural fibre reinforced composites", Composites, Part B 30 (3): pp.309–320.

[64] Rana, A.K., Mitra, B.C. and Banerjee, A.N., 1999, "Short jute fibre-reinforced polypropylene composites: dynamic mechanical study", J. Appl. Polym. Sci.71:pp.531–539.

[65] Manikandan Nair, K.C., Diwan, S.M. and Thomas, S., 1996, "Tensile properties of short sisal fiber reinforced polystyrene composites", J. Appl

Polym. Sci. 60: pp.1483–1497.

[66] El-Tayeb, N.S.M., 2009, "Development and characterisation of low-cost polymeric composite materials", Materials and Design 30: pp.1151–1160.

[67] Jacoba, M. Thomas, S. and Varugheseb, K.T., 2004, "Mechanical properties of sisal/oil palm hybrid fiber reinforced natural rubber composites", Compos. Sci. Technol. 64: pp. 955–965.

[68] Pothana, L.A., Oommen, Z. and Thomas, S., 2003, "Dynamic mechanical analysis of banana fiber reinforced polyester composites", Compos. Sci. Technol. 63 (2): pp.283–293.

[69] Yousif, B.F. and EI-Tayeb, N.S.M., 2006, "Mechanical and tribological characteristics of OPRP and CGRP composites", in: The Proceedings ICOMAST, GKH Press, Melaka, Malaysia, pp. 384–387,

[70] Tong, J., Arnell, R.D. and Ren, L.-Q., 1998, "Dry sliding wear behaviour of bamboo", Wear 221: pp.37–46.

[71] Tong, J., Ma, Y., Chen, D., Sun, J. and Ren, L., 2005, "Effects of vascular fiber content on abrasive wear of bamboo", Wear 259: pp.37–46.

[72] Hornsby, P.R., Hinrichsen, E. and Tarverdi, K., 1997, "Preparation and properties of polypropylene composites reinforced with wheat and flax straw fibres", Part II. Analysis of composite microstructure and mechanical properties, J. Mater. Sci. 32: pp. 1009–1015.

[73] Pothan, L.A., Thomas, S. and Neelakantan, N.R., 1997, "Short banana fibre reinforced polyester composites: mechanical, failure and aging characteristics", J. Reinf. Plast. Comp. 16: pp.744.

[74] Gassan J., 2002, "A study of fiber and interface parameters affecting the fatigue behaviour of natural fiber composites", Composite Part A 33: pp.369–374.

[75] Hepworth, D.G., Hobson, R.N., Bruce, D.M. and Farrent, J.W., 2003, "The use of unretted hemp in composite manufacture", Composites A 31: pp.1279–1283.

[76] Joseph, P.V., Kuruvilla, J. and Sabu T., 2002, "Short sisal fibre reinforced polypropylene composites: the role of interface modification on ultimate properties", Comps. Interf. 9 (2): pp.171–205.

[77] El-Sayed, A.A., El-Sherbiny, M.G., Abo-El-Ezz, A.S. and Aggag, G.A., 1995, " Friction and wear properties of polymeric composite materials for bearing

applications", Wear 184: pp.45–53.

[78] Rowell, R.M., 1997, "Chemical modification of agro-resources for property enhancement", Paper and Composites from Agro-based Resources, CRC Press. p. 351-375.

[79] Espert, A., Vilaplana, F. and Karlsson, S., 2004, "Comparison of water absorption in natural cellulosic fibres from wood and one-year crops in polypropylene composites and its influence on their mechanical properties", Compos Part A ; 35: pp.1267–76.

[80] Sanadi, A.R., CaulField, D.F. and Jacobson, R.E., 1997, "Agro-Fibre Thermoplastic Composites", Paper and composites from agro-based resources, Boca Raton: CRC Press: Lewis Publishers, Chapter 12, pp. 377-401.

[81] Maya Jacob John, Anandjiwala Rajesh D., 2008, "Recent Developments in Chemical Modification and Characterization of Natural Fiber-Reinforced Composites", Polymer composites, pp.187-207.

[82] Joseph, K., Thomas, S. and Pavithran, C., 1996, "Effect of chemical treatment on the tensile properties of short sisal fibre-reinforced polyethylene composites", Polymer 37: pp. 5139–49.

[83] Joseph, P.V., Joseph, K. and Thomas, S., 1999, "Effect of processing variables on the mechanical properties of sisal-fiber-reinforced polypropylene composites", Compos Sci Techol., 59: pp.1625–40.

[84] George, J., Bhagawan, S.S. and Thomas, S., 1998, "Effects of environment on the properties of low-density polyethylene composites reinforced with pineapple-leaf fiber", Compos. Sci. Techno., 58: pp.1471–85.

[85] Joseph, P.V., Rabello, M.S., Mattoso, L.H.C., Joseph, K., and Thomas, S., 2002, "Environmental effects on the degradation behaviour of sisal fibre reinforced polypropylene composites", Composites Science and Technology, **62**(10-11): pp.1357-1372.

[86] Stark, N., 2001, "Influence of moisture absorption on mechanical properties of wood flour-polypropylene composites", J. Thermoplast. Compos. Mater.,14: pp.421–32.

[87] Yuan, X., Jayaraman, K. and Bhattacharya, D., 2002, "Plasma treatment of sisal fibers and its effects on tensile strength and interfacial bonding", In Proceedings the Third International Symposium on Polymer Surface Modification: Relevance to Adhesion, Journal of Adhesion Science and

Technology Special Publication (0):1-25.Newark, NJ: MST Conferences, LLC.

[88] Stamboulis, A., Baillie, C.A., Garkhail, S.K., Van Melick, H.G.H. and Peijs T., 2000, "Environmental durability of flax fibers and their composites based on polypropylene matrix", Applied Composite Materials, 7: pp.273-294.

[89] Thomas, Selvin P., Sreekumar, P.A., Saiter, J.M., Joseph K., Unnikrishnan, G. and Thomas, S., 2009, "Effect of fiber surface modification on the mechanical and water absorption characteristics of sisal/polyester composites fabricated by resin transfer molding", Compos Part A 40: pp.1777–1784

[90] Singleton, A.C.N., Baillie, C.A., Beaumont, P.W.R. and Peijs, T.,2003,Compos B: Eng 34:519

[91] Rana AK, Mandal A, Bandyopadhyay B. Short jute fiber reinforced composites: effect of compatibilizer, impact modifier and fiber loading. Compos Sci Technol 2003; 63: pp.801–806.

[92] Mukherjee, R.N., Pal S.K., Sanyal S.K., Phani K.K., 1984, "Role of interface in fiber reinforced polymer composites with special reference to natural fibers." Journal of Polymer Material, (1),: pp. 69-81.

[93] Gassan J, Bledzki AK, 1999, "Alkali treatment of jute fibers: relationship between structure and mechanical properties." Journal of Applied Polymer Science, (71): p. 623-629.

[94] Zadorecki P., Flodin P., 1985, "Surface modification of cellulose fibers. I. Spectroscopic characterization of surface-modified cellulose fibers and their copolymerization with styrene." J Appl Polym Sci, (30): pp. 2419–2429.

[95] Zadorecki, P. and Flodin, P., 1985, "Surface modification of cellulose fibres. II. The effect of cellulose fibre treatment on the performance of cellulose–polyester composites." J Appl Polym Sci, (3): p. 3971–3983.

[96] Xue, Li., Lope G. and Panigrahi, S., "Chemical treatments of natural fiber for use in natural fiber reinforced composites: A review".Springer Science, Volume 15, (2007) p. 25-33.

[97] Mohanty, A.K., Misra, M. and Drzal, L.T., 2001, Compos Interfaces 8: p.313.

[98] Agrawal, R., Saxena, N.S., Sharma, K.B., Thomas, S. and Sreekala, M.S., 2000, Material Science Engg. A 277: p.77.

[99] Jahn, A., Schroder, M.W., Futing, M. and Schezel, K, Diepenbrock, 2002, Wear , Spectrochim,Acta A: Mol Biomol Spectrosc 58: p.2271.

[100] Paul, S., Puja, N. and Rajive, G., 2003. Molecules 8: pp.374

[101] Joseph, K., L.H.C. Mattoso, R.D. Toledo, S. Thomas, de-Carvalho, L.H., Pothen, L., Kala, S. and James, B., 2000,"Natural fiber reinforced thermoplastic composites', In Natural Polymers and Agrofibers Composites, ed. E. Frollini, A.L. Leão and L.H.C. Mattoso, 159-201. Sãn Carlos, Brazil: Embrapa, USP-IQSC, UNESP

[102] Wang, B., 2004, MSc. Thesis. University of Saskatchewan.

[103] Sreekala, M. S.; Kumaran, M. G.; Sabu, M. G., 1998, "Oil Palm Fibers: Morphology, Chemical Composition, Surface Modification, and Mechanical Properties", J Appl Polym Sci, 66(5), pp.821-835

[104] Ray, D. and Sarkar, B. K., 2001, "Characterization of alkali-treated jute fibers for physical and mechanical properties", J Appl Polym Sci , **80**, pp. 1013–1020.

[105] Aziz, S. H., and Ansell, M. P., 2004, "The effect of alkalization and fibre alignment on the mechanical and thermal properties of kenaf and hemp bast fibre composites: Part 1 – polyester resin matrix", Compos Sci Technol, 64: pp.1219.

[106] Samal, R. K., Acharya, S., Mohanty, M. and Ray, M. C., 2001, "FTIR spectra and physico-chemical behavior of vinyl ester participated transesterification and curing of jute", J Appl Polym Sci., 79, pp. 575.

[107] Higgins, G. H., V. Goldsmith, and A. N. Mukherjee, 1958, J. Polym. Sci., 32: pp.57.

[108] Roncero, M.B., Torres, A.L., Colom, J.F., and Vidal, T., 2005, "The effect of xylanase on lignocellulosic components during the bleaching of wood pulps", Bioresource Technology, 96(1): p. 21-30.

[109] Tanaka, K., Minoshima, K., Grela, W. and Komai, K., 2002, "Characterization of the aramid/epoxy interfacial properties by means of pull-out test and influence of water absorption", Composites Science and Technology, 62: pp. 2169-2177.

[110] Raj, R.G., Kokta, B.V., Grouleau, G., and Daneault, C., 1990, "The influence of coupling agents on mechanical properties of composites containing cellulosic fillers", Polymer.-Plast.Technol.Eng, 29(4): p. 339-353.

[111] Newson, W.R. and Maine, F.W., 2002, "Second generation woodfibre-polymer composites", In Progress in Woodfibre-Plastic Composites. Toronto, Canada.

[112] Abdul Khalil, H.P.S., Chow, W.C., Rozman, H.D., Ismail, H., Ahmad, M.N., and Kumar, R.N., 2001, "The effect of anhydride modification of sago starch on the tensile and water absorption properties of sago-filled linear low-density polyethylene (LLDPE)", Polym.-Plast.Technol.Eng, 40(3): p. 249-263.

[113] Lin, J.C., Chang, L.C., Nien, M.N. and Ho, H.L., 2006, "Mechanical behavior of various nano-particle filled composites at low-velocity impact", Comp Struct. 27: pp.30–36.

[114] Jayaraman, K., 2003, "Manufacturing sisal-polypropylene composites with minimum fiber degradation", Comp Sci Tech, 63: pp.367–74.

[115] Fujii, T., 1975, *J. Jpn. Soc. Comp. Mater.*, **1,** 35 (1975).

[116] Joseph, P.V., Mathew, G., Joseph, K., Groeninckx G. and Thomas, S., 2003, "Dynamic mechanical properties of short sisal fiber reinforced polypropylene composites", Comp A ;34:275–90.

[117] Karmakar, A., Chauhan, S.S., Modak, J.M. and Chanda, M., 2007, "Mechanical properties of wood-fiber reinforced polypropylene composites", Comp A, 38: pp.227–33.

[118] Thwe M.M. and Liao, K., 2003, "Environment degradation of bamboo/glass fibre hybrid polypropylene composites", J Mater Sci Lett, 38:pp.363–81.

[119] Sreenivasan, S., Iyer, P.B, and Krishna Iyer K.R., 1996, "Influence of delignification and alkali treatment on the fine structure of coir fibers (Cocos Nucifera)", J Mater Sci, 31: pp.721–726.

[120] Britton, P., Hodzic, A., Curro, R., Shu, L., Berndt, C.C. and Shanks, R.A., 2006, "Mechanical properties of PHB-Bagasse Composites", Proc ACUN-5, Developments in composites: Advanced, Infrastructural, natural, and Nano-composites, UNSW, Sydney, Australia , July 11-14.

[121] Mariatti, M., Jannah, M., Abu Bakar, A. and Abdul Khalil, H. P. S., 2008, "Properties of Banana and Pandanus Woven Fabric Reinforced Unsaturated, Polyester Composites", Journal of Composite Materials, 42 (9); pp.931-941

[122] Csari, P., Davies, P., and Mazeas, F., 2001, "Sea Water Aging of Glass Reinforced Composites: Shear Behavior and Damage Modeling", Journal of Composite Materials, 35: pp.1343–1371.

[123] Marom, G., 1985, "The role of water transport in composite materials", In: Comyn J, editor. "Polymer permeability", Elsevier Applied Science; chapter-9.

[124] Chiou, J.S. and Paul, D.R., 1986, "Sorption equilibria and kinetics of ethanol in miscible poly(vinylidene fluoride)/poly(methyl methacrylate) blends", Journal of Polymer Engineering Science, 26: pp.1218-1227.

[125] Marcovich, N.E., Reboredo, M.M. and Aranguren, M.I., 1999, "Moisture diffusion in polyesterwood flour composites", Polymer 40(26): pp.7313-7320.

[126] Wang, W., Sain, M. and Cooper, P.A., 2006, "Study of moisture absorption in natural fibre plastic composites", 2006, Composites Science and Technology, 66(3-4): pp.379-86

[127] Shen, C.H. and Springer, G.S., 1976, "Moisture Absorption and Desorption of Composite Materials," Journal of Composite Materials, 10: pp.1-20.

[128] Deo, C.R. and Acharya, S. K., 2010, "Effect of Moisture Absorption on Mechanical Properties of Chopped Natural Fiber Reinforced Epoxy Composite", Journal of Reinforced Plastics and Composites Online First, published on March 4, doi: 10.1177/ 073168440935-3352.

[129] Shi, S.Q. and Gardner, D.J., 2006, "Effect of density and polymer content on the hygroscopic thickness swelling rate of compression molded wood fiber/polymer composites", Wood Fiber Sci. 38: pp.520–526.

[130] Matuana, L.M., Balatinecz, J.J., Sodhi, R. S. and Park, C.B., 2001, "Surface characterization of esterified cellulosic fibres by XPS and FTIR spectroscopy", Wood Science and Technology; 35(3): pp.191-201.

[131] Amontons, G., 1699, Mem. Acad. T. , Ser. A: pp 257-282.

[132] Petrov, N.P., 1893, "Friction in machines and the effect of the lubricant", Inzh. Ah, 1893, pp 71-140, Vol. 2; pp. 227-279.

[133] Tower, B., 1983, "First report on friction experiments", Proc., Inst. Mech. Eng., London, Nov: pp. 632-659.

[134] Renolds, O., 1886, "On the theory of lubrication and its application to Mr. Beauchamp Tower's experiments", Plilos. Trans. T. Soc. London, Vol. 177, pp. 157-234.

[135] Holm, R., 1983, "The frictional force over the real area of Contact", Wiss. Vereoff. Siemens Werken, Vol. 17 (4), pp. 38-42.

[136]. Peterson, M. B., 1990, "Advanced in tribo-materials-I Achievements in Tribology", Amer, Soc, Mech. Eng., Vol.1, New York; pp.91-109.

[137] Rigney, D.A., 1981, In: D.A. Rigney (Ed.), "Fundamentals of Friction and Wear of Materials", American Society for Metals, Metals Park, Ohio; pp.1–12.

[138] Ashby, M.F. and Lim, S.C., 1990, “Wear-mechanism maps”, Scripta Metallurgical et Materialia, Vol.24: pp. 805-810.

[139] Wang, Y., Lei, T.C. and Gao, C.Q., 1990, “Influence of isothermal hardening on the sliding wear behaviour of 52100 bearing steel’, Tribology International, Vol. 23(1): pp. 47-53.

[140] Lim, S. C., 1998, “Recent developments in wear mechanism Maps”, Tribology International Vol. 31, Nos 1–3, pp. 87–97.

[141] Eyre, L.S., 1976, “Wear Characteristics of metals”, Tribology International, October-1976, pp. 203-212.

[142] Dowson, 1985, “Wear oh where”, International Conference on wear of Materials, Vancouver Canada, April 14-18,

[143] Blau, J., 1997, “Fifty years of research on the wear of metals”, Tribology International, Vol. 30(5): pp. 321-331.

[144] Barwell, F. T. and Strang, C. D., 1952, “Metallic Wear”, Proc. Roy. Soc. London, A, 212 (III): pp. 470-477.

[145] Archard, J.F., 1953, “Contact Rubbing of flat Surfaces”, J. Appl, Phys 24: pp. 981-988.

[146] Archard, J.F. and Hirst, W, 1957, “The Wear of Metal Under Unlubricated Conditions”, Proc. Roy. Soc. London, A, Vol. 238: pp 515-528.

[147] Kragelski, I. V., 1983, "Grundlagen der Berechnung von Reibung und VerschleiR”, Carl Hanser Verag. Miinchenu. Wien.

[148] Fleischer, G., 1973, “Energetische Methode der Bestimmung des VerschleiRes”, Schtnierungsrechnik 4(9): pp. 269-274.

[149] Gahr, K.H.Z., 1987, “Microstructure and wear of materials”, Tribology series 10, Elsevier Science Publishers.

[150] Stachowiak, G.W. and Batchelor, A.W., 1993, Engineering tribology. Amsterdam: Elsevier.

[151] Friedrich, K., 1986, “Friction and wear of polymer composites”, In: Friedrich K, editor. Composite materials series-1, Amsterdam: Elsevier; Chapter-8.

[152] Thorp, J.M., 1982, “Abrasive wear of some commercial polymers”, Tribol. Int., 15: pp.89–135.

[153] Budinski, K.G., 1997, “Abrasion resistance of plastics”, Wear; 203 (204): pp.302–309.

[154] Evans, D.C., and Lancaster, J.K., 1979. “The Wear of Polymers”, In: Scott, D. (Ed.), Treatise on Materials Science and Technology, New York, USA; Academic Press, Vol. 13, pp. 85—139.

[155] Unal, H., Sen, U. and Mimaroglu, A., 2005, “Abrasive behaviour of polymeric materials”, Mater. Des. 26: pp.705–710.

[156] Unal, H., Sen, U. and Mimaroglu, A., 2004, “Dry Sliding Wear Characteristics of Some Industrial Polymers Against Steel Counter Face”, Journal of Tribo, 37: pp.727–732.

[157] Shipway, P.H. and Ngao, N.K., 2003, “Microscale abrasive wear of polymeric materials”, Wear; 255: pp.742–750.

[158] Harsha, A.P. and Tewari, U.S., 2003, “Two-body and three-body abrasive wear behaviour of polyaryletherketone composites”, Polymer Testing; 22: pp. 403–418.

[159] Cirino, M., Pipes, R.B. and Friedrich, K., 1987, “The Abrasive Wear Behavior of Continuous Fiber Polymer Composites”, J. Mater. Sci., 22: pp.2481–2492.

[160] Cirino, M., Friedrich, K. and Pipes, R.B., 1988, “Evaluation of Polymer Composites for Sliding and Abrasive Wear Application”, Composites, 19: pp.383–392.

[161] Chand, N., Nayak, A. and Neogi, S., 2000, “Three-Body Abrasive Wear of Short Glass Fiber Polyester Composite”, Wear, 242: pp.32–46.

[162] Bijwe, J., Logani, C.M. and Tewari, U.S., 1989, “Influence of fillers and fibre reinforcement on abrasive wear resistance of some polymeric composites”, In: Proceeding of the International Conference on Wear of Materials, Denver, CO, USA, April 8–14, pp. 75–92.

[163] Liu, C., Ren, L., Arnell, R.D. and Tong, J., 1999, “Abrasive wear behavior of particle reinforced ultrahigh molecular weight polyethylene composites”, Wear; 225–229: pp.199–204.

[164] Chand, N. and Dwivedi, U.K., 2006, “Effect of coupling agent on abrasive wear behaviour of chopped jute fibre-reinforced polypropylene composites”, Wear; 261 (10): pp.1057–1063.

[165] Zhang, H., Zhang, Z., Guo, F., Jiang, W. and Liu W.M., 2009, “Study on the tribological behavior of hybrid PTFE/ cotton fabric composites filled with Sb_2O_3 and melaminecyanurate”, Tribol. Int.; 42(7): pp.1061–1066.

[166] Hashmi, S.A.R., Dwivedi, U.K. and Chand, N., 2007, "Graphite modified cotton fiber reinforced polyester composites under sliding wear conditions, Wear; 262 (11–12): pp.1426–1432.

[167] Yousif, B.F. and El-Tayeb, N.S., 2007, "The effect of oil palm fibers as reinforcement on tribological performance of polyester composite", Surface Review and Letters (SRL); 14 (6): pp.1095–1102.

[168] Yousif, B.F., 2009, "Frictional and wear performance of polyester composites based on coir fibers",Proc IME J. J. Eng Tribol.;223(1): pp.51–9.

[169] Chin, C.W. and Yousif, B.F., 2009, "Potential of kenaf fibers as reinforcement for tribological applications", Wear; 267: pp.1550–1557

[170] Yousif, B.F., Lau, Saijod, T.W. and Mc-William, S., 2010, "Polyester composite based on betelnut fibre for tribological applications", Tribology International; 43: pp.503–511.

[171] Lai, W.L. and Mariatti, M., 2008, "The properties of woven betel palm (areca catechu) reinforced polyester composites", J. Reinf. Plast. Compos.; 27: pp.925-935

[172] Dwivedi, U.K. and Chand, N., 2008, "Influence of Wood Flour Loading on Tribological Behavior of Epoxy Composites", Polymer Composites; 29: pp.1189-1192

[173] Dwivedi, U. K., Ghosh, A., and Chand, N., 2007, "Abrasive wear behaviour of bamboo powder filled polyester composites," BioResources; 2(4): pp.693-698.

[174] Soda, N., 1975, "Wear of some F.F.C metals during unlubricated sliding part-1. Effects of load, velocity and atmospheric pressure on wear",. Wear; 33: pp.1-16.

[175] Burwell, J.T. and Strang, C.D., 1953, 'Metallic wear', Proc.Soc (London), 212 A May: pp.470-477.

[176] Burwell, J.T., 1957, "Survey of possible wear mechanisms", Wear-1; 58: pp.119-141.

[177] Zumgahr, K.H., 1987, "Microstructure and wear of materials", Elsevier, Amsterdam.

[178] Ko, P.L., 1987, "Metallic wear-a review with special references to vibration-induced wear in power plant components", Tribology International, April,Vol.20, No.1: pp.66-78.

[179] Verma, A. P. and Sharma, P. C., 1992, "Abrasive Wear Behaviour of GRP Composite", The Journal of the Institute of Engineers (India) , Pt MC2,Vol.72, pp. 124.

[180] Wu, J. and Cheng, X.H., 2006, "The tribological properties of Kevlar pulp reinforced epoxy composites under dry sliding and water lubricated condition", Wear; 261: pp.1293–1297

[181] Sung, N.-H. and Suh, N. P., 1978, "Effect of fiber orientation on friction and wear of fiber reinforced polymeric composites", Wear; 53: pp.129-141

[182] Lyhmn, C., 1987, "Tribological behaviour of unidirectional polypropylene sulfide carbon fiber reinforced laminate composites", Wear; 117: pp.147–59.

[183] Cirino, M., Friedrich, K. and Pipes, R. B., 1988, "The effect of fiber orientation on the abrasive wear behavior of polymer composite materials," Wear; 121, pp.127-141

[184] Vishwananth, B., Verma, A. P., Rao, V. S. K., 1993, "Effect of reinforcement on friction and wear of fabric reinforced polymer composites", Wear, **167**, pp.93-99

[185] Shim, H.H., Kwon, O.K., Youn, J.R., 1992, "Effects of fibre orientation and humidity on friction and wear properties of graphite fibre composites", Wear; 157: pp.141-149.

[186] K. Joseph, S. Varghese, G. Kalaprasad, S. Thomas, L. Prasannakumar, P. Koshy, and C. Pavithram, 1996, *Eur. Polym. J.*, **32**, pp. 1243.

[187] Z. Lu , K. Friedrich, W. Pannhorst, J. Heinz, 1993, "Wear and friction of a unidirectional carbon fiber-glass matrix composite against various counterparts", Wear**,** 162-164, 1103-1113

[188] Eleiche, A.M., Amin, G.M., 1986, "The effect of unidirectional cotton fibre reinforcement on the friction and wear characteristics of polyester", Wear 112, 67.

[189] Chand, N., Dwivedi, U.K. and Acharya, S.K., 2007, "Anisotropic abrasive wear behaviour of bamboo (Dentrocalamus strictus)", Wear, 262, pp. 1031–1037

[190] Chand, N. and Dwivedi, U.K., 2007, "High stress abrasive wear study on bamboo", Journal of Materials Processing Technology 183, pp. 155–159.

[191] Tong, J., Ren, L., Li, J., Chen, B., 1995, "Abrasive wear behaviour of bamboo", Tribology International 28(5), pp. 323.

[192] Chand, N. and Dwivedi, U.K., 2007, "Influence of Fiber Orientation on High Stress Wear Behavior of Sisal Fiber-Reinforced Epoxy Composites", polymer composites, pp. 437-441.

[193] Chand, N. and Dwivedi, U.K., 2009, "Influence of Fibre Orientation on Friction and Sliding Wear Behaviour of Jute Fibre Reinforced Polyester Composite", Appl. Compos. Mater, 16: pp. 93–100.

[194] C.W. Chin, B.F. Yousif, 2009, Potential of kenaf fibres as reinforcement for tribological applications, Wear, 267 (9-10), pp. 1550-1557.

[195] Finnie, I., 1995, "Some reflections on the past and future of erosion: Part-I", Wear; 186/187: pp.1-101.

[196] Meng, H. C. and Ludema, K. C., 1995, "Solid Particle Erosion Resistance of Ductile Wrought Super Alloys and Their Weld Overlay Coatings", ibid, 181–183: pp.443.

[197] Bitter, J.G.A., 1963, "A study of erosion phenomena", Part I. Wear; 6: pp.5–21.

[198] Hutchings, I.M., Winter, R.E. and Field, J.E, 1976, "Solid particle erosion of metals: the removal of surface material by spherical projectiles", Proc Roy Soc Lond, Ser A; 348: pp.379-392.

[199] Pool, K.V., Dharan, C.K.H. and Finnie, I., 1986, "Erosive wear of composite materials", Wear;107: pp.1-12.

[200] Kulkarni, S.M., Kishore, K., 2001, "Influence of matrix modification on the solid particle erosion of glass/epoxy composites", Polymer and Polymer Composites;9: pp.25-30.

[201] Rajesh, J.J, Bijwe, J., Tewari, U.S. and Venkataraman, B., 2001, "Erosive wear behavior of various polyamides", Wear; 249: pp.702 – 714.

[202] Harsha, A.P., Tewari, U.S., Venkataraman, B., 2003, "Solid particle erosion behaviour of various polyaryletherketone composites", Wear; 254: pp. 693–712.

[203] Roy, M., Vishwanathan, B. and Sundararajan, G., 1994, "The solid particle erosion of polymer matrix composites", Wear; 171: pp.149–161.

[204] Hager A, Friedrich K, Dzenis YA, Paipetis SA. Study of erosion wear of advanced polymer composites. In: Street K, editor. ICCM-10 Conference Proceedings, Whistler, BC, Canada. Cambridge (UK): Woodhead Publishing; 1995. p. 155–62.

[205] Barkoula, N.M. and Karger-Kocsis, J., 2002, "Review-processes and influencing parameters of the solid particle erosion of polymers and their composites", J. Mater. Sci.; 37: pp. 3807–3820.

[206]. Tewari, U.S., Harsha, A.P., Hager, A.M. and Friedrich, K., 2003, "Solid particle erosion of carbon fibre– and glass fibre–epoxy composites", Compos Sci Technol.; 63: pp.549–57.

[207] Bhushan, B., 1999, " Principles and applications of tribology",New York: Wiley.

[208] Harsha, A.P. and Thakre, A.A., 2007, "Investigation on solid particle erosion behaviour of polyetherimide and its composites", Wear; 262: pp.807–818.

[209] Bijwe, J., Indumathi, J., John, R.J. and Fahim, M., 2001, "Friction and wear behavior of polyetherimide composites in various wear modes", Wear; 249: pp.715–726.

[210] Bijwe, J., Indumathi, J. and Ghose, A.K., 2002, "On the abrasive wear behavior of fabric-reinforced polyetherimide composites", Wear; 253: pp.768–777.

[211] Ruff, A.W. and Ives, L.K., 1975, "Measurement of solid particle velocity in erosive wear", Wear; 35: pp.195–199.

[212] Sundararajan, G. and Roy, B.V., 1990, "Erosion efficiency– a new parameter to characterize the dominant erosion mechanism", Wear; 140: pp.369–381.

[213] Suresh, A. and Harsha, A.P., 2006, "Study of erosion efficiency of polymers and polymer composites", Polymer testing; 25: pp.188-196.

[214] Barkoula, N.M. and Karger-Kocsis, J., 2002, "Effects of fibre content and relative fibre-orientation on the solid particle erosion of GF/PP composites", Wear; 252: pp.80–87.

[215] Biswas, S. and Satapathy, A., 2010, "A Comparative Study on Erosion Characteristics of Red Mud Filled Bamboo-Epoxy and Glass-Epoxy Composites", Journal of Materials and Design; 4: pp. 1752-1767.

[216] Miyazaki , N. and Hamao, T., 1994, "Solid Particle Erosion of Thermoplastic Resins Reinforced by Short Fibers", Journal of Composite Materials; 28: pp.871-883.

[217] Srivastava, V.K. and Pawar, A.G., 2006, "Solid particle erosion of glass fiber reinforced fly-ash filled epoxy resin composites", Composites Science and Technology; 66: pp.3021–3028.

[218] Sari, N. and Sinmazcelik, T., 2007, "Erosive wear behaviour of carbon fibre/polyetherimide composites under low particle speed", Materials Design; 28: pp.351–355.

[219] Myers, Raymond H., Khuri, Andre, I. and Carter, Walter H., Jr., 1989, "Response surface methodology: 1966-1988. Technometrics31(2): pp.137-153.

[220] Montgomery, D.C., 2005, "Design and Analysis of Experiments: Response surface method and designs", New Jersey: John Wiley and Sons, Inc.

[221] Sahin, Y. and Motorcu, A.R., 2005, "Surface roughness model for machining mild steel", Mater Des;26: pp.321–326.

[222] Noordin, M.Y., Venkatesh, V.C., Sharif, S., Elting, S. and Abdullah, A., 2004, "Application of response surface methodology in describing the performance of coated carbide tools when turning AISI 1045 steel", J Mater Process Technol.; 145: pp.46–58.

[223] Gunaraj, V. and Murugan, N., 1999, "Application of Response Surface Methodology for Predicting Weld Bead Quality in Submerged Arc Welding of Pipes", Journal of Materials Processing Technology; 88: pp.266-275.

[224] Lin, J. F. and Chou, C.C., 2002, "The Response Surface Method and the Analysis of Mild Oxidational Wear", Tribology International; 35: pp.771-785.

[225] Sagbas, A., Kahraman, F. and Esme, U., 2009, "Modeling and Predicting Abrasive Wear Behaviour Of Poly Oxy Methylenes Using Response Surface Methodolgy and Neural Networks", MetalurgiJa; 48 (2): pp.117-120

[226] Khuri, A.I. and Cornell, J.A., 1987, "Response Surfaces. Designs and Analyses", Vol. 81 of Statistics, Textbooks and Monographs, Marcel Dekker, Inc. ASQC, New York.

[227] Box, G. and Hunter, J., 1957, "Multi-factor experimental designs for exploring response surfaces", Ann. Math. Stat.; 21 (1): pp.195–241.

[228] Box, G.E.P., Hunter, W.H. and Hunter, J.S., 1978, "Statistics for experiments", 10th Edn. New York, Wiley.

[229] Majumder, A. and Goyal, A., 2008, "Enhanced production of exocellular glucansucrase from Leuconostoc dextranicum NRRL B1146 using response surface method", Bioresour Technol.; 99: pp.3685–3691.

PUBLICATIONS

International Journal:

1) Chittaranjan Deo and S.K. Acharya. 'Solid Particle Erosion of Lantana-Camara Fiber Reinforced Polymer Matrix Composite.' Polymer-Plastic technology and Engineering, 48: 1084-1087, 2009.

2) Chittaranjan Deo and S.K. Acharya.' Effect of moisture absorption on mechanical properties of chopped natural fiber reinforced epoxy composite.' Journal of Reinforced Plastic and Composite. Online First, published on March 4, 2010, (Online) DOI: 10.1177/0731684409353352.

3) Chittaranjan Deo and S.K. Acharya. 'Effects of Load and Sliding Velocity on Abrasive Wear of Lantana-Camara Fiber Reinforced Polymer Matrix Composite.' Journal of Engineering Tribology. Online First, published on November 25, 2009, (Online) DOI: 10. 1243/13506501JET699.

4) Chittaranjan Deo & S. K. Acharya, "Influence of Fiber Orientation on Abrasive Wear Behaviour of Lantana-Camara Fiber Reinforced Polymer Composite." Journal of Polymer-Plastics Technology and Engineering. (Under review)

5) Chittaranjan Deo & S. K. Acharya, Abrasive Wear Behaviour of Natural Fiber (Lantana-Camara) Reinforced Epoxy Composites: Influence of Fiber Content and Normal Load, Journal of Bio Resources**.** (Under review)

6) Chittaranjan Deo & S. K. Acharya, Influence of Fiber Treatment on Wear Performance of Lantana-Camara / Epoxy Composites", Journal of the Brazilian Society of Mechanical Sciences and Engineering. (Under review)

National Journal

1) Chittaranjan Deo & S. K. Acharya, "Effect of fiber content on abrasive wear of Lantana-Camara fiber reinforced polymer matrix composite", Indian journal of Engineering and Materials. (Accepted for publication)

International/ National Conferences:

1) Deo, C.R., Acharya, S.K. 'Solid Particle Erosion of Random Oriented Chopped Lantana-Camara Fiber Reinforced Polymer Matrix Composite'. 6th International Conference on Industrial Tribology, New Delhi, November 6-8, 2008.

2) Deo, C.R., Acharya, S.K. 'Abrasive Wear Performance of Lantana Camara Fiber Reinforced Polymer Matrix Composite'. National Symosium for Material Research Scholars (MR09), IIT, Bombay, May 8-9, 2009.

3) Deo, C.R., Acharya, S.K. 'Effect of Load on Abrasive Wear Behaviour of Lantana Camara Fiber Reinforced Polymer Composites.' International Conference on Mechanical and Electrical Technology (ICMET-2009), held in conjunction with IEEE ICCSIT 2009 August 8 - 11, 2009, Beijing, China

4) Deo, C.R., Acharya, S.K. 'Abrasive Wear Behaviour of Natural Short Fiber Reinforced Polymer Matrix Composite'. National Conference on Advances In Mechanical Engineering, (AME-09), Vidya Vikas Institute Of Engineering And Technology, Mysore, Oct 05, 2009.

5) Deo, C.R., Acharya, S.K. 'Effect of Environment on Mechanical Properties of Natural Fiber (Lantana-Camara) Epoxy Composite.' National conference on Advanced Manufacturing Technique, (NCAMT-2009), School of Mechanical Engineering, Shri Mata Vaishno Devi University, Katra, Jammu & Kashmir. Nov 05-06, 2009.

6) Acharya, S.K., Deo, C.R., and Mishra, C., 'Effect of Fiber Modification on Abrasive Wear Behaviour of Chopped Natural Fiber Reinforced Polymer Matrix Composite.' National conference on Advanced Manufacturing Technique, (NCAMT-2009), School of Mechanical Engineering, Shri Mata Vaishno Devi University, Katra, Jammu & Kashmir. Nov 05-06, 2009.

7) Deo, C.R., Acharya, S.K. 'Effect of Fiber Orientation on Abrasive Wear Behaviour of Natural Fiber (Lantana-Camara) Reinforced Polymer Composite. ISTAM-2009, Netaji Subhas Institute of Technology, New Delhi, Dec 18-21, 2009.

8) Deo, C.R., Acharya, S.K. ‘Effect of Water Absorption on Mechanical Properties of Lantana-Camara Fiber Reinforced Epoxy Composite.’ International Conference on Materials Mechanics and Management, (IMMM-2010), College of Engineering, Trivandrum, Kerala, Jan 14-16, 2010.

9) Deo, C.R., Acharya, S.K. ‘Influence of Fiber Orientation on Abrasive Wear Behaviour of Lantana-Camara Fiber Reinforced Polymer Composite: Wear Anisotropy’, International Conference on Recent Trends in Materials and Characterization (RETMAC-2010), NIT, Karnataka, Surathkal, India, February 14-15, 2010

10) Deo, C.R., Acharya S.K. ‘Abrasive Wear Behaviour of Natural Fiber Reinforced Polymer Composite: A statistical analysis, National Conference on Recent Advances in Fluid and Solid Mechanics (RAF & SM-2010), Department of Civil Engineering, NIT, Rourkela, Feb 27-28, 2010.

BIBLIOGRAPHY

Mr. Chitta Ranjan Deo is a faculty member in the Department of Mechanical Engineering, Synergy Institute of Engineering & Technology, Dhenkanal, Orissa, India-759001. He has 13 years of research and teaching experience in his field. He did M.E. in Production Engineering. This dissertation is being submitted for the fulfillment of the Ph.D. degree. The contact address is:

Chitta Ranjan Deo
Department of Mechanical Engineering
Synergy Institute of Engineering & Technology
Phone: 06762-225905/226708.
NH-42 Bypass, Dhenkanal, Orissa, India-759001
Phone: 06762-225905/226708.

D/30, OTM-Staff Colony, Choudwar
Cuttack, Orissa, India-754025
Mobile No.- +919437122252
E-mail: chittadeo@gmail.com